Analysis of heat shock protein 30 gene expression and function in *Xenopus laevis* A6 kidney epithelial cells

by

Saad Khan

A thesis
presented to the University of Waterloo
in fulfillment of the
thesis requirement for the degree of
Doctor of Philosophy
in
Biology

Waterloo, Ontario, Canada, 2014

Author's Declaration

I hereby declare that I am the sole author of this thesis. This is a true copy of the thesis including any required final revisions, as accepted by my examiners.

I understand that my thesis may be made electronically available to the public

Abstract

Heat shock proteins (HSPs) are molecular chaperones that assist in protein synthesis, folding and degradation and prevent stress-induced protein aggregation. The present study examined the pattern of accumulation of HSP30 and HSP70 in cells recovering from heat shock as well as the effect of proteasome inhibition on cytoplasmic/nuclear and endoplasmic reticulum (ER) molecular chaperone accumulation, large multimeric HSP30 complexes, stress granule and aggresome formation in *Xenopus laevis* A6 kidney epithelial cells. Initial immunoblot analysis revealed the presence of elevated levels of HSP30 after 72 h of recovery. However, the relative levels of HSP70 declined to near control levels after 24 h. The relative levels of both *hsp30* and *hsp70* mRNA were reduced to low levels after 24 h of recovery from heat shock. Pretreatment of cells with cycloheximide, a translational inhibitor, produced a rapid decline in HSP70 but not HSP30. The cycloheximide-associated decline of HSP70 was blocked by the proteasomal inhibitor, MG132, but had little effect on the relative level of HSP30. Also, treatment of cells with the phosphorylation inhibitor, SB203580, in addition to cycloheximide treatment enhanced the stability of HSP30 compared to cycloheximide alone. Immunocytochemical studies detected the presence of HSP30 accumulation in a granular pattern in the cytoplasm of recovering cells and its association with aggresome-like structures, which was enhanced in the presence of SB203580. To verify if proteasome inhibition in A6 cells induced the formation of similar HSP30 granules, immunoblot and immunocytochemical analyses were performed. MG132, celastrol and withaferin A enhanced ubiquitinated proteins, inhibited chymotrypsin-like activity of the proteasome and induced the accumulation of cytoplasmic/nuclear HSPs, HSP30 and HSP70 as well as ER chaperones, BiP and GRP94 and heme oxygenase-1. Northern blot experiments determined that

proteasome inhibitors induced an accumulation in *hsp30*, *hsp70* and *bip* mRNA but not *eIF1α*. The final part of this study demonstrated that treatment of A6 cells with proteasome inhibitors or sodium arsenite or cadmium chloride induced HSP30 multimeric complex formation primarily in the cytoplasm. Moreover, these stressors also induced the formation of RNA stress granules, pre-stalled translational complexes, which were detected via TIA1 and polyA binding protein (PABP), which are known stress granule markers. These stress granules, however, did not co-localize with large HSP30 multimeric complexes. In comparison, proteasome inhibition or treatment with sodium arsenite or cadmium chloride also induced the formation of aggresome-like structures, which are proteinaceous inclusion bodies formed as a result of an abundance of aggregated protein. Aggresome formation was identified by monitoring the presence of vimentin and γ-tubulin, both of which are cytoskeletal proteins and serve as markers of aggresome detection. Aggresome formation, which was also verified using the ProteoStat assay, co-localized with large HSP30 multimeric complexes. Co-immunoprecipitation experiments revealed that HSP30 associated with γ-tubulin and β-actin in cells treated with proteasome inhibitors or sodium arsenite or cadmium chloride suggesting a possible role in aggresome formation. In conclusion, this study has shown that the relative levels of heat shock-induced HSP30 persist during recovery in contrast to HSP70. While HSP70 is degraded by the ubiquitin-proteasome system, it is likely that the presence of HSP30 multimeric complexes that are known to associate with unfolded protein as well as its association with aggresome-like structures may delay its degradation. Finally, proteasome inhibition, sodium arsenite and cadmium chloride treatment of A6 cells induced cytoplasmic/nuclear and ER chaperones as well as resulting in the

formation stress granules and aggresome-like structures which associated with large HSP30 multimeric complexes.

Acknowledgements

First and foremost, I would like to thank God for giving me perseverance, ambition and drive to complete my PhD and for making this part of my life's journey full of joyful moments. My time at the Heikkila Lab will be cherished forever as I was able to forge some of the fondest memories in recent times. I want to dedicate this thesis to my grandparents, especially my mom's father, Dr. Zaheer Uddin for his love, prayers and passion for science. I truly believe that it is my elder's prayers that have given me the strength to embark and successfully complete this big endeavour in my life. I have many people to thank and I would like to start off by thanking, my supervisor, Dr. John J. Heikkila for this opportunity as well as his patience, guidance and advice throughout the past 6 years. He is truly an amazing individual and I have gained lots of experience both professionally and in my personal life. I would also like to thank Lisa (John's wife) for her welcoming dinners and great stories. In addition, I would like to thank my committee members, Dr. Bernard R. Glick and Dr. Mungo Marsden for taking the time out of their busy schedules to review my work, provide insightful advice and helpful feedback at every step of the way through this long journey. I also want to thank my externals Dr. Richard D. Mosser and Dr. Russell Tupling for examining my thesis in detail and providing excellent advice and especially for being nice to me during my defense. I would also like to thank all the members of Club Heikkila who have stuck by me and provided me with 6 years of ultimate fun: Jordan Young, Shantel Walcott, Ashley Rammeloo, Jara Brunt, Jin Duan, Ahmed J. El-Zahabi, Danny Chan, Imran Khamis, Charles M. Pickard and Ena Music thank you for making this lab the most wonderful at the University of Waterloo and make other labs in the Department of Biology envious of us. I want to make a special mention to Imran, for his insane support and listening to my wild

conjectures for the past 3 years. I would also like to extend a big thank you to Linda Zepf, Jennifer Collins and all the other administrative staff for their assistance and advice to allow me to successfully defend my thesis. I want to thank our wonderful group of research technicians and laboratory assistants in the Department of Biology for their support, especially Dale Weber and Mishi Groh for checking up on me constantly during my long trips to the confocal room. I want to thank my family and friends, especially my parents and brothers for sticking by me through these 6 years and wishing and praying for me to do well in life all the time. To my younger brothers, you are the best brothers anyone can wish for and thank you for all your support through my undergraduate, masters and PhD study and it was great times for us living in Waterloo together as a family. We became tighter at Waterloo, a home away from home. Last but not least, I want to thank the most important person in my life, a person who has become my life, without whom, I can't imagine to spend a single day, my wife, Ayesha. Thank you for being a part of my life and for unrelenting support that you have provided me throughout my PhD. These years will always be special for me since it's during this time that I met you and our love grew. It's your continuous support and love that got me to complete this PhD on time and in the grandest of fashions. You are the most wonderful, amazing human being that I have ever met.. You bring out the best in me and have always gotten me to try to strive for the best. The passion for being the best has driven me to do my best and make you proud and this is the result of that hard work that we have put in together. I thank God every day for bringing you into my life and pray that we spend many more years together.

Table of Contents

List of Figures

List of Tables

List of Abbreviations

ANOVA	analysis of variance
APS	ammonium persulfate
ATF6	activating transcription factor 6
BCA	bicinchoninic acid
BCIP	5-bromo-4-chloro-3-indolyl phosphate
BiP	immunoglobulin-binding protein
BSA	bovine serum albumin
C	control
$CdCl_2$	cadmium chloride
CHOP	CCAAT/-enhancer-binding protein homologous protein
CT	chymotrypsin
DAPI	4,6-diamidino-2-phenylindole
DMSO	dimethylsulphoxide
DBD	DNA binding domain
EDTA	ethylene-diamine-tetraacetic acid
eIF1α	elongation initiation factor 1 alpha
eIF2α	elongation initiation factor 2 alpha
ER	endoplasmic reticulum
ERAD	ER-associated degredation
ERSE	ER stress response element
FBS	fetal bovine serum
G3BP	ras GTPase-activating protein-binding protein
GCN2	general control nonderepressable 2
GRP94	glucose regulated protein 94
HDAC6	histone deacetylase 6
HBSS	Hank's balanced salt solution
HEPES	4-(2-hydroxyethyl)-1-piperazineethanesulfonic acid
HO-1	heme oxygenase-1
HR-A/B/C	hydrophobic repeat sequence
HSC	heat shock cognate
HSE	heat shock element
HSF	heat shock factor
HSP	heat shock protein
hsp	heat shock protein gene or mRNA
HSR	heat shock response
IRE1	inositol-requiring kinase 1
L-15	Leibovitz-15
LSCM	laser scanning confocal microscopy

MAPK	mitogen activated protein kinase
MBT	mid-blastula transition
MG132	carbobenzoxy-L-leucyl-L-leucyl-L-leucinal
MHC	major histocompatibility complex
mtHSP70	mitochondrial HSP70
NA	sodium arsenite
NBT	4-nitro blue tetrazolium
Nrf-2	nuclear factor-2
PABP	polyA binding protein
PBS	phosphate buffered saline
PERK	protein kinase (PKR) endoplasmic reticulum kinase
PGPH	peptidyl-glutamyl peptide hydrolyzing
PKR	RNA-activated protein kinase
ROS	reactive oxygen species
SDS	sodium dodecyl sulfate
SDS-PAGE	sodium dodecyl sulfate-polyacrylamide gel electrophoresis
SHSP	small heat shock protein
TBS-T	tris buffered saline solution – Tween20
TDF	transcription factor domain
TEMED	tetra-methyl-ethylene-diamine
TIA	T-cell intracellular antigen
TNF	tumour necrosis factor
TRAP1	TNF receptor-associated protein 1
Tris buffer	tris(hydroxymethyl)aminomethane
TRITC	rhodamine-tetramethylrhodamine-5-isothiocyanate phalloidin
UPR	unfolded protein response
UPS	ubiquitin-proteasome system
WA	withaferin A

Chapter 1: Introduction

1.1 Introduction

Organisms have evolved stress-responsive intracellular networks that can identify, monitor and respond to stressful stimuli (Morimoto, 2008). At the molecular level, environmental and physiological stressors can disrupt protein function and stability causing proteins to unfold or misfold into non-native conformations (Morimoto, 1998; Balch et al., 2008). Polypeptides that are abnormally folded are prone to cytotoxic aggregation, which can result in aberrant cellular processes and/or disease (Morimoto, 2008). As a result, molecular chaperone systems, such as heat shock proteins (HSPs), have evolved to assist in the refolding of unfolded/misfolded proteins and inhibit the formation of cytotoxic protein aggregates.

1.2 Heat shock proteins

HSPs are molecular chaperones that are involved in many cellular processes including protein synthesis, folding and assembly, membrane translocation and degradation. HSPs also bind to denatured proteins and assist in their refolding to their native state or target them for degradation in order to prevent stress-induced protein aggregation. HSPs have been well documented in a wide variety of organisms (Katschinski, 2004). There are at least 6 different HSP families that have been characterized to date including small HSPs (sHSPs), HSP40, HSP60, HSP70, HSP90 and HSP100 (Katschinski, 2004; Morimoto, 2008). *Hsp* gene expression patterns vary between organisms, tissues types, and developmental stages (Lindquist, 1986; Heikkila et al., 1997). Some *hsp* genes are expressed constitutively while others are stress-inducible (Katschinski, 2004).

1.2.1 Small heat shock proteins (sHSPs)

The sHSPs (16 – 42 kDa) are an evolutionarily divergent superfamily of proteins with the exception of an 80-100 amino acid conserved α-crystallin domain (MacRae, 2000; Van Montfort et al., 2001). The number, size and sequence of the family members vary between species (Arrigo and Landry, 1994; Stromer et al., 2003). The major sHSP families include HSP27 and the α-crystallins. Despite their lack of conservation, most sHSPs usually have three functional domains. These regions include the conserved α-crystallin domain, an amino-terminal extension and a carboxy-terminal extension. The secondary structure of the α-crystallin domain consists of β-strands organized into β-sheets that are required for dimer formation, the basic functional units of sHSP complexes (Buchner et al., 1998; MacRae, 2000). The N-terminal extension is poorly conserved except for the Trp-Asp-Pro-Phe (WDPF) sequence, which may play a role in oligomer formation (Lambert et al., 1999; Ganea, 2001). The C-terminal extension, which is poorly conserved and variable in length, was shown to be essential for stabilization of the quaternary structure, solubility and chaperone activity (MacRae, 2000; Fernando and Heikkila, 2000; Morris et al., 2008).

SHSPs have the ability to form highly polymeric structures that are necessary for their chaperone functions *in vivo* (Sun and MacRae, 2005; Hilario et al., 2011). Various functions that have been suggested for sHSPs include resistance against apoptosis, acquisition of thermotolerance, actin capping/decapping activity and cellular differentiation (Arrigo, 1998; MacRae, 2000; Van Montfort et al., 2001; Heikkila, 2010). As a result, the role of sHSPs in several medical conditions such as multiple sclerosis, cardiovascular diseases, oncogenesis and neurodegenerative diseases have been investigated (Jolly and

Morimoto, 2000; Westerheide and Morimoto, 2005; Ghayour-Mobarhan et al., 2012; Vidyasagar et al., 2012).

Another small HSP is HSP32. However, HSP32 is not a member of the sHSP superfamily since it was discovered to be heme oxygenase-1, an oxidative stress-inducible enzyme that catalyzes the breakdown of heme into bilirubin, iron and carbon monoxide (Keyse and Tyrrell, 1989; Elbirt et al., 1998). The *ho-1* gene is expressed primarily in the spleen, where senescent erythrocytes are sequestered and hemoglobin is degraded, as well as in kidney and liver (Raju et al., 1997). HO-1 accumulation was induced by agents that cause oxidative stress including sodium arsenite, UV radiation, hyperoxia, glutathione depletion and proteasomal inhibition (Keyse and Tyrrell, 1989; Elbirt et al., 1998; Oguro et al., 1998, Otterbein et al., 1999). More specifically, the *ho-1* gene is induced via the nuclear factor-like 2 (Nrf2) pathway, which can be activated by many compounds including proteasome inhibitors such as bortezomib, curcumin or MG132 as well as heavy metals like sodium arsenite and cadmium (Alam et al., 2000; Wu et al., 2004; Yamamoto et al., 2010; Kastle et al., 2012; Wang et al., 2013; Furfaro et al., 2014). Heat shock also induced HO-1 expression in various rat organs, European sea bass liver, mouse Sertoli cells, human fibroblasts and hepatoma cells (Taketani et al., 1988; Keyse and Tyrrell, 1989; Mitani et al., 1990; Raju and Maines, 1994; Lee et al., 1996; Hachfi et al., 2012; Li et al., 2014). However, heat shock did not enhance HO-1 accumulation in human alveolar macrophages, fibroblasts, hepatoma, glioma, HeLa, or HL60 cells (Yoshida et al., 1988; Keyse and Tyrrell, 1989; Taketani et al., 1989; Mitani et al., 1990; Okinaga et al., 1996).

1.2.1.1 HSP27

HSP27, also known as HSPB1, is the most extensively studied sHSP and is present in a variety of organisms. HSP27 is constitutively present in cells, but is also elevated in response to heat shock and other stressors (Arrigo and Landry, 1994; De Thonel et al., 2012; Garrido et al., 2012; Arrigo and Gibert, 2013). *Hsp27* genes were developmentally regulated in mouse, *Drosophila* and zebrafish and their expression varied depending on the tissue type and developmental stage (Davidson et al., 2002; Michaud et al., 2002; Mao and Sheldon, 2006; Middleton and Sheldon, 2013). Normally, HSP27 exists as large oligomers and under stress is phosphorylated by the p38 MAPK pathway resulting in conversion to smaller oligomers (Landry et al., 1992; Rogalla et al., 1999; Parcellier et al., 2005; Bryantsev et a. 2007; Bukach et al., 2009). In mammalian systems, HSP27 is expressed in various tissues including lens, heart, kidney, bladder, stomach, skin and muscle and is involved in cellular processes such as signal transduction, differentiation and modulation of cytoskeletal proteins (Lavoie et al., 1993; Garrido et al., 1997; Mehlen et al., 1997; Garrido et al., 2006; Wettstein et al., 2012). Additionally, HSP27 was shown to modulate transcription, translation and transduction pathways as well as being involved in tumor cell survival and cytoskeletal integrity (Arrigo and Gibert, 2013). HSP27 was found to function as an antioxidant by lowering levels of reactive oxygen species by increasing levels of glutathione (Arrigo et al., 2005). HSP27 is localized primarily in the cytoplasm but has the ability to translocate to the nucleus during stressful conditions (Guo et al., 2012; Mymrikov et al., 2012; Schmidt et al., 2012; Tang et al., 2013). Interestingly, mutated HSP27 was reported to be involved in the development of many neurodegenerative diseases (Evgrafov et al., 2004; Arrigo et al., 2007; Stetler et al., 2009; Mymrikov et al., 2011; Gurgis et al., 2014).

1.2.1.2 Crystallins

Crystallins are a group of sHSPs that are associated with the lens of the vertebrate eye. There are 3 main classes of crystallins, namely, α, β and γ-crystallin (Wistow, 2012). The major family of crystallin that is ubiquitously present in different species is the α-crystallin, which has two isoforms, αA-crystallin and αB-crystallin. Crystallin's primary function is to produce lens transparency and prevent the aggregation of misfolded proteins (Clark et al., 2012). αB-crystallin, also known as HSPB5, is a stress-induced sHSP that is expressed in many tissues including muscle, heart, kidney, lungs, colon and most importantly the lens (Arrigo and Gibert, 2013). It has numerous cellular functions including the prevention of protein aggregation by binding client proteins, cytoskeletal protection by binding intermediate filaments, regulating cellular growth and adhesion as well as protein transport (Arrigo and Gibert, 2013). αB-crystallin forms oligomers similar to HSP27, however these structures are less dynamic and range from 400 to 700 kDa (Arrigo and Simon, 2010). Similar to HSP27, mutations in α-crystallins were associated with various pathologies including cataract, neural and cardiovascular disorders (Vicart et al., 1998; Koteiche and Mchaourab, 2006; Arrigo et al., 2007). Recently, α-crystallins were reported to play an important role in tumorogensis as constitutive levels of αB-crystallins were detected in gliomas, prostate cancer, oral squamous cell carcinomas, renal cell carcinomas and head and neck cancer (Arrigo et al., 2007; Chen et al., 2012).

1.2.1.3 HSP30

The HSP30 family of stress-inducible sHSPs have only been detected in frog, fish and bird species (Bienz, 1984; Krone et al., 1992; Norris and Hightower, 2002; Franck et al., 2004; Katoh et al., 2004; Kondo et al., 2004; Wang et al., 2007; An et al., 2014). The number of *hsp30* genes can vary from species to species. For example, at least 5 members were isolated from *Xenopus laevis* (Bienz, 1984; Krone et al., 1992) and 10 from *Rana catesbeiana*, the American bullfrog (Helbing et al., 1996). In fish, only one *hsp30* gene was identified in zebrafish whereas up to 18 isoforms were identified in the desert topminnow (*Poeciliid*) (Norris et al., 1995; Elicker and Hutson, 2007). In birds, at least one *hsp30-like* gene, *hsp25*, was identified in chicken (Katoh et al., 2004).

Rana catesbeiana HSP30 has not been widely studied but Mulligan-Tuttle and Heikkila (2007) demonstrated that *Rana hsp30* mRNA and HSP30 protein were not constitutively present in the *Rana* FT fibroblast cell line. However, they were strongly induced in response to heat shock and localized primarily in a granular pattern in the nucleus and cytoplasm. Kaldis et al. (2004) demonstrated that *Rana* HSP30 displayed chaperone activity as it inhibited heat-induced citrate synthase aggregation *in vitro*. Additionally, *Rana* HSP30 maintained heat-treated luciferase in a folding competent state as determined using a *Xenopus* oocyte refolding assay. Furthermore, it was suggested that *Rana* HSP30 may have a protective role during development, since it occurred constitutively in the liver of metamorphosing tadpoles (Helbing et al., 1996). The pattern of *Xenopus laevis hsp30* gene expression and function will be discussed in section 1.4.2.

Studies with the Atlantic salmon, *Salmo salar* determined that it had a stress-inducible HSP30 homolog. For example, Lund et al. (2002) reported increased levels of

hsp30 mRNA in salmon when their incubation temperature was raised from 16 °C to 22-25 °C. Similarly, desert topminnow *hsp30* was not expressed constitutively but was heat-inducible and transient in its expression (Norris et al., 1997). Finally, the accumulation of *hsp30* mRNA was observed in primary cell cultures derived from goldfish caudal fin when temperatures were elevated from 20 to 40 °C (Kondo et al., 2004).

Chicken HSP25, a member of the HSP30 family, was not constitutively expressed but was stress-inducible in all tissues examined (Kawazoe et al., 1999). HSP25 accumulation was induced by various stressors including heat shock, sodium arsenite and the proteasomal inhibitor, lactacystin (Kawazoe et al., 1999; Wang et al., 1981; Katoh et al., 2004). Additionally, HSP25 was determined to co-localize with γ-tubulin and accumulate in the perinuclear region (Wieske et al., 2001; Katoh et al., 2004). Finally, Katoh et al. (2004) demonstrated that overexpression of chicken HSP25 in HeLa cells resulted in inclusion body formation.

1.2.2 Heat shock protein 70 (HSP70)

The HSP70 family of molecular chaperones are found in all organisms and are responsible for the regulation of protein folding under normal and stressful conditions (Katschinski, 2004). This molecular chaperone family contains constitutively expressed as well as stress-inducible members that interact with exposed hydrophobic surfaces of unfolded or partially-folded proteins and refold them in an ATP-dependent manner (Katschinski, 2004). HSP70 family members include heat shock protein 70 (HSP70), heat shock cognate 70 (HSC70), mitochondrial HSP70 and endoplasmic reticulum (ER)-resident immunoglobulin binding protein (BiP), also known as glucose regulated protein 78.

1.2.2.1 HSP70

HSP70 contains a highly conserved ATPase domain, a peptide-binding domain and a G/C-rich domain required for binding with other co-chaperones (Beere et al., 2000; Daugarud et al., 2007). The N-terminal ATPase domain is involved in hydrolyzing ATP while the peptide-binding domain is involved in binding and release of non-native proteins. Additionally, a Glu-Glu-Val-Asp (EEVD) motif is present in the C-terminal region and allows HSP70 to interact with other HSPs and co-chaperones such as HSP40 (Katschinski, 2004; Daugaard et al., 2007). Binding at this motif maybe also be responsible for HSP70 chaperone function and target protein specificity. Human cytosolic HSP70 is expressed in a tissue-specific and cell-cycle dependent manner during normal steady-state conditions (Daugaard et al., 2007). Upregulation of *hsp70* gene expression was reported in cells encountering stressful conditions including elevated temperature, mycotoxin treatment, proteasome inhibition and exposure to arsenite or cadmium (Golli-Bennour and Bacha, 2011; Xiong et al., 2013). During these periods of stress, HSP70 protects the cell from aggregation of unfolded protein and also directs the refolding of these proteins (Kim et al., 2013). HSP70 was shown to play an inhibitory role in stress kinase pathways (Sreedhar and Csermely, 2004) and prevention of apoptosis (Beere and Green, 2001; Stankiewicz et al., 2009). In addition to possessing a chaperone function, HSP70 also inhibited apoptosis by recruiting and deactivating caspases (Beere et al., 2000; Daugaard et al., 2007; Schlecht et al., 2011). Furthermore, high levels of HSP70 were often associated with many types of cancers and have been implicated in cancer cell survival (Aghdassi et al., 2007; Ciocca et al., 2013).

1.2.2.2 Immunoglobulin-binding protein

Immunoglobulin-binding protein (BiP), is an ER-resident molecular chaperone primarily involved in ER protein quality control and in regulating the unfolded protein response by binding to unfolded proteins in the ER lumen (Wu et al., 2006). BiP is composed of three main domains: the ATPase domain, the peptide-binding domain and the C-terminal domain (King et al., 2001). Similar to cytosolic HSP70, BiP is an ATP-dependent chaperone. Other functions of BiP include maintaining calcium homeostasis by sequestering calcium within the ER, assisting in degradation of proteins through the ERAD pathway (see section 1.4), signal transduction associated with initiating the unfolded protein response (UPR; see section 1.4), cytoprotective and anti-apoptotic effects by binding to caspase-7 and caspase-12 on the cytosolic side of the ER (Coe and Michalak, 2009; Dudek et al., 2009; Weng et al., 2011). *Bip* gene expression is induced by the UPR (see section 1.4), which is triggered by increased levels of unfolded protein in the ER (Gal-Yam et al., 2006; Zhang and Zhang, 2010). BiP levels were reported to increase in response to glucose starvation, treatment with glycosylation inhibitor, tunicamycin, and calcium ionophore, A23187 (Kim et al., 2005; Xu et al., 2009). Marinesco-Sjogren syndrome, an autosomal dominant polycystic liver disease, and Wolcott-Rallison syndrome are just some of the diseases that are associated with dysfunction of BiP and its co-chaperones (Senee et al., 2004; Anttonen et al., 2005; Waanders et al., 2006). More recently, overexpression of BiP was associated with various cancer types. BiP was shown to act as a receptor on the plasma membrane of many tumour cells resulting in cancer cell survival, proliferation and metastasis (Su et al., 2010; Zhang and Zhang, 2010).

1.2.3 Heat shock protein 90 (HSP90)

The HSP90 family of HSPs contains four members including two cytosolic HSP90 isoforms, HSP90α and HSP90β, mitochondrial chaperone known as TRAP1 (TNF receptor-associated protein 1) and ER-associated glucose-regulated protein 94 (GRP94; Felts et al., 2000). Both HSP90 isoforms contain essential ATP-dependent chaperone activity and are constitutively present at a high level in the cell (Sangster et al., 2004). Hereafter in this thesis HSP90 will refer to the HSP90α isoform.

1.2.3.1 HSP90

HSP90 is a ubiquitious molecular chaperone found in all eukaryotes in high abundance in the cytoplasm and nucleus and is fundamental to eukaryotic viability (Pearl et al., 2008; Erlejman et al., 2014). HSP90 was determined to associate with the transcription factor, heat shock factor 1 (HSF1), steroid receptors and signal transduction proteins involved in cell growth and proliferation (Zhao and Houry, 2005; Pearl et al., 2008). HSP90's interaction with co-chaperones including HSP70, HSP40 and p23 is essential for its proper function (Pratt, 1997; Taipale et al., 2010). HSP90 contains the N-terminal domain required for dimerization and ATP binding, a middle domain and a C-terminal domain to bind client proteins and co-chaperones. HSP90 also undergoes various post-translational modifications including phosphorylation, acetylation and oxidation, which regulate its function (Erlejman et al., 2014). HSP90 prevents denaturation and aggregation of proteins under normal conditions, assists in assembly/disassembly of multi-protein complexes and ensures proper folding and translocation of signalling molecules (Buchner, 1999; Sangster et al., 2004). Due to its involvement in many cellular pathways, especially in key processes in

oncogenesis such as stabilization of mutant proteins, angiogenesis, self-sufficiency in growth signals and metastasis, HSP90 has become a key target for treating various cancers (Whitesell and Lindquist, 2005; Trepel et al., 2010).

1.2.3.2 GRP94

GRP94 is an ER-resident protein that is upregulated as part of the unfolded protein response (described in Section 1.4). GRP94 was shown to be induced by a number of ER stressors including disturbances in calcium homeostasis, inhibition of glycosylation or hypoxia (Lee, 2001; Marzec et al., 2012). GRP94 contains the same domains as HSP90 and has similar functions. For example, the N-terminal domain residues in GRP94 that process ATP catalysis are the same as those in HSP90. However, unlike HSP90, GRP94 does not bind any co-chaperones and functions solely based on conformational changes within its domains (Marzec et al., 2012). GRP94 primarily functions as a chaperone and folds protein in the ER lumen including substrates of the immunoglobulin family (Marzec et al., 2012). Additionally, GRP94 is important for proper translocation and folding of Toll-like receptors and integrins (Wu et al., 2012).

1.3 Heat shock response

The heat shock response (HSR) is a universal cellular homeostatic mechanism that has been well characterized in both prokaryotes and eukaryotes. It is activated in response to stressful stimuli including elevated temperatures, heavy metals or disease states (Morimoto, 2008). These stresses can induce an accumulation of unfolded protein, which can interfere with regular cellular processes. Accumulation of unfolded protein triggers the upregulation of

hsp genes through the transcription factor, heat shock factor (HSF), which binds to the heat shock element (HSE), an enhancer found in the regulatory/promoter region of *hsp* genes (Morimoto, 1998; 2008).

1.3.1 Heat shock factors (HSFs)

C. elegans, Drosophila and *S. cervisiae* have a single HSF in contrast to plants and vertebrates, which have multiple HSFs with specialized functions (Morimoto and Santoro, 1998; Voellmy, 2004; Fujimoto and Nakai, 2010). To date, 4 HSFs have been identified and characterized in vertebrates including HSF1, HSF2, HSF3 and HSF4. In mammals, HSF1 is the primary eukaryotic transcription factor responsible for the stress-induced expression of *hsp* genes and is functionally equivalent to the HSF found in *Drosophila* and yeast (Morimoto, 1998; Core and Lis, 2008; Sakurai and Enoki, 2010). Detectable levels of HSF2 were observed in embryonic tissues and specifically contributed to the developmental regulation of *hsp* gene expression in various organisms including mouse, rat, chicken and zebrafish (Rallu et al., 1997; Voellmy, 2004; Abane and Mezger, 2010). HSF3 in combination with HSF1 was required for stress-induced expression of *hsps* in birds (Nakai, 1999; Fujimoto and Nakai, 2010). Recently, mouse HSF3 was found to have similar functionality to that of chicken HSF3 (Fujimoto et al., 2010). Finally, HSF4, which was reported to have DNA damage repair capabilities, was expressed in specific mammalian tissues including heart, brain, skeletal muscle and pancreas and consisted of two isoforms (HSF4a and HSF4b; Nakai et al., 1997; Tanabe et al., 1999; Pirkkala et al., 2001; Cui et al., 2012).

1.3.2 Structure of HSF1

HSF1 is the stress-inducible member of the HSF family, which is responsible for the activation of the heat shock response in eukaryotes (Voellmy, 2004; Fujimoto and Nakai, 2010). HSF1 consists of a helix-turn-helix DNA binding motif, a carboxy-terminal transcriptional transactivation domain and an oligomerization domain consisting of a hydrophobic repeat sequence (HR-A/B) essential for trimer formation (Fig. 1; Voellmy, 2004; Sakurai and Enoki, 2010; Fujimoto and Nakai, 2010). An additional hydrophobic repeat sequence (HR-C) is located adjacent to the transcription activation domain. Under normal conditions interactions between HR-A/B and HRC contribute to the suppression of HSF1 trimerization, while a conserved sequence located between HR-A/B and HR-C is thought to negatively regulate DNA-binding and transcriptional activation (Fujimoto and Nakai, 2010).

1.3.3 Stress-induced regulation of *hsp* genes

In eukaryotes, stress-inducible *hsp* genes are regulated primarily at the transcriptional level via the interaction of HSF1 with the heat shock element (HSE), which is generally present in the 5' promoter of all *hsp* genes (Morimoto, 1998; Katschinski, 2004; Voellmy, 2004; Sakurai and Enoki, 2010). Normally HSF1 is bound to HSP90 and histone deacetylase 6 (HDAC6) and exists as an inactive monomer in the cytoplasm and/or nucleus. In response

Figure 1. General structure of HSF1. Schematic representation of HSF1 structural motifs that correspond to the helix-turn-helix DNA binding domain, hydrophobic repeat sequences (HR-A/B and HR-C), the carboxy terminal transcription activation domain, and regulatory domains associated with the suppression of HSF1 activity (adapted from Voellmy, 2004).

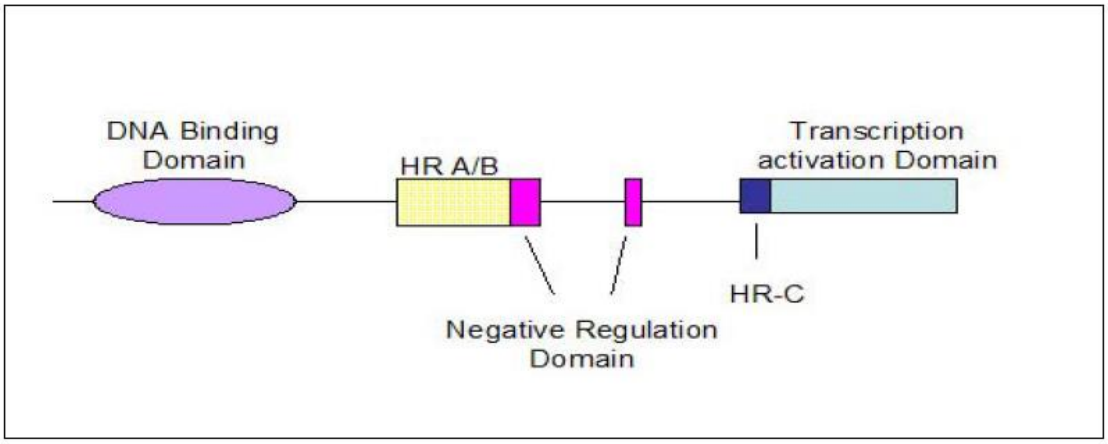
DNA Binding
Domain
HR A/B
Transcription
activation Domain
HR-C
Negative Regulation
Domain

to an increase in the intracellular levels of unfolded or misfolded proteins, HSP90 and HDAC6 are recruited to aid in protein folding and to prevent their aggregation, thereby allowing HSF1 monomers to trimerize (Fig. 2; Bouyalt et al., 2007; Sakurai and Enoki, 2010). This trimerization results in the activation of HSF1 and subsequent localization to the nucleus to initiate transcription of *hsp* genes. HSF1 also undergoes phosphorylation at serine and threonine residues that can lead to potential activation or inactivation of HSF1. Constitutively phosphorylated serine residues suppress HSF1 activation, while inducible phosphorylated serine residues promote HSF1 activity (Holmberg et al., 2002; Bjork and Sistonen, 2010). Sumoylation, the post-translational process by which a small ubiquitin-like modifier (SUMO) is added to proteins, can also play a role in regulating DNA binding activity and transcriptional activation of HSF1 (Hong et al., 2001; Anckar et al., 2006; Bjork and Sistonen, 2010).

1.4 Unfolded protein response

The unfolded protein response (UPR) is a complex signalling response in eukaryotes that is activated in response to an increase in unfolded or misfolded proteins in the ER. Secreted, organelle-targeted or membrane-bound proteins are processed in the ER and shipped through vesicular transport to various components in the cell (Ni and Lee, 2007). If these proteins are misfolded due to any pathological or physiological condition and cannot be repaired, then they are targeted for degradation by the ubiquitin-proteasome system (UPS) using the ER-associated degradation (ERAD) pathway (Malhi and Kaufman, 2011).

Figure 2. Stress-induced regulation of heat shock response. (1) External stressful stimuli cause native proteins in the cell to unfold. (2) HSP90 and HDAC6 are bound to HSF1 under normal conditions in the cell. (3) HSP90 and HDAC6 are recruited to prevent aggregation of unfolded proteins. (4) This allows HSF1 monomers to trimerize and translocate to the nucleus. (5) The HSF1 trimer than binds to the heat shock element at the 5' promoter of *hsp* genes. (6) HSF1 binding to the HSE results in the transcription of stress-induced HSPs including HSP90.

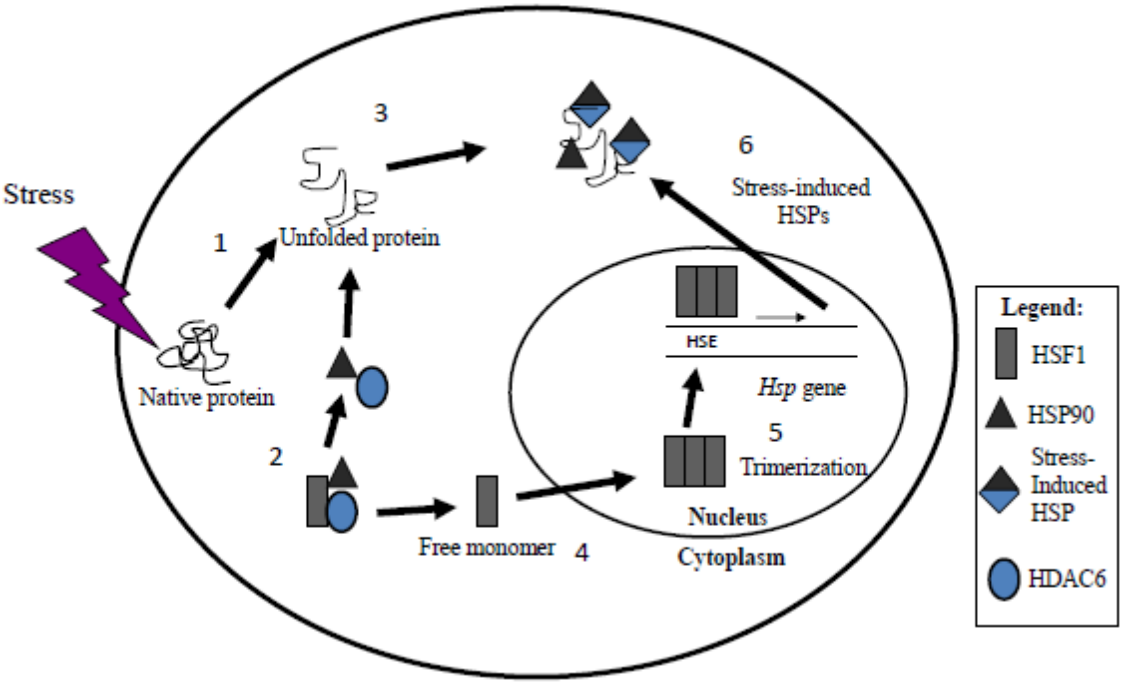
Stress
1
Native protein
Unfolded protein
3
2
Free monomer
4
HSE
Hsp gene
5
Trimerization
Nucleus
Cytoplasm
6
Stress-induced HSPs
Legend:
HSF1
HSP90
Stress-Induced HSP
HDAC6

ERAD along with the resident molecular chaperones present in ER provide a quality control system that ensures unfolded proteins do not accumulate in the ER. If unfolded proteins continue to accumulate in the ER, then the cell activates the UPR, which is mediated by three transmembrane receptors: activating transcription factor 6 (ATF6), inositol-requiring kinase 1 (IRE1) and double-stranded RNA-activated protein kinase (PKR)-like endoplasmic reticulum kinase (PERK; Malhi and Kaufman, 2011). These proteins are normally bound to and inactivated by BiP, an ER-resident molecular chaperone of the HSP70 family. In the presence of an increased amount of misfolded proteins in the ER, BiP dissociates from the transmembrane proteins and associates itself with the exposed hydrophobic surfaces of the unfolded/misfolded proteins allowing for the activation of PERK, ATF6 and IRE1 (Fig. 3; Chakrabarti et al., 2011). The PERK pathway causes translational attenuation through the phosphorylation of eIF2α and transduces both pro- and anti-apoptotic signals. Subsequently, ATF6 activation, due to dissociation of BiP from ATF6, results in the translocation of ATF6 to the Golgi, where it is cleaved from the membrane anchor (Chen et al., 2002). The released ATF6 translocates to the nucleus and binds promoters containing the ER stress response element (ERSE) thus upregulating genes encoding molecular chaperones such as BiP and proteins involved in the ERAD pathway (Fig. 3; Adachi et al., 2008).

1.5 Ubiquitin-proteasome system

The ubiquitin-proteasome system (UPS) is the principle mechanism used by all cells to degrade proteins and maintain protein homeostasis in the cell. It is essential for many fundamental processes in the cell including cellular differentiation, cell cycle progression, proliferation and apoptosis (Mani and Gelmann, 2005; Landis-Piwowar et al., 2006).

Figure 3. The Unfolded protein response. 1) Native proteins in the ER unfold under stressful conditions. 2) BiP bound to ATF6 in the ER membrane is released and binds unfolded proteins. 3) This allows the dimerization of ATF6 and cleavage of its transcription factor domain (TFD). 4-5) TFD migrates to the nucleus and causes an up-regulation of ATF6 target genes including the *bip* gene. 6) Proteins that cannot be refolded are targeted for degradation through the ER-associated degradation (ERAD) pathway.

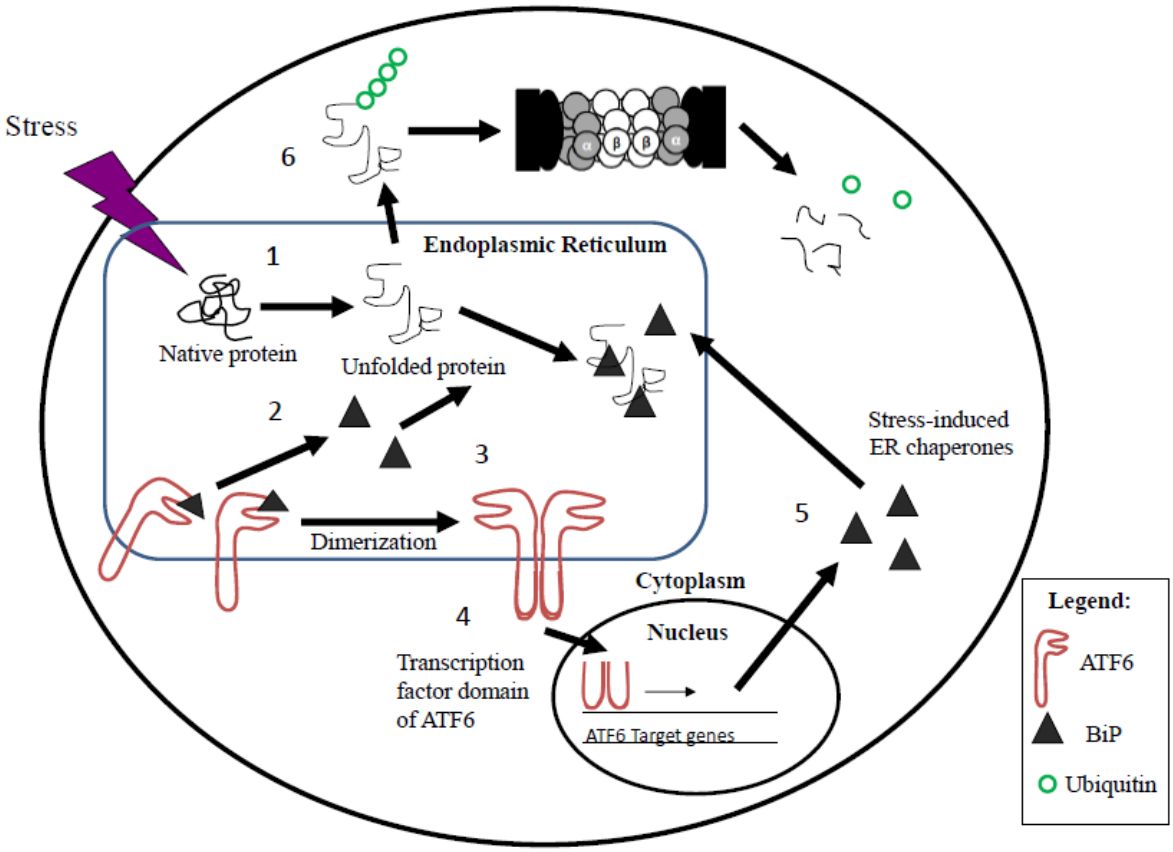
Stress
6
Endoplasmic Reticulum
1
Native protein
Unfolded protein
2
3
Dimerization
Stress-induced
ER chaperones
5
Cytoplasm
Nucleus
4
Transcription
factor domain
of ATF6
ATF6 Target genes
Legend:
ATF6
BiP
Ubiquitin

The pathway is broken down into two successive steps: the addition of ubiquitin molecules to proteins targeted for degradation followed by their degradation by the 26S proteasome (Fig. 4A; Yang et al., 2008).

1.5.1 Protein ubiquitination

Ubiquitin is a 76 amino acid protein that serves as a marker for proteasome degradation when it is attached to lysine residues of a targeted protein. The process of ubiquitination is controlled by a set of ubiquitin-activating and -conjugating enzymes (E1-E4; Yang et al., 2008; Lehman, 2009). First, ubiquitin-activating enzyme (E1) activates ubiquitin in an ATP-dependent manner through the adenylylation and formation of a thiol-ester bond at its C-terminus. Subsequently, ubiquitin is transferred to a cysteine residue within one of several distinct ubiquitin-conjugating enzymes (E2). With the aid of a third enzyme, an E3 ubiquitin ligase, ubiquitin is transferred to a lysine residue of a substrate protein. This mechanism continues until the substrate protein is polyubiquitinated (Hershko and Ciechanover, 1998). E4 enzymes facilitate the formation of these polyubiquitin chains (Koegl et al., 1999). Following, ubiquitination, the substrate protein is then delivered by ubiquitin receptor proteins to the proteasome.

1.5.2 The Proteasome

The 26S proteasome is a complex of multiple protein subunits containing a 19S regulator and a 20S proteolytic core (Gallastegui and Groll, 2010; Figure 4B). The 19S

Figure 4. Ubiquitin proteasome system. A) Unfolded protein is targeted for degradation by ubiquitin-conjugating enzymes that create a polyubiquitin chain and attach it to the lysine residues. The ubiquitinated protein is then cleaved into polypeptides by the 26S Proteasome and the ubiquitin molecules are recycled. B) The structure of 26S Proteasome containing 19S regulatory subunit and the 20S proteolytic core consisting of 2 α and 2 β rings. (Adapted from Lee and Goldberg, 1998).

A

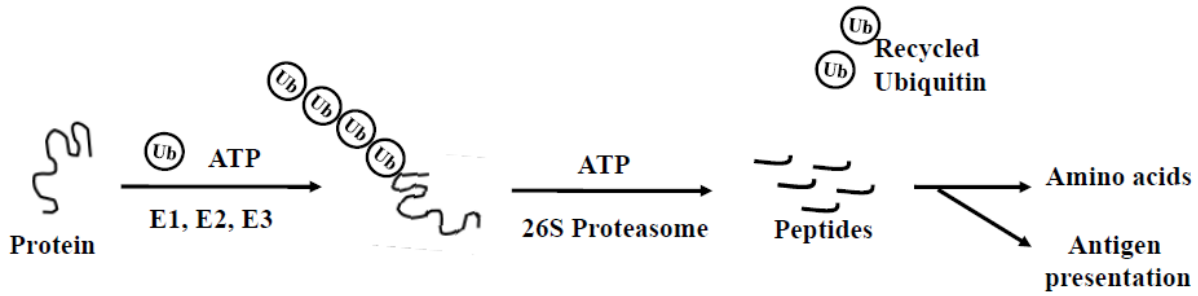
Ub
Ub
Ub
Ub
Ub
Recycled
Ubiquitin
Ub
ATP
E1, E2, E3
Protein
ATP
26S Proteasome
Peptides
Amino acids
Antigen
presentation

B

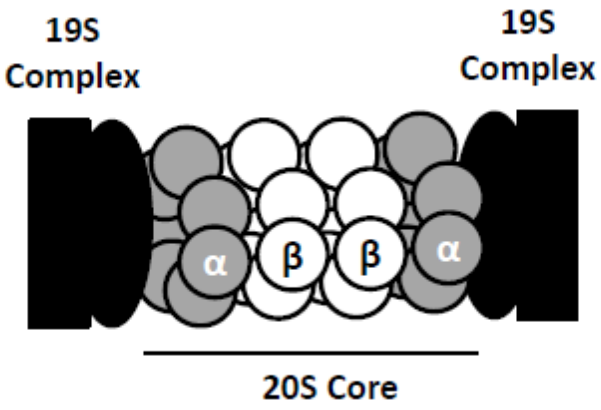
19S
Complex
19S
Complex
α
β
β
α
20S Core

regulator serves to control which proteins will be degraded by identifying ubiquitinated proteins and then subsequently deubiquitinating them and passing them onto the 20S catalytic core for degradation. The 20S proteolytic core contains chymotrypsin-like (CT-like), trypsin-like (T-like) and peptidyl-glutamyl peptide hydrolyzing-like (PGPH-like) peptidases (Murata et al., 2009; Sahara et al., 2014). The 20S core degrades proteins into oligopeptides and ubiquitin is released and recycled.

1.5.3 Proteasome inhibitors

Proteasomal inhibition was shown to have a number of cellular effects including an increase in ubiquitinated protein, a decrease in the rate of protein hydrolysis and disruption of protein homeostasis (Yang et al., 2008). In mammalian systems, proteasome inhibition induced HSP70 in canine kidney cells, HSP27, HSP60, HSP70 and HSP90 in neonatal rat cardiomyocytes, HSP72 in caco-2 cells, and HSP27 and αB crystallin in murine lens epithelial cells (Bush et al., 1997; Stangl et al., 2002; Pritts et al., 2002; Awasthi and Wagner, 2005). Inhibition of the ubiquitin-proteasome pathway has been associated with a variety of neurological and protein-misfolding diseases including Alzheimer's, Parkinson's and Huntington's Disease (Masilah et al., 2000; Ross and Pickart, 2004; Jankowska et al., 2013; Lee et al., 2013).

1.5.3.1 MG132

Carbobenzoxy-leucyl-L-leucyl-L-leucinal (Fig. 5A), more commonly known as MG132, is a peptide aldehyde and functions as a reversible inhibitor of the 26S proteasome (Rock et al., 1994; Lee and Goldberg, 1998; Guo and Peng, 2013). MG132 inhibits the 20S

proteasome activity by covalently binding to the active site of the β-subunits and effectively blocking proteolytic activity. MG132 has become a widely employed research tool due to study the impact of proteasomal inhibition on various cellular processes including the upregulation of the heat shock and unfolded protein response. For example, MG132 was shown to increase levels of HSP70 and induce the unfolded protein response in a dopaminergic neuronal N27 cell line (Xiong et al., 2013). Additionally, this study also demonstrated the formation of aggresome-like inclusion bodies when cells were incubated for an extended time with MG132 and that they were cleared through the autophagy-lysosomal pathway. Moreover, Park et al. (2011) demonstrated that MG132-induced apoptosis in human Jurkat T cells via ER-stress mediated apoptotic pathway and also upregulated UPR-related chaperones such as BiP. This was also confirmed in human colon cancer cells as MG132 treatment resulted in ER stress (Williams et al., 2013). Additionally, MG132 treatment of mouse embryonic fibroblasts resulted in the activation of HSF1 and resulted in the transcription of *hsp* genes (Lecomte et al., 2013). Microarray analysis of heat shock and MG132 induced-HSP accumulation in a mouse fibrosarcoma cell line suggested multiple pathways such as cytokine induction, extracellular matrix remodelling in addition to the heat shock response that might be activated (Kim et al., 2011). Recently, Kastle et al. (2012) demonstrated that MG132 enhanced the accumulation of HO-1 in human fibroblast cells and this phenomenon was mediated by means of the p38MAPK pathway and Nrf-2.

1.5.3.2 Celastrol

Celastrol (3-Hydroxy-9β,13α-dimethyl-2-oxo-24,25,26-trinoroleana-1(10),3,5,7-tetraen-29-oic acid) is a quinone triterpene (Fig. 5C). It is extracted from the root of a plant

belonging to the *Celastraceae* family of plants that has been used for hundreds of years in traditional Chinese medicine to treat rheumatoid arthritis, bacterial infections and fever (Westerheide et al., 2004). Interestingly, it was found that celastrol suppressed protein aggregates and toxicity in HeLa cells expressing polygutamine aggregates (Zhang and Sarge, 2007). Also, celastrol treatment improved brain function and provided neuroprotection in rat models for Huntington's, Parkinson's and amyotrophic lateral sclerosis (ALS) diseases (Kiaei et al., 2005; Cleren et al., 2005). Previous studies examining celastrol demonstrated that it inhibits the CT-like activity of the 26S proteasome by associating with the β5 subunit of the proteasome (Yang et al., 2006). In mammalian cells, celastrol was determined to inhibit proteasome activity and induce *hsp* accumulation (Westerheide et al., 2004; Yang et al., 2006; Trott et al., 2008; Wang et al., 2011). This inhibition of the proteasome was suggested as a major contributor to celastrol's effectiveness in inducing apoptosis in cancer cells (Salminen et al., 2010).

1.5.3.3 Withaferin A

Withaferin A (WA) is a steroidal lactone that is extracted from the roots of Ashwaganda (*Withania somnifera*), a plant that has been used extensively in Aryuvedic Indian medicine for centuries (Mandal et al., 2008). Its IUPAC name is (4β,5β,6β,22R)-4,27-Dihydroxy-5,6:22,26-diepoxyergosta-2,24-diene-1,26-dione. Previously, WA was shown to inhibit angiogenesis by preventing activation of NF-κB as well as having anti-tumor activity (Mohan et al., 2004; Malik et al., 2007; Yang et al., 2007; Mandal et al., 2008). Additionally, WA inhibited CT-like activity of the purified rabbit 20S proteasome and 26S proteasome in human prostate cancer cells *in vitro* and *in vivo*, respectively (Yang et al., 2007).

Figure 5. Structures of selected proteasomal inhibitors. A) MG132. B) withaferin A. C) celastrol.

A

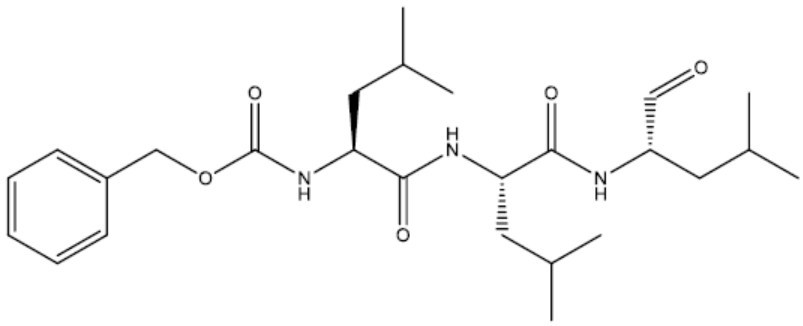

B

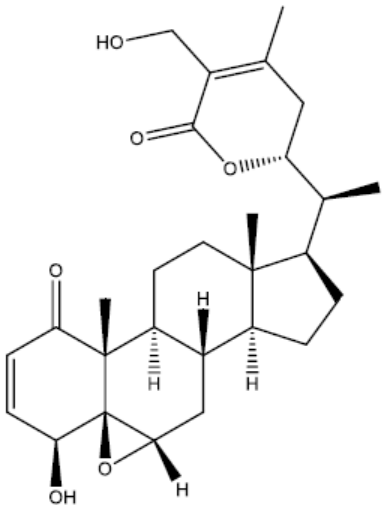

C

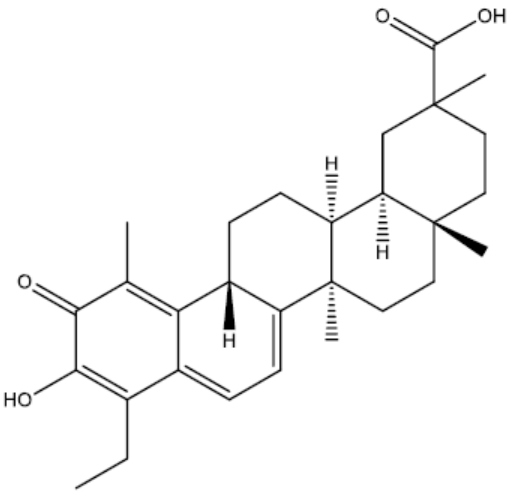

Molecular docking results indicated that withaferin A (Fig 5B) bound to the active N-terminal Thr1 residue of the β5 subunit of the 20S proteasome. Recently, it was shown that inhibition of HSP90 in WA-treated cells resulted in an increase accumulation of HSP70 (Yu et al., 2010). Also, Santagata et al. (2012) showed that the α, β unsaturated carbonyl with potential for high thiol reactivity was essential for WA-induced HSP accumulation in glioma tumour cells. More recently, WA-associated cytotoxicity in glioblastomas involved the induction of the heat shock response through oxidative stress and by altering the MAPK signalling pathway (Grogan et al., 2013). Finally, several studies demonstrated that withaferin A treatment resulted in activation of the MAP kinases p38 and JNK (Mandal et al., 2008; Oh et al., 2008).

1.6 Chemical stressors

1.6.1 Arsenic

Arsenic is a chemical stressor that is abundantly present in the environment in a variety of forms including arsenite and contributes to renal, cardiovascular and hepatic diseases worldwide (Del Razo et al., 2001). Arsenic exposure has been associated with a variety of cancers that affect major organs including liver, lungs, kidney, bladder and skin. At the cellular level, arsenic in the form of arsenite was shown to induce cytoskeletal collapse, apoptosis, metabolic abnormalities and oxidative stress (Li and Chou, 1992; Liu et al., 2001; Bode and Dong, 2002). Previously, arsenite also substituted for phosphate in cells and affected cellular processes such as DNA replication and ATP synthesis (Del Razo et al., 2001). Additionally, arsenite induced toxicity at the cellular level through the production of reactive oxygen species and generation of free radicals, which induced oxidative damage to

proteins. An increase in the relative levels of unfolded or damaged proteins caused by arsenite led to the activation of HSF1 and the accumulation of HSPs (Voellmy, 2004; Khalil et al., 2006; Guo et al., 2011). Recent mammalian studies demonstrated that arsenite acted as a proteasome inhibitor since it inhibited CT-like activity of the proteasome and increased relative levels of ubiquitinated proteins (Tsou et al., 2005; Medina-Diaz et al., 2009).

1.6.2 Cadmium

Cadmium is a toxic heavy metal that has been identified as a human carcinogen. It tends to accumulate in the human body, primarily in the kidney, due to anthropogenic sources (Mendez-Armenta and Rios, 2007). Waisberg et al. (2003) reported that cadmium can cause cancers of the lung, prostate and pancreas due to inhalation of tobacco smoke, contaminated food and air pollution. At the cellular level, cadmium induced the production of reactive oxygen species, reacted with thiol groups to denature proteins and substituted for zinc to form abnormally folded proteins (Waisberg et al., 2003; Galazyn-Sidorczuk et al., 2009). Additionally, cadmium was shown to inhibit proteasome activity and disrupt E-cadherin mediated cell adhesion (Joseph et al., 2001; Yu et al., 2008). Cadmium was also found to induce *hsp* and metallothionein expression (Bonham et al., 2003; Liu et al., 2006; Mouchet et al., 2006; Blechinger et al., 2007). Prolonged exposure to cadmium also resulted in enhanced accumulation of HSPs in renal epithelial cells and rat liver cells (Goering et al., 1993; Bonham et al., 2003).

1.7 RNA stress granules

Stress or RNA granules are cytoplasmic foci composed of untranslated mRNA, RNA binding proteins such as T-cell intracellular antigen (TIA), polyA-binding protein (PABP), small ribosomal subunits and a complex assembly of initiation factors (Thomas et al., 2011). These complexes, which are usually 0.1 to 2 μm in size, form in cells exposed to adverse environmental conditions causing translation initiation inhibition via the phosphorylation of eIF2α (Zurla et al., 2011). Stress granules have been hypothesized to stabilize and protect mRNA during times of stress (Buchan and Parker, 2009). Stress granule assembly is thought to occur by phosphorylation of eIF2α and is activated by distinct eIF2α kinases depending on the stress (Kedersha et al., 1999). Stress granules have yet to be purified from stressed cells and are only identified by markers such as mRNA-binding proteins TIA1, PABP or G3BP (Anderson and Kedersha, 2006).

Previously it was shown that proteasomal inhibition induced the formation of stress granules in HeLa and human embryonic kidney 293 cells by phosphorylating eIF2α via the general control nonderepressable 2 (GCN2) stress kinase (Mazroui et al., 2007). Recently, Fournier et al. (2010) demonstrated that another proteasomal inhibitor and chemotherapeutic agent, bortezomib, also induced the formation of stress granules in HeLa cells. Additionally, it was recently discovered that HDAC6 plays a critical role in stress granule assembly and inhibition of HDAC6 activity resulted in abolishment of stress granule formation (Kwon et al., 2007). Moreover, stress granule formation is thought to occur by movement of components via the microtubule network to the perinuclear region in the cytoplasm since disruption of the microtubule network inhibited stress granule formation (Ivanov et al., 2003; Kwon et al., 2007).

1.8 Aggresomes

Aggresomes are specialized cellular structures containing misfolded, ubiquitinated proteins in a cage of intermediate filaments and cytoskeletal proteins such as vimentin (Johnson et al., 1998). Aggresome formation results in response to a variety to stressors that induce a high number of misfolded proteins. Misfolded proteins tend to aggregate and travel to perinuclear regions on microtubule networks since studies have shown that aggresome formation was blocked by drugs, such as nocodazole, that depolymerize microtubules (Garcia-Mata et al., 1999; Kopito, 2000). While aggresome composition tends to vary based on cell type, common components are present and serve as markers including vimentin and γ-tubulin. Various studies reported that molecular chaperones such as HSP27, αB crystallin, HSP40 and HSP70 may be involved in the formation of aggresome (Ito et al., 2002; Zhang and Qian, 2011).

Aggresomes have a cytoprotective function by becoming cytoplasmic recruitment centers for misfolded, damaged or mutated proteins (Taylor et al., 2003) For example, Taylor et al. (2003) demonstrated that aggresomes assisted in the rapid turnover of polyglutamine-aggregates, which was slowed down by inhibiting the formation of aggresomes. Various stressors were found to induce aggresome formation in mammalian systems (Ito et al., 2002; Song et al., 2008; Bolhuis and Richter-Landsberg, 2010; Jacobson et al., 2012; Taylor et al., 2012; Xiong et al., 2013). For example, proteasome inhibition induced aggresome formation in human embryonic kidney cells, oligodendroglia and glioma cells (Ito et al., 2002; Taylor et al., 2012). Also, sodium arsenite and cadmium chloride induced the formation of

aggresomes in kidney and yeast cell lines (Heir et al., 2006; Song et al., 2008; Jacobson et al., 2012).

1.9 *Xenopus laevis* as a model organism

The South African clawed frog, *Xenopus laevis*, has been used extensively as a model system in various research areas including vertebrate development. The large size (1.1 mm in diameter) of the *Xenopus* oocyte/eggs facilitated the in vivo analysis of microinjected DNA, mRNA and protein (Etkin, 1982; Ovsenek et al., 1990; Tam and Heikkila, 1995; Sive et al., 2010; Heikkila, 2010; Moody, 2012). In fact, it was the first in vivo system in which heterologous promoter/gene constructs were expressed. Also, pioneering work with *Xenopus* embryos by various researchers including the Nobel Laureate, Dr. John Gurdon, successfully cloned *Xenopus* animals by transferring somatic nuclei into enucleated eggs. In developmental studies, *X. laevis* eggs can be externally fertilized and the embryos develop rapidly at room temperature. Furthermore, many *X. laevis* genes have been isolated and characterized. As aquatic animals, *Xenopus* have a high tolerance for dynamic environmental conditions and possess physiological traits that are common to most vertebrates thus ensuring that data collected through these systems is applicable to mammals (Burggren and Warburton, 2007).

1.9.1 A6 kidney epithelial cell line

Xenopus continuous cell lines are useful tools for *in vitro* molecular analyses. A number of *Xenopus* cell lines have been developed over the years including A6, B3.2, KR, XF, XL2, XL110, XL-177 and XTC-2 (Smith and Tata, 1991). The most popular cell line

used today is the A6 somatic cell line, which was also used in the present study. The *X. laevis* A6 kidney epithelial cell line was isolated from the renal uriniferous tubules of the adult male *Xenopus* by Rafferty (1968). It is easy to maintain and has a quick doubling time, making it an ideal tool for cellular and molecular biology research. Unlike other untransformed *Xenopus* cell lines, A6 cells continue to divide after reaching confluency. The A6 kidney epithelial cell line has been used widely in diverse areas of research, from genetic profiling under zero gravity to the function of Cystic Fibrosis transmembrane conductance regulator channels and the role of renal epithelial sodium channels in hypertension (Guerra et al., 2004; Ikuzawa et al., 2007; Wang et al., 2009).

Additionally, the induction of the heat shock response following exposure to environmental stressors such as heat shock, sodium arsenite, hydrogen peroxide and cadmium chloride has been well characterised in *X. laevis* A6 kidney epithelial cells (Ohan et al., 1998; Phang et al., 1999; Muller et. al, 2004; Gellalchew and Heikkila, 2005; Woolfson and Heikkila, 2009; Heikkila, 2010; Brunt et al., 2011; Khamis and Heikkila, 2013). Furthermore, proteasomal inhibitors such as lactacystin, MG132, celastrol and curcumin were shown to inhibit chymotrypsin (CT)-like activity of the proteasome, enhance the relative levels of ubiquitinated protein and induce accumulation of HSPs in A6 cells (Young and Heikkila, 2010; Walcott and Heikkila, 2010; Khan and Heikkila, 2011). Finally, sodium arsenite and cadmium chloride were found to inhibit proteasome function since these stressors inhibited CT-like activity and enhanced accumulation of ubiquitintated proteins in A6 cells (Brunt et al., 2012).

1.9.2 *Xenopus laevis* HSP30 family

HSP30 is a member of the sHSP superfamily of molecular chaperones. All of the *hsp30* gene family members examined to date, except *hsp30E* for which there is only a partial sequence, are intronless and denoted *hsp30A-E*. *Hsp30A* and *hsp30B* genes were first identified by Bienz (1984). However, *hsp30A* contained an insertional mutation with a stop codon in the coding region producing only a 10 kDa protein. The *hsp30B* gene contained a frameshift mutation and was considered a pseudogene. *Hsp30C* and *hsp30D* were isolated and completely sequenced by Krone et al. (1992) and encoded 24 kDa proteins (Krone et al., 1992). Only the promoter and the N-terminal coding region of *hsp30E* were isolated. Analysis of the HSP30 amino acid sequence revealed the presence of a C-terminal α-crystallin domain (ACD) flanked by poorly conserved N-terminal region and C-terminal extension. HSP30 is the dominant stress-inducible sHSP in *Xenopus* and has counterparts in birds, fish and other frogs but not in mammals as mentioned previously. *Xenopus* HSP27 is a homolog of the human HSP27 and has only 19 % sequence identity with *Xenopus* HSP30C as mentioned previously (Tuttle et al., 2007). Similarly, in the minnow, HSP27 shared greater identity with human and avian HSP27 than with HSP30 (Norris et al., 1997). This suggested that the HSP30 and HSP27 families of proteins are unique. Extensive immunoblot and immunocytochemical analyses did not detect the presence of *hsp27* mRNA or HSP27 protein in *Xenopus laevis* A6 cells (Gauley and Heikkila, unpublished data).

Initial studies determined that heat shock-induced *hsp30* genes were developmentally regulated. During embryogenesis, *hsp30C* was first heat-inducible at the late neurula/early taildbud stage of *Xenopus* development, while *hsp30D* was not heat-inducible until midtailbud (Heikkila, 2003). In contrast, *Hsp90*, *Hsp70* and *Hsp47* genes were heat shock-

inducible after the midblastula stage (Ali et al., 1996a; Ali et al., 1996b; Lang et al., 2000; Hamilton and Heikkila, 2006; Heikkila, 2010). In *X. laevis* A6 kidney epithelial cells, various stresses including heat shock, sodium arsenite, herbimycin A, cadmium and hydrogen peroxide were found to induce *hsp30* gene expression (Briant et al., 1997; Ohan et al., 1998; Phang et al., 1999; Muller et al., 2004; Woolfson and Heikkila, 2009; Young et al., 2009; Khamis and Heikkila, 2013). Immunocytochemical analysis of A6 cells revealed that heat shock or sodium arsenite-induced HSP30 accumulation occurred primarily in the perinuclear region in a granular or punctate pattern (Gellalchew and Heikkila, 2005). Interestingly, exposure of A6 cells to concurrent mild sodium arsenite and heat stress greatly enhanced *hsp30* gene expression compared to each stressor individually (Young et al., 2009). Recent studies determined that proteasomal inhibitors, such as lactacystin, MG132, celastrol and curcumin, induced HSP30 accumulation in A6 cells (Young and Heikkila, 2010; Walcott and Heikkila, 2010; Khan and Heikkila, 2011). Immunocytochemical analysis revealed that these proteasomal inhibitors induced the formation of large HSP30 cytoplasmic structures (Young and Heikkila, 2010; Khan and Heikkila, 2011). It was hypothesized that these large HSP30 structures might be stress granules or aggresomes.

HSP30C and HSP30D were determined to function as molecular chaperones since they inhibited heat-induced target protein aggregation and maintained heat- or chemically-denatured luciferase in a folding competent state (Fernando and Heikkila, 2000; Fernando et al., 2002; Abdulle et al., 2002). For example, *Xenopus* HSP30C and HSP30D prevented heat- and chemically-induced aggregation of citrate synthase in an ATP-independent fashion (Fernando and Heikkila, 2000; Abdulle et al., 2002). Additionally, site-specific mutagenesis also revealed that the C-terminal region was essential for proper HSP30 folding and optimal

chaperone activity (Fernando and Heikkila, 2000; Abdulle et al., 2002; Fernando et al., 2002). Finally, Fernando et al. (2003) demonstrated that HSP30 was phosphorylated *in vivo* by the p38 MAPK pathway during recovery from stress and resulted in production of smaller oligomeric structures and inhibition of molecular chaperone activity.

1.9.3 *Xenopus laevis* HSP70 family

The *Xenopus* HSP70 family consists of constitutively expressed HSC70, stress-inducible HSP70, mitochondrial HSP70 (mtHSP70) and BiP. Members of the stress-inducible HSP70 family were first isolated from *Xenopus* by Bienz (1984). Coding regions of *hsc70.I, hsc70.II* and *bip* genes were isolated and characterized in our laboratory (Ali et al., 1996a; Ali et al., 1996b; Miskovic et al., 1997).

1.9.3.1 *Xenopus laevis* HSP70

Several studies demonstrated that *hsp70* mRNA and protein were present constitutively during *Xenopus* oogenesis (Bienz, 1984; Davis and King, 1989, Horrell et al., 1987). *Hsp70A* and *Hsp70B* transcripts were maintained throughout oocyte maturation, fertilization and cleavage. During development *hsp70* mRNA was first heat inducible after the midblastula transition (MBT), which marks the activation of the zygotic genome (Krone and Heikkila, 1988; Ovsenek and Heikkila, 1990). Additionally, whole mount *in situ* hybridization, which was employed to detect the spatial pattern of heat-inducible *hsp70* mRNA in embryos, determined that it accumulated in a tissue-specific manner in embryos after the midblastula stage (Lang et al., 2000). As found with HSP30, HSP70 accumulation in A6 cells was induced in response to a variety of stressors including heat shock, sodium

arsenite, cadmium and proteasomal inhibitors including MG132, lactacystin, celastrol and curcumin (Heikkila, 2004, Woolfson and Heikkila, 2009; Young et al., 2009; Young and Heikkila, 2010; Walcott and Heikkila, 2010; Khan and Heikkila, 2011; Khamis and Heikkila, 2013).

1.9.3.2 *Xenopus laevis* BiP

Xenopus BiP shared greater amino acid sequence identity with BiP from other vertebrates than with *Xenopus* HSP70 (Miskovic et al., 1997). Analysis of the protein domains of *Xenopus* BiP determined that it contained an N-terminal ATPase domain, similar to HSP70, as well as a C-terminal KDEL (ER-retention signal sequence). In developmental studies, northern blot and immunoblot analyses determined that constitutive levels of *bip* mRNA and BiP protein were present in unfertilized eggs and at all developmental stages examined (Winning et al., 1989; 1991; Miskovic and Heikkila, 1999). This was confirmed by whole mount *in situ* hybridization experiments, which detected *bip* mRNA across the surface of the gastrula embryo while in neurulae it was present in the neural folds, neural plate and around the blastopore (Miskovic and Heikkila, 1999). In neurula and later stages, *bip* mRNA accumulation was enhanced after treatment with the calcium ionophore, A23187 and tunicamycin. Also, constitutive levels of *bip* mRNA were detected in all adult tissues examined (Miskovic et al., 1997). Finally, in *Xenopus* A6 cells, *bip* mRNA was detected constitutively and enhanced by tunicamycin, dithiothreitol and A23187 (Miskovic et al., 1997).

1.10 Research objectives

While much is known about stress-induced sHSP regulation and function in mammals, less is known about these molecular chaperones, such as HSP30, in *Xenopus* laevis. The primary question that I wanted to address in this thesis was whether *Xenopus* HSP30 multimeric complexes associated with aggresomes and/or stress granules in A6 kidney epithelial cells. The present study has focused on an examination of the relative levels of HSP30 and HSP70 during recovery from heat stress as well as the intracellular localization and possible function of proteasomal inhibitor-induced HSP30 in *Xenopus laevis* A6 kidney epithelial cells. Furthermore, this thesis has investigated, for the first time inA6 cells, the formation of stress granules and aggresomes and their possible association with HSP30 multimeric complexes. The specific questions that were examined in the thesis are as follows:

1) What are the relative levels of HSP30 and HSP70 accumulation in A6 cells during recovery from heat shock?
2) Is the p38 MAPK pathway involved in the formation of HSP30 multimeric complexes during recovery from thermal stress?
3) What effect do proteasome inhibitors (MG132, withaferin A, celastrol, cadmium and arsenite) have on HSP30, HSP70, BiP, GRP94 and heme oxygenase-1 accumulation?
4) Do stress-induced stress (RNA) granules and/or aggresomes form in A6 cells in response to proteasomal inhibitors?
5) Is there an association of large HSP30 multimeric complexes with stress granules and/or aggresomes in A6 cells treated with proteasomal inhibitors?

Chapter 2: Experimental Procedures

2.1 Maintenance and treatment of *Xenopus laevis* A6 kidney epithelial cells

X. laevis A6 cells were obtained from the American Type Culture Collection (ATCC, Rockville, MD) and were grown in 70 % Leibovitz L-15 Media containing 10 % (v/v) fetal bovine serum (100 U/ml) and 1 % penicillin/streptomycin (100 units penicillin, 100 µg/ml streptomycin; all purchased through Sigma-Aldrich, Oakville, ON) at 22 °C in T75 cm^2 BD falcon culture flasks (BD Biosciences, Mississauga, ON). Upon confluency, cells were washed with 1 ml of versene [0.02 % (w/v) KCl, 0.8 % (w/v) NaCl, 0.02 % (w/v) KH_2PO_4, 0.115 % (w/v) Na_2HPO_4, 0.02 % (w/v) sodium ethylenediaminetetra-acetic acid (Na_2 EDTA)], followed by a 1 min incubation with 2 ml of fresh versene. Then 1 ml of 1X trypsin (Sigma-Aldrich) diluted in 100 % Hank's Balanced Salt Solution (HBSS; Sigma-Aldrich) was added until cells began to detach from the flask. Ten ml of fresh L-15 media was then added to the detached cells. The cell suspension was then divided evenly into additional flasks. Cell treatments were performed 2 days after cell passaging to allow the cells to reach 90-100 % confluence.

For initial set of experiments, cells were heat shocked in a water bath set at 33 °C for 2 h and allowed to recover at 22 °C. Flasks of cells were treated either before for 2 h or after heat shock for the duration of the treatment with 100 µM cycloheximide (dissolved in water; Sigma-Aldrich), 10 µM SB203580 (dissolved in dimethyl sulfoxide (DMSO); Sigma-Aldrich) or 30 µM MG132 (carbobenzoxy-L-leucyl-L-leucyl-L-leucinal dissolved in DMSO; Sigma-Aldrich; Young and Heikkila, 2010). For the study of ER and cytosolic molecular chaperones as well as presence of aggresomes or stress granules, cells were either maintained at 22 °C containing the vehicle, DMSO (Control cells) or treated with 7 µM A23187

(dissolved in DMSO; Sigma-Aldrich), 30 μM MG132, 2.5 μM celastrol (dissolved in DMSO; Cayman Chemical, Ann Arbor, MI, USA; Walcott and Heikkila, 2010) or 5 μM withaferin A (dissolved in DMSO; Enzo Life Sciences, Plymouth Meeting, PA) at 22 °C for periods of time ranging from 2 to 24 h. Cells were rinsed using 65 % HBSS and removed via scraping in 1 ml of 100 % HBSS. Cells were centrifuged at 21,920 x g for 1 min and the resulting pellets were stored at -80 °C until protein or RNA isolation.

2.2 Cell-based proteasome assay

To evaluate the effect of A23187, celastrol, withaferin A or MG132 on proteasomal activity in A6 cells, The Proteasome-Glo Chymotrypsin-Like cell based luminescent assay kit was obtained from Promega (Promega, Madison, WI). Proteasome-Glo Cell-Based Reagents each contain a specific luminogenic proteasome substrate (Suc- Leu-Leu-Val-Tyr-Glo substrate for chymotrypsin-like activity) in a buffer optimized for cell permeabilization, proteasome activity and luciferase activity. The proteasome cleavage generates an aminoluciferin substrate that is consumed by luciferase to produce a luminescent signal at a rate proportional to proteasome activity. Proteasome-Glo™ Cell-Based Buffer and Luciferin Detection Reagent were equilibrated to room temperature in the dark and mixed with the Suc-Leu-Leu-Val-Tyr-aminoluciferin (Suc-LLVY-aminoluciferin) substrate to produce the Proteasome-Glo™ Reagent, which was used to detect the chymotrypsin-like activity. Flasks of A6 cells were treated with 7 μM A23187 or 30 μM MG132 for 24 h, or 2.5 μM celastrol or 5 μM withaferin A for 18 h. After treatments, cells were washed with 2 mL of versene and then with 1 mL of 1X trypsin until the cells began to detach from the T75 cm^2 BD falcon culture flask. Nine ml of fresh L-15 media was then added to the flask and the media was

pipetted up and down to rinse the flask surface and allow for even distribution. The cell suspension was then removed from the flask and placed into a 15 mL falcon tube. Cells were pelleted at 4 °C by gentle centrifugation at 2,400 x g for 5 min. Following centrifugation excess media was removed and pellets were washed in 5 mL of fresh L-15 media and then centrifuged again at 2,400 x g for 5 min at 4 °C. A6 cells were then resuspended in 5 mL of fresh L-15 media. For each sample, the total number of cells per mL was determined using a Bright-Line haemocytometer (Hausser Scientific, Horsham, PA).

Approximately 15,000 cells per well were added to white-walled 96 well plates along with an L-15 blank. Proteasome-Glo™ Reagent was allowed to reach room temperature before being added to the 96-well plate in a 1:1 ratio (100 µL sample: 100 µL reagent). The contents of the plate were then mixed for 2 min on the shaker and allowed to incubate at room temperature for 45 min before detection of luminescence. The luminescence of each sample was measured using the Victor^3 luminometer (Perkin Elmer Inc., Waltham, MA) containing a filter set at 340/480 nm. Values were then compared to a blank control (Proteasome-Glo cell-based reagent + L-15 media) and a no-treatment control (Proteasome-Glo cell-based reagent + L-15 containing DMSO). Measurements were repeated 3 times and statistical analysis was performed through analysis of variance (ANOVA) followed by Tukey's Multiple comparison post-test.

2.3 Antisense riboprobe production

2.3.1 *Hsp30C, hsp70, bip* and *eIF1α* template construction

The open reading frame of the *hsp30C* gene was previously inserted into the pRSET expression vector (Invitrogen, Carlsbad, California) by Pasan Fernando (Fernando and

Heikkila, 2000). The coding region of *hsp70* genomic DNA was previously isolated (Lang et al., 2000) and inserted into the plasmid pSP72 (Promega, Nepean, Ontario). The BiP cDNA was cloned into the *Xho*I and *Eco*RI sites of pBluescript KS+ (Gibco/BRL Laboratories, Burlington, ON) (Miskovic *et al*, 1997). The eIF1α cDNA clones (Genbank accession No. BG160504) in pCMV-Sport6 vectors (Invitrogen Life Technologies, Frederick, MD) were obtained from the ATCC. Plasmids containing the *hsp30C, hsp70, bip* and *eIF1α* insert were transformed into *Escherichia coli* DH5α cells (Fig. 6). Individual colonies were inoculated into 15 mL centrifuge tubes and grown overnight in 5 mL of LB broth [1% (w/v) tryptone-peptone, 0.5% (w/v) yeast extract, 1% (w/v) NaCl, pH 7.5] containing 100 μg/mL ampicillin (Bioshop, Burlington, Ontario) at 37 ºC.

2.3.2 Plasmid isolation and *in vitro* transcription

Bacterial cells were pelleted in a centrifuge at 2,400 x g for 10 min at 4 ºC. Plasmid DNA was isolated using phenol: chloroform extraction and re-suspended in 50 μL distilled water and stored at -20 °C. The plasmid containing the *hsp30C, hsp70, bip* or *eIF1α* insert as mentioned above was linearized using the PvuII, MluNI, BamHI or SmaI restriction enzyme, respectively (Figure 6, Roche, Indianapolis, IN). *In vitro* transcription was used to generate digoxygenin (DIG)-labelled riboprobes. Each *in vitro* transcription reaction contained 4 μL of linearized DNA template, 4 μL of rNTP mix [2.5 mM rGTP, 2.5 mM rATP, 2.5mM rCTP, 1.625 mM rUTP (Promega), 0.875 mM DIG-11-UTP (Roche), 1.5 μL diethylpyrocarbonate (DEPC)-treated water, 4 μL of 100 mM dithiothreitol to a final concentration of 20 mM (Promega), 4 μL of 5X transcription buffer to a final concentration of 1X (Fermentas, Burlington, Ontario), 0.5 μl Rnase inhibitor (Fermentas) and 40 U of SP6 RNA polymerase

Figure 6. Templates for *hsp30C, hsp70, bip* and *eIf1α in vitro* transcription. A) The coding region of the *hsp30* gene was previously cloned in the pRSETB plasmid into the *BamHI* and *EcoRI* sites (Fernando and Heikkila, 2003). To generate antisense riboprobe template, the plasmid was linearized with *PvuII* and transcribed with SP6 polymerase. B) The coding region of the *hsp70* gene contained in pXL16P (Bienz, 1984) was cloned into the *SmaI* and *Pst1* sites of pSP72 (Promega), generating pSP72-hsp70. To generate antisense riboprobe template, the plasmid was linearized with *MluNI* and transcribed with SP6 polymerase. C) The BiP cDNA was cloned into the *Xho*I and *EcoRI* sites of pBluescript KS+ (Miskovic *et al*, 1997). BiP antisense riboprobe was generated by linearization of the plasmid with *Bam*HI and transcribed with T7 polymerase. D) The coding region of eIF1α was cloned into pCMV-SPORT6, generating pCMV-SPORT6-eIf1α (ATCC). To synthesize antisense riboprobe, pCMV-SPORT6-ef-1was linearized with *SmaI* and transcribed *in vitro* with T7 polymerase.

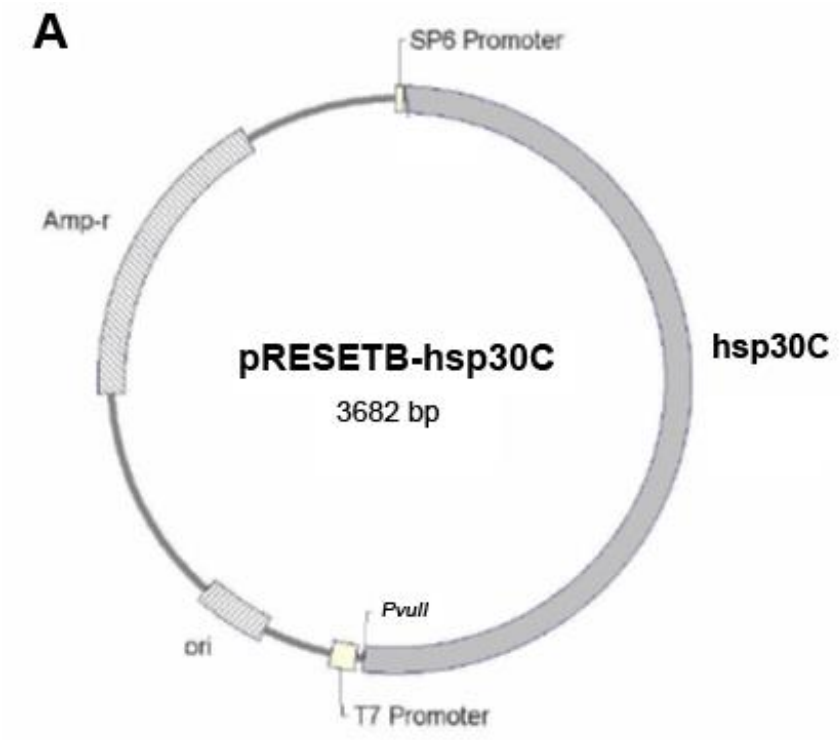
A
SP6 Promoter
Amp-r
pRESETB-hsp30C
3682 bp
hsp30C
PvuII
ori
T7 Promoter

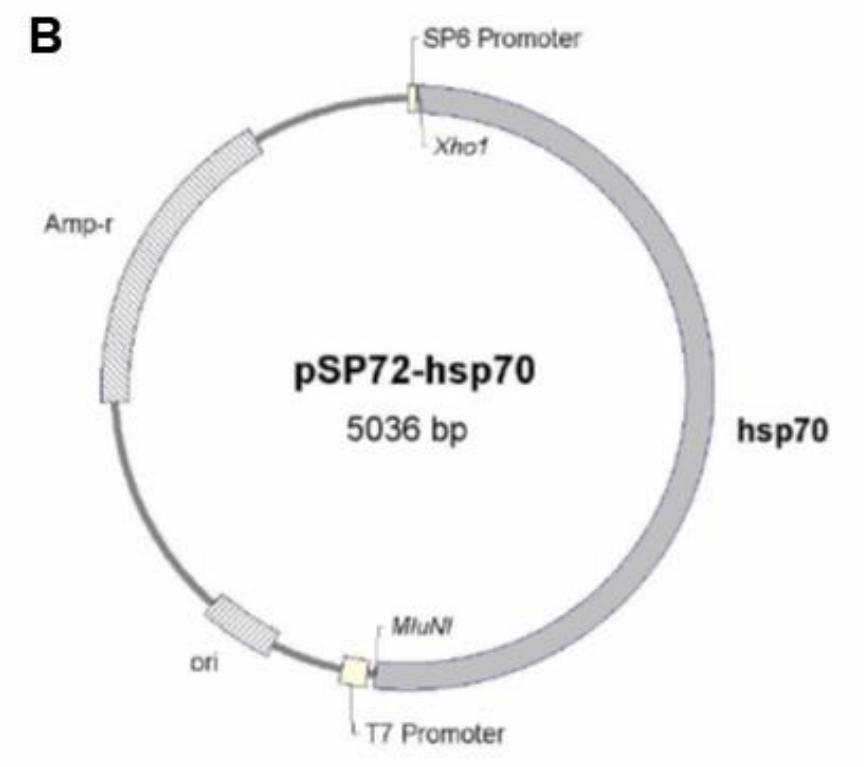
B
SP6 Promoter
Xho1
Amp-r
pSP72-hsp70
5036 bp
hsp70
MluNI
ori
T7 Promoter

C

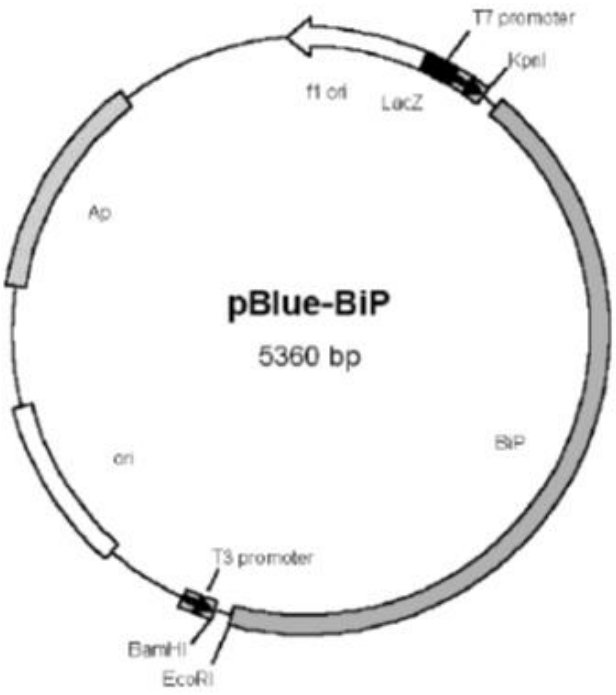
T7 promoter
KpnI
f1 ori
LacZ
Ap
pBlue-BiP
5360 bp
ori
BiP
T3 promoter
BamHI
EcoRI

D

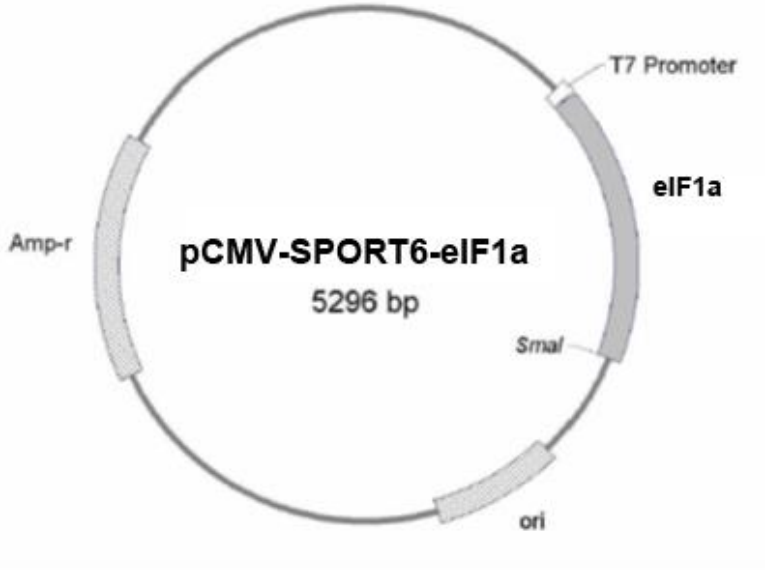
T7 Promoter
eIF1a
Amp-r
pCMV-SPORT6-eIF1a
5296 bp
SmaI
ori

for *hsp30C* and *hsp70* or T7 RNA polymerase for *bip* and *eIF1α* (Roche)]. The *in vitro* transcription reaction was performed for 1 h at 37°C. To remove any remaining DNA template, 2 µL of RNase-free DNase 1 (Roche) was added for 10 min at 37 ºC. *In vitro* transcripts were then precipitated with the addition of 10 µL of 3 M sodium acetate (pH 5.2), 80 µL of TES [10 mM Tris (pH 7.4), 5 mM EDTA (pH 8.0), 1% (w/v) SDS] and 220 µL of ice-cold 100% filtered ethanol and re-suspended in 21 µL of DEPC-treated water. One µL was electrophoresed to verify the presence of the *in vitro* transcript. The remaining 20 µL was stored at -80 ºC until Northern hybridization analysis.

2.4 RNA isolation

RNA was isolated from A6 cells using the QIAgen RNeasy Mini Kit (QIAgen, Mississauga, Ontario) as described in the RNeasy Mini Handbook (2009) animal cell protocol. Isolated RNA was suspended in DEPC-treated water and quantified using the NanoDrop ND-1000 (NanaDrop, Waltham, Massachusetts) spectrophotometer at a wavelength of 260 nm. RNA integrity was analyzed by electrophoresing 2 µg of each RNA sample on a 1.2% (w/v) formaldehyde agarose gel [1.2% (w/v) agarose, 10% (v/v) 10X MOPS, 16% (v/v) formaldehyde]. Prior to loading, 10 µL of loading buffer [1 µL 10X MOPS, 1.6 µL formaldehyde, 2 µL RNA loading dye (0.2% bromophenol blue, 1 mM EDTA (pH 8.0), 50% (v/v) glycerol), 5 µL formamide, 0.5 µg/mL ethidium bromide] was added to each sample. Samples were then heat denatured for 10 min at 68 ºC, cooled on ice for 5 min, and then loaded onto the gel and electrophoresed for 1 h at 90 V. Distinct 18S and 28S rRNA banding indicated intact RNA.

2.5 Northern hybridization analysis

For Northern hybridization analysis, an antisense riboprobe for *Xenopus hsp30C, Xenopus hsp70, Xenopus bip* and *eIf1α* (see Section 2.3) was used. Ten μg of total isolated RNA was electrophoresed in a 1.2 % formaldehyde agarose gel as described previously. The loading buffer contained all components except ethidium bromide and the gel was electrophoresed for 3 h at 70V. Following electrophoresis, the RNA in the gel was denatured by soaking the gel in 0.05 N NaOH for 20 min. Then the gel was rinsed in DEPC-treated water and soaked twice for 20 min each in fresh 20X SSC buffer [3 M sodium chloride, 300 mM sodium citrate]. The RNA was then transferred overnight to a positively charged nylon membrane (Roche) by capillary action.

The following morning, RNA on the membrane was UV-crosslinked twice using a UVC-515 Ultraviolet Multilinker. The quality of the transfer was checked using 1X reversible blot stain (Sigma Aldrich). The stained blot was scanned and then incubated in 50 mL of pre-heated prehybridization buffer [50% (v/v) formamide, 5X SSC, 0.02% (w/v) SDS, 0.01% (w/v) N-lauryl sarcosine, 2% (w/v) blocking reagent] in a hybridization bag at 68 ºC for 4 h in a Shake N' Bake Hybridization Oven. After prehybridization, the buffer was replaced with hybridization buffer (same components as prehybridization buffer) containing 20 μL of either *hsp30C, hsp70, bip* or *eIf1α* DIG-labelled antisense riboprobe and the membrane was returned to the hybridization oven overnight.

The following morning, the membrane was then washed to remove any unbound probe. It was first washed twice in 2X SSC at room temperature, then once each in 0.5X SSC and 0.1X SSC, both at 68ºC for 15 min. Each of these three SSC washing solutions contained 0.1% (w/v) SDS. The blot was then equilibrated for 1 min at room temperature in washing

buffer [100 mM maleic acid buffer, 0.3% (v/v) Tween-20 (Sigma Aldrich)] and blocked using blocking solution [2% (w/v) blocking reagent, 10% (v/v) maleic acid buffer] for 1 h at room temperature. The blot was then incubated in blocking solution containing 1:8000 alkaline phosphatase conjugated anti- DIG-Fab fragments for 30 min. The membrane was then washed twice in washing buffer for 10 min each and then equilibrated in detection buffer [0.1 M Tris-HCl (pH 9.5), 0.1 M NaCl] for 2 min prior to detection using CDP-star, a chemiluminescent reagent, which was applied to the membrane and allowed to develop in a hybridization bag for 10 min. The membrane was then visualized on a DNR Chemiluminescent Imager (DNR Bioimaging Systems, Kirkland, Quebec) for up to 15 min depending on the strength of the signal.

2.6 Protein isolation, quantification and immunoblot analysis

2.6.1 Protein isolation and quantification

Protein was isolated from A6 cells using a lysis buffer solution at pH 7.4 containing 200 mM sucrose, 2 mM EDTA, 40 mM NaCl, 30 mM HEPES, 1% (w/v) SDS and 1 % protease inhibitor cocktail (Promega). It should be noted here that the lysis buffer used for samples in preparation for western blotting with mouse anti-ubiquitin antibody contained 10 mM N-ethylmaleimide (Sigma-Aldrich) to inhibit deubiquitination of proteins. The cells were homogenized in the lysis buffer by sonication (output 4.5, 60% duty cycle) on ice for 15 bursts using a Fisher Scientific Sonic Dismembrator 100 (Fisher Scientific) and subsequently centrifuged at 21,920 x g for 30 min at 4 °C. The supernatant containing the protein sample was removed.

Protein was quantified using a bicinchoninic acid (BCA) protein assay kit (Pierce, Rockford, IL). A bovine serum albumin (BSA; BioShop) protein standard was created by diluting BSA in distilled water at concentrations ranging from 0 to 2 mg/ml. Protein samples were diluted to a concentration of 1:2 in distilled water. Ten µL of BSA standards and protein samples were transferred in triplicate into a 96 well clear polystyrene plate. Then 80 µL of BCA reagent A and B (Pierce) at a ratio 50:1 were added to the BSA and protein samples. The plate was incubated at 37 °C for 30 min and then read at 562 nm using a Versamax Tunable microplate reader (Molecular Devices, Sunnyvale, CA). A standard curve was created using the concentrations of the BSA protein standards, which was used to determine the concentration of the protein samples. Protein samples were stored at -20 °C until further use.

2.6.2 Immunoblot analysis

Immunoblot analysis was performed using 20, 40 or 60 µg of protein (the highest amount was used for the analysis of ubiquitinated protein) and sodium dodecyl sulfate-polyacrylamide gel electrophoresis (SDS-PAGE) as described previously (Khan and Heikkila, 2011). Specifically, separating gels [10-12% (v/v) acrylamide, 0.32% (v/v) n'n'-bis methylene acrylamide, 0.375 M Tris (pH 8.8), 1% (w/v) SDS, 0.2% (w/v) ammonium persulfate (APS), 0.14% (v/v) tetramethylethylenediamine (TEMED)] were prepared, poured and allowed to polymerize for 25 min with 100% ethanol layered on top. Ethanol was poured off and the stacking gel [4% (v/v) acrylamide, 0.11% (v/v) n'n'-bis methylene acrylamide, 0.125 M Tris (pH 6.8), 1% (w/v) SDS, 0.4% (w/v) APS, 0.21 % (v/v) TEMED] was prepared, poured and allowed to polymerize for 25 min. A6 cell protein samples were

aliquoted and loading buffer [0.0625M Tris (pH 6.8), 10% (v/v) glycerol, 2% (w/v) SDS, 5% (v/v) β-mercaptoethanol, 0.00125% (w/v) bromophenol blue] was added, to a final concentration of 1X. Samples and molecular weight markers (BioRad, Mississauga, ON) were denatured via boiling for 10 min, cooled on ice for 5 min and pulse-centrifuged prior to loading. Polyacrylamide gels were electrophoresed on a BioRad Mini Protean III gel system (BioRad) with 1X running buffer [25mM Tris, 0.2M glycine, 1 mM SDS] at 90 V until samples reached the separating gel, at which time the voltage was turned up to 160 V until the dye front reached the bottom of the gel.

Pure nitrocellulose transfer blot membranes (BioRad) were incubated for 30 min in transfer buffer [25 mM Tris, 192 mM glycine, 20% (v/v) methanol]. After electrophoresis, the stacking gel was cut away and the remainder of the gel was soaked in transfer buffer for 15 min. Protein was transferred to the nitrocellulose membrane with a Trans-Blot Semi-Dry Transfer Cell (BioRad) at 25 volts for 20 min. Blots were then stained with Ponceau S stain [0.19% (w/v) Ponceau S (Sigma-Aldrich), 5% (v/v) acetic acid] for 10 min to determine transfer efficiency. The membrane was destained with MilliQ water and then scanned photographed. The membrane was subsequently blocked in 5 % blocking solution [20 mM Tris (pH 7.5), 0.1% Tween 20 (Sigma-Aldrich), 300 mM NaCl, 5% (w/v) Nestle® Carnation skim milk powder] for 1 h to prevent non-specific binding. Immunodetection was carried out via either the use of polyclonal rabbit anti-*Xenopus* HSP30 antibody (Fernando and Heikkila, 2003); 1:500 dilution, the polyclonal rabbit anti-*Xenopus* HSP70 antibody (Gauley et al., 2008); 1:250 dilution, the polyclonal rabbit anti-BiP antibody (Sigma-Aldrich); 1:1000 dilution, the monoclonal rat anti-GRP94 antibody (Cedarlane); 1:1000 dilution, the polyclonal rabbit anti-actin antibody (Sigma-Aldrich); 1:200 dilution, the monoclonal mouse

Table 1. Dilution specifications for antibodies used in western blot analysis

Primary Antibody		Secondary Antibody		Comments
Name	**Dilution**	**Name**	**Dilution**	
Rabbit anti-*Xenopus* HSP30	1:500	Goat anti-rabbit IgG AP-conjugate	1:2000	Prepared by Heikkila lab
Rabbit anti-*Xenopus* HSP70	1:250	Goat anti-rabbit IgG AP-conjugate	1:3000	Prepared by Abgent (San Diego, CA)
Rabbit anti-BiP	1:1000	Goat anti-rabbit IgG AP-conjugate	1:3000	Purchased from Sigma Aldrich
Rat anti-GRP94	1:1000	Goat anti-rat IgG AP-conjugate	1:3000	Purchased from Cedarlane
Rabbit anti-actin	1:200	Goat anti-rabbit IgG AP-conjugate	1:3000	Purchased from Sigma Aldrich
Mouse anti-ubiquitin	1:150	Goat anti-mouse IgG AP-conjugate	1:1000	Purchased from Zymed
Rabbit anti-p38 MAPK	1:200	Goat anti-rabbit IgG AP-conjugate	1:2000	Purchased from Cell Signal Technology
Rabbit anti-phospho p38 MAPK	1:200	Goat anti-rabbit IgG	1:2000	Purchased from Cell Signal Technology

anti-ubiquitin antibody (Zymed, San Francisco, CA); 1:150 dilution or the polyclonal rabbit anti-p38 MAPK (Cell Signal Technology; 1:200 dilution) or the polyclonal rabbit anti-phosphorylated p38 MAPK (Cell Signal Technology; 1:200 dilution) (Table 1). Excess unbound antibody was removed by rinsing the membrane with 1X TBS-T [20 mM Tris, 300 mM NaCl, (pH 7.5), 0.1% (v/v) Tween 20]. The membrane was then incubated for 1 h with blocking solution containing the secondary antibody (alkaline phosphatase-conjugated goat-anti-rabbit, rat or mouse (BioRad)). The secondary antibody dilution was dependent on the primary antibody employed, which is outlined in table 1. For detection, the membrane was incubated in alkaline phosphatase detection buffer [alkaline phosphatase buffer (100 mM Tris base, 100 mM NaCl, 50 mM $MgCl_2$ (pH 9.5)), 0.3% 4-nitro blue tetrazolium (NBT; Roche), 0.17% 5-bromo-4-chloro-3-indolyl phosphate, toluidine salt (BCIP; Roche)] until the bands were visible.

2.7 Pore exclusion limit gel electrophoresis

Immediately following treatment, A6 cells were collected as described previously (see section 2.1) and 300 uL of prepared lysis buffer [50 mM Tris (pH 7.5), 1% Nonidet P-40, 2 mM EDTA, 100 mM NaCl, 50 mM $MgCl_2$, 10 mM N-Ethylmaleimide and 1X Protease inhibitor cocktail (Promega)] was added to each sample. The cell pellet was resuspended using a pipet and the cell lysate was incubated on a rotator for 2 h at 4 °C. Cellular debris, nuclei and insolubilized material was pelleted using a refrigerated Eppendorf microcentrifuge at 21,920 x g at 4 °C for 10 min. The supernatant was transferred to a fresh tube and loading buffer without SDS and β-mercaptoethanol [0.0625M Tris (pH 6.8), 10% (v/v) glycerol and 0.00125 % (w/v) bromophenol blue] was added to a final concentration of 1X.

The protein samples were resolved on a previously prepared 2 to 22.5 % (0 to 12.5 % glycerol) gradient gel. The gradient gel was prepared using 2 solutions, namely, degassed, chilled, 2 % acrylamide, 0.375 M Tris (pH 8.8) and 22.5 % acrylamide, 0.375 M Tris (pH 8.8), 12.5% glycerol, which were loaded into the reservoir and mixing chamber, respectively, of a BioRad gradient maker. APS and TEMED were added to initiate polymerization, and the acrylamide solutions were mixed in the mixing chamber of the gradient maker by a stir bar as the solution was pumped into the BioRad multicasting chamber via a peristaltic pump. The liquid filled the gel sandwiches (1.0 mm spacer) in the chamber from the top, generating 2 to 22.5 % (0 to 12.5 % glycerol; top to bottom) continuous acrylamide gradient gels. The combs (1.0 mm 1-D comb position at the top) were added and gels were left to polymerize for 1 h, after which the combs were removed and wells were washed with MilliQ water. The gels were then chilled at 4 °C until ready to use. The gels were electrophoresed in 1X running buffer without SDS [25mM Tris, 0.2M glycine] at 90 V for 3 h at 4 °C to separate the proteins to their pore exclusion limits (Fernando and Heikkila, 2003). Following electrophoresis the gels were transferred to nitrocellulose membranes and immunoblotted with anti-*Xenopus* HSP30 antibody as described previously (see section 2.6.2).

2.8 Co-immunoprecipitation analysis

Immediately following treatment, A6 cells were rinsed using 65 % HBSS and 10 mM N-ethylmaleimide and removed via scraping in 1 ml of 100 % HBSS. Cells were centrifuged at 21,920 x g for 1 min and the resulting pellets were flash frozen in liquid nitrogen and stored at -80 °C until further use. Cell pellets were thawed on ice and 400 uL of solubilizing buffer [50 mM Tris (pH 7.5), 1% Nonidet P-40, 2 mM EDTA, 100 mM NaCl, 50 mM

$MgCl_2$, 10 mM N-ethylmaleimide and 1X Protease inhibitor cocktail (Promega)] was added to each sample. The cell pellet was resuspended using a pipet and all clumps were dispersed using a 20 G needle followed by incubation on a rotator for 2 h at 4 °C. Cellular debris and nuclei was pelleted using a refrigerated Eppendorf microcentrifuge at 21,920 x g at 4 °C for 10 min. The supernatant was transferred to a fresh tube and the amount of protein was quantified using the BCA method as described in Section 2.6.1.

Three hundred micrograms of cell lysate was transferred to a new tube and combined with 10 μg of affinity-purified rabbit anti-*Xenopus* HSP30 antibody or 15 μg of monoclonal mouse anti-γ-tubulin antibody. The antibody-cell lysate mixture was incubated on a rotator overnight at 4 °C. One hundred micrograms of the remaining cell lysate was added to loading buffer [0.0625M Tris (pH 6.8), 10% (v/v) glycerol, 2% (w/v) SDS, 5% (v/v) β-mercaptoethanol, 0.00125% (w/v) bromophenol blue] to a final concentration of 1X, boiled for 10 min and stored at -20 °C until further use. The following day, 100 μL of Protein G Sepharose beads (Sigma Aldrich) per sample were washed with solubilizing buffer for 5 min at 4 °C and then spun at 1,000 x g for 1 min at 4 °C. This was repeated twice before the beads were placed on ice prior to incubation with the antibody-lysate mixture.

The antibody-lysate mixture was added to the 100 μL of beads and incubated on the rotator at 4 °C for 2 h. After 2 h of incubation, the beads were spun at 1,000 x g for 1 min at 4 °C. The supernatant was removed and 200 μL of the supernatant was added to loading buffer and marked as “Flow Through”. The beads were then rinsed 3 times with solubilizing buffer for 5 min at 4 °C. Finally, the beads were resuspended in 100 μL of loading buffer and boiled for 10 min and kept at –20 °C until further use. The samples were then electrophoresed be means of SDS-PAGE and proteins were transferred onto a nitrocellulose

membrane. Immunoblot analysis utilized polyclonal rabbit anti-*Xenopus* HSP30 antibody (Fernando and Heikkila, 2003); 1:500 dilution, the monoclonal mouse anti-γ-tubulin antibody (Sigma-Aldrich); 1:1000 dilution, the polyclonal rabbit anti-BiP antibody (Sigma-Aldrich); 1:1000 dilution and the polyclonal rabbit anti-actin antibody (Sigma-Aldrich); 1:200.

2.9 Densitometry and statistical analysis

Densitometric analyses within the range of linearity were performed using ImageJ (1.42q) software on all blots as described previously (Khan and Heikkila, 2011). Briefly, experiments were repeated in triplicate, and the average densitometric values were expressed as a percentage of the maximum hybridization band (for HSP30, HSP70 or HO-1) or as fold-increase with respect to control cells (for BiP or GRP94). The data were graphed with standard error of the mean represented as vertical error bars. Statistical analysis through one way analysis of variance (ANOVA) followed by Tukey's Multiple comparison post-test were performed with this data to determine if statistically significant differences existed between samples. Confidence levels used were 90% ($p < 0.1$; Δ) and 95% ($p < 0.05$; *).

2.10 Immunocytochemistry and laser scanning confocal microscopy

Cells were prepared for imaging by laser scanning confocal microscopy (LSCM) on 22 x 22 mm glass coverslips in sterile petri dishes. In order to clean the glass coverslips, they were placed in small Coplin jars to ensure full contact with the base solution [49.5% (v/v) ethanol, 0.22M NaOH] for 30 min with periodic shaking at room temperature. The coverslips were then rinsed under running distilled water for 3 h and dried on Whatman paper. A6 cells were grown on flame sterilized cover slips for 24 h at 22 °C.

For experiments involving recovery from heat stress, the petri dishes were wrapped with parafilm, sealed in a plastic bag and then placed in a heated water bath set at 33 °C for 2 h and allowed to recover at 22 °C. Cells on coverslips were heat shocked and then treated for the duration of the experiment with 100 µM cycloheximide after 2 h of recovery followed by incubation with 30 µM MG132 after 6 h in recovery. Some cells were also treated 0.5 h before heat shock with 10 µM SB203580 for the duration of the experiment. For the remaining experiments the cells were either maintained at 22 °C or treated with 7 µM A23187, 30 µM MG132, 2.5 µM celastrol, 5 µM withaferin A, 20 µM sodium arsenite or 100 µM cadmium chloride for 16 h.

Following the treatments, cells were rinsed with phosphate buffered saline [PBS; 1.37 M NaCl, 67 mM Na_2HPO_4, 26 mM KCl, 14.7 mM KH_2PO_4, 1 mM $CaCl_2$, 0.5 mM $MgCl_2$, pH 7.4] and fixed using 3.7% (w/v) paraformaldehyde (pH 7.4 in PBS; BDH, Toronto, ON) for 15 min. A6 cells were rinsed 3 times with PBS for 5 min each and permeabilized using 0.3% Triton X-100 (Sigma-Aldrich) for 10 min. A6 cells were then rinsed 3 times with PBS and incubated with 3.7 % (w/v) bovine serum albumin fraction V (BSA; Fischer Scientific) for 1 h or overnight on the shaker at 4 °C. The BSA fraction V was filter-sterilized using a 0.45 µm filter (Pall Filtration Corp., St. Laurent, QC) to remove debris that might negatively affect the imaging.

The following day cells were incubated with affinity-purified rabbit anti-*Xenopus* HSP30 antibody (1:500), affinity-purified rabbit anti-BiP antibody (1:1000; Sigma Aldrich), monoclonal mouse anti-PABP antibody (1:100; Novus Biologicals, Littleton, CO), affinity-purified rabbit anti-TIA1 antibody (1:100; Cedarlane), monoclonal mouse anti-γ-tubulin antibody (1:100; Sigma Aldrich) or monoclonal mouse anti-vimentin antibody (1:50; Dako

Canada Ltd., Burlington, ON) in 3.7 % BSA for 1h. Following three washes with PBS, indirect labeling of A6 cells was performed using fluorescent-conjugated secondary antibodies including goat anti-rabbit Alexa Fluor 488 (Invitrogen Molecular Probes, Carlsbad, CA) at 1:2000, or goat anti-mouse Alexa Fluor 488 (Invitrogen Molecular Probes) at 1:1000 or goast anti-mouse Alexa Fluor 555 (Invitrogen Molecular Probes) at 1:1000 in 3.7 % BSA for 30 min in the dark. To visualize the actin cytoskeleton, A6 cells were incubated with rhodamine-tetramethylrhodamine-5-isothiocyanate phalloidin (TRITC; Invitrogen Molecular Probes) for 15 min at 1:100 in 3.7 % BSA in the dark. A ProteoStat aggresome detection kit (Enzo Life Sciences, Plymouth Meeting, PA) was used to monitor the presence of aggresome-like structures as per manufacturer's instructions. The cover slips were dried and mounted on glass slides with Vectashield mounting medium containing 4, 6-diamidino-2-phenylindole (DAPI; Vector Laboratories Inc., Burlingame, CA) to stain nuclei. Coverslips were permanently attached to glass slides by using clear nail polish and examined by laser scanning confocal microscopy by using a Zeiss Axiovert 200 microscope and ZEN 2009 software (Carl Zeiss Canada Ltd., Mississauga, ON).

Chapter 3: Results

3.1 Distinct patterns of HSP30 and HSP70 degradation in cells recovering from heat stress

3.1.1 Elevated levels of HSP30 in A6 cells recovering from thermal stress

Preliminary experiments compared the effect of elevated temperatures on HSP30 and HSP70 accumulation in *X. laevis* A6 cells. Cells incubated at elevated temperatures of 33 or 35 °C resulted in enhanced accumulation of both HSP30 and HSP70 in comparison to cells maintained at 22 °C (Fig. 7). Actin levels remained constant throughout these treatments. I then compared the relative levels of HSP30 and HSP70 in *Xenopus laevis* A6 kidney epithelial cells at different time periods during recovery from a heat shock. Immunoblot analysis revealed that after a 2 h heat shock treatment at 33 °C, the relative levels of HSP30 accumulation during recovery at 22 °C increased to peak levels at 8 h and then declined to 81% after 24 h and to 67% and 21% after 48 and 72 h of recovery, respectively (Fig. 8). In other immunoblot experiments, HSP30 was still detectable after 96 h of recovery (data not shown). In contrast, the relative levels of HSP70 peaked 2 h after recovery from heat shock and then declined to 71% by 8h, 26% at 24 h and only 5% and 2% at 48 and 72 h, respectively. In these experiments the relative levels of actin were not affected as indicated by densitometric analyses (data not shown).

3.1.2 Pattern of *hsp30* and *hsp70* mRNA decay during recovery from heat shock

Given the extended pattern of decay in the relative levels of HSP30 compared to HSP70, northern blot analysis was performed to determine if they reflected the relative levels

Figure 7. HSP30, HSP70 and actin accumulation in A6 cells subjected to heat shock. Cells were maintained at 22 °C or treated at 33 °C or 35 °C for 2 h followed by a 2 h recovery at 22 °C. After treatment, cells were harvested and total protein was isolated. Twenty μg of protein was then resolved on a 12% SDS-polyacrylamide gel. Protein was transferred to nitrocellulose membranes and probed with anti-HSP30, anti-HSP70 or anti-actin polyclonal antibodies as described in Material and methods. These data are representative of three separate experiments.

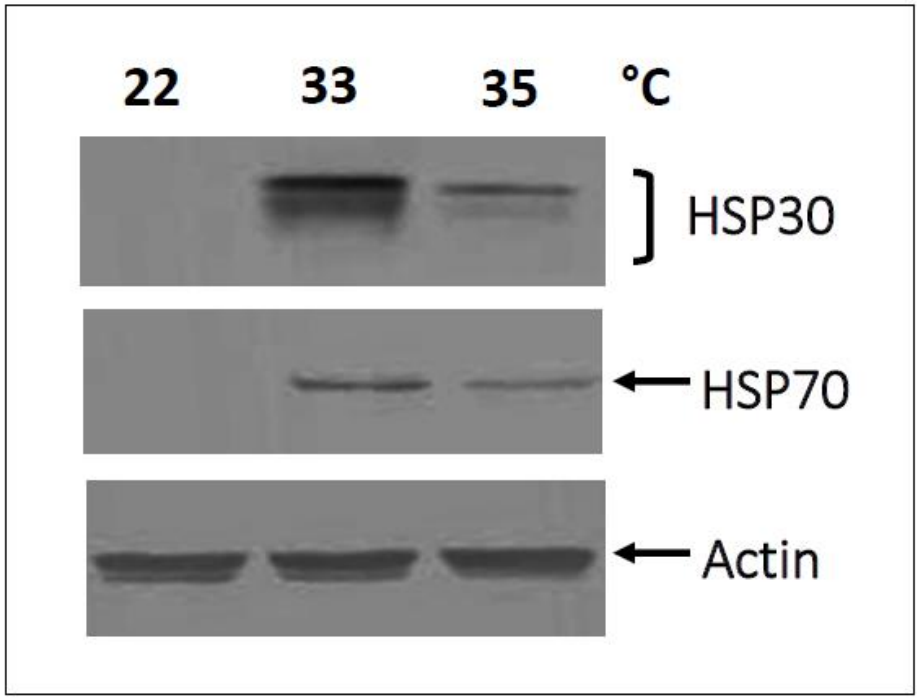
22
33
35
°C
HSP30
HSP70
Actin

Figure 8. Relative levels of HSP30 and HSP70 accumulation in cells recovering from heat shock. A) Cells were maintained at 22 °C (C) or incubated at 33 °C for 2 h and subsequently allowed to recover at 22 °C for different time intervals ranging from 0 to 72 h. Total protein was isolated and 40 µg was subjected to immunoblot analysis using anti-HSP30, anti-HSP70 or anti-actin polyclonal antibodies as described in Materials and methods. These data are representative of three separate experiments. B) Image J software was used to perform densitometric analysis of signal intensity for HSP30 (black) and HSP70 (white) protein bands as described in Materials and methods. The data are expressed as a percentage of the maximum band (33 °C with 8 h recovery for HSP30 and 33 °C with 2 h recovery for HSP70) while the standard errors are represented by vertical error bars. Statistical Analysis was performed as described in Materials and methods.

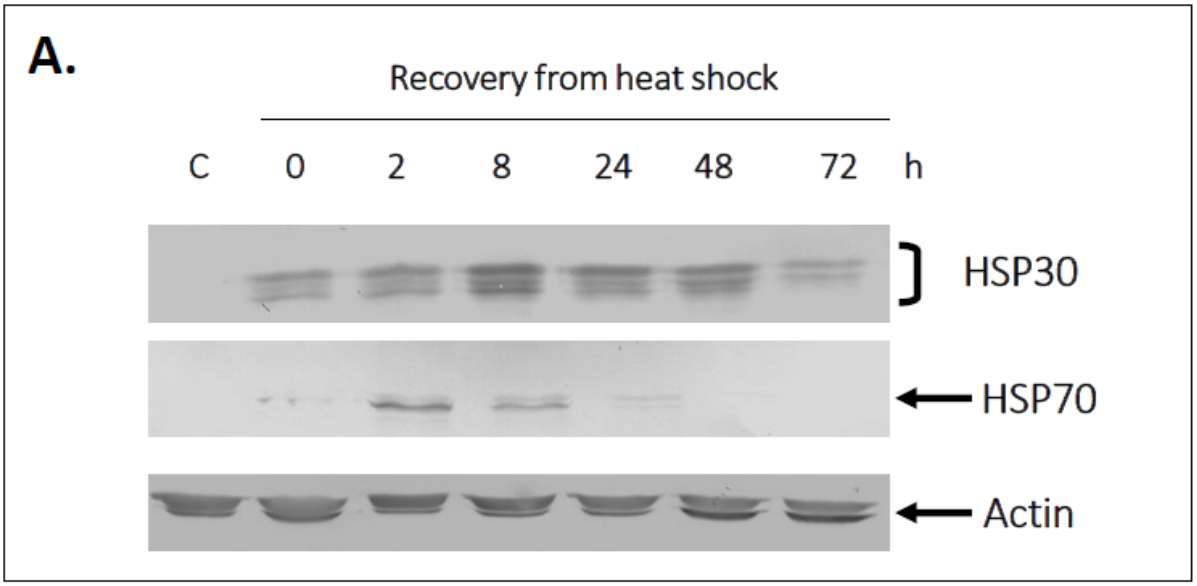
A.
Recovery from heat shock
C
0
2
8
24
48
72
h
HSP30
HSP70
Actin

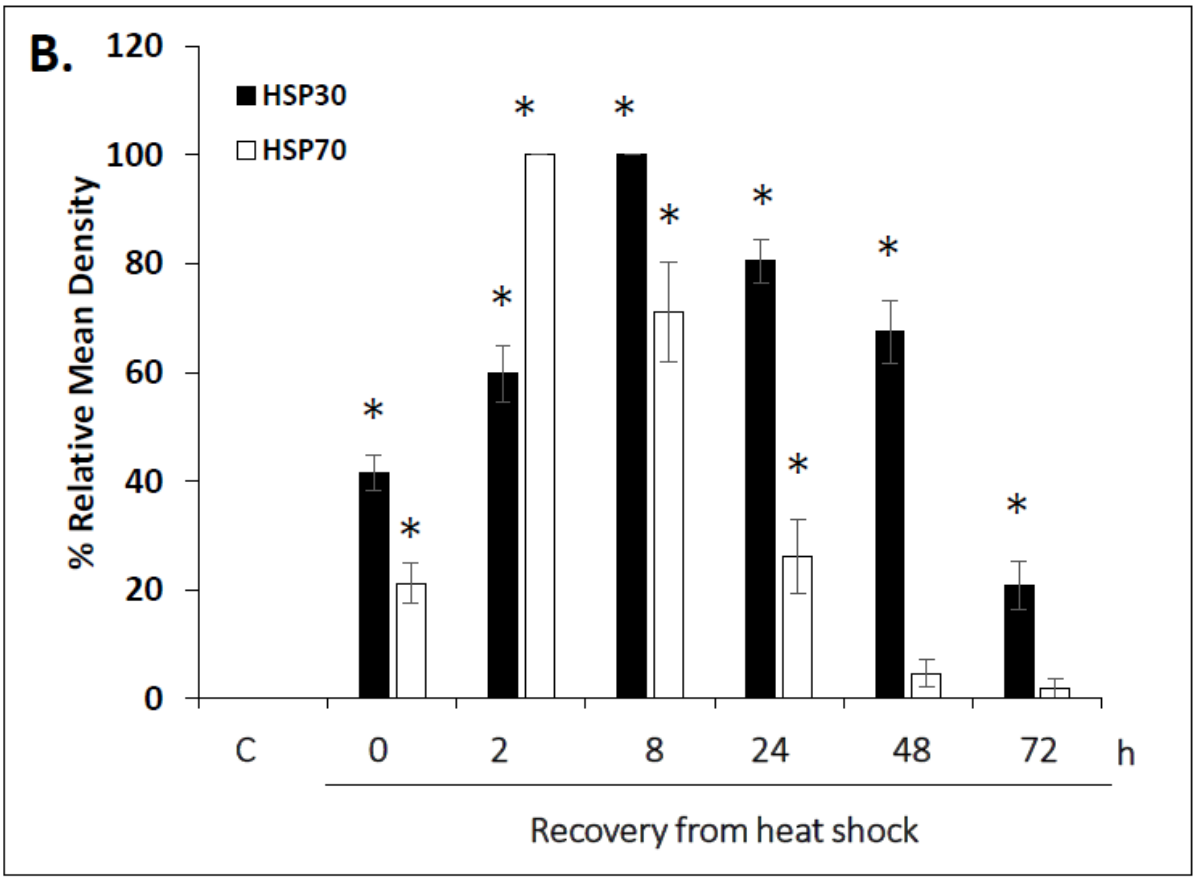
B.
HSP30
HSP70
% Relative Mean Density
120
100
80
60
40
20
0
C
0
2
8
24
48
72
h
Recovery from heat shock

of their mRNAs. As shown in Figure 9, maximum levels of *hsp30* and *hsp70* mRNA accumulation occurred at 33 °C with no recovery. The relative levels of both *hsp30* and *hsp70* mRNA then declined in a similar fashion after 2 to 24 h of recovery with no detectable levels of either mRNA after 48 h of recovery at 22 °C. The relative levels of *eIf1α* mRNA were relatively consistent during the recovery period.

3.1.3 Effect of cycloheximide on HSP30 and HSP70 accumulation in cells recovering from thermal stress

The next phase of this study examined the effect of the translational inhibitor, cycloheximide, on the pattern of HSP30 and HSP70 decay during recovery from heat shock using immunoblot analysis. As shown in Figure 10, cells pretreated with 100 µM cycloheximide for 2 h before a 33 °C heat shock completely inhibited the accumulation of HSP30 and HSP70. Given these results, cells were treated with this concentration of cycloheximide immediately after the cells were transferred from 33 to 22 °C for up to 36 h of recovery. Maximum HSP30 and HSP70 accumulation occurred in cells with no recovery. After 2 h of recovery the relative levels of HSP30 dropped to 85% compared to cells with no recovery. This relative level of HSP30 was maintained at 8 h followed by a drop to 61% at both 16 and 24 h with a slight reduction to 57% after 36 h of recovery. In contrast, HSP70 levels displayed a faster decay during recovery from heat shock than HSP30. Compared to peak levels, HSP70 was reduced to 25% after 8 h and 4% after 16 h of recovery. HSP70 was not detected in samples after 24 or 36 h of recovery. Also, the relative levels of actin were unchanged throughout this experiment. Given the prolonged elevation of HSP30 during recovery in the presence of cycloheximide, the localization of HSP30 was examined by

Figure 9. *Hsp30, hsp70* and *eIF1α* mRNA accumulation in cells recovering from heat stress. A) A6 cells were maintained at 22 °C (C) or incubated at 33 °C for 2 h and subsequently allowed to recover at 22 °C from 0 to 72 h. Cells were harvested and total RNA was isolated and quantified as described in Materials and methods. Ten µg of total RNA was analyzed by northern hybridization analysis using *hsp30, hsp70* and *eIF1α* antisense riboprobes. These data are representative of three separate experiments. B) Image J software was used to perform densitometric analysis of signal intensity of *hsp30* (black) and *hsp70* (white) mRNA bands as described in Materials and methods. The data are expressed as a percentage of the maximum band (33 °C with no recovery for either *hsp30* or *hsp70*) while the standard errors are represented by vertical error bars.

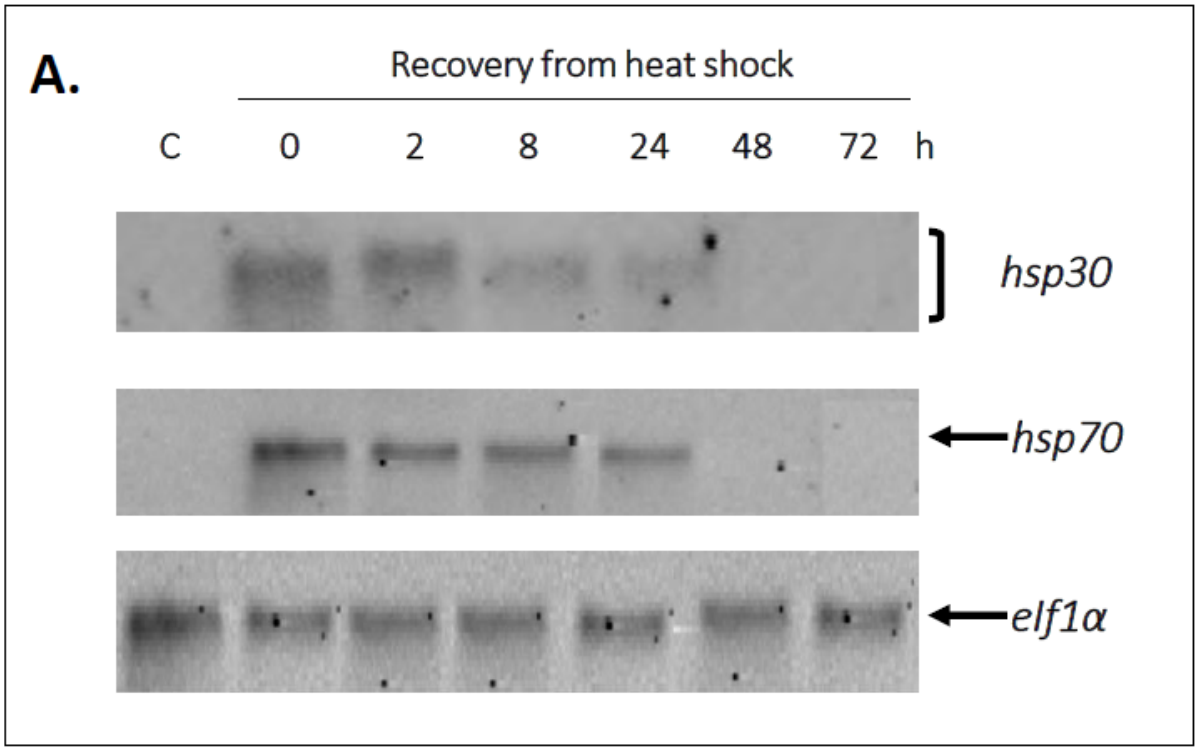
A.
Recovery from heat shock
C
0
2
8
24
48
72
h
hsp30
hsp70
elf1α

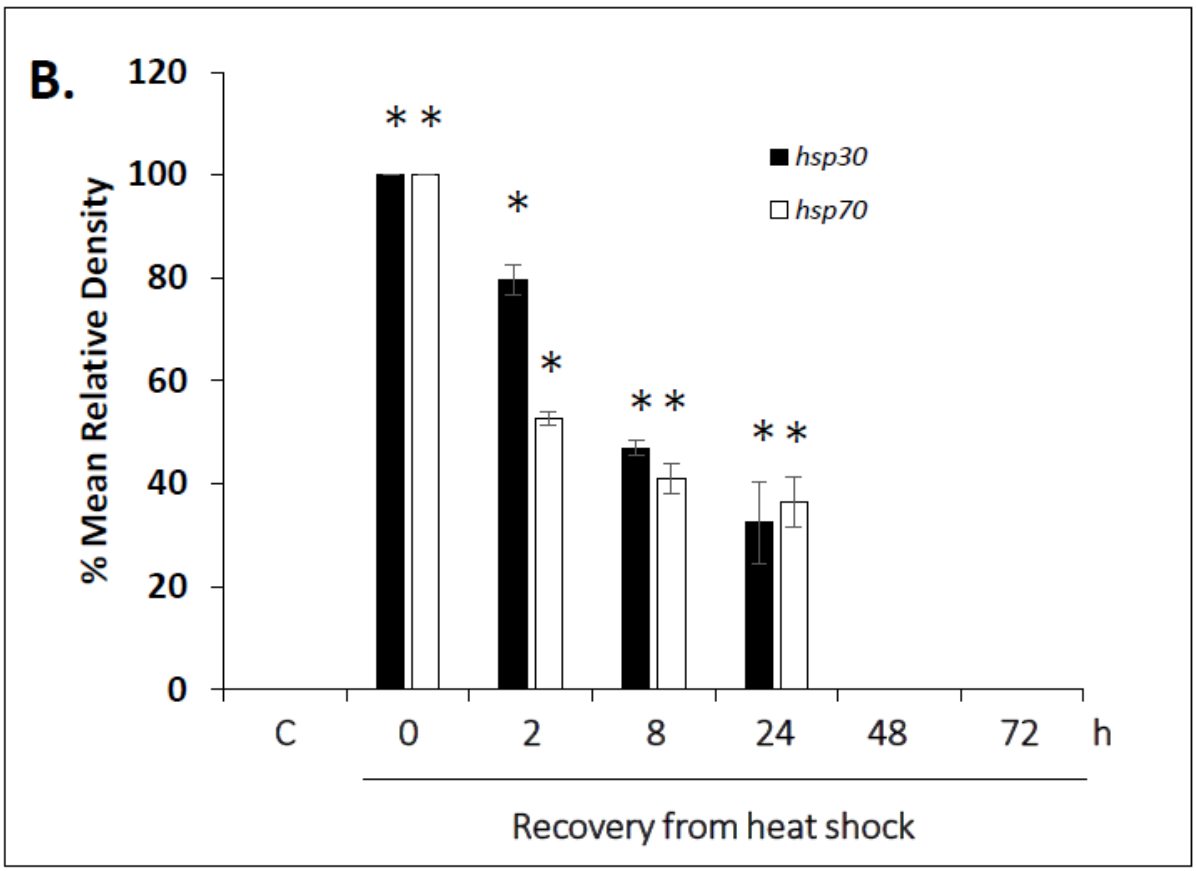
B.
% Mean Relative Density
120
100
80
60
40
20
0
hsp30
hsp70
C
0
2
8
24
48
72
h
Recovery from heat shock

Figure 10. Effect of cycloheximide on the relative levels of HSP30 and HSP70 in A6 cells recovering from heat stress. A) Cells were maintained at 22 °C (C) or treated with 100 µM cycloheximide (CHX) for 2 h prior to incubation at 33 °C for 2 h plus a 2 h recovery (H) or incubated at 33 °C for 2 h followed by the immediate addition of cycloheximide to a final concentration of 100 µM and then incubated at 22 °C for different time intervals ranging from 0 to 36 h. Cells were harvested and total protein was isolated and analyzed by immunoblotting using anti-HSP30, anti-HSP70 or anti-actin polyclonal antibodies as described in Materials and methods. These data are representative of three separate experiments. B) Image J software was used to perform densitometric analysis of signal intensity for HSP30 (black) and HSP70 (white) protein bands as described in Materials and methods. The data are expressed as a percentage of the maximum band (33 °C with no recovery for HSP30 and HSP70). The standard errors are represented by vertical error bars.

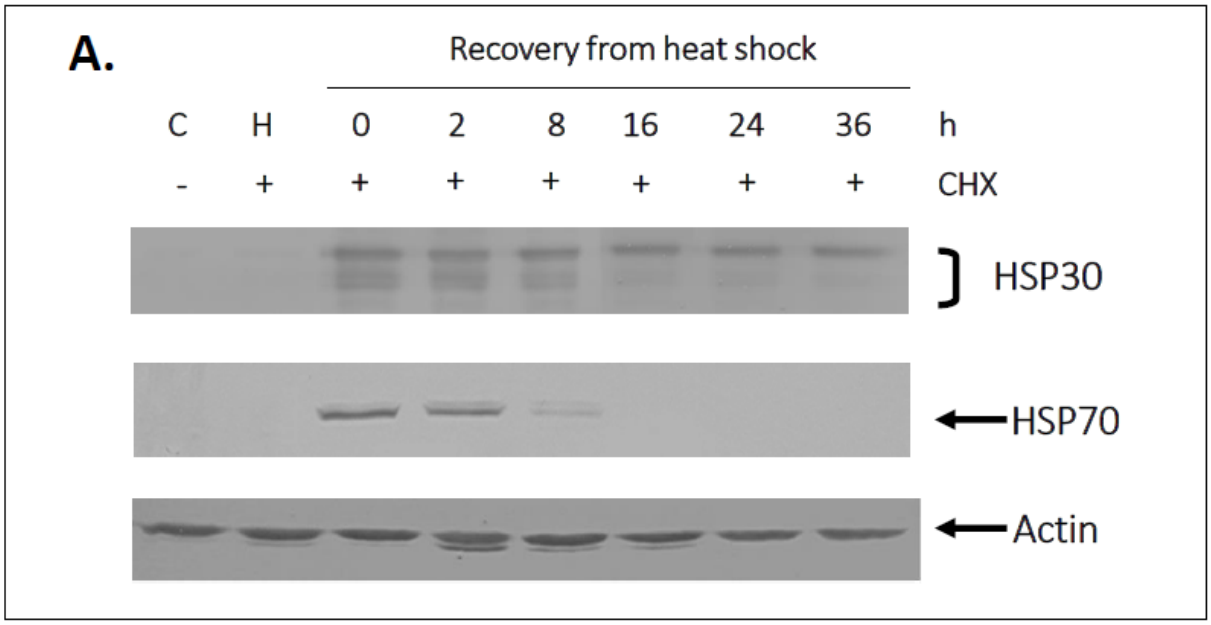
A.
Recovery from heat shock
C H 0 2 8 16 24 36 h
- + + + + + + + CHX
HSP30
HSP70
Actin

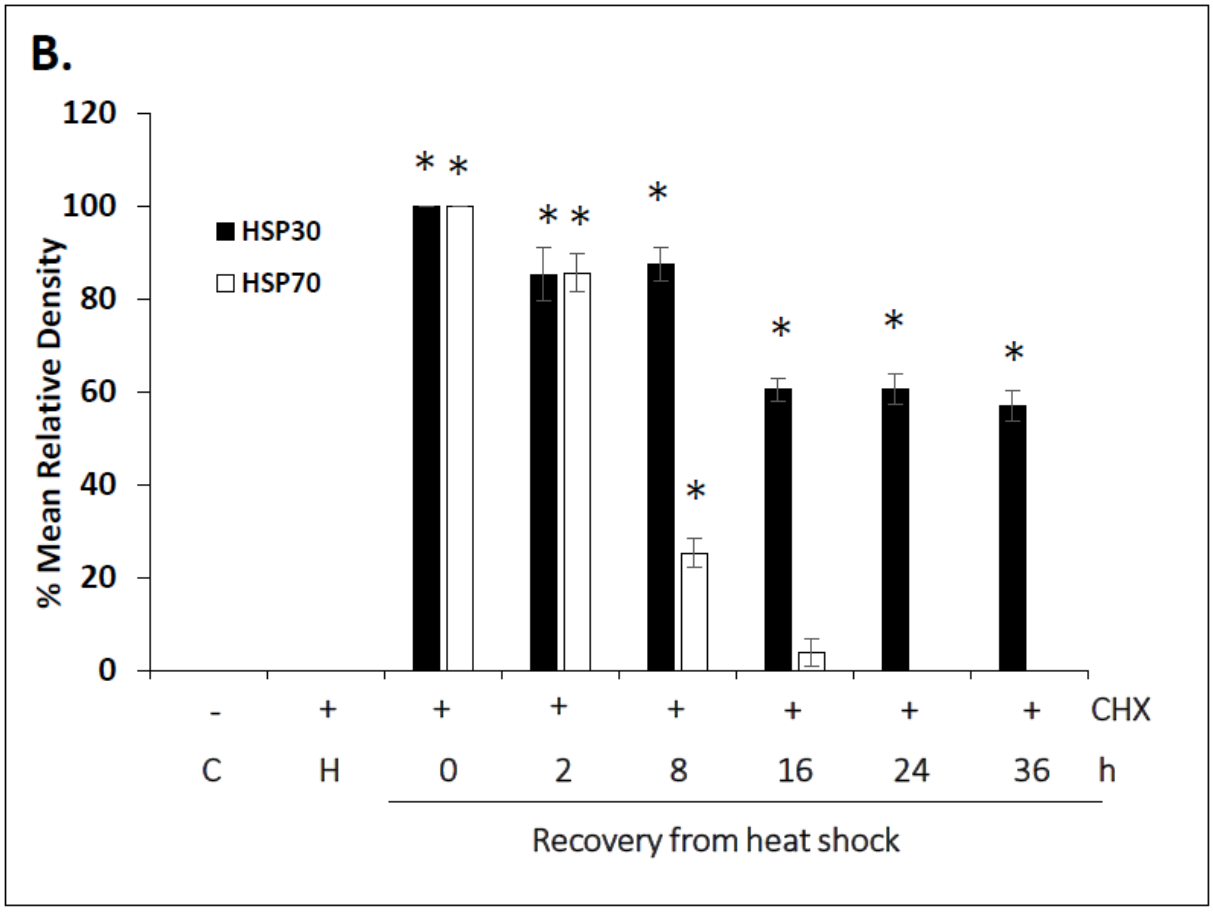
B.
120
100
80
60
40
20
0
% Mean Relative Density
HSP30
HSP70
- + + + + + + + CHX
C H 0 2 8 16 24 36 h
Recovery from heat shock

immunocytochemistry (Fig. 11). As shown in Figure 11A, immunocytochemistry did not detect the presence of HSP30 in control or in cells pretreated with cycloheximide prior to heat shock in contrast to cells treated at 33 °C for 2 h. In cells recovering from heat stress, HSP30 occurred in 90 percent of cells in a granular pattern after 8 h of recovery and stayed elevated up to 36 h after recovery. Additionally, cells treated with cycloheximide during recovery from the 33 °C treatment also showed HSP30 accumulation in 60 percent of cells primarily in the cytoplasm in a granular pattern (Fig. 11C). This accumulation pattern was observed in cells recovering up to 36 h. Unfortunately, HSP70 was not examined because the affinity-purified, polyclonal anti-HSP70 antibody, which was utilized successfully in immunoblot analysis, was unable to specifically detect HSP70 by immunocytochemistry (Gauley et al., 2008). Examination of the F-actin cytoskeleton revealed the presence of membrane ruffling in cells recovering from heat shock and after the addition of cycloheximide. This phenomenon was detectable in cells after 2 h of recovery and appeared to peak at 8 h with less ruffling of the cytoskeleton at 24 h followed by a more control-like appearance of the cytoskeleton after 36 h.

3.1.4 Effect of cycloheximide and MG132 on HSP30 and HSP70 accumulation in cells recovering from thermal stress

The eukaryotic proteasome, which is involved in the degradation of most proteins in the cell, can be reversibly inhibited by MG132. To determine if proteasomal inhibition affected the degradation of HSP30 and HSP70, A6 cells were treated with MG132 in addition to cycloheximide as shown in Figure 12. In these experiments, cells were heat shocked at 33 °C and then allowed to recover in the presence of cycloheximide at 22 °C

Figure 11. Localization of heat shock-induced HSP30 in cells during recovery with or without cycloheximide. A) Cells were cultured on base-washed coverslips and maintained at 22 °C (Control) or treated at 33 °C with or without a 2 h pretreatment of 100 µM cycloheximide. B & C) Cells were also incubated at 33 °C for 2 h and then allowed to recover at 22 °C for 2, 8, 24 or 36 h with (panel C) or without (panel B) 100 µM cycloheximide. Actin and nuclei were stained directly with phalloidin conjugated to TRITC (red) and DAPI (blue), respectively. HSP30 was indirectly detected with an anti-HSP30 antibody and a secondary antibody conjugated to Alexa-488 (green). From left to right, the columns display fluorescence detection channels for actin, HSP30 and merger of actin, DAPI and HSP30. White arrows indicate membrane ruffling of the F-actin cytoskeleton. The 20 µm white scale bars are indicated at the bottom right section of each panel. These results are representative of 3 separate experiments.

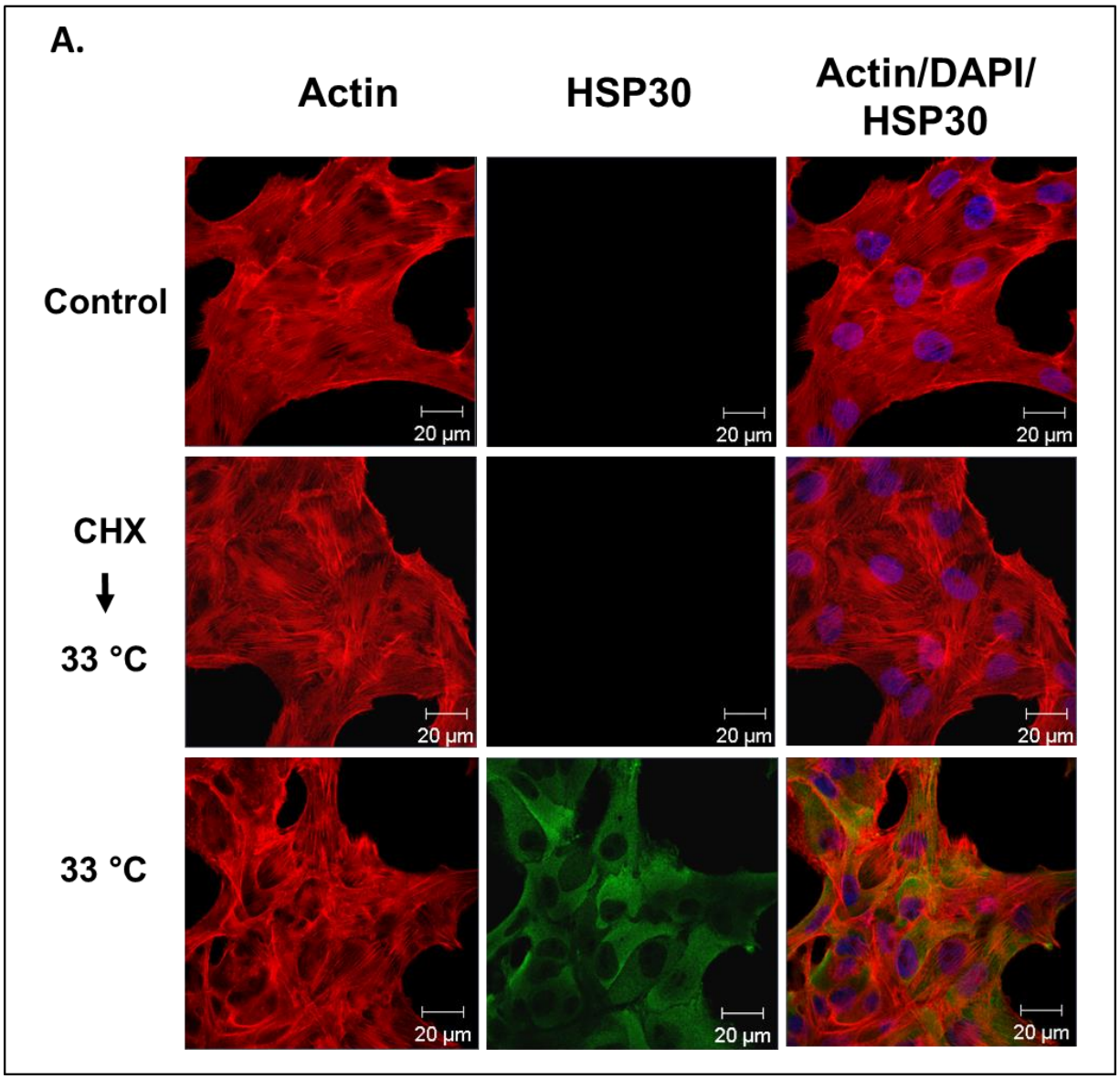
A.
Actin
HSP30
Actin/DAPI/
HSP30
Control
CHX
33 °C
33 °C
20 µm

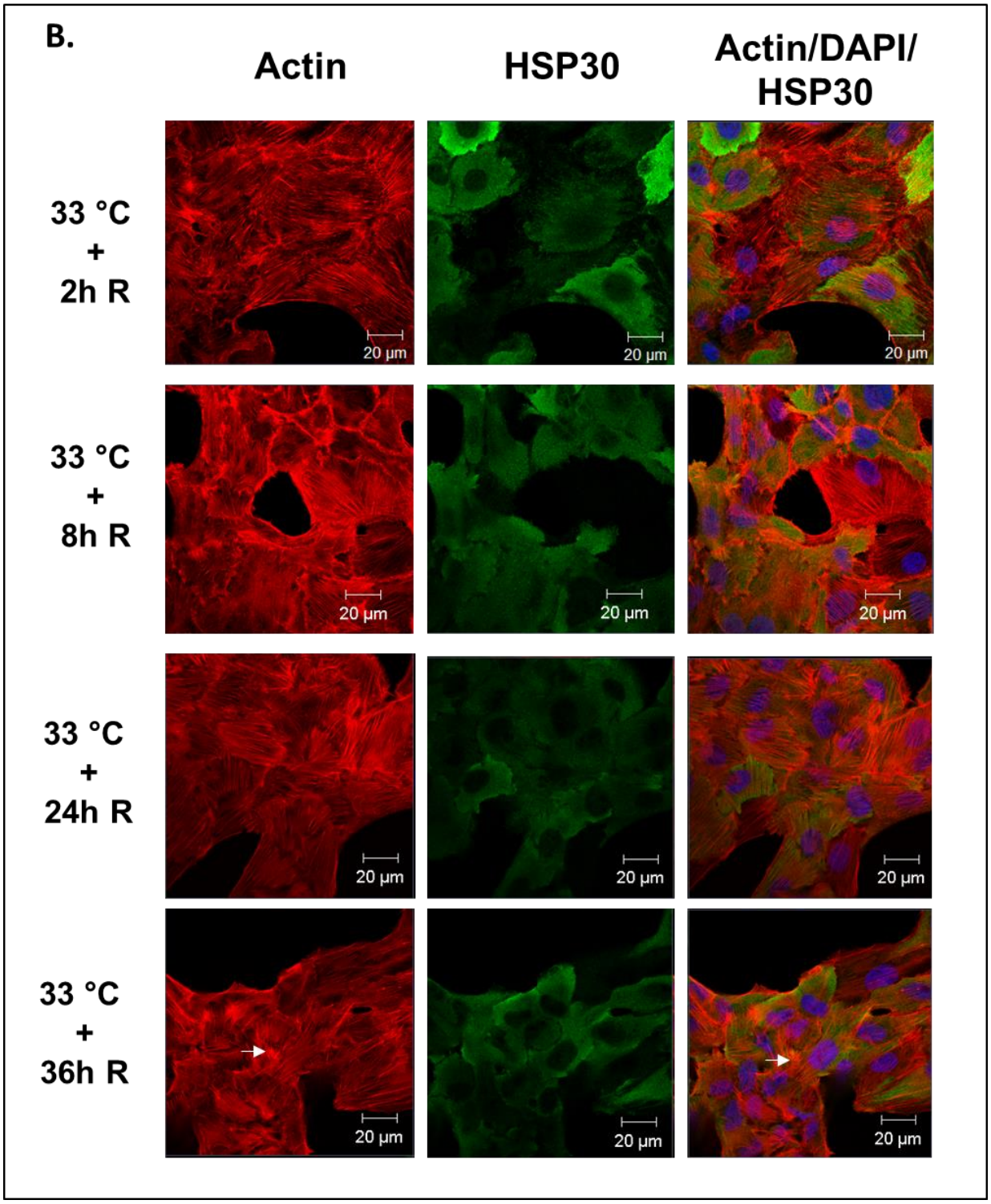
B.
Actin
HSP30
Actin/DAPI/
HSP30
33 °C
+
2h R
33 °C
+
8h R
33 °C
+
24h R
33 °C
+
36h R
20 µm

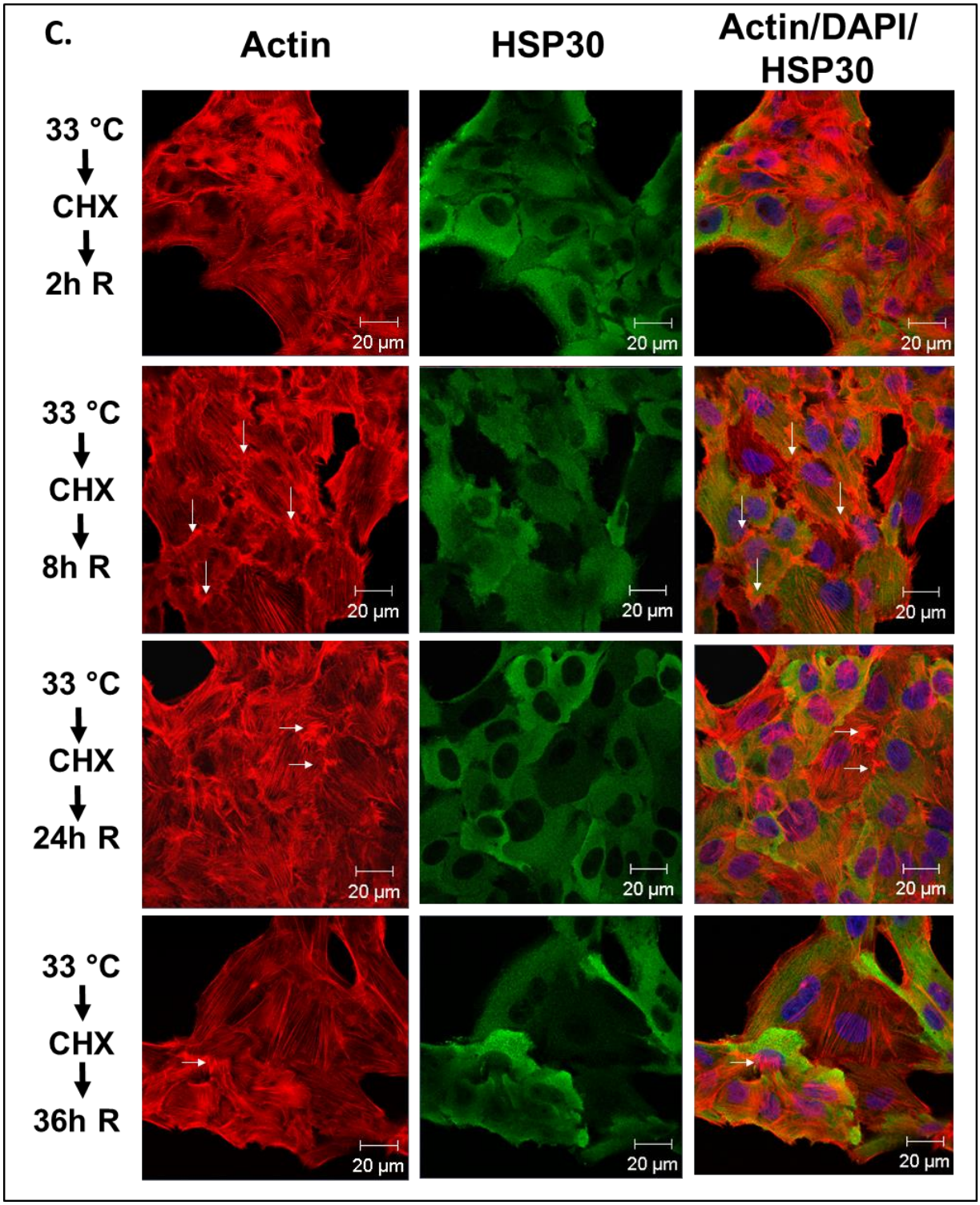
C.
Actin
HSP30
Actin/DAPI/
HSP30
33 °C
CHX
2h R
33 °C
CHX
8h R
33 °C
CHX
24h R
33 °C
CHX
36h R
20 µm

Figure 12. Effect of cycloheximide or cycloheximide plus MG132 on HSP30 and HSP70 levels in A6 cells recovering from heat shock. A) Cells were maintained at 22 °C (C1) or treated with 100 µM cycloheximide (CHX) at 22 °C for 6 h prior to the addition of MG132 to a final concentration of 30 µM for 36 h at 22 °C (C2). Some cells were heat shocked at 33 °C for 2 h followed by recovery for up to 36 h at 22 °C in the presence of 100 µM cycloheximide with the addition of MG132 to a final concentration of 30 µM at the 6 h time point. Cells were harvested and total protein was analyzed by immunoblotting using anti-HSP30, anti-HSP70 or anti-actin polyclonal antibodies as described in Materials and methods. These data are representative of three separate experiments. B) Image J software was used to perform densitometric analysis of signal intensity for HSP30 (black) and HSP70 (white) protein bands as described in Materials and methods. The data are expressed as a percentage of the maximum band (33 °C with no recovery for HSP30 and HSP70). The standard errors are represented by vertical error bars.

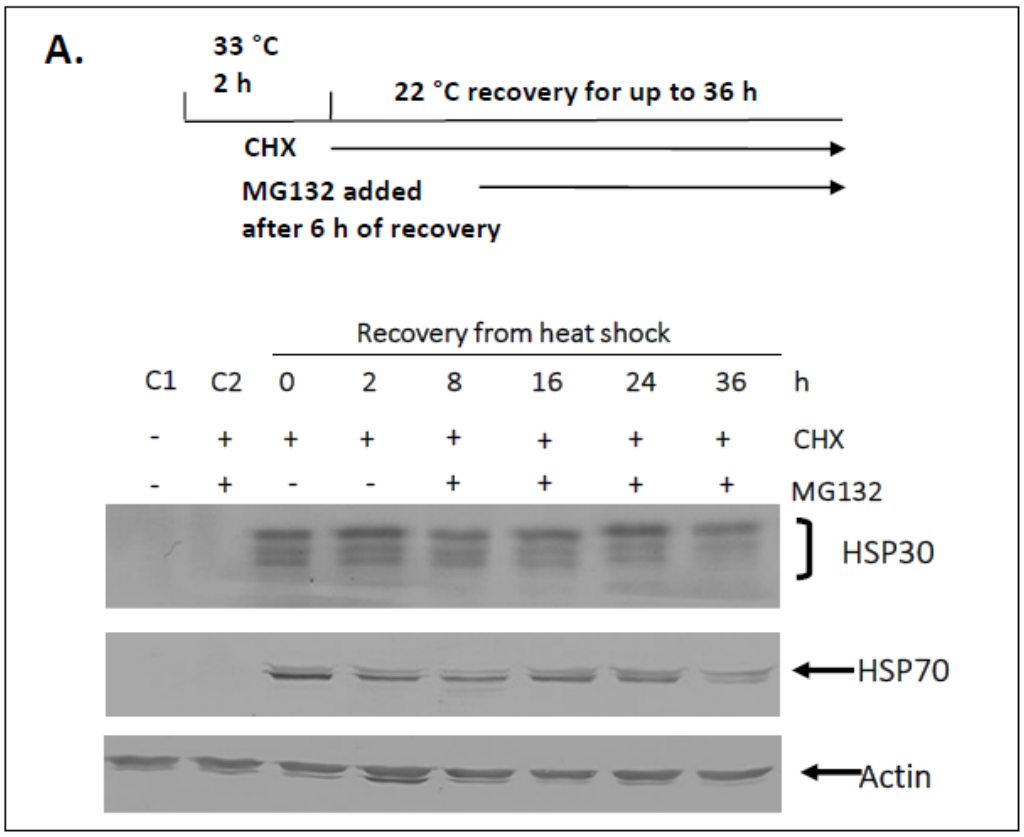
A.
33 °C
2 h
22 °C recovery for up to 36 h
CHX
MG132 added
after 6 h of recovery
Recovery from heat shock
C1 C2 0 2 8 16 24 36 h
- + + + + + + + CHX
- + - - + + + + MG132
HSP30
HSP70
Actin

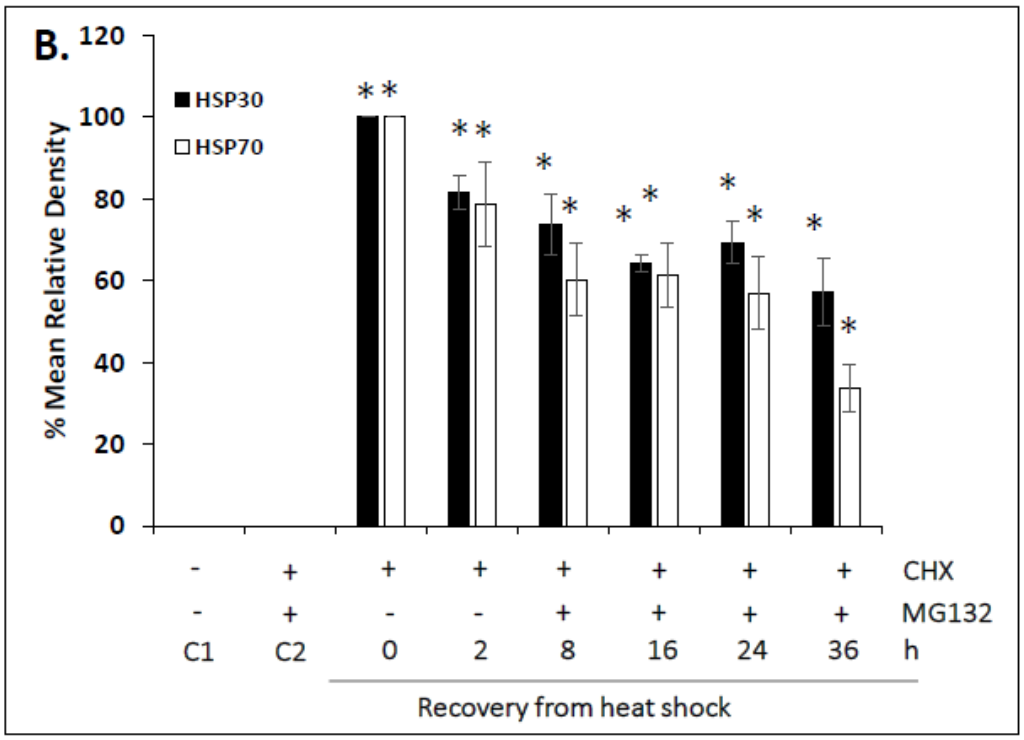
B.
% Mean Relative Density
120
100
80
60
40
20
0
HSP30
HSP70
- + + + + + + + CHX
- + - - + + + + MG132
C1 C2 0 2 8 16 24 36 h
Recovery from heat shock

followed by the addition of MG132 after 6 h of recovery. Immunoblot analysis revealed that maximum levels of HSP30 and HSP70 occurred in cells subjected to heat stress with no recovery. After 16 h of recovery from heat shock in the presence of cycloheximide and MG132, the relative levels of both HSP30 and HSP70 were approximately 64 and 61% of the maximum values, respectively. Thereafter, the relative level of HSP30 after 36 h of recovery was 57% while HSP70 was reduced to 33% of maximum value. In control experiments, cells that were incubated at 22 °C (C1) or pretreated with cycloheximide at 22 °C for 6 h and then treated with MG132 for 36 h (C2) showed no detectable levels of HSP30 or HSP70.

Immunocytochemical analysis determined that cells pretreated with cycloheximide and then incubated with MG132 displayed no HSP30 accumulation (Fig. 13). In cells recovering from heat shock, treatment with cycloheximide and MG132 revealed the continued presence of HSP30 in a granular pattern in over 60% of the cells after 36 h. Finally, examination of the F-actin organization revealed a disorganized cytoskeleton with ruffled edges in cells recovering in cycloheximide and MG132 for 8 and 24 h. This F-actin membrane ruffling decreased over time since more control-like stress fibers were visible in cells recovering for 36 h (white arrows, Fig. 13).

3.1.5 HSP30 stability and oligomerization during recovery from heat shock is regulated by p38 phosphorylation in A6 cells

Enhanced accumulation of HSP30 during recovery from stress could be due to the formation of multimeric HSP30 complexes (Ohan et al., 1998; Fernando and Heikkila, 2000; Fernando et al., 2003) that might not be readily degraded by the proteasome. To test this, we used the pyridinylimidazole drug SB203580, an inhibitor of p38 phosphorylation.

Figure 13. Localization of heat shock-induced HSP30 in cells recovering in the presence of cycloheximide plus MG132. Cells were cultured on base-washed coverslips and maintained at 22 °C (Control) or pretreated with 100 µM cycloheximide and subsequently treated with 30 µM MG132 for 36 h. Cells were also incubated at 33 °C for 2 h and subsequently allowed to recover at 22 °C in 100 µM cycloheximide for 8, 24 or 36 h with the addition of 30 µM MG132 at the 6 h time point. Actin and nuclei were stained directly with phalloidin conjugated to TRITC (red) and DAPI (blue), respectively. HSP30 was indirectly detected with an anti-HSP30 antibody and a secondary antibody conjugated to Alexa-488 (green). From left to right, the columns display fluorescence detection channels for actin, HSP30 and merger of actin, DAPI and HSP30. White arrows indicate ruffling of the F-actin cytoskeleton. The 20 µm white scale bars are indicated at the bottom right section of each panel. These results are representative of 3 separate experiments.

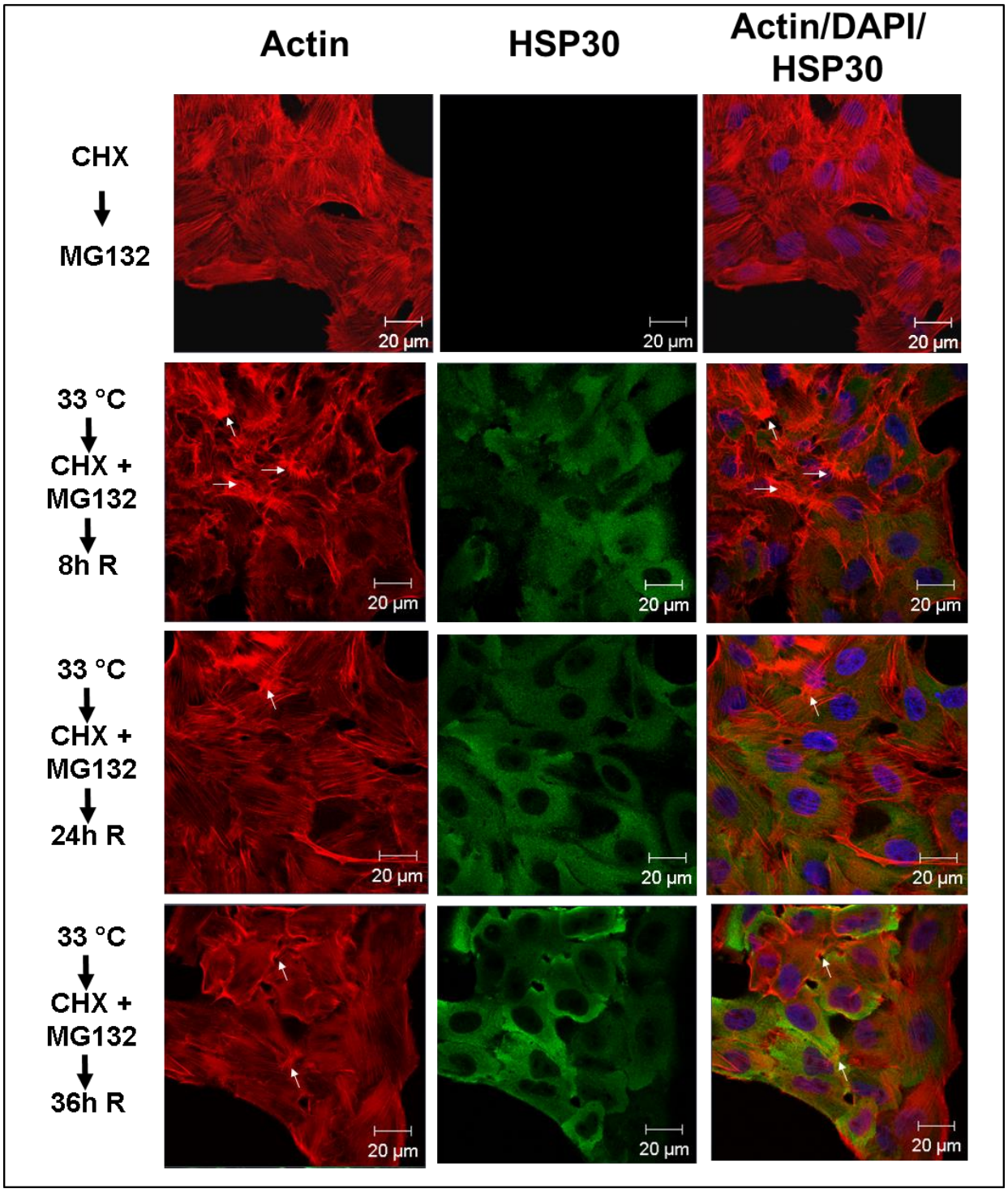
Actin
HSP30
Actin/DAPI/
HSP30
CHX
MG132
33 °C
CHX +
MG132
8h R
33 °C
CHX +
MG132
24h R
33 °C
CHX +
MG132
36h R
20 µm

P38 is part of the p38 MAP kinase pathway that was found to phosphorylate *Xenopus* HSP30 *in vitro* and resulted in the breakdown of HSP30 multimeric complexes into smaller oligomers (Fernando et al., 2003). In the present study, pretreatment of A6 cells with SB203580 resulted in enhanced accumulation of HSP30 in cells recovering from the 33 °C heat shock (Fig. 14A). However, p38 and actin levels did not change in response to SB203580 pretreatment. Additionally, in cells treated with SB203580 during recovery from heat shock for 8 or 24 h had decreased relative levels of phosphorylated p38 compared to cells without the inhibitor (Fig. 14A). Furthermore, the number of cells showing the presence of HSP30 increased from 25% to 90 % when cells were pretreated with SB203580 and allowed to recover for 8 h from a 33 °C heat treatment (Fig. 15). Similarly, only 15 % of cells recovering from 33 °C thermal stress for 24 h accumulated HSP30 in comparison to 90 % of the cells that had been pretreated with SB203580.

It was previously determined that phosphorylation of HSP30 induced the breakdown of multimeric structures into smaller units *in vitro* (Fernando et al., 2003). The presence of multimeric HSP30 complexes in A6 cells recovering from thermal stress was detected by means of native pore-exclusion limit electrophoresis followed by immunoblotting and immunodetection. In cells recovering from a 33 °C heat shock for 24 h, HSP30 complexes were detected at approximately 140 and 67 kDa (Fig. 14B). In comparison, cells pretreated with SB203580 and allowed to recover for 24 h after a 33 °C heat shock showed the presence of relatively large HSP30 complexes migrating from approximately 667 to 220 kDa (asterisks, Fig. 14B). As shown in Figure 16, immunocytochemical analysis revealed the presence of large HSP30 immunoreactivity structures (white arrows) in the cytoplasm of cells that had recovered from heat shock in the presence of SB203580 for 2 or 24 h compared

Figure 14. Effect of SB203580 on the relative levels of HSP30, p38 and phosphorylated p38 in cells recovering from thermal stress. A) A6 cells were incubated at 22 °C or 33 °C for 2 h with 2 or 24 h recovery, with (+) or without (-) SB203580 (SB) and subsequently treated with cycloheximide (CHX). Cells were harvested and total protein was analyzed by immunoblotting using anti-HSP30, anti-HSP70, anti-p38, anti-phospho p38 (p-p38) or anti-actin polyclonal antibodies as described in Materials and methods. These results are representative of 3 separate experiments. B) A6 cells were incubated 22 °C or 33 °C for 2 h with 24 h recovery, with (+) or without (-) SB203580 (SB). Cells were harvested and total protein was analyzed by native pore-exclusion limit electrophoresis. This was followed by immunoblotting using the anti-HSP30 polyclonal antibody as described in Materials and methods. Approximate molecular mass in kDa are indicated on the left of the figure. Asterisks with arrows indicate the position of HSP30 complexes. These results are a representative of 4 separate experiments.

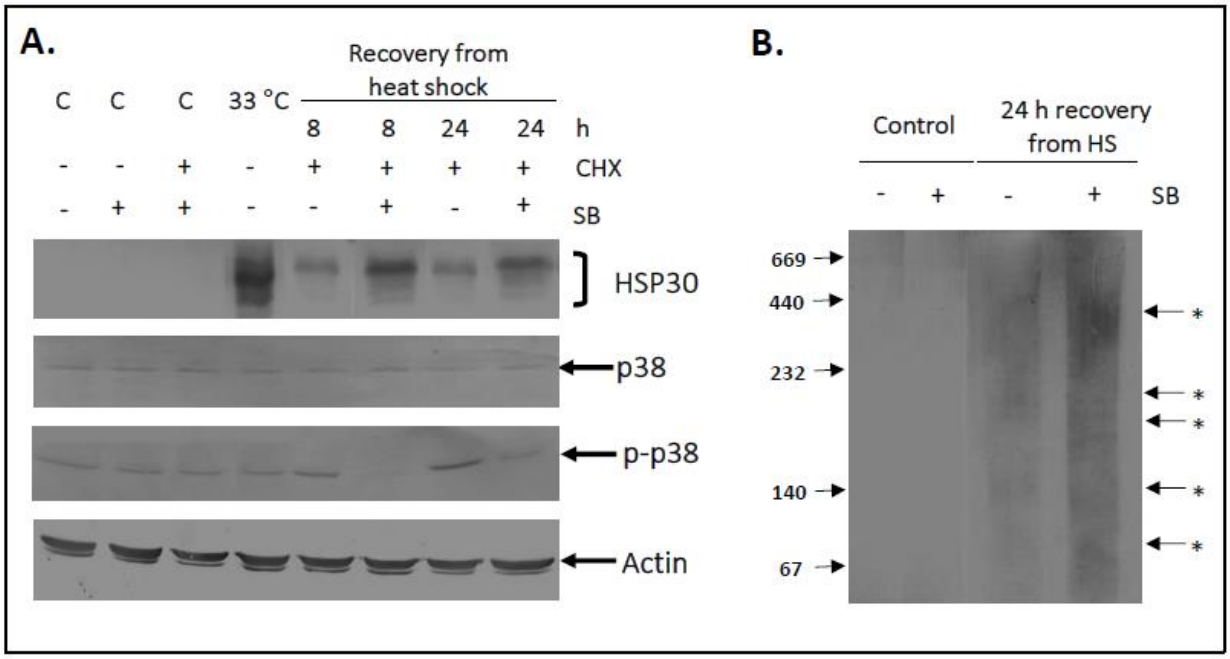
A.
Recovery from heat shock
C C C 33 °C 8 8 24 24 h
- - + - + + + + CHX
- + + - - + - + SB
HSP30
p38
p-p38
Actin
B.
Control
24 h recovery from HS
- + - + SB
669
440
232
140
67
*
*
*
*
*

Figure 15. Localization of HSP30 in cells treated with SB203580 and cycloheximide during recovery from thermal stress. A6 cells were incubated at 22 °C or 33 °C for 2 h with 2 or 24 h recovery, with (+) or without (-) SB203580 (SB) and subsequently treated with cycloheximide (CHX). Actin and nuclei were stained directly with phalloidin conjugated to TRITC (red) and DAPI (blue), respectively. HSP30 was indirectly detected with an anti-HSP30 antibody and a secondary antibody conjugated to Alexa-488 (green). The 20 µm white scale bars are indicated at the bottom right section of each panel. These results are representative of 3 separate experiments.

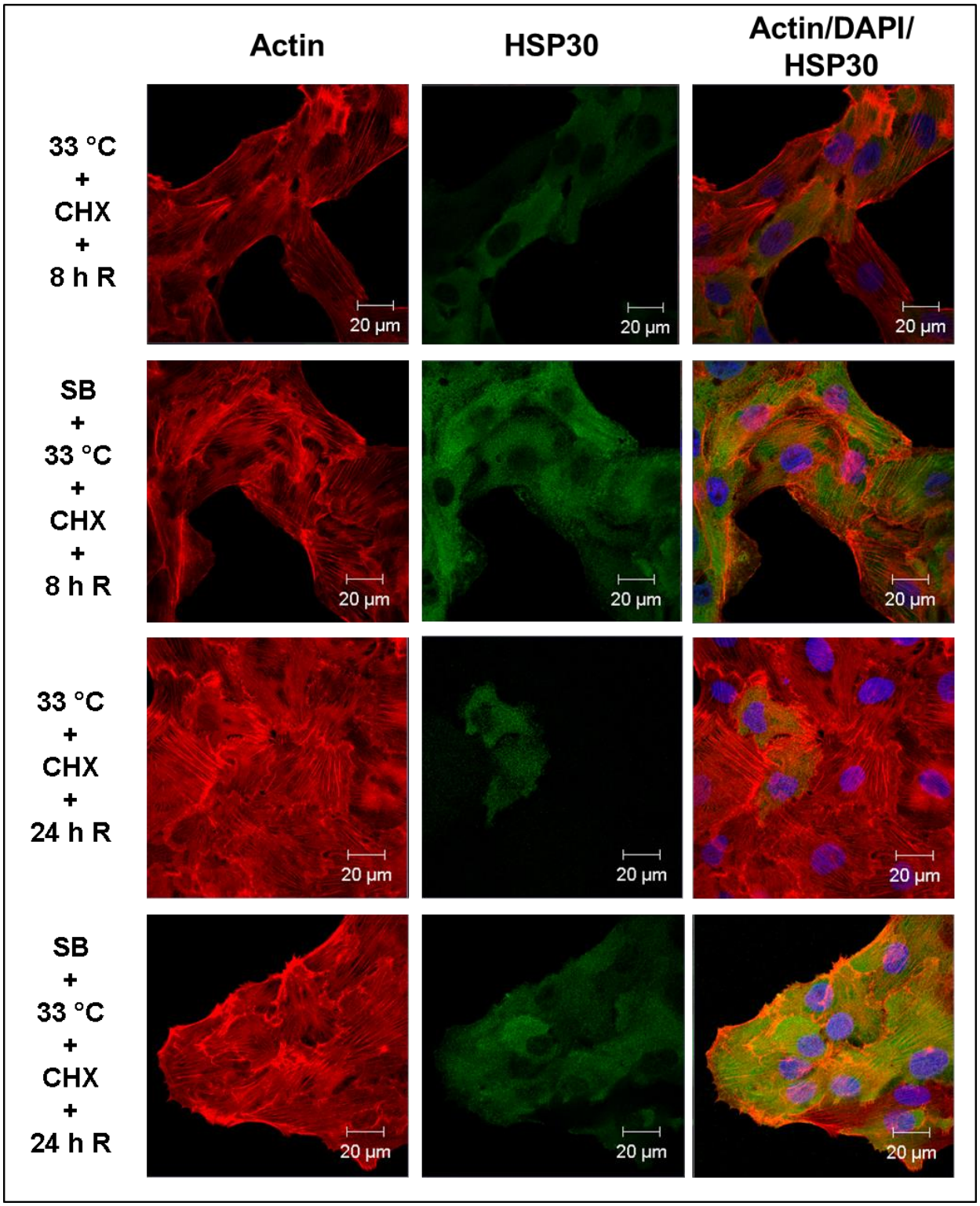
Actin
HSP30
Actin/DAPI/
HSP30
33 °C
+
CHX
+
8 h R
SB
+
33 °C
+
CHX
+
8 h R
33 °C
+
CHX
+
24 h R
SB
+
33 °C
+
CHX
+
24 h R
20 µm

to cells not treated with the phosphorylation inhibitor. In some cells, these large structures surrounded HSP30 non-immunoreactive areas in the cytoplasm. In previous studies, we detected the presence of relatively large HSP30 immunoreactivity complexes that were suggested to be associated with possible aggresome-like structures (Young and Heikkila, 2010; Khan and Heikkila, 2011). Given these findings, we employed a ProteoStat aggresome assay (Shen et al., 2011; Nakajima and Suzuki, 2013) to detect the presence of aggresome-like structures in A6 cells recovering from heat shock. As shown in Figure 16, cells that had recovered for 2 h after heat shock displayed a relatively low level of aggresome-like structures, which increased in size and number in the perinuclear region when the recovery period was extended to 24 h. The presence of SB203580 during recovery from heat shock resulted in an increase in the size of these aggresome-like structures. A careful immunocytochemical analysis through the use of Z-stacking revealed that HSP30 enveloped some of these aggresome-like structures as well as occurring within them. In control cells, aggresome-like structures were not detected (data not shown).

3.2 Proteasome inhibitors induce cytosolic and ER molecular chaperones

3.2.1 Effect of celastrol, withaferin A, MG132 and A23187 on ubiquitinated protein accumulation and inhibition of chymotrypsin-like activity

In the previous section, an association of HSP30 with aggresome-like structures during recovery from heat shock was detected. Since aggresomes are produced in response to proteasomal inhibition, I examined in detail the effect of various proteasomal inhibitors on the relative levels of cytoplasmic and endoplasmic reticulum chaperone levels in the *Xenopus* A6 cell line. Initial experiments were performed to examine the effect of 3 proteasomal

Figure 16. Association of HSP30 multimeric complexes with aggresome-like structures in cells recovering from heat stress. A6 cells were incubated at 33 °C for 2 h with 2 or 24 h recovery, with (+) or without (−) SB203580 (SB). ProteoStat aggresome detection kit was used to directly stain aggresome-like structures and nuclei were stained directly DAPI (blue). HSP30 was detected indirectly with an anti- HSP30 antibody and a secondary antibody conjugated to Alexa-488 (green). From left to right, the columns display fluorescence detection channels for HSP30, ProteoStat assay, and merger of ProteoStat assay, DAPI and HSP30. The white arrows indicate large HSP30 immuno-reactivity structures and dense aggresome-like structures. In the bottom two rows, the white rectangle contains aggresome-like structures, which are duplicated and enlarged at the bottom left corner (inset) of each panel. The 20 μm white scale bars are indicated at the bottom right section of each panel. These results are representative of 3 separate experiments.

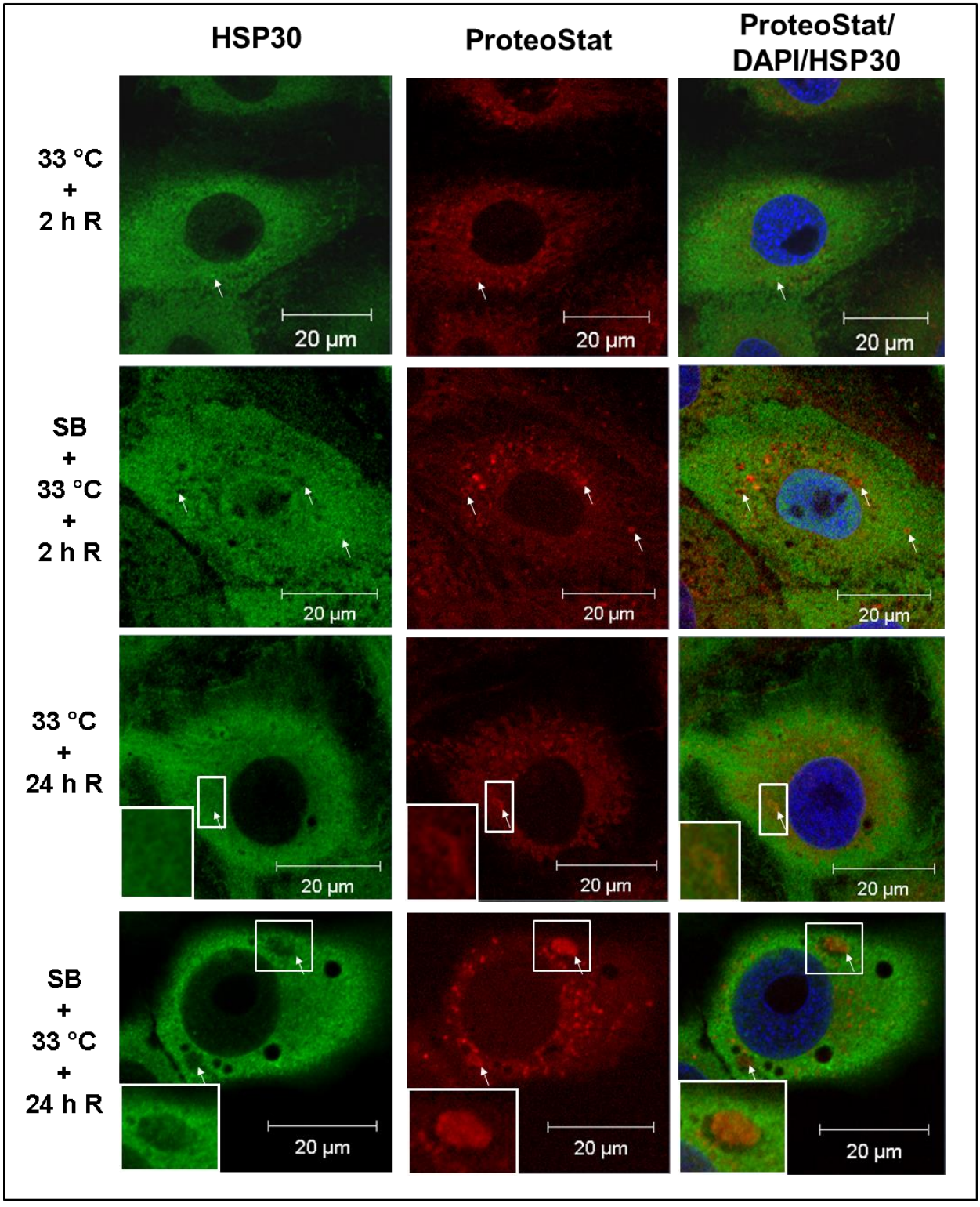
HSP30
ProteoStat
ProteoStat/
DAPI/HSP30
33 °C
+
2 h R
SB
+
33 °C
+
2 h R
33 °C
+
24 h R
SB
+
33 °C
+
24 h R
20 µm

inhibitors, MG132, celastrol and withaferin A on the relative levels of ubiquitinated proteins and proteasomal chymotrypsin (CT)-like enzyme activity. The concentrations of the proteasomal inhibitors employed in this study were determined previously to induce HSP30 and HSP70 accumulation in either *Xenopus* A6 cells or mammalian cells (Yang et al., 2007; Young and Heikkila, 2010; Walcott and Heikkila, 2010).

Immunoblot analysis revealed that relative levels of ubiquitinated proteins in cells treated with 2.5 μM celastrol or 5 μM withaferin A for 16 h or 30 μM MG132 for 24 h at 22 °C were 5 to 6-fold higher than observed in control cells (Fig. 17). However, treatment of cells with 7 μM A23187, a calcium ionophore and activator of the unfolded protein response (Drummond et al., 1987; Winning et al., 1989; Li et al., 1993; Miskovic and Heikkila, 1999), for 24 h did not result in a significant increase in ubiquitinated protein levels (Fig. 17). Furthermore, treatment of cells with higher concentrations of A23187 (10 to 14 μM) did not result in enhanced accumulation of ubiquitinated protein relative to control (data not shown). Additionally, cells treated with 7 μM A23187 for 24 h, 2.5 μM celastrol for 16 h, 30 μM MG132 for 24 h or 5 μM withaferin A for 16 h showed a decrease in CT-like activity of 15, 66, 82 and 65 %, respectively, as shown in Fig. 17C.

3.2.2 Proteasome inhibitors induced *hsp30, hsp70, bip* mRNA and HSP30, HSP70, BiP and GRP94 accumulation in A6 cells

The relative levels of *hsp30*, *hsp70*, *bip* and *eIf1α* mRNA, in response to treatment with proteasome inhibitors or A23187 was determined using Northern blot analysis. Previously our laboratory reported that A6 cells treated with classical proteasome inhibitors including MG132 and lactacystin induced *hsp30* mRNA accumulation (Young and Heikkila,

Figure 17. Effect of A23187, celastrol, withaferin A and MG132 on relative levels of ubiquitinated protein and chymotrypsin-like activity. A) Cells were maintained at 22 °C, treated with 7 μM A23187 for 24 h (A23187), treated with 2.5 μM celastrol for 16 h (CEL), treated with 5 μM withaferin A for 16 h (WA) or treated with 30 μM MG132 for 24 h (MG132) at 22 °C. Protein was transferred to nitrocellulose membrane from SDS polyacrylamide gels and probed with a mouse anti-ubiquitin monoclonal antibody as described in Materials and methods. The positions of molecular mass standards in kDa are shown in the first lane (M). These data are representative of three separate experiments. B) Image J software was used to perform densitometric analysis of the signal intensity for ubiquitinated protein bands of western blot images as described in Materials and methods. The data are expressed as a percentage of the lane with maximum density (MG132) while the standard error is represented by vertical error bars. The level of significance of the differences between samples was calculated by one-way ANOVA with a Tukey's post-test. Significant differences between the control cells and A6 cells treated with 2.5 μM celastrol (16 h), 5 μM withaferin A (16 h) or 30 μM MG132 (24 h), are indicated as * ($p < 0.05$). These data are representative of three separate experiments. C) Effect of A23187, celastrol, withaferin A or MG132 on chymotrypsin (CT)-like activity of A6 cells. Cells were maintained at 22 °C, treated with 7 μM A23187 for 24 h (A23187), treated with 2.5 μM celastrol for 16 h (CEL), treated with 5 μM withaferin A for 16 h (WA) or treated with 30 μM MG132 for 24 h (MG132) at 22 °C. Cells were suspended in L-15 media and 15,000 cells per well were placed in a 96-well plate. A cell-based CT-like assay was used to monitor the proteolytic activity as described in Materials and methods. The CT-like activity was measured and expressed as a percentage of the CT-like activity observed in control cells. The

level of significance of the differences between samples was calculated by one-way ANOVA with a Tukey's post-test. Significant differences between control cells and cells treated with celastrol, withaferin A or MG132 are indicated as * ($p < 0.05$).

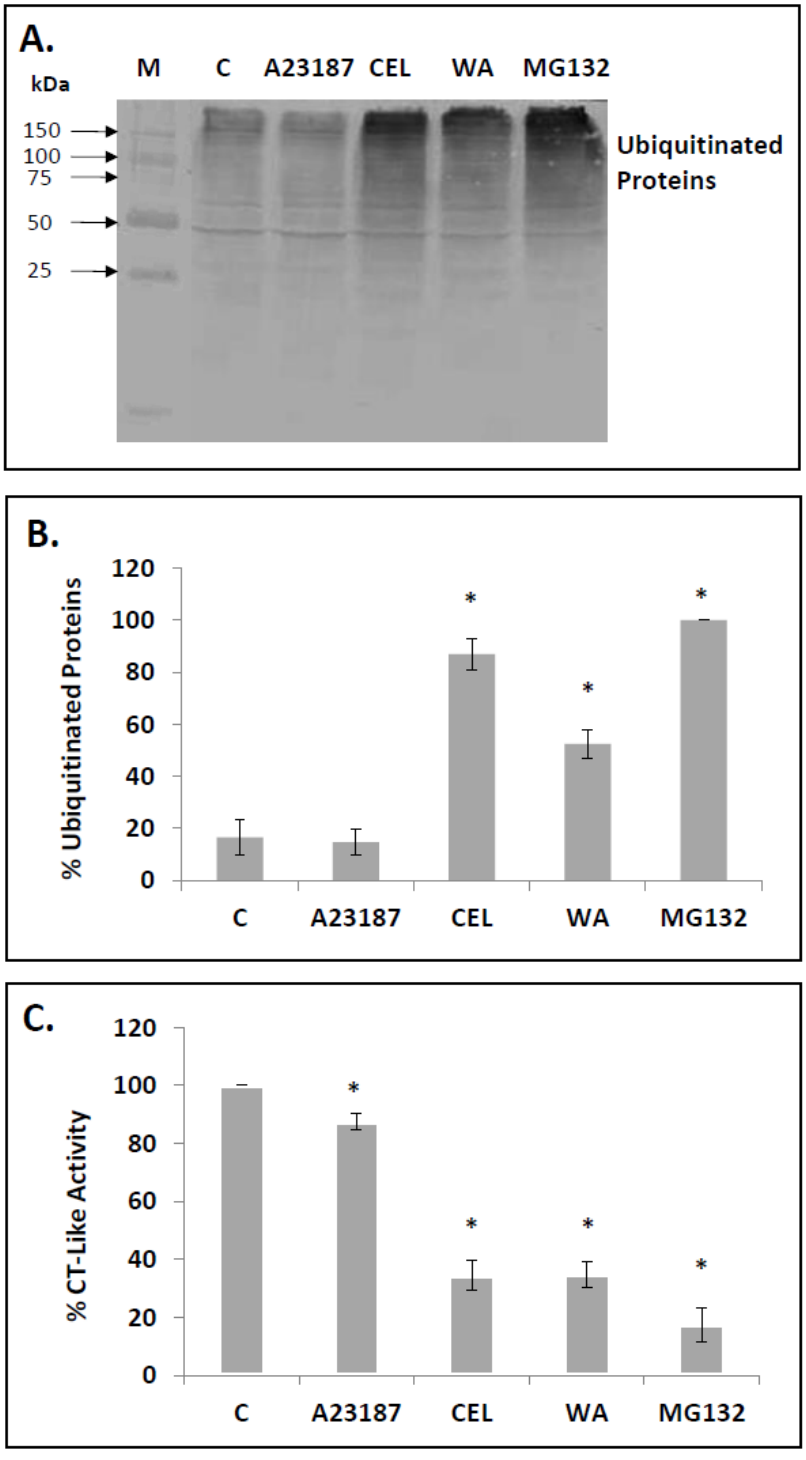

2010). In the present study, an increased accumulation of *hsp30* and *hsp70* mRNA was observed in cells treated with 2.5 µM celastrol, 5 µM withaferin A or 30 µM MG132 but not with A23187 when compared to control cells (Fig. 18A). Moreover, as shown in Figure 18A, enhanced levels of *bip* mRNA were detected in cells treated with 7 µM A23187, 2.5 µM celastrol, 5 µM withaferin A or 30 µM MG132 in comparison to control cells. Densitometric analysis revealed a 7-, 5-, 5- or 6-fold increase in *bip* mRNA levels in cells treated with A23187, celastrol, withaferin A or MG132, respectively (Fig. 18B). The relative levels of *eIf1α* mRNA remained unchanged throughout the course of these treatments.

HSP30, HSP70, BiP and GRP94 protein accumulation in response to proteasome inhibitors or A23187 treatment of A6 cells was determined by immunoblot analysis. Treatment of A6 cells with 2.5 µM celastrol, 5 µM withaferin A or 30 µM MG132 for 24 h resulted in significantly enhanced accumulation of HSP30 and HSP70 accumulation in comparison to control cells (Fig. 19). Treatment with 7 µM A23187 did not induce any HSP30 or HSP70 accumulation. In comparison, 7 µM A23187 induced a 2-fold accumulation of BiP and GRP94. This study also determined that treatment of cells with 2.5 µM celastrol, 5 µM withaferin A or 30 µM MG132 for 24 h resulted in 2-, 2- and 3-fold increases in BiP accumulation respectively (Fig. 19). These stressors also significantly increased GRP94 accumulation in comparison to control cells (Fig 19).

3.2.3 Temporal pattern of proteasomal inhibitor-induced HSP30, HSP70, BiP and GRP94 accumulation

In time course studies of A6 cells treated with 30 µM MG132 or 2.5 µM celastrol at 22 °C, an enhanced accumulation of HSP30, HSP70, BiP and GRP94 was first detected at 8

Figure 18. Effect of A23187, celastrol, withaferin A and MG132 on *hsp30, hsp70, bip* and *eIF1α* mRNA levels. A) Cells were maintained at 22 °C or treated with 7 μM A23187 for 24 h (A23187), 2.5 μM celastrol for 16 h (CEL), 5 μM withaferin A for 16 h (WA) or 30 μM MG132 for 24 h (MG132) at 22 °C. Cells were harvested and total RNA was isolated. Total RNA (10 μg) was analyzed by Northern hybridization analysis using *hsp30, hsp70, bip* and *eIF1α* antisense riboprobes as described in Materials and methods. These data are representative of three separate experiments. B) Image J software was used to perform densitometric analysis of the signal intensity for *hsp30* (black), *hsp70* (white) and *bip* (grey) mRNA levels of northern blot images as described in Materials and methods. The data are expressed as a percentage of the maximum signal (30 μM MG132 for 24 h for *hsp30* and *hsp70* and 7 μM A23187 for 24 h for *bip*). The standard error is represented by vertical error bars. The level of significance of the differences between samples was calculated by one-way ANOVA with a Tukey's post-test. Significant differences between the control cells and treated cells are indicated as * ($p < 0.05$).

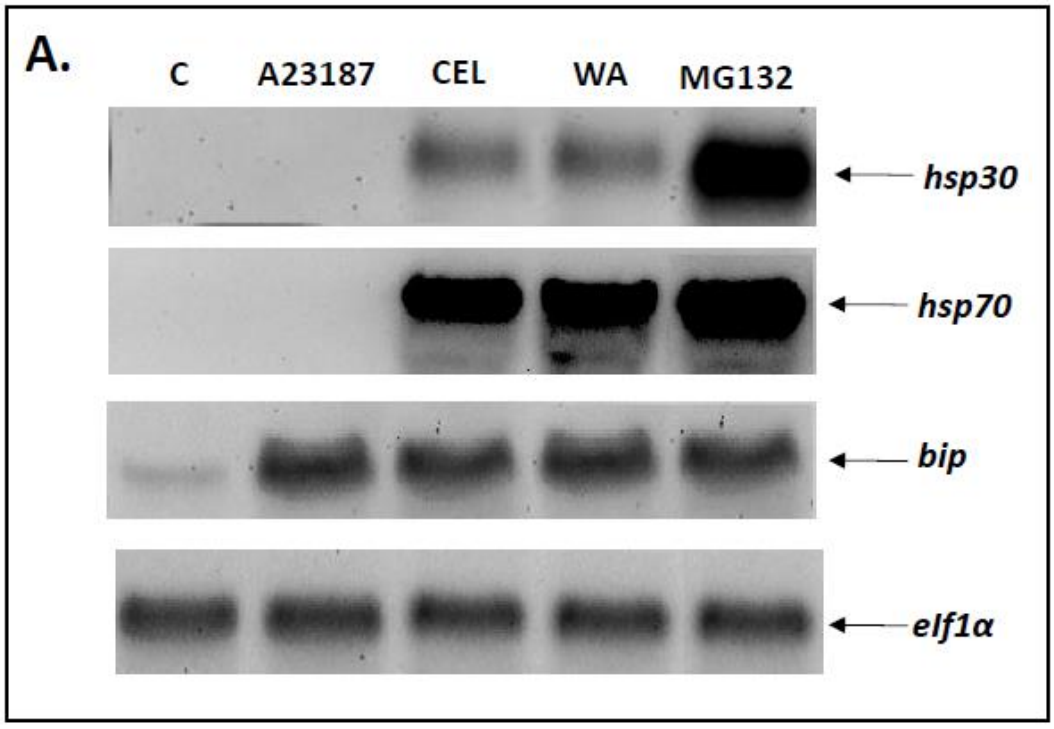
A.
C
A23187
CEL
WA
MG132
hsp30
hsp70
bip
elf1α

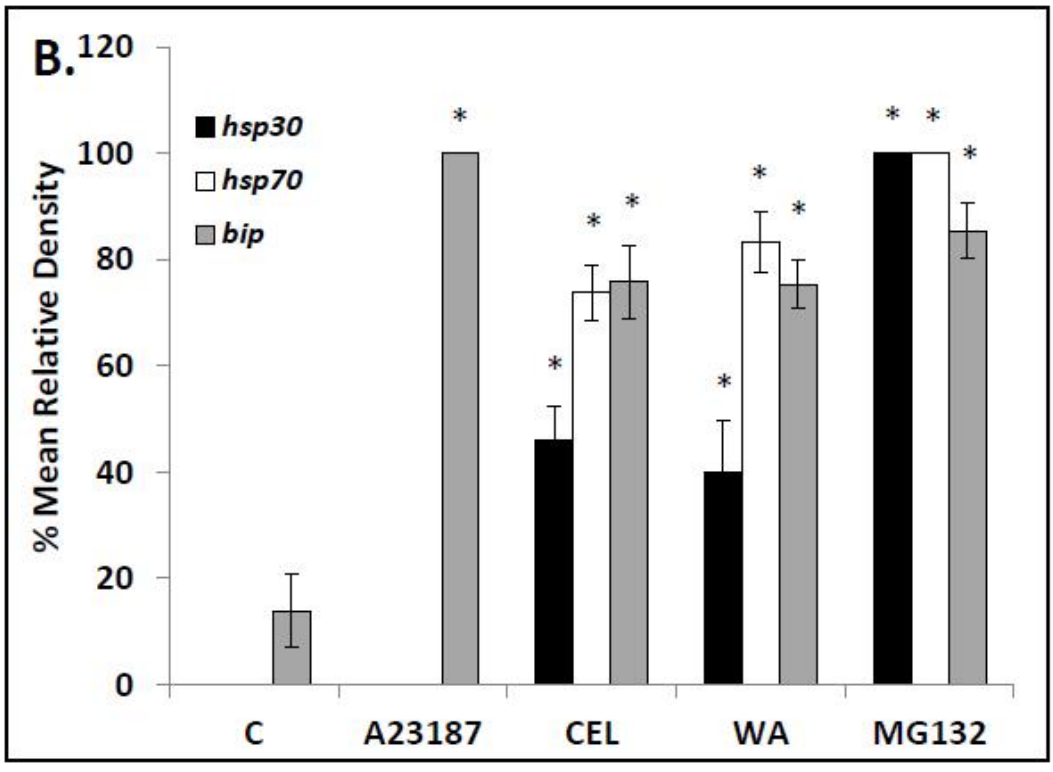
B.
% Mean Relative Density
120
100
80
60
40
20
0
hsp30
hsp70
bip
C
A23187
CEL
WA
MG132

Figure 19. Effect of A23187 and proteasome inhibitors on HSP30, HSP70, BiP and GRP94 accumulation. A) Cells were maintained at 22 °C or treated with 7 μM A23187 for 24 h (A23187), 2.5 μM celastrol for 16 h (CEL), 5 μM withaferin A for 16 h (WA) or 30 μM MG132 for 24 h (MG132) at 22 °C. Cells were harvested and total protein was isolated. Forty μg of different protein samples were then analyzed by Western blot analysis using anti-HSP30, anti-HSP70, anti-BiP, anti-GRP94 or anti-actin antibodies as described in Material and methods. These data are representative of three separate experiments. B & C) Image J software was used to perform densitometric analysis of the signal intensity for HSP30 (black; panel B), HSP70 (white; panel B), BiP (black; panel C) and GRP94 (white; panel C) protein bands of western blot images as described in Materials and methods. The data are expressed for each treatment as percentage of the maximum signal (30 μM MG132 for 24 h for HSP30 and HSP70 accumulation; Panel B or as a ratio to control levels (for BiP and GRP94 accumulation; Panel C). The standard error is represented by vertical error bars. The level of significance of the differences between samples was calculated by one-way ANOVA with a Tukey's post-test. Significant differences between the control cells and treated cells are indicated as * ($p < 0.05$) or Δ ($p < 0.10$).

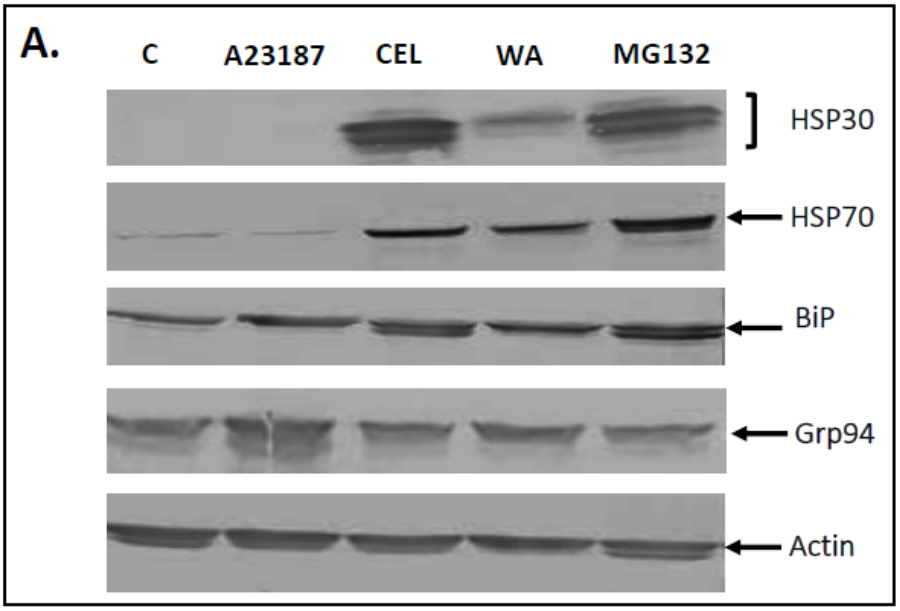
A.
C
A23187
CEL
WA
MG132
HSP30
HSP70
BiP
Grp94
Actin

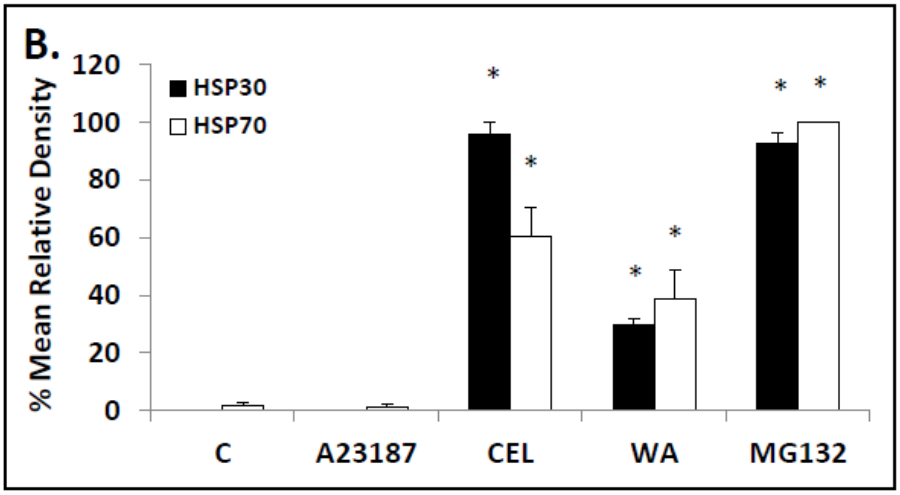
B.
% Mean Relative Density
120
100
80
60
40
20
0
HSP30
HSP70
C
A23187
CEL
WA
MG132

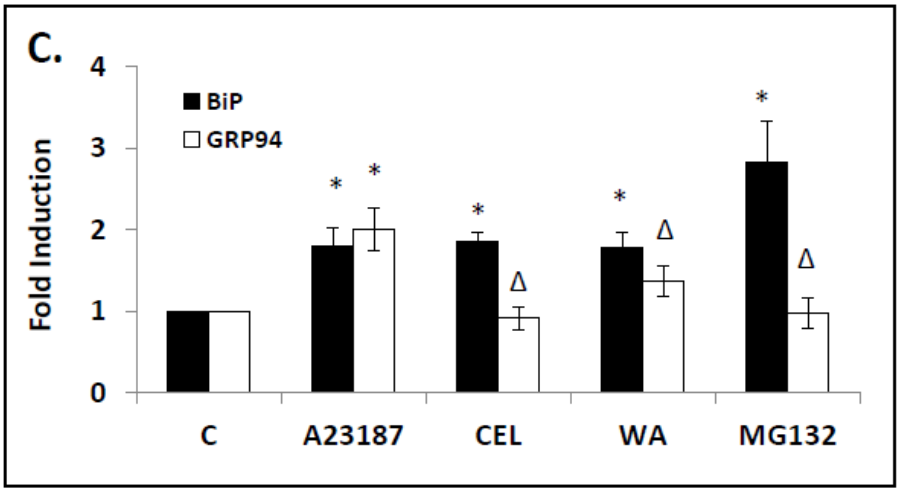
C.
Fold Induction
4
3
2
1
0
BiP
GRP94
C
A23187
CEL
WA
MG132

h (Fig. 20, 21). Thereafter, levels of HSP30 increased 5- or 3-fold in MG132 or celastrol-treated cells, respectively, in comparison to the 8 h treatment. In contrast, the relative level of HSP70 was elevated 20-fold, while BiP levels increased only 2- to 2.5-fold in cells treated with MG132 or celastrol for 24 h (Fig. 20, 21). MG132 and celastrol treatments also significantly increased GRP94 accumulation in A6 cells, while actin levels remained constant. Similar results for HSP30 accumulation were observed in cells treated with 5 μM withaferin A (Fig. 22). Significantly enhanced accumulation was initially observed in cells treated for 8 h and increased 3-fold in cells treated for 24 h. In contrast, a slightly different temporal phenomenon with respect to HSP70 and BiP accumulation was found for cells treated with 5 μM withaferin A. Withaferin A induced only a 1.5-fold increase in HSP70 accumulation at 24 h compared to cells treated with withaferin A for 8 h (Fig 22). Additionally, significantly enhanced accumulation (1.5-fold) in BiP levels were not observed in cells until 16 or 24 h of withaferin A treatment (Fig. 22). However, similar to celastrol, MG132 and WA also induced expression of GRP94 to significantly higher levels compared to control cells. Actin levels were not affected by these treatments.

3.2.4 Intracellular localization and accumulation of HSP30 and BiP in proteasome inhibited A6 cells

As shown in Figures 23 and 24, the intracellular localization of HSP30 and BiP was examined in cells treated with A23187, MG132, celastrol or withaferin A using immunocytochemistry and laser scanning confocal microscopy (LSCM). Comparable studies with HSP70 or GRP94 were not carried out since these antibodies were unable to specifically detect HSP70 or GRP94 by immunocytochemistry, even though they easily detected these

Figure 20. Temporal pattern of MG132-induced HSP30, HSP70, BiP and GRP94 accumulation. A) Cells were maintained at 22 °C or exposed to 30 μM MG132 for time intervals ranging from 2 to 24 h. Cells were harvested and total protein was isolated. The different protein samples were then analyzed by immunoblot analysis. These data are representative of three separate experiments. B & C) Image J software was used to perform densitometric analysis of the signal intensity for HSP30 (black; panel B), HSP70 (white; panel B), BiP (black; panel C), GRP94 (white; panel c) protein bands of western blot images as described in Materials and methods. The data are expressed for each treatment as a percentage of the maximum band (30 μM MG132 for 24 h for HSP30 and HSP70 accumulation) or as a ratio to control levels (for BiP and GRP94 accumulation). The standard error is represented by vertical error bars. The level of significance of the differences between samples was calculated by one-way ANOVA with a Tukey's post-test. Significant differences between the control cells and MG132-treated cells are indicated as * ($p < 0.05$) or Δ ($p < 0.10$).

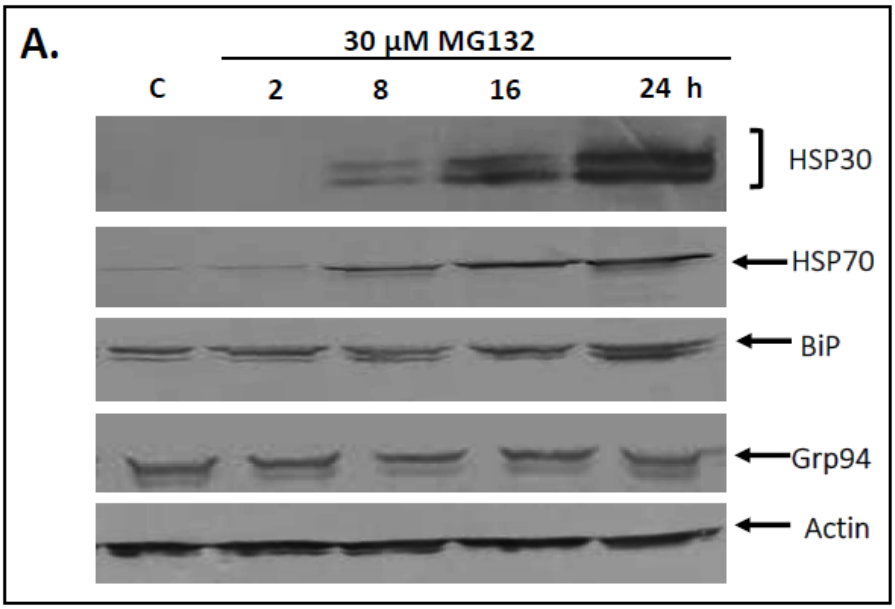
A.
30 μM MG132
C
2
8
16
24 h
HSP30
HSP70
BiP
Grp94
Actin

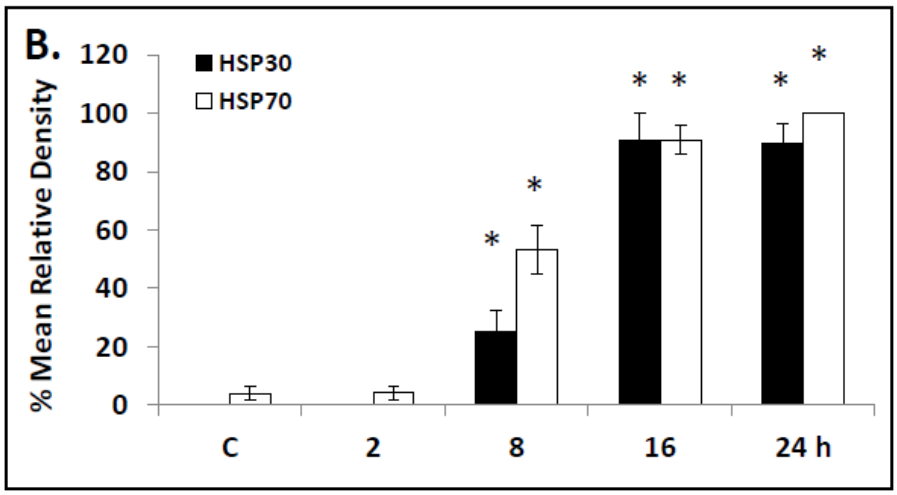
B.
% Mean Relative Density
HSP30
HSP70
120
100
80
60
40
20
0
C
2
8
16
24 h

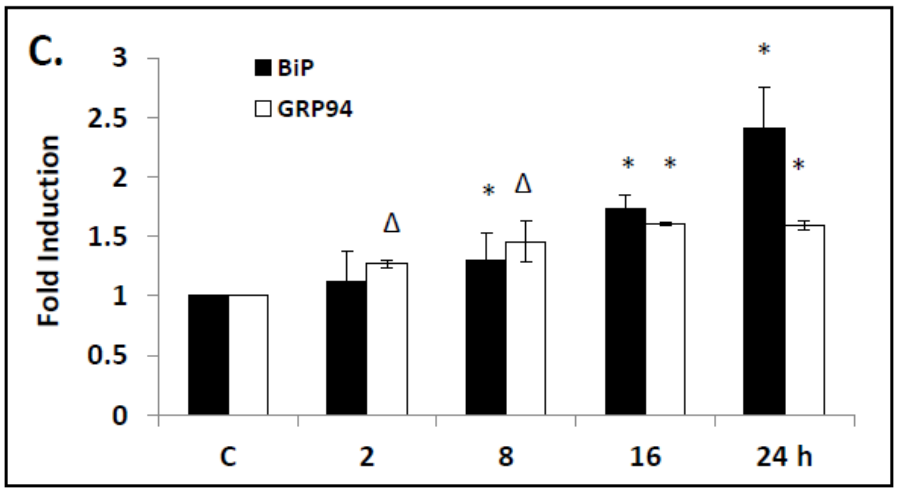
C.
Fold Induction
BiP
GRP94
3
2.5
2
1.5
1
0.5
0
C
2
8
16
24 h

Figure 21. Time course of celastrol-induced HSP30, HSP70, BiP and GRP94 accumulation. A) Cells were maintained at 22 °C or exposed to 2.5 μM celastrol for time intervals ranging from 2 to 24 h at 22 °C. Cells were harvested and total protein was isolated and then analyzed by immunoblot analysis. These data are representative of three separate experiments. B & C) Image J software was used to perform densitometric analysis of the signal intensity for HSP30 (black; panel B), HSP70 (white; panel B), BiP (black; panel C) or GRP94 (white; panel C) protein bands of western blot images as described in Materials and methods. The data are expressed as percentage of the maximum signal (2.5 μM celastrol for 24 h for HSP30 or HSP70 accumulation) or as a ratio to control levels (for BiP and GRP94 accumulation). The standard error is represented by vertical error bars. The level of significance of the differences between samples was calculated by one-way ANOVA with a Tukey's post-test. Significant differences between the control cells and celastrol-treated cells are indicated as * ($p < 0.05$) or Δ ($p < 0.10$).

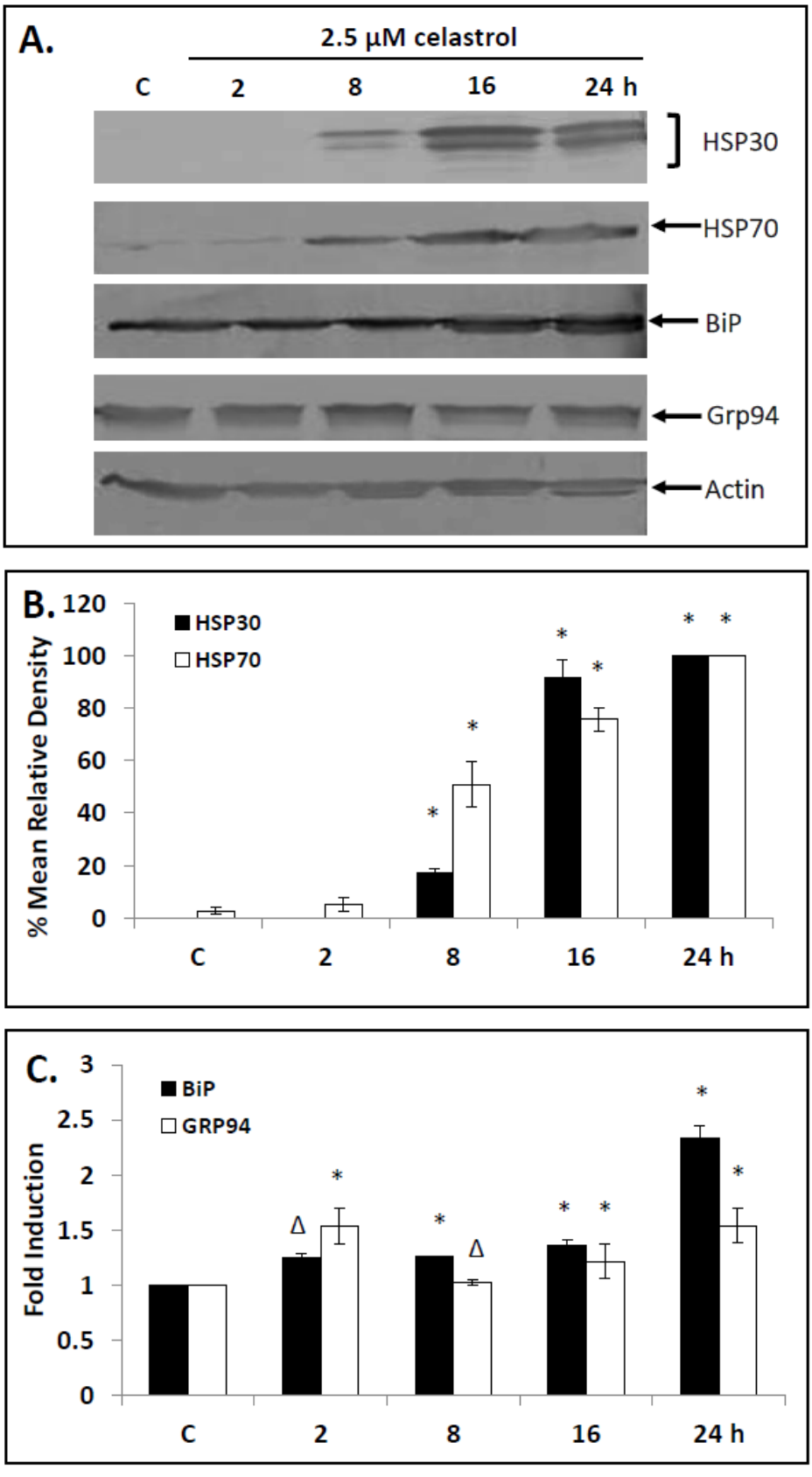
A.
2.5 µM celastrol
C
2
8
16
24 h
HSP30
HSP70
BiP
Grp94
Actin
B.
% Mean Relative Density
HSP30
HSP70
120
100
80
60
40
20
0
C
2
8
16
24 h
C.
Fold Induction
BiP
GRP94
3
2.5
2
1.5
1
0.5
0
C
2
8
16
24 h

Figure 22. Time course of withaferin A-induced HSP30, HSP70, BiP and GRP94 accumulation. A) Cells were maintained at 22 °C or exposed to 5 μM withaferin A for time intervals ranging from 2 to 24 h at 22 °C. Cells were harvested and total protein was isolated and then analyzed by immunoblot analysis. These data are representative of three separate experiments. B) Image J software was used to perform densitometric analysis of the signal intensity for HSP30 (black; panel B), HSP70 (white; panel B), BiP (black; panel C) and GRP94 (white; panel C) protein bands of western blot images as described in Materials and methods. The data are expressed as percentage of the maximum signal (5 μM withaferin A for 24 h for HSP30 and HSP70) or as a ratio to control levels (for BiP and GRP94 accumulation). The standard error is represented by vertical error bars. The level of significance of the differences between samples was calculated by one-way ANOVA with a Tukey's post-test. Significant differences between the control cells and withaferin A-treated cells are indicated as * ($p < 0.05$) or Δ ($p < 0.10$).

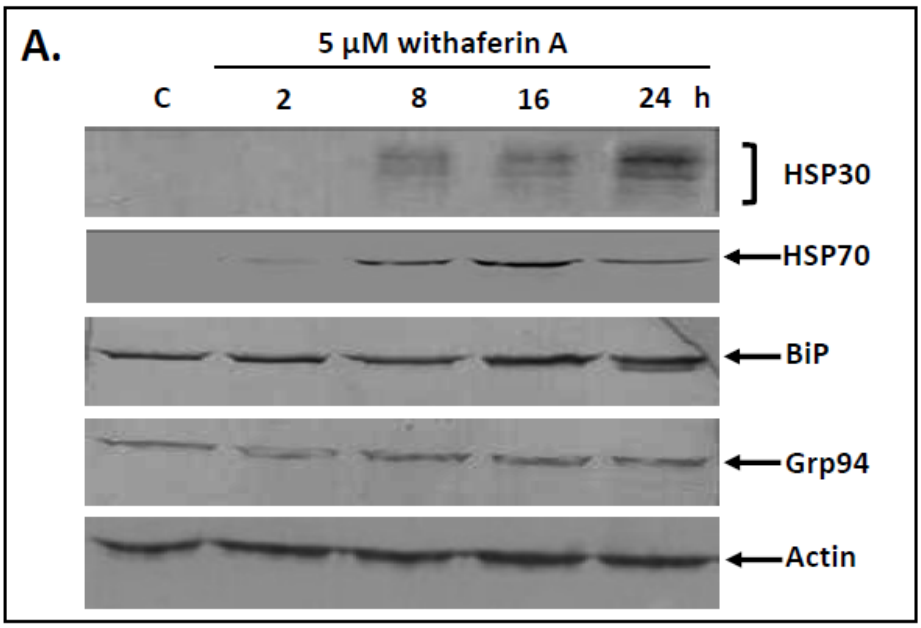
A.
5 μM withaferin A
C
2
8
16
24 h
HSP30
HSP70
BiP
Grp94
Actin

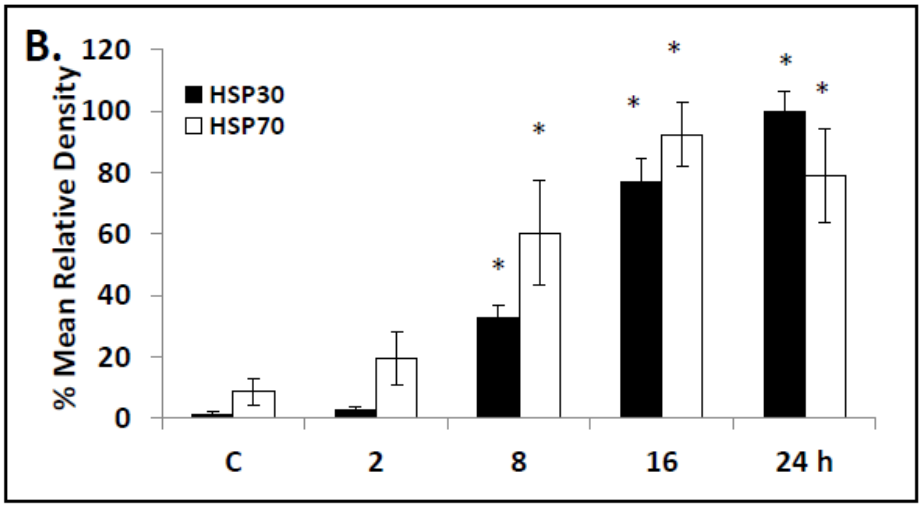
B.
% Mean Relative Density
120
100
80
60
40
20
0
HSP30
HSP70
C
2
8
16
24 h

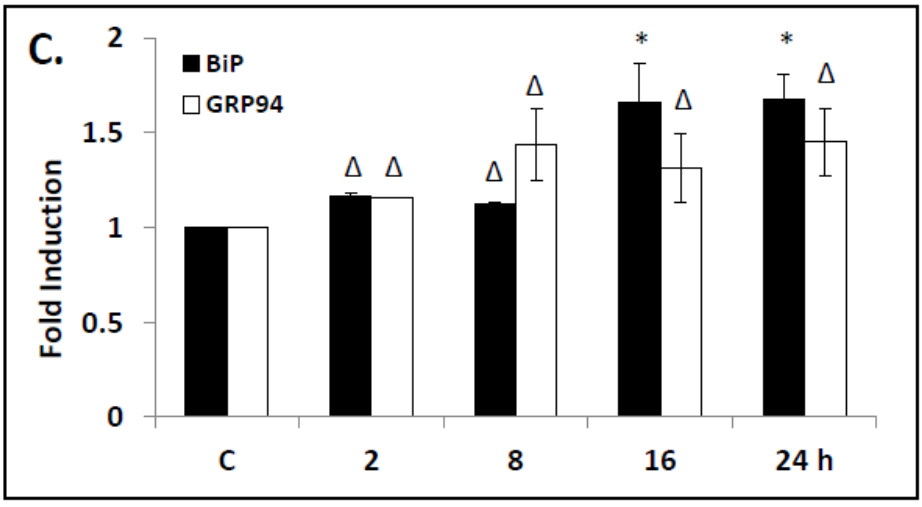
C.
Fold Induction
2
1.5
1
0.5
0
BiP
GRP94
C
2
8
16
24 h

chaperones in immunoblot analyses. Cells treated with 30 µM MG132 for 24 h, 2.5 µM celastrol for 8 h or 5 µM withaferin A for 16 h at 22 °C resulted in the localization of HSP30 in the cytoplasm in a granular or punctuate pattern. HSP30 was not detectable in control cells maintained at 22 °C or cells treated with 7 µM A23187 for 24 h (Fig. 23). In comparison, A6 cells maintained at 22 °C displayed BiP localization diffusely throughout the cytoplasm (Fig. 24). Cells treated with 7 µM A23187, 30 µM MG132 for 24 h, 2.5 µM or 5 µM withaferin A for 16 h at 22 °C resulted in enhanced accumulation of BiP primarily in the cytoplasm in a punctate pattern and occasionally at the periphery of the cell membrane in comparison to control cells. Additionally, in withaferin A-treated cells relatively large BiP staining structures were found at the periphery of the nucleus in comparison to cells treated with A23187, which demonstrated intense BiP staining in the perinuclear region. Examination of general morphology and F-actin organization revealed that cells exposed to A23187, MG132 or withaferin A displayed intact cytoskeleton and visible actin stress fibers, similar to control cells. However, cells treated with 2.5 µM celastrol for 8 h displayed a collapse of the cytoskeleton in most cells while BiP accumulation was found diffusely throughout the cytoplasm with enhanced levels toward the periphery of the cell.

3.2.5 Withaferin A and celastrol induce heme oxygenase-1 (HO-1) accumulation in a time and concentration dependent manner

In an ancillary study, stress-induced HSP30 accumulation in A6 cells was also compared with the accumulation of the stress-induced enzyme, heme oxygenase-1 (HO-1). HO-1 is involved in heme catabolism into biliverdin which is then further converted to

Figure 23. Intracellular localization of HSP30 in response to proteasome inhibition. Cells were grown on glass coverslips and were maintained at 22 °C or treated with 7 μM A23187 or 30 μM MG132 for 24 h, 2.5 μM celastrol (CEL) for 8 h or 5 μM withaferin A (WA) for 16 h at 22 °C. Actin and nuclei were stained directly with phalloidin conjugated to TRITC (red) and DAPI (blue), respectively. HSP30 was indirectly detected with an anti-*Xenopus* HSP30 antibody and a secondary antibody conjugated to Alexa-488 (green). From left to right the columns display fluorescence detection channels for actin, BiP and merger of actin, DAPI and BiP. The 20-μm white scale bars are indicated at the bottom right section of each panel. These results are representative of 3 different experiments.

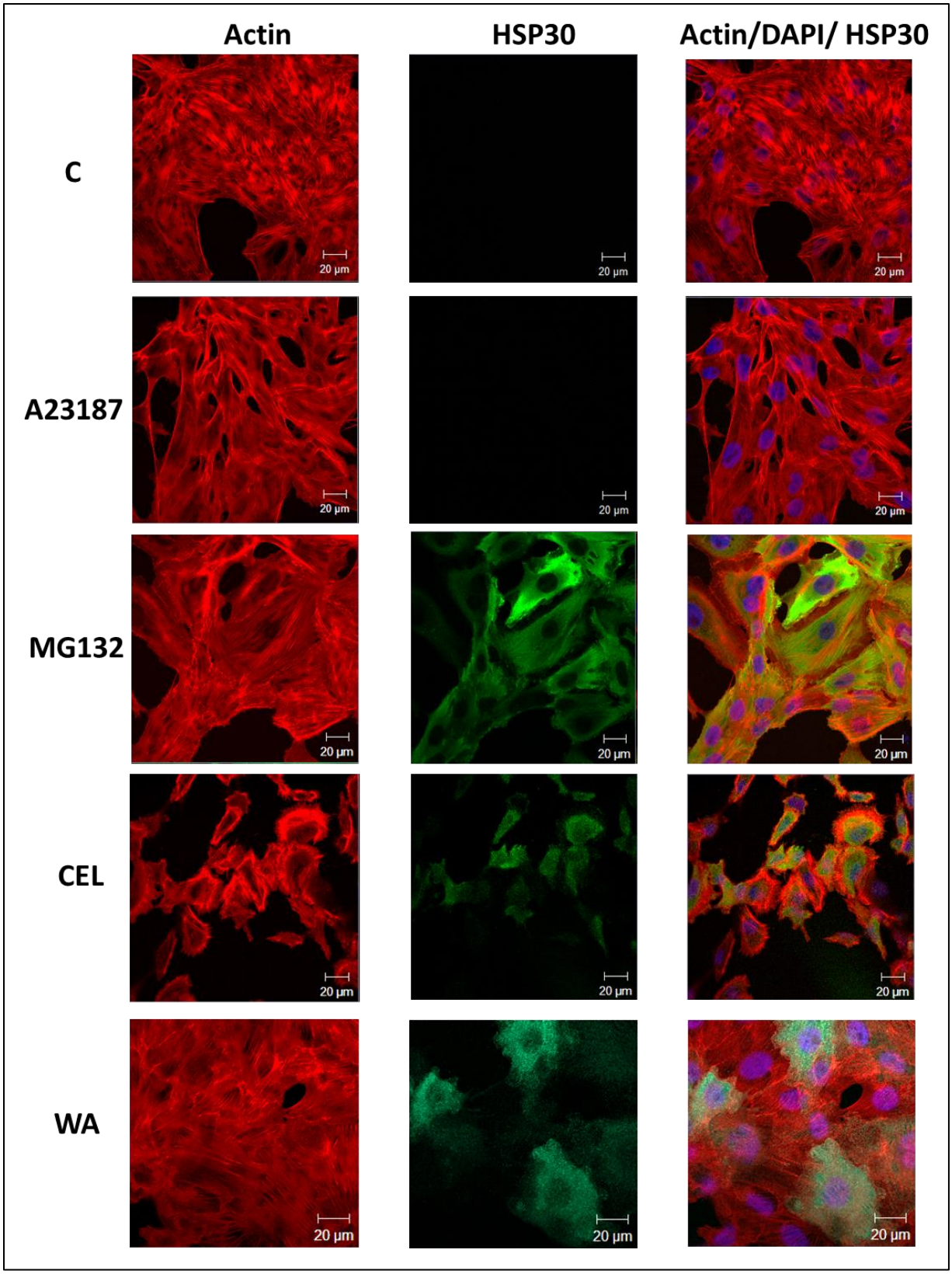
Actin
HSP30
Actin/DAPI/ HSP30
C
A23187
MG132
CEL
WA
20 µm

Figure 24. Intracellular localization of BiP in response to proteasome inhibition. Cells were grown on glass coverslips and were maintained at 22 °C or treated with 7 μM A23187 or 30 μM MG132 for 24 h, 2.5 μM celastrol (CEL) for 8 h or 5 μM withaferin A (WA) for 16 h at 22 °C. Actin and nuclei were stained directly with phalloidin conjugated to TRITC (red) and DAPI (blue), respectively. BiP was indirectly detected with an anti-BiP antibody and a secondary antibody conjugated to Alexa-488 (green). From left to right the columns display fluorescence detection channels for actin, BiP and merger of actin, DAPI and BiP. The white arrows indicate perinuclear localization while the yellow areas show the presence of BiP near the cell membrane. The 20-μm white scale bars are indicated at the bottom right section of each panel. These results are representative of 3 different experiments.

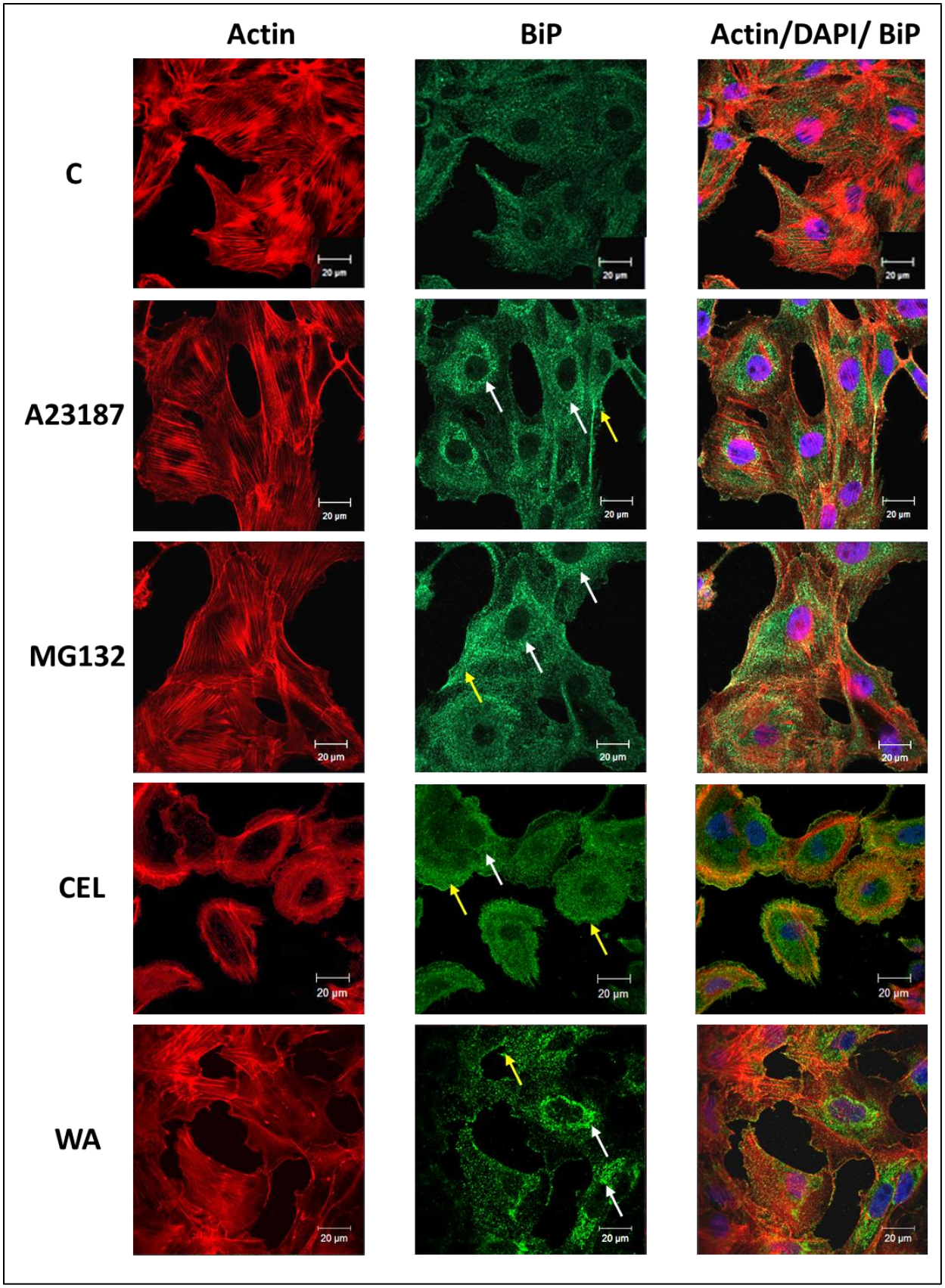
Actin
BiP
Actin/DAPI/ BiP
C
A23187
MG132
CEL
WA
20 µm

bilirubin, an antioxidant (Par et al., 2010). Also, HO-1 was strongly induced by reactive oxygen species as well as proteasomal inhibitors such as MG132, lactacystin and bortezomib (Lee et al., 1996; Wu et al., 2004; Kastle et al., 2012; Furfano et al. 2014). Anti-human HO-1 antibody (Enzo Life Sciences) employed in this part of the study was created from a human peptide that has 100 % amino acid sequence identity with the comparable region in *Xenopus* HO-1. Cells treated with withaferin A and celastrol showed concentration- and time-dependent increases in HO-1 and HSP30 accumulation (Fig. 25, 26). As shown in Figure 25, immunoblot analysis of cells treated for 24 h demonstrated HO-1 accumulation occurred initially in cells treated with 1 μM withaferin A (Fig. 25A). In contrast, HSP30 accumulation was detected in cells treated with 2.5 μM withaferin A. However, maximum accumulation was observed in cells treated with 5 μM withaferin A for both HO-1 and HSP30 (Fig. 25B). In time course studies, HO-1 and HSP30 accumulation was initially detected in cells treated with 5 μM withaferin A for 8 h (Fig. 25C). Maximum levels of HO-1 were observed in cells treated with 5 μM withaferin A for 16 h while the maximum level of HSP30 was observed at 24 h (Fig. 25D). Densitometric analysis revealed a 100-fold increase in HO-1 levels occurred in cells treated with 5 μM withaferin A for 16 h in comparison to cells treated for only 8 h (Fig. 25D). Similarly, celastrol also induced concentration and time-dependent increases in HO-1 and HSP30 accumulation (Fig. 26). HO-1 accumulation was first detectable in cells treated with 1 μM celastrol while maximal levels occurred with 2.5 μM celastrol (Fig. 26A). In comparison, HSP30 accumulation was initially observed in cells treated with a higher concentration of 2.5 μM celastrol while maximal accumulation occurred in cells treated with 5 μM celastrol (Fig. 26A). In time course studies, celastrol-induced HO-1 and HSP30 accumulation occurred initially in cells treated with 2.5 μM celastrol for 8 h and maximal

Figure 25. Withaferin A-induced HO-1 and HSP30 accumulation occurs in a concentration- and time-dependent manner. A) Cells were maintained at 22 °C (C) or treated with 1, 2.5, 5 or 10 μM withaferin A for 24 h at 22 °C. Cells were harvested and total protein was isolated. Forty μg of different protein samples were then analyzed by Western blot analysis using anti-HO-1, anti-HSP30 or anti-actin antibodies as described in Material and methods. These data are representative of three separate experiments. B) Image J software was used to perform densitometric analysis of the signal intensity for HO-1 (black) or HSP30 (white) protein bands of western blot images as described in Materials and methods. The data are expressed as percentage of the maximum signal (5 μM WA for 24 h for HO-1 and HSP30). C) Cells were maintained at 22 °C (C) or treated with 5 μM withaferin A (WA) for 2 to 24 h at 22 °C. Cells were harvested and total protein was isolated. Forty μg of different protein samples were then analyzed by Western blot analysis using anti-HO-1, anti-HSP30 or anti-actin antibodies as described in Material and methods. These data are representative of three separate experiments. D) Image J software was used to perform densitometric analysis of the signal intensity for HO-1 (black) or HSP30 (white) protein bands of western blot images as described in Materials and methods. The data are expressed as percentage of the maximum signal (5 μM WA for 16 h for HO-1 or 5 μM WA for 24 h for HSP30). The standard error is represented by vertical error bars. The level of significance of the differences between samples was calculated by one-way ANOVA with a Tukey's post-test. Significant differences between the control cells and withaferin A-treated cells are indicated as * ($p < 0.05$).

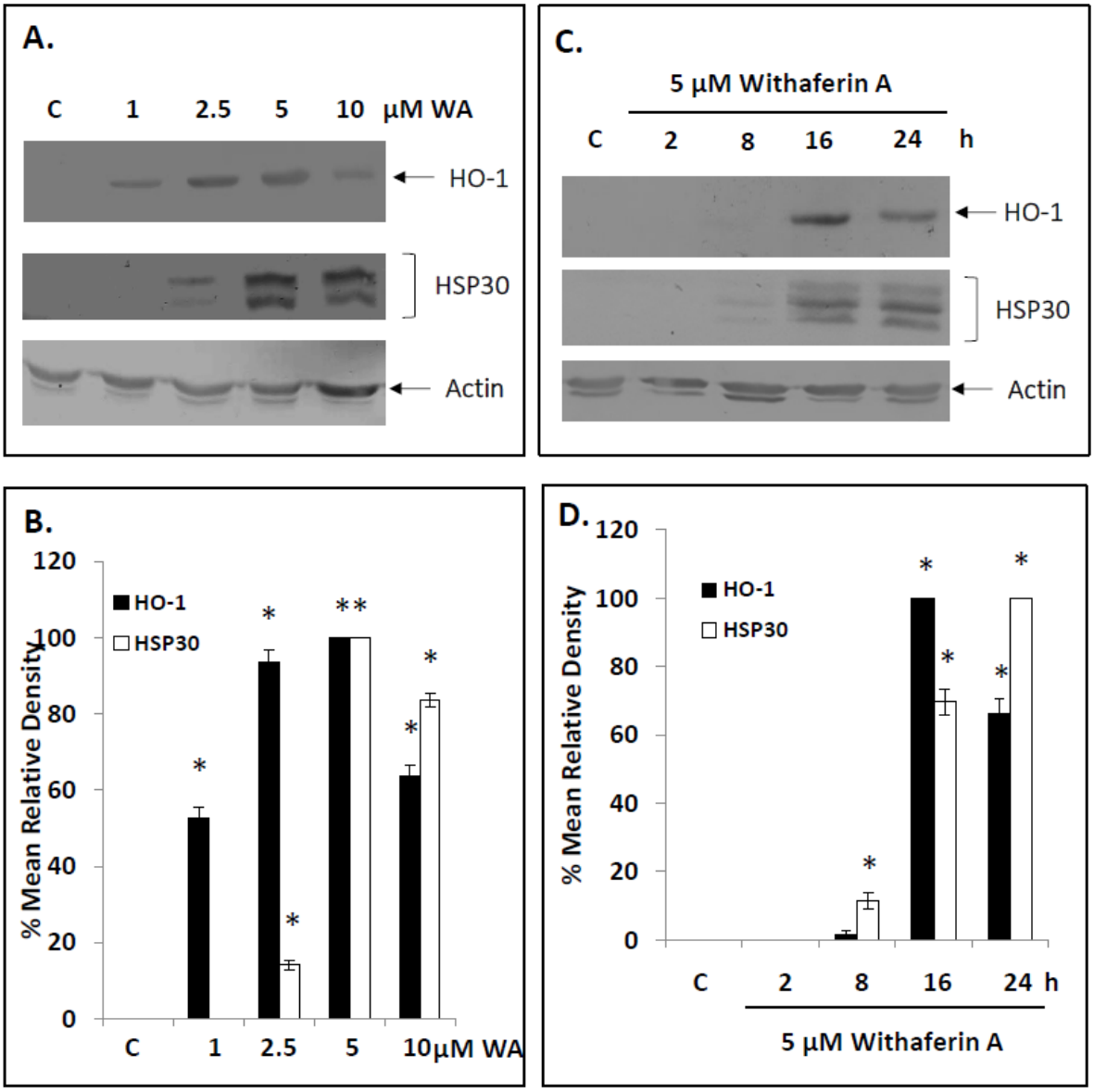
A.
C 1 2.5 5 10 μM WA
HO-1
HSP30
Actin
C.
5 μM Withaferin A
C 2 8 16 24 h
HO-1
HSP30
Actin
B.
% Mean Relative Density
HO-1
HSP30
C 1 2.5 5 10μM WA
D.
% Mean Relative Density
HO-1
HSP30
C 2 8 16 24 h
5 μM Withaferin A

Figure 26. Concentration- and time-dependent HO-1 and HSP30 accumulation in A6 cells treated with celastrol. A) Cells were maintained at 22 °C (C) or treated with 1, 2.5, 5 or 7.5 μM celastrol for 24 h at 22 °C. Cells were harvested and total protein was isolated. Forty μg of different protein samples were then analyzed by Western blot analysis using anti-HO-1, anti-HSP30 or anti-actin antibodies as described in Material and methods. These data are representative of three separate experiments. B) Image J software was used to perform densitometric analysis of the signal intensity for HO-1 (black) or HSP30 (white) protein bands of western blot images as described in Materials and methods. The data are expressed as percentage of the maximum signal (2.5 μM celastrol for 24 h for HO-1 and 5 μM celastrol for 24 h for HSP30). C) Cells were maintained at 22 °C (C) or treated with 2.5 μM celastrol for 2 to 24 h at 22 °C. Cells were harvested and total protein was isolated. Forty μg of different protein samples were then analyzed by Western blot analysis using anti-HO-1, anti-HSP30 or anti-actin antibodies as described in Material and methods. These data are representative of three separate experiments. D) Image J software was used to perform densitometric analysis of the signal intensity for HO-1 (black) or HSP30 (white) protein bands of western blot images as described in Materials and methods. The data are expressed as percentage of the maximum signal (2.5 μM celastrol for 24 h for HO-1 and HSP30). The standard error is represented by vertical error bars. The level of significance of the differences between samples was calculated by one-way ANOVA with a Tukey's post-test. Significant differences between the control cells and celastrol-treated cells are indicated as * ($p < 0.05$).

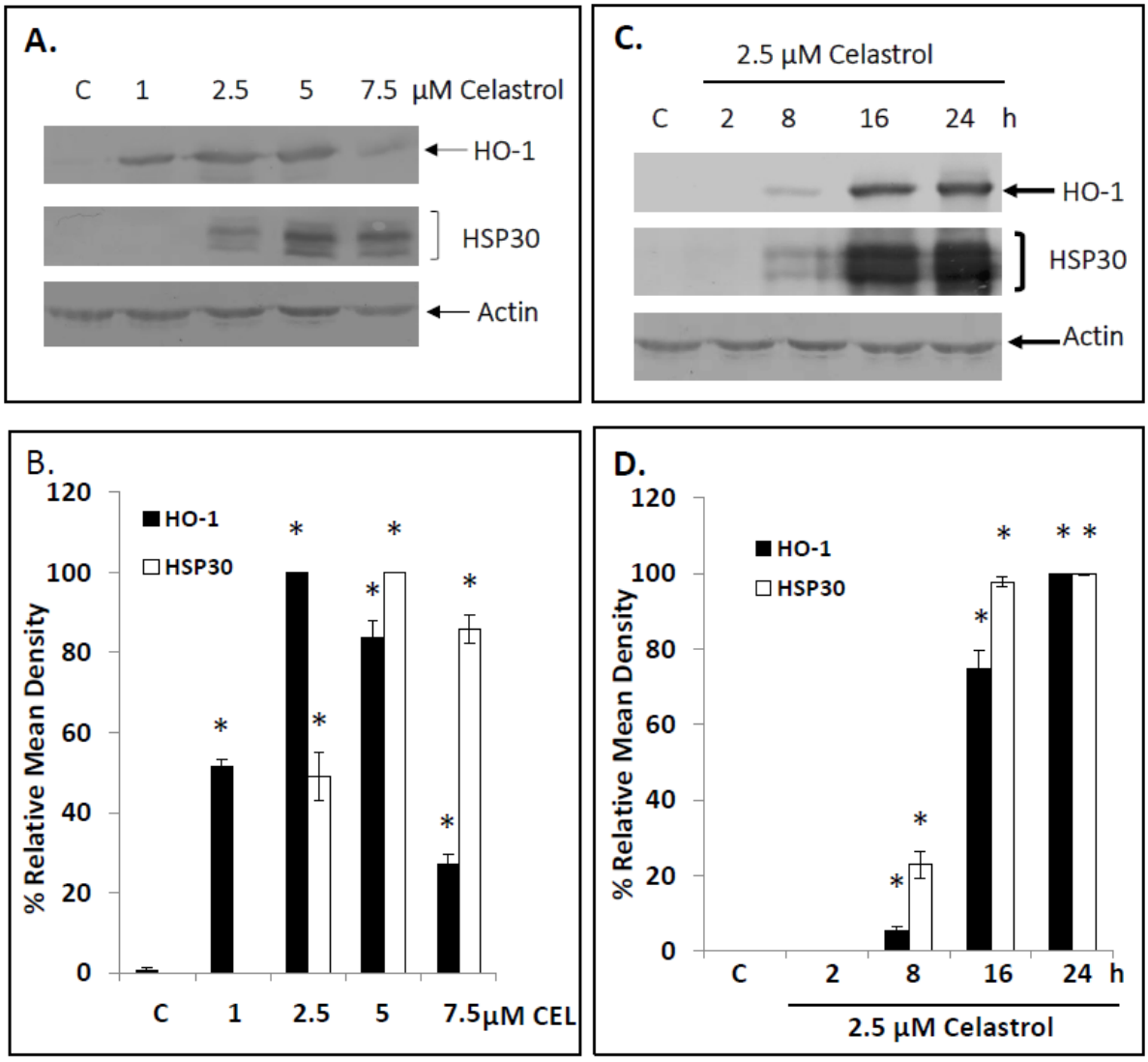
A.
C 1 2.5 5 7.5 μM Celastrol
HO-1
HSP30
Actin
C.
2.5 μM Celastrol
C 2 8 16 24 h
HO-1
HSP30
Actin
B.
% Relative Mean Density
HO-1
HSP30
C 1 2.5 5 7.5μM CEL
D.
% Relative Mean Density
HO-1
HSP30
C 2 8 16 24 h
2.5 μM Celastrol

levels were observed in cells treated for 24 h (Fig. 26C). A 20-fold increase in HO-1 accumulation was observed in cells treated for 8 h in comparison for 16 h. This was greater than the 4-fold increase observed with HSP30 during the same time period (Fig. 26D).

Immunocytochemistry and laser scanning confocal microscopy revealed that HO-1 accumulation primarily occurred in the cytoplasm in a diffuse and granular pattern (Fig. 27). As seen in Figure 27, MG132-, celastrol- and withaferin A-induced HO-1 accumulation occurred in over 90 % of cells. Some actin re-organization to the periphery was present in cells treated with celastrol and withaferin A.

3.3 MG132, withaferin A, sodium arsenite and cadmium chloride treatment results in stress granule, aggresome and large HSP30 multimeric structure formation in A6 cells

3.3.1 Proteasome inhibition, sodium arsenite and cadmium chloride induce large HSP30 multimeric complexes

In the present study and in previous reports from our laboratory, we observed the presence of large HSP30 staining structures in withaferin A, MG132, sodium arsenite or cadmium chloride treated cells (Wolffson and Heikkila, 2009; Walcott and Heikkila, 2010; Young and Heikkila, 2010). MG132, celastrol and withaferin A treatments induced large HSP30 staining structures as highlighted by white rectangular boxes in Figure 28. Similarly, treatments with sodium arsenite and cadmium chloride also induced these large HSP30 staining structures in the perinuclear region (Fig. 28B). Actin re-organization and ruffling at the periphery of the cells were also observed in some of these treatments. Given these findings, it was possible that stress-induced HSP30 may have associated with other stress-

Figure 27. Intracellular localization of HO-1 in response to proteasome inhibition. Cells were grown on glass coverslips and were maintained at 22 °C or treated with 30 μM MG132 for 16 h, 2.5 μM celastrol (celastrol) for 16 h or 5 μM withaferin A (WA) for 16 h at 22 °C. Actin and nuclei were stained directly with phalloidin conjugated to TRITC (red) and DAPI (blue), respectively. HO-1 was indirectly detected with an anti-HO-1 antibody and a secondary antibody conjugated to Alexa-488 (green). From left to right the columns display fluorescence detection channels for actin, HO-1 and merger of actin, DAPI and HO-1. The 20-μm white scale bars are indicated at the bottom right section of each panel. These results are representative of 3 different experiments.

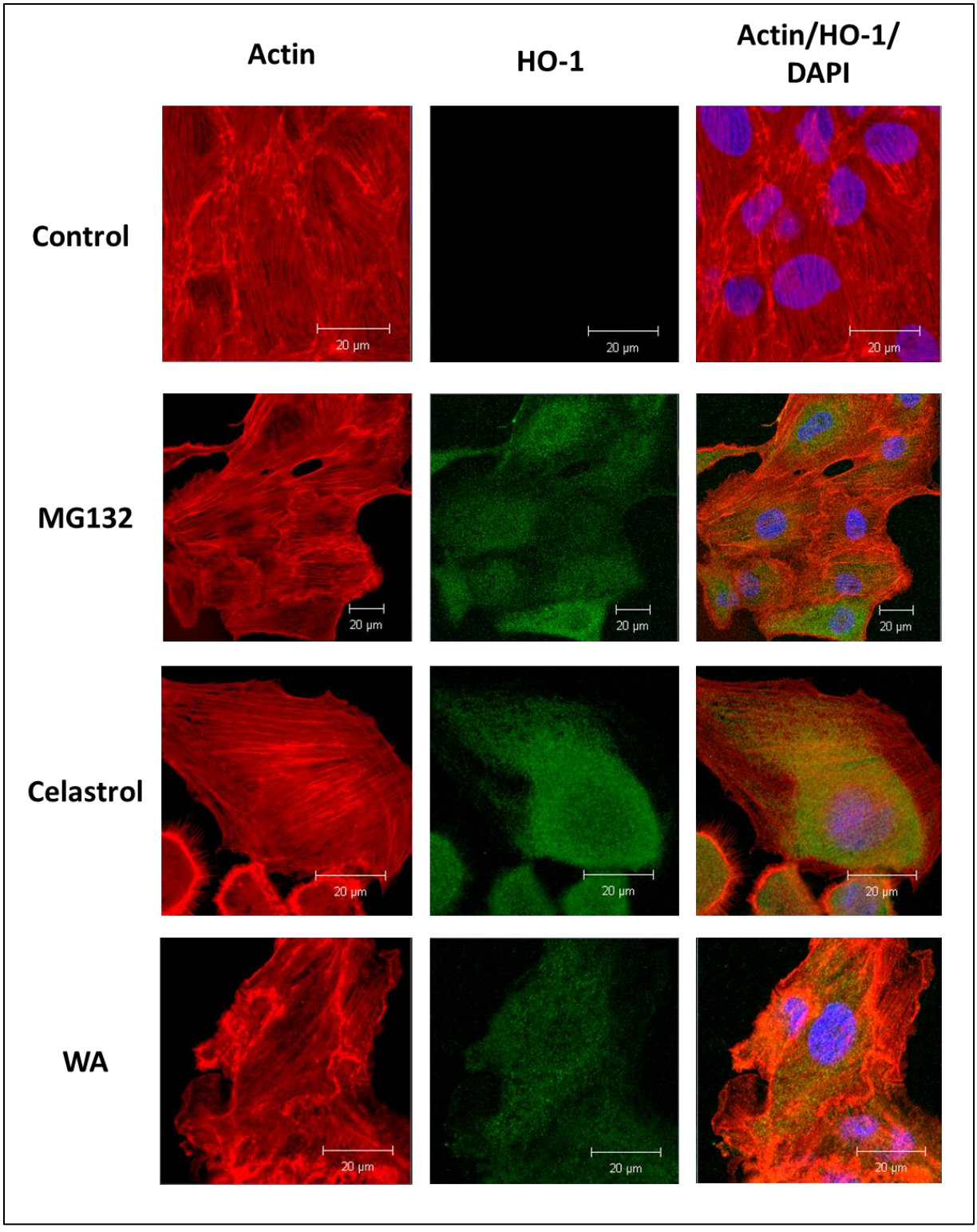
Actin
HO-1
Actin/HO-1/
DAPI
Control
MG132
Celastrol
WA
20 μm

Figure 28. Intracellular localization of HSP30 and presence of large HSP30 structures in response to proteasome inhibition. A) Cells were grown on glass coverslips and were maintained at 22 °C or treated with 30 μM MG132 for 16 h, 2.5 μM celastrol (celastrol) for 16 h or 5 μM withaferin A (WA) for 16 h at 22 °C. B) Cells were also treated with 20 μM sodium arsenite (NA) for 16 h or 100 μM cadmium chloride ($CdCl_2$) for 16 h at 22 °C. Actin and nuclei were stained directly with phalloidin conjugated to TRITC (red) and DAPI (blue), respectively. HSP30 was indirectly detected with an anti-HSP30 antibody and a secondary antibody conjugated to Alexa-488 (green). From left to right the columns display fluorescence detection channels for actin, HSP30 and merger of actin, DAPI and HSP30. The 20-μm white scale bars are indicated at the bottom right section of each panel. Large HSP30 staining structures are delineated with a white box and shown as a figure inset. These results are representative of 3 different experiments.

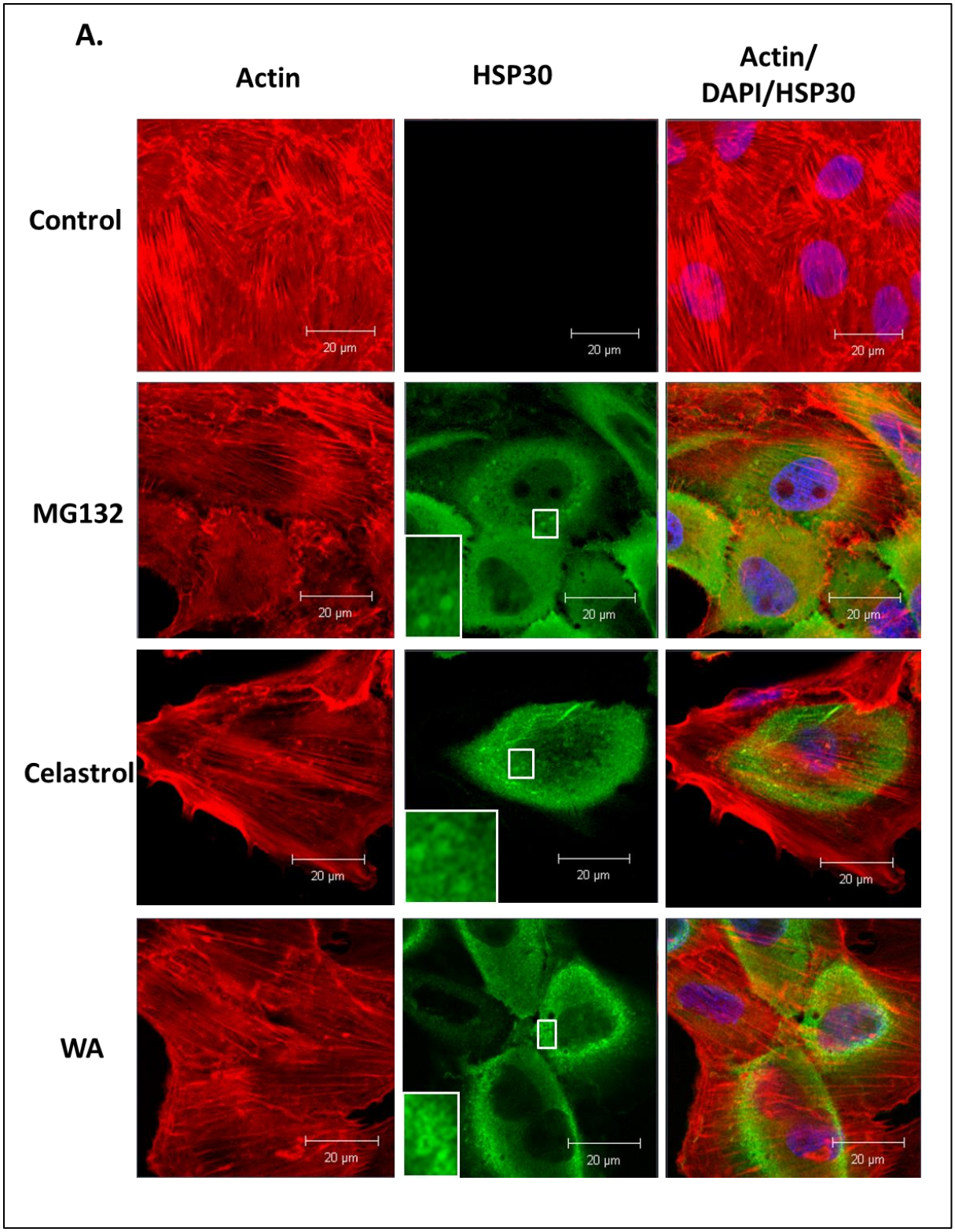
A.
Actin
HSP30
Actin/
DAPI/HSP30
Control
MG132
Celastrol
WA
20 µm

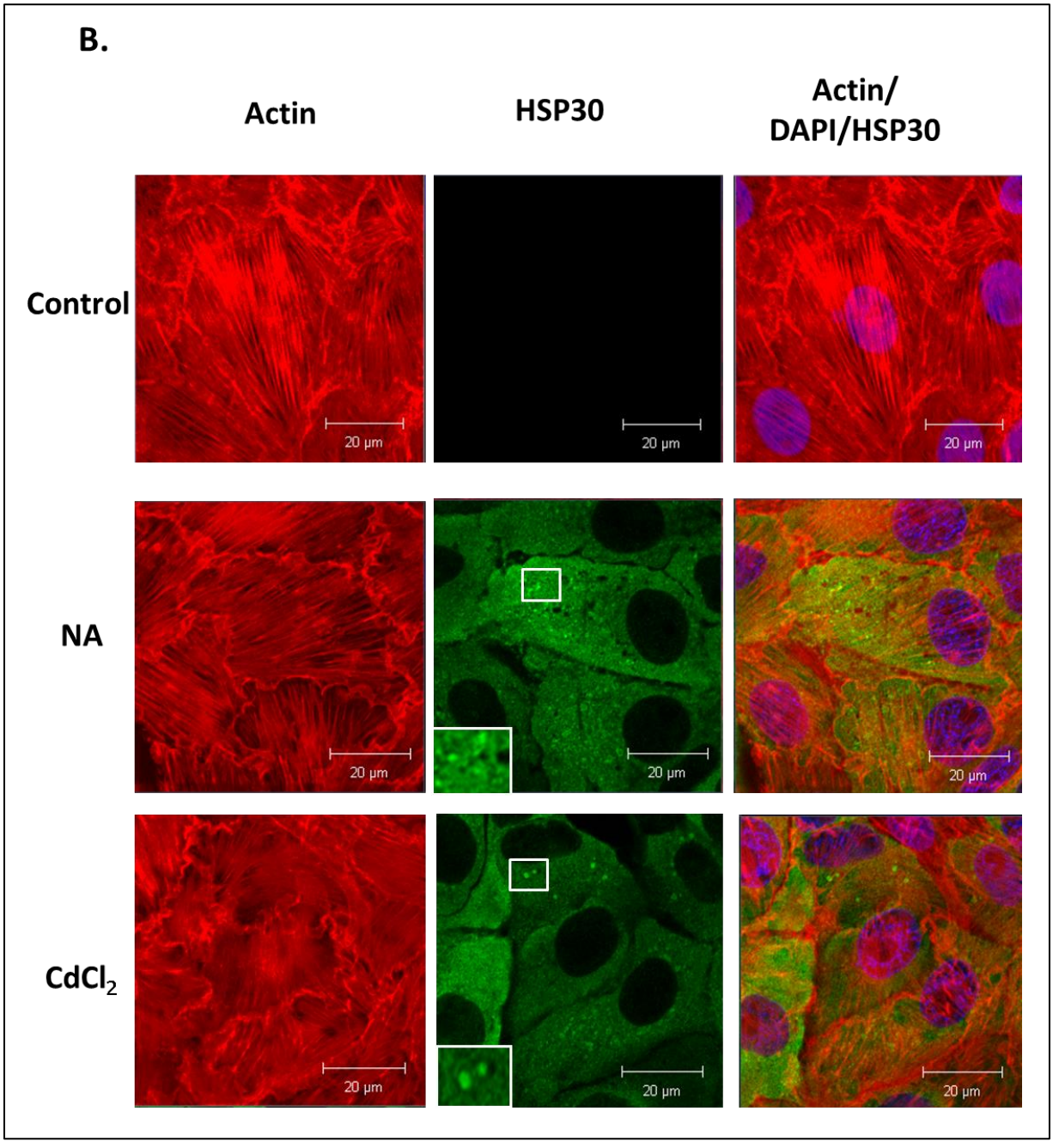
B.
Actin
HSP30
Actin/
DAPI/HSP30
Control
NA
CdCl2
20 µm

inducible structures such RNA stress granules or aggresomes.

3.3.2 MG132, withaferin A, sodium arsenite and cadmium chloride induce stress granule formation in A6 cells

Stress granules are RNA-protein complexes composed of stalled pre-initiated mRNA bound to 40S ribosomal subunit, poly(A)-binding protein (PABP) and various eukaryotic protein synthesis elongation factors (Anderson and Kedersha, 2006). Previous studies in mammalian systems have shown a possible association of hsp27 with heat shock-induced stress granules (Kedersha et al., 2005). In this study, the presence of stress granules in A6 cells was determined by immunocytochemistry employing antibodies that react with TIA1 and PABP, which are marker proteins for stress granules. As shown in Figure 29, immunocytochemical analysis and laser scanning confocal microscopy revealed the presence of stress granules in A6 cells treated with either MG132 or sodium arsenite but not with heat shock. A6 cells treated with MG132 or sodium arsenite displayed an increase in PABP and TIA1 staining in the cytoplasm primarily in the perinuclear region in comparison to control cells. Additionally, both PABP and TIA1 co-localized in A6 cells treated with MG132 or sodium arsenite, confirming the presence of stress granules by two different markers. However, as shown in Figure 30, PABP did not co-localize with HSP30 in cells treated with MG132, sodium arsenite or cadmium chloride. More specifically, PABP was present in cells treated with MG132 in the cytoplasm in areas that had no HSP30 staining (Fig. 30B). Similarly, cells treated with sodium arsenite displayed no co-localization of HSP30 with PABP (Fig. 30C).

Figure 29. Presence of stress granules in cells treated with MG132 or sodium arsenite. Cells were grown on glass coverslips and were maintained at 22 °C (Control), incubated at 33 °C or treated with 30 μM MG132 for 16 h or 20 μM sodium arsenite (NA) for 16 h at 22 °C. Stress granule markers such as poly(A)-binding protein (PABP) was detected indirectly with an anti-PABP antibody and a secondary antibody conjugated to Alexa-555 (red). TIA1 (granule associated RNA binding protein) was detected indirectly with an anti-TIA1 antibody and a secondary antibody conjugated to Alexa-488 (green). Nuclei were stained directly with DAPI (blue). From left to right the columns display fluorescence detection channels for PABP, TIA1 and merger of PABP, DAPI and TIA1. The 20-μm white scale bars are indicated at the bottom right section of each panel. These results are representative of 3 different experiments.

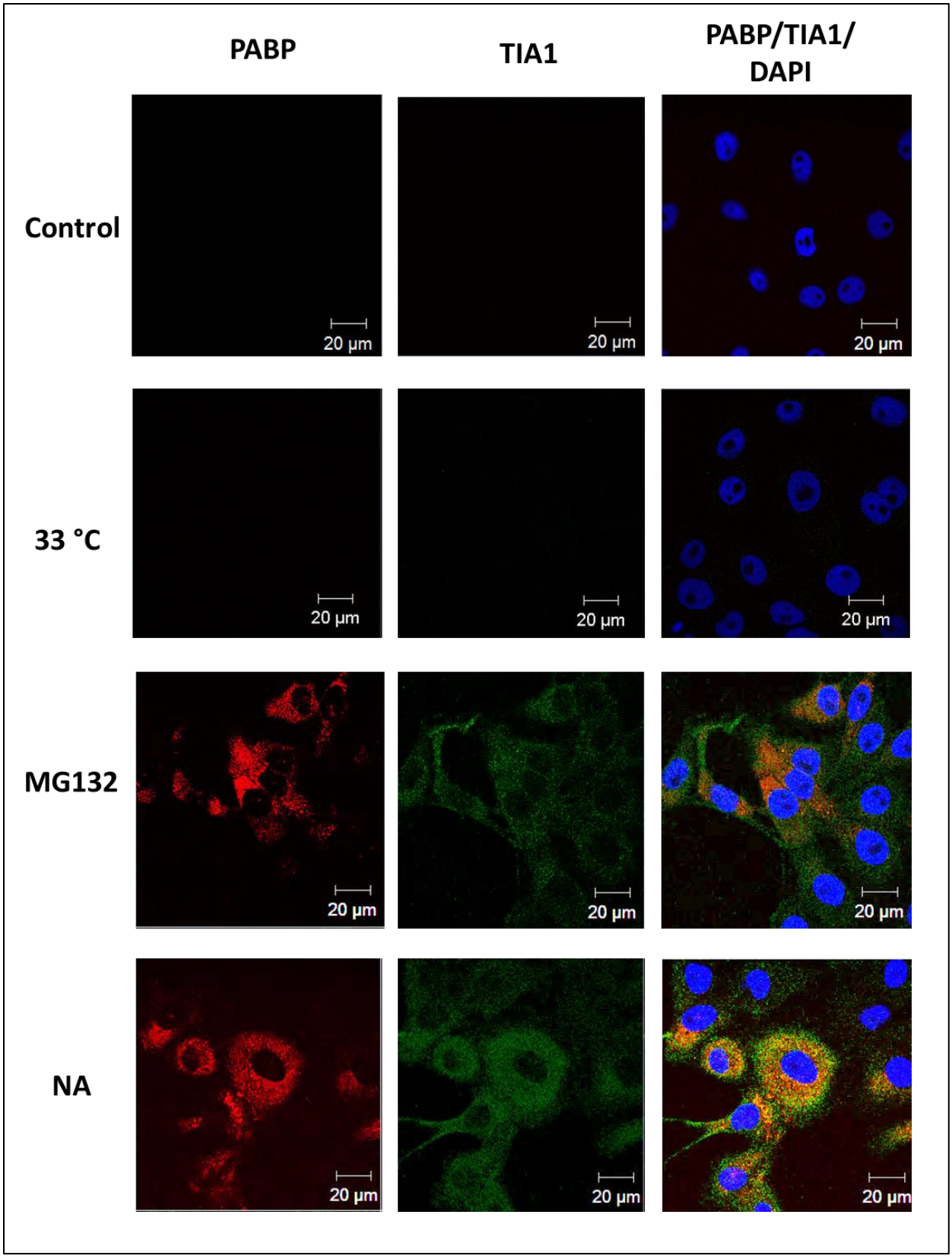
PABP
TIA1
PABP/TIA1/
DAPI
Control
33 °C
MG132
NA
20 µm

Figure 30. Association of stress granules with HSP30 in cells treated with MG132, sodium arsenite and cadmium chloride. A) Cells were grown on glass coverslips and were maintained at 22 °C (Control) or treated with 30 μM MG132 for 16 h, 20 μM sodium arsenite (NA) for 16 h or 100 μM cadmium chloride ($CdCl_2$) at 22 °C. The stress granule marker, PABP, was detected indirectly with an anti-PABP antibody and a secondary antibody conjugated to Alexa-555 (red). HSP30 was detected indirectly with an anti-HSP30 antibody and a secondary antibody conjugated to Alexa-488 (green). Nuclei were stained directly with DAPI (blue). From left to right the columns display fluorescence detection channels for PABP, HSP30 and merger of PABP, DAPI and HSP30. B & C) Magnified images of MG132 treated cells (panel B) and sodium arsenite treated cells (panel C) are delineated with a white box. The 20-μm white scale bars are indicated at the bottom right section of each panel. These results are representative of 3 different experiments.

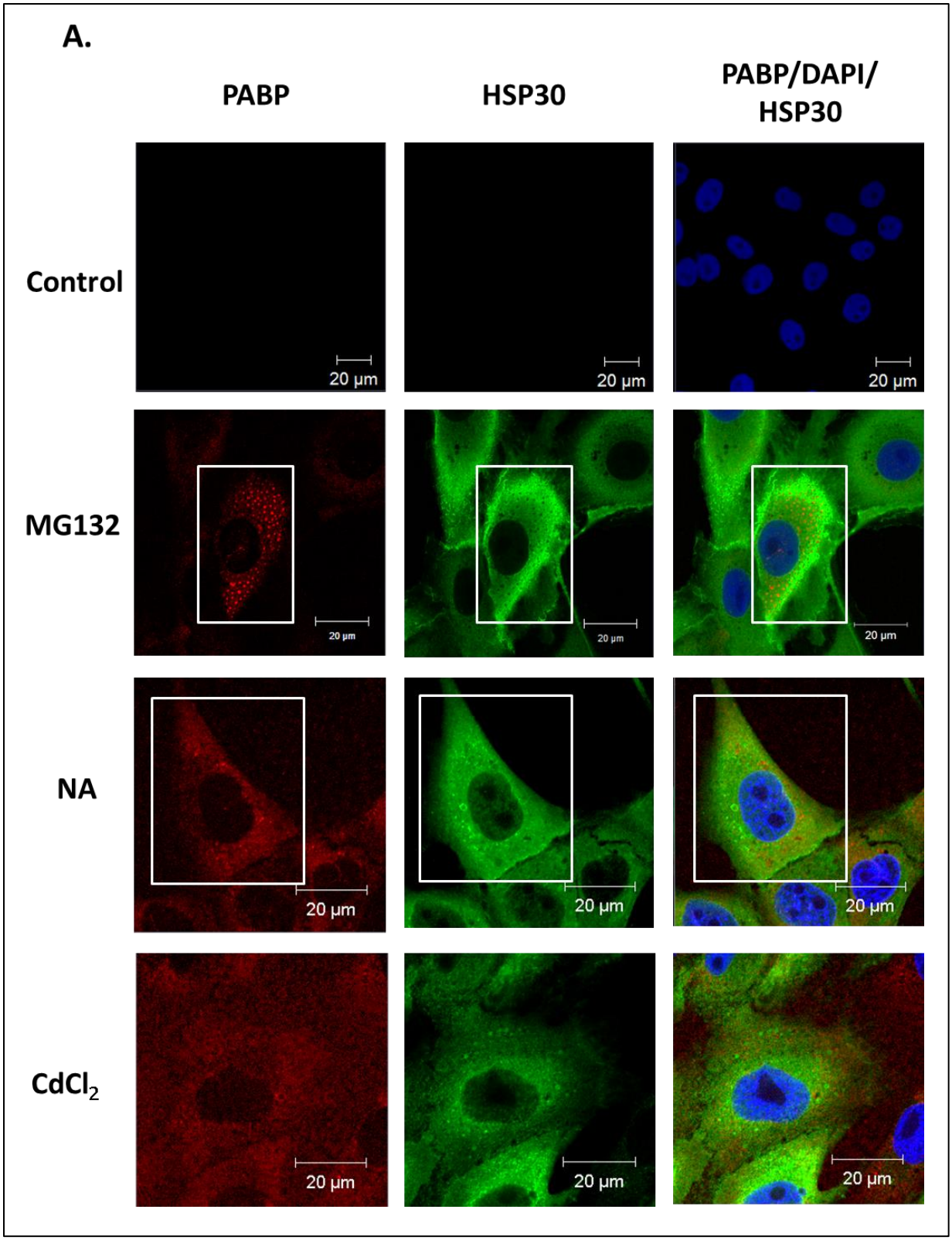
A.
PABP
HSP30
PABP/DAPI/
HSP30
Control
MG132
NA
CdCl2
20 µm

B.

MG132

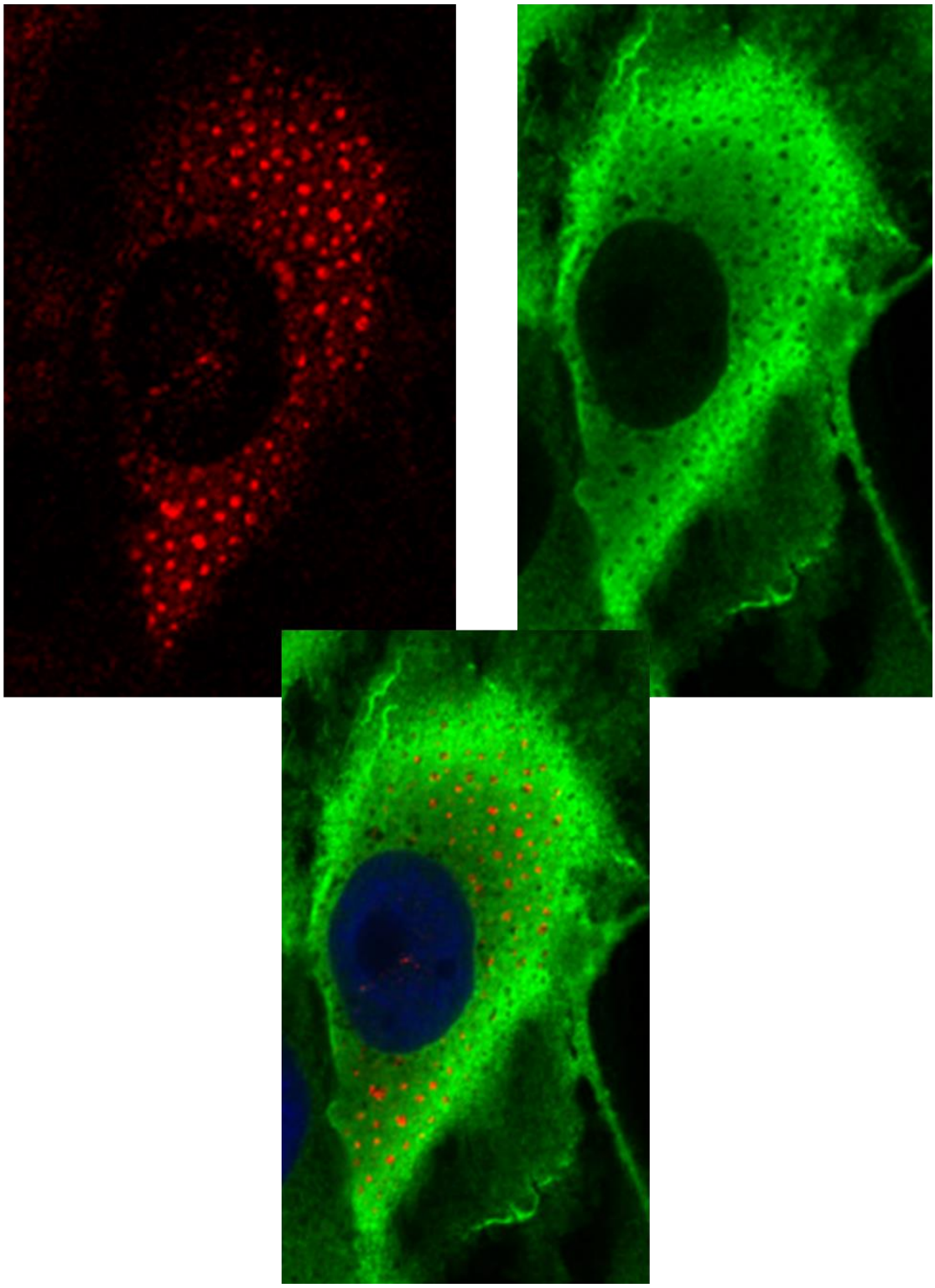

C. NA

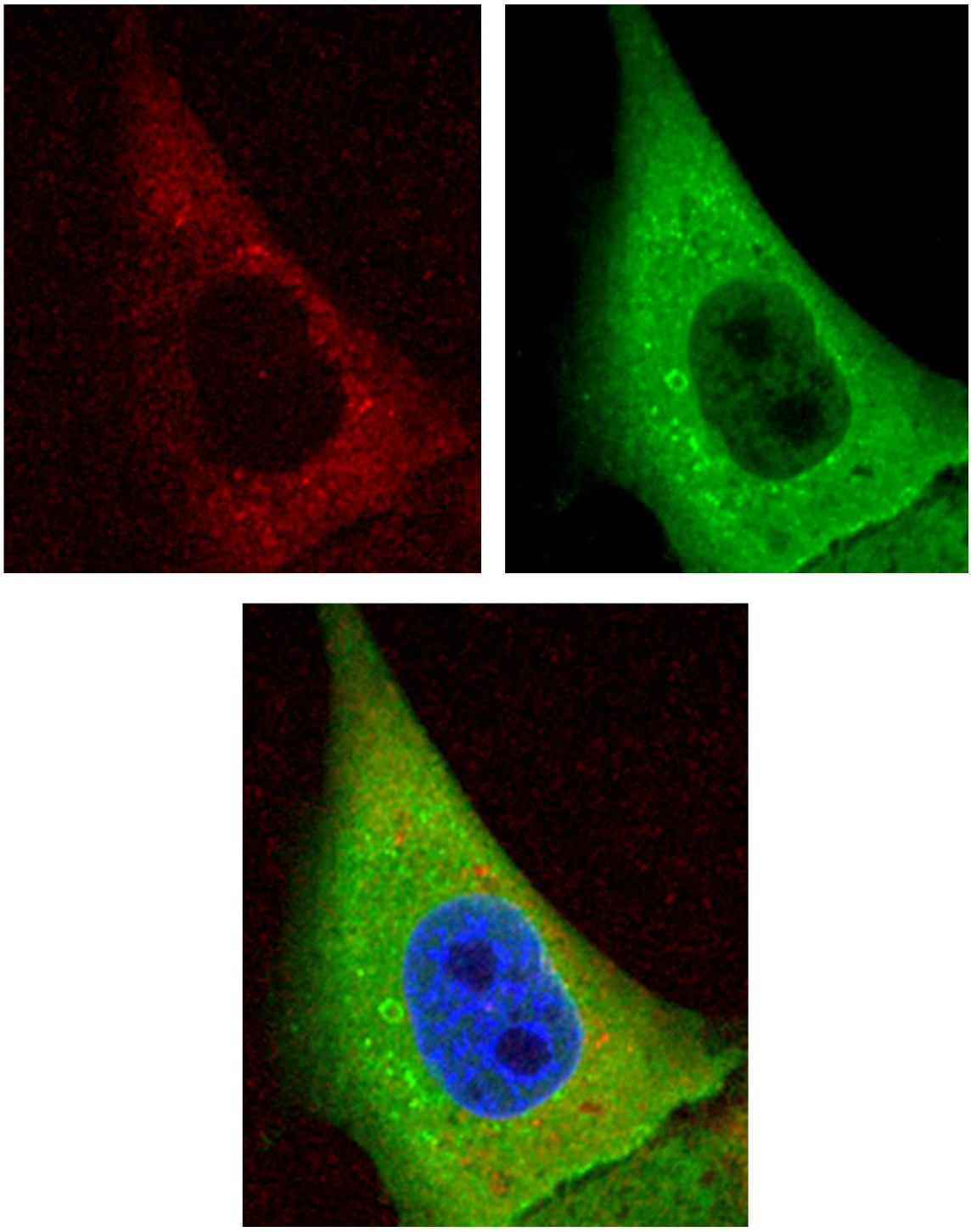

3.3.3 Formation of aggresomes in response to proteasome inhibition, arsenite or cadmium exposure

Since, HSP30 did not co-localize with stress-induced RNA granules, we examined the possibility that HSP30 associated with stress-induced aggresomes. Aggresomes are specialized cellular structures containing misfolded, ubiquitinated proteins in a cage of intermediate filaments and cytoskeletal proteins including vimentin and γ-tubulin (Johnston et al., 1998). Previous studies reported that treatment of human cultured cells with proteasome inhibitors such as MG132 resulted in aggresome formation (Zaarur et al., 2008; Bolhuis & Richter-Landsberg, 2010; Xiong et al., 2013). Vimentin and γ-tubulin have been used as cytological markers for the presence of stress-induced aggresomes (Garcia-Mata et al., 1999; Bauer & Richter-Landsberg, 2006; Xiong et al., 2013). Also available is the ProteoStat aggresome detection kit (Enzo Life Sciences, Farmingdale, NY; Amijee et al., 2009; Shen et al., 2011).

In the present study, we employed anti-vimentin and anti-γ-tubulin antibodies as well the ProteoStat aggresome detection kit to examine the presence of stress-induced aggresomes in A6 cells. Cells maintained at 22 °C did not display aggresome-like structures in the cytoplasm as determined by the ProteoStat assay (Red channel, Fig. 31A). Additionally, in control cells γ-tubulin was not associated with aggresome-like structures but rather localized primarily in the cytoplasm and formed a mesh-like network (Fig. 31A). In comparison, cells incubated at 33 °C or treated with MG132 or withaferin A induced the formation of large putative aggresomes in the perinuclear region as detected by the ProteoStat assay (Fig. 31A). These putative aggresomes stained using the ProteoStat assay were also recognized by the anti-γ-tubulin antibody (Fig. 31A). Moreover, treatment of cells with sodium arsenite or

Figure 31. Treatment of cells with MG132, withaferin A, sodium arsenite or cadmium chloride results in the formation of aggresome-like structures. A) Cells were grown on glass coverslips and maintained at 22 °C (Control), incubated at 33 °C or treated with 30 μM MG132 for 16 h or 5 μM withaferin A (WA) for 16 h at 22 °C. B) Cells were also treated with 20 μM sodium arsenite (NA) for 16 h or 100 μM cadmium chloride ($CdCl_2$) at 22 °C. The ProteoStat aggresome detection kit was used to directly stain aggresome-like structures while nuclei were stained directly with DAPI (blue). Gamma-tubulin was detected indirectly with an anti-γ-tubulin antibody and a secondary antibody conjugated to Alexa-488 (green). From left to right, the columns display fluorescence detection channels for ProteoStat assay, γ-tubulin and merger of ProteoStat assay, DAPI and γ-tubulin. These results are representative of 3 separate experiments.

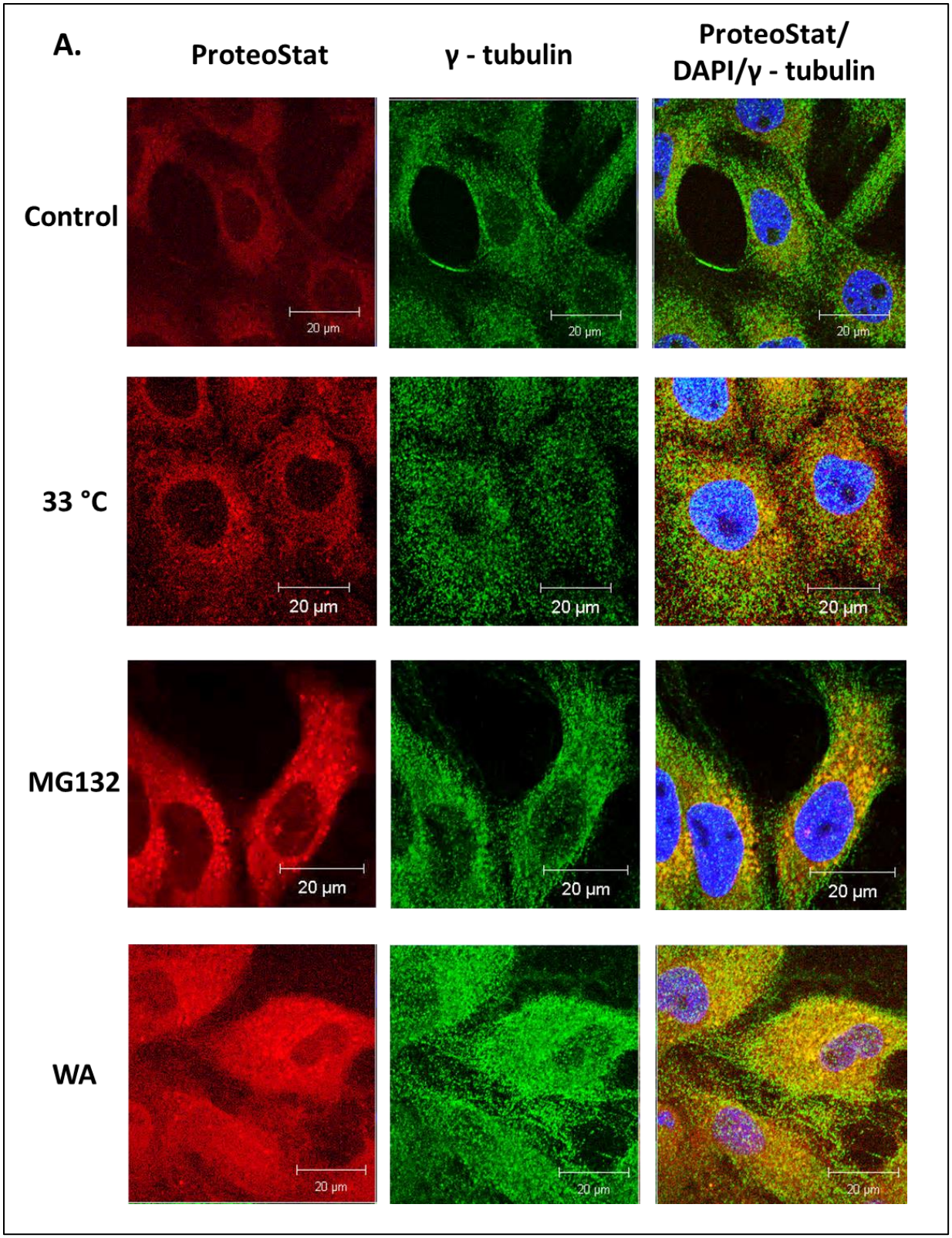
A.
ProteoStat
γ - tubulin
ProteoStat/
DAPI/γ - tubulin
Control
33 °C
MG132
WA
20 µm

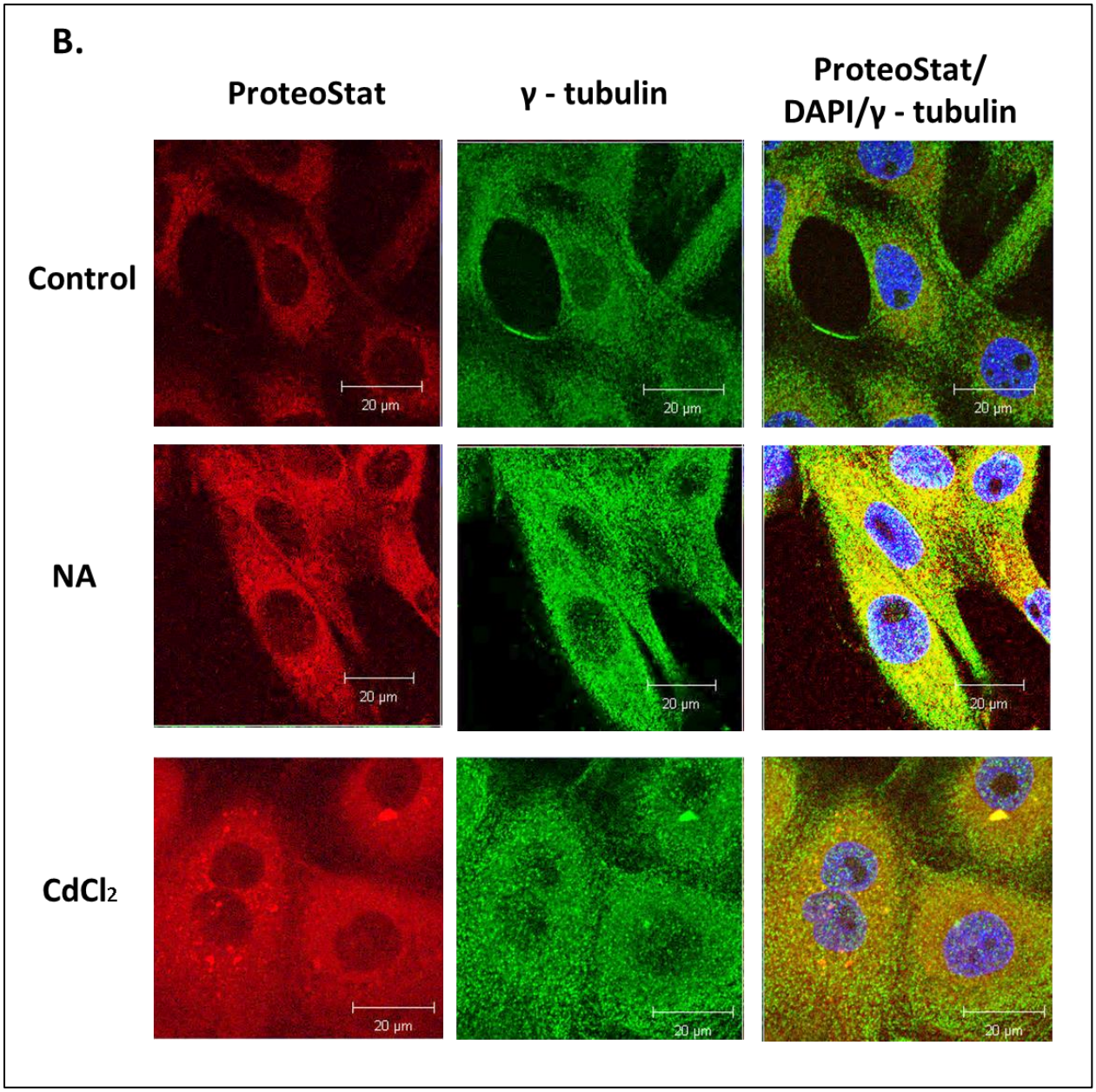
B.
ProteoStat
γ - tubulin
ProteoStat/
DAPI/γ - tubulin
Control
NA
CdCl2
20 µm

cadmium chloride also resulted in the formation of aggresomes as detected through γ-tubulin and ProteoStat assay co-localization (Fig. 31B). To further confirm the presence of aggresome in response to MG132, withaferin A, sodium arsenite or cadmium chloride and to verify that the ProteoStat assay was indeed detecting aggresomes, we used an antibody against vimentin. As shown in Figure 32, vimentin and ProteoStat co-localized in cells maintained at 22 °C or treated with the selected chemical stressors. Moreover, cells treated with MG132 or withaferin A showed an increased number of aggresomes present in the perinuclear region (Fig. 32A). This phenomenon was also observed in cells treated with sodium arsenite or cadmium chloride (Fig. 32B). Taken together, these findings confirmed that treatment of A6 cells with MG132, withaferin A, sodium arsenite or cadmium chloride induced aggresome formation in comparison to control cells.

3.3.4 HSP30 associates with aggresomes in cells treated with heat shock, MG132, withaferin A, sodium arsenite or cadmium chloride

The next phase of this study was to determine whether large HSP30 staining structures associated with stress-induced aggresomes in A6 cells. In cells maintained at 22 °C, neither HSP30 accumulation nor aggresomes were detected using the anti-HSP30 antibody and the ProteoStat assay, respectively. In comparison, cells heat shocked at 33 °C demonstrated the presence of large HSP30 structures which co-localized with aggresomes. A6 cells treated with MG132 or withaferin A also displayed large HSP30 structures in the cytoplasm as well as the presence of aggresomes (Fig. 33A). Additionally, some large HSP30 structures actively formed rings around the aggresomes as shown in the insets of figure 33A. Z-stacking revealed that HSP30 not only enveloped the aggresome but was also found

Figure 32. Co-localization of vimentin with aggresome-like structures in A6 cells treated with MG132, withaferin A, sodium arsenite or cadmium chloride. A & B) Cells were grown and treated as previously described in Figure 31. The ProteoStat aggresome detection kit (red) directly stained aggresome-like structures, while nuclei were stained with DAPI (blue). Vimentin was detected indirectly with an anti-vimentin antibody and a secondary antibody conjugated to Alexa-488 (green). From left to right, the columns display fluorescence detection channels for ProteoStat assay, vimentin and merger of ProteoStat assay, DAPI and vimentin. These results are representative of 3 separate experiments.

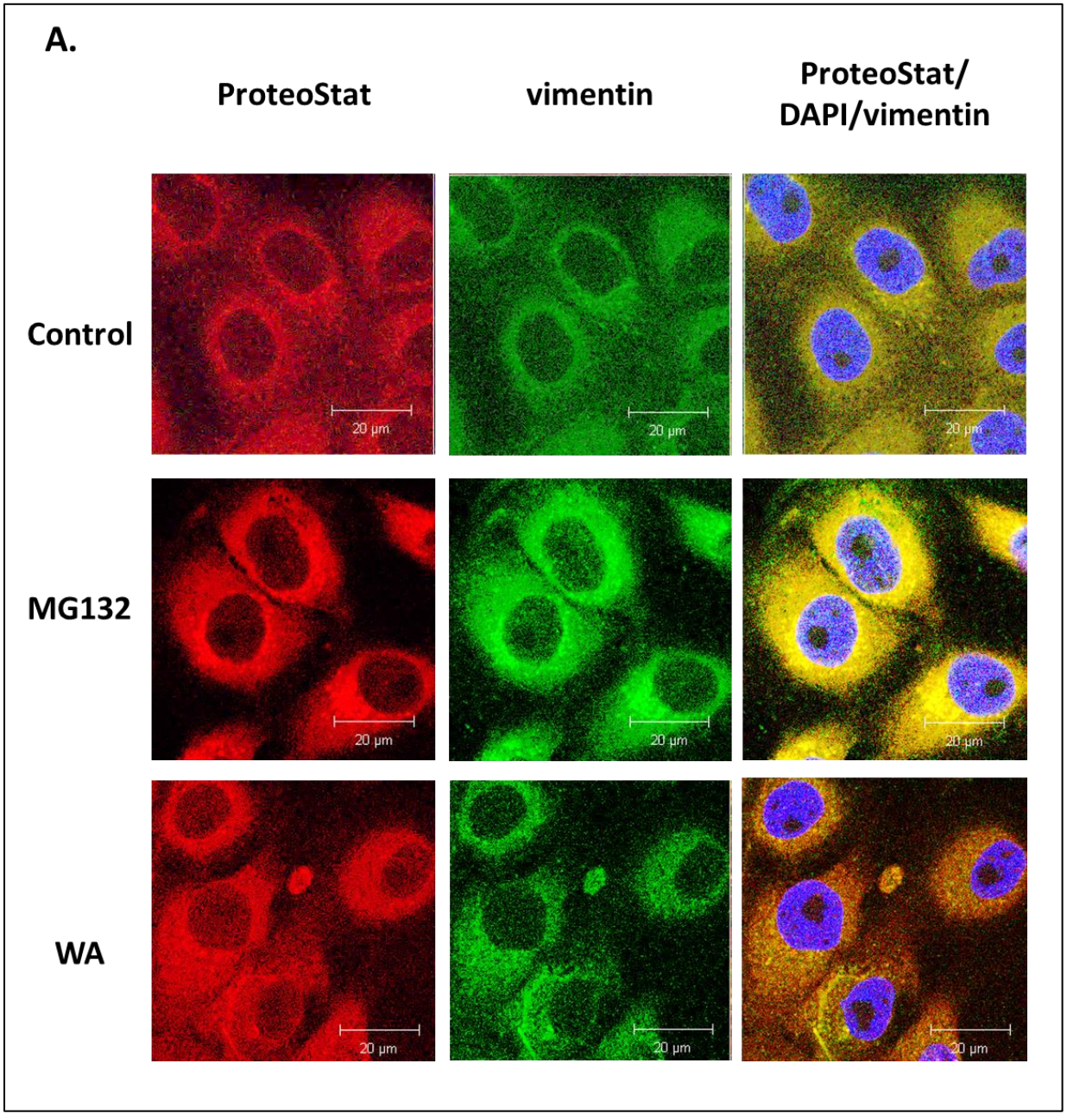
A.
ProteoStat
vimentin
ProteoStat/
DAPI/vimentin
Control
MG132
WA
20 µm

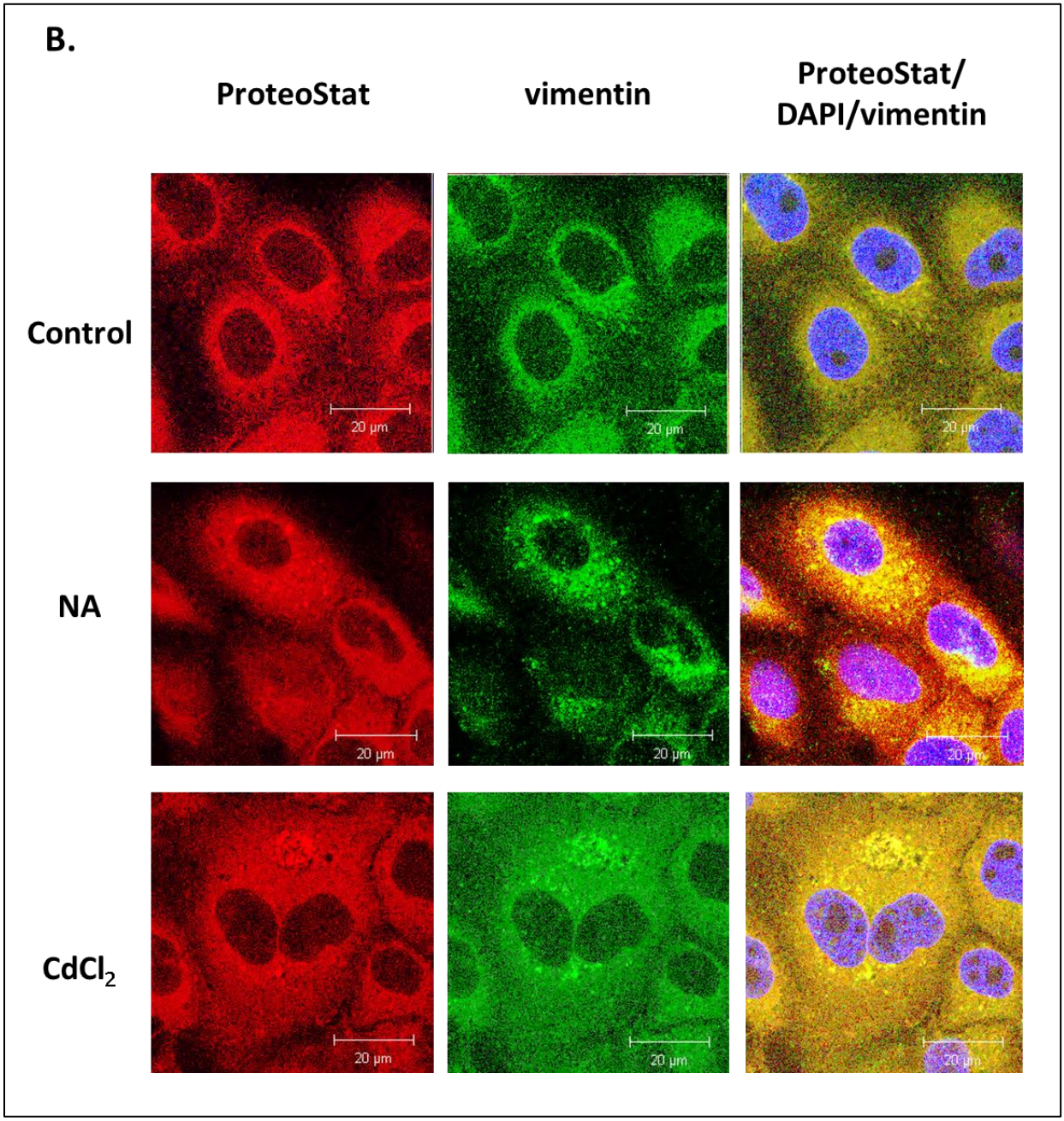
B.
ProteoStat
vimentin
ProteoStat/
DAPI/vimentin
Control
NA
CdCl2
20 µm

Figure 33. Association of large HSP30 structures and aggresome-like structures in response to MG132, withaferin A, sodium arsenite or cadmium chloride treatment. A & B) Cells were grown on glass coverslips and treated as described in Figure 31. The ProteoStat aggresome detection kit (red) directly stained aggresome-like structures. HSP30 was detected indirectly with an anti-*Xenopus* HSP30 antibody and a secondary antibody conjugated to Alexa-488 (green). Nuclei were stained directly with DAPI (blue). From left to right, the columns display fluorescence detection channels for ProteoStat assay, HSP30 and merger of ProteoStat assay, DAPI and HSP30. Aggresomes and large HSP30 structures are magnified, delineated with a white box and shown as a figure inset. These results are representative of 3 separate experiments.

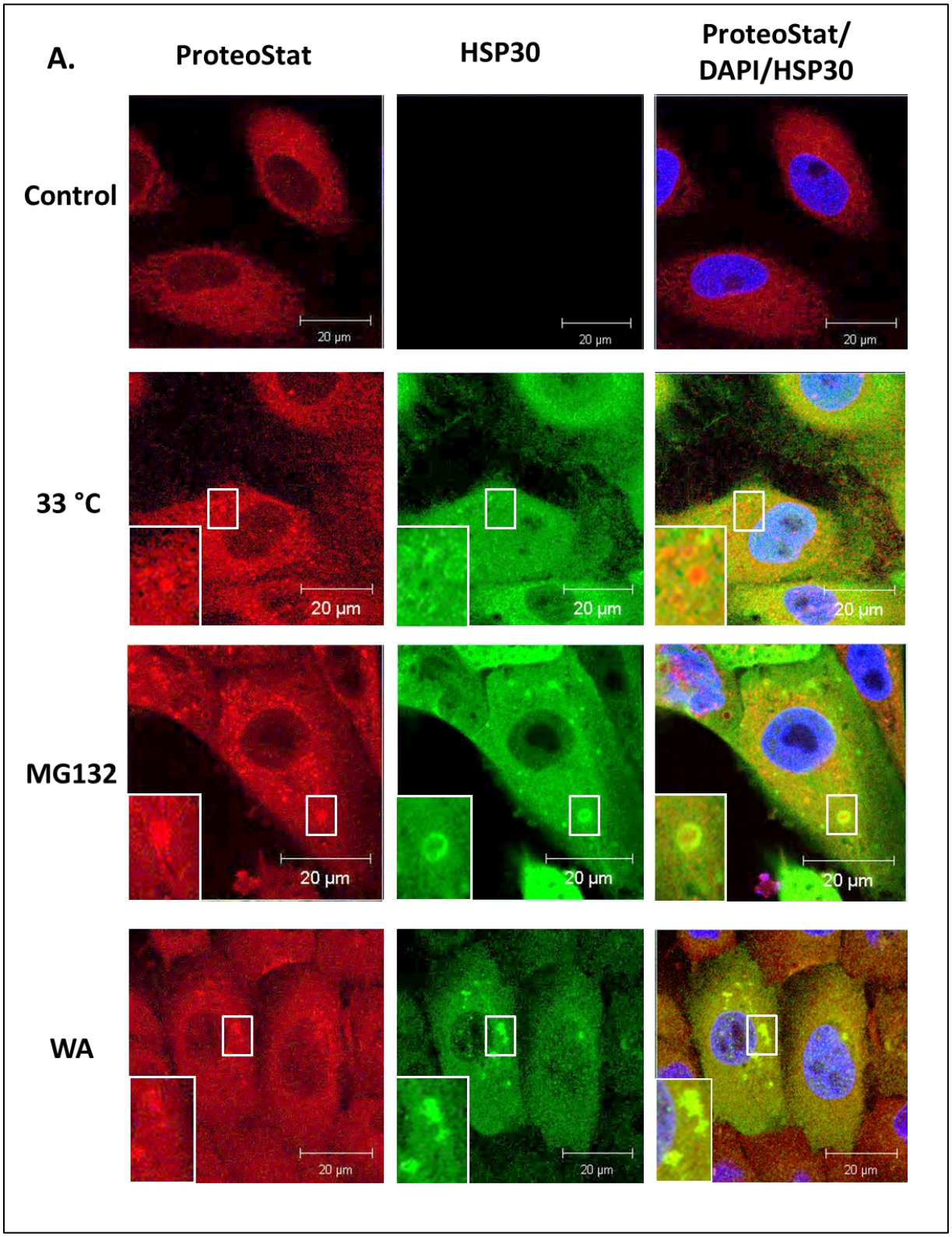
A.
ProteoStat
HSP30
ProteoStat/
DAPI/HSP30
Control
33 °C
MG132
WA
20 µm

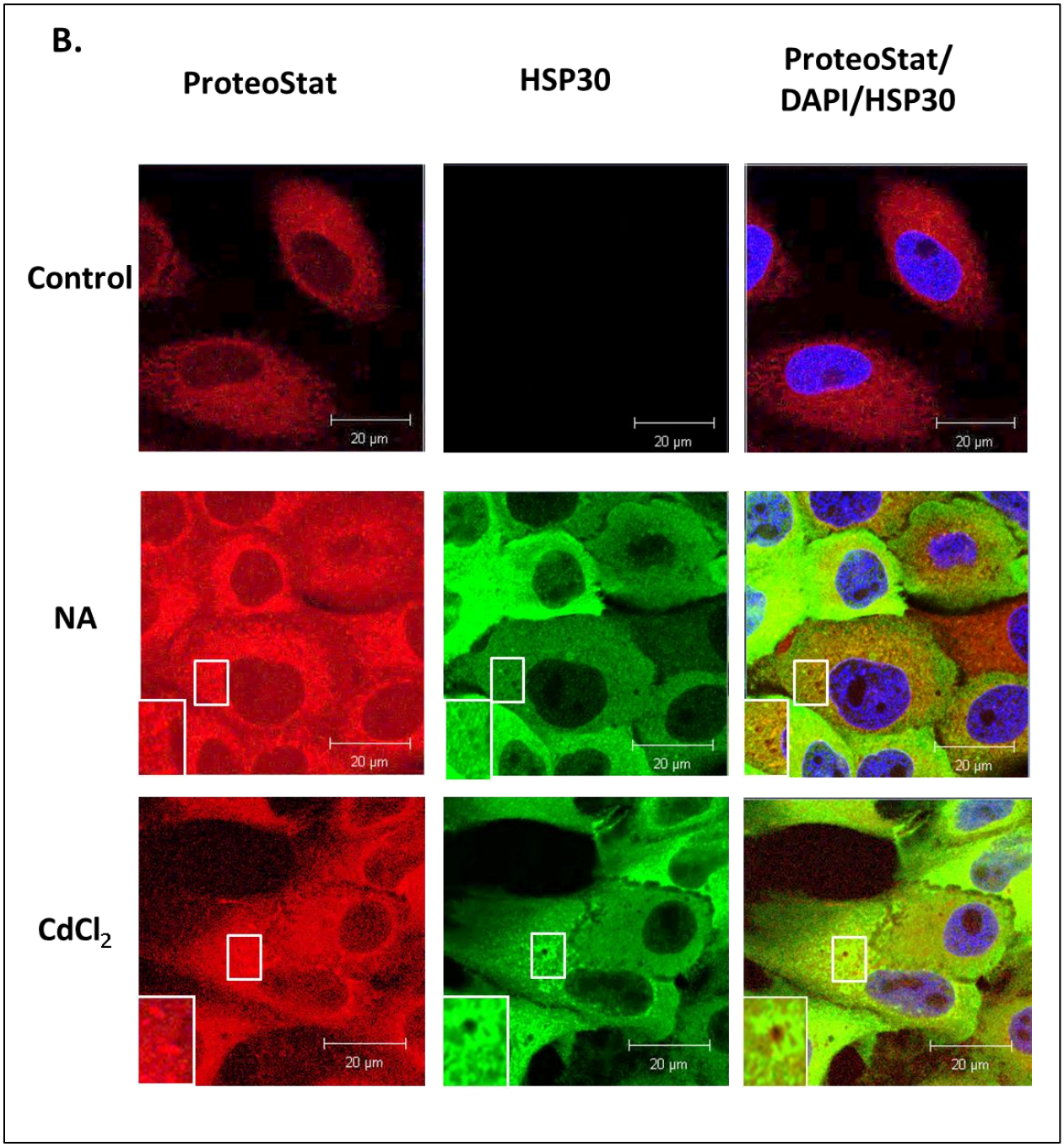
B.
ProteoStat
HSP30
ProteoStat/
DAPI/HSP30
Control
NA
CdCl2
20 µm

within the aggresome (data not shown). This phenomenon was also observed in cells treated with arsenite or cadmium (Fig. 33B).

These previous results were further verified using γ-tubulin as a marker in the detection of aggresomes in A6 cells. As shown in Figure 34, A6 cells incubated at 33 °C showed enhanced HSP30 accumulation and presence of some large HSP30 structures in comparison to cells maintained at 22 °C. These HSP30 staining structures co-localized with γ-tubulin (Fig. 34A). Similarly, A6 cells treated with MG132 or withaferin A resulted in an increase in HSP30 accumulation in the cytoplasm as well as the appearance of aggresomes as shown by γ-tubulin association with these large structures (Fig. 34A). Some aggresomes co-localized with large HSP30 structures as shown in Figure 34A insets. Again, Z-stacking analysis determined that the large multimeric complexes of HSP30 enveloped the aggresome while smaller HSP30 complexes were present within the aggresome (data not shown). Additionally, sodium arsenite and cadmium chloride also induced these structures and displayed co-localization between HSP30 and γ-tubulin (Fig. 34B).

To further validate an association between HSP30 and γ-tubulin, co-immunoprecipitation studies using anti-*Xenopus* HSP30 antibody and anti- γ-tubulin antibody followed by immunoblot analysis were performed. As shown in Figure 35, HSP30 was successfully precipitated using anti-*Xenopus* HSP30 antibody in cells treated with MG132, withaferin A, sodium arsenite or cadmium chloride. Additionally, HSP30 co-immunoprecipitated γ-tubulin and β-actin in treated cells and not in control cells (Fig. 35). In comparison, BiP, an ER-resident molecular chaperone did not co-immunoprecipitate with HSP30 in any of the treatments. To corroborate the first co-immunoprecipitation experiment, the procedure was repeated using the anti-γ-tubulin antibody for immunoprecipitation.

Figure 34. Association of large HSP30 structures and γ-tubulin in response to proteasome inhibition. A & B) Cells were treated as previously described in Figure 31. Gamma-tubulin was detected indirectly with an anti- γ-tubulin antibody and a secondary antibody conjugated to Alexa-555 (red). HSP30 was detected indirectly using an anti-*Xenopus* HSP30 antibody and a secondary antibody conjugated to Alexa-488 (green). Nuclei were stained directly with DAPI (blue). From left to right, the columns display fluorescence detection channels for γ-tubulin, HSP30, and merger of HSP30, DAPI and γ-tubulin. Large HSP30 staining structures along with areas of γ-tubulin staining are magnified, delineated with a white box and shown as a figure inset. These results are representative of 3 separate experiments.

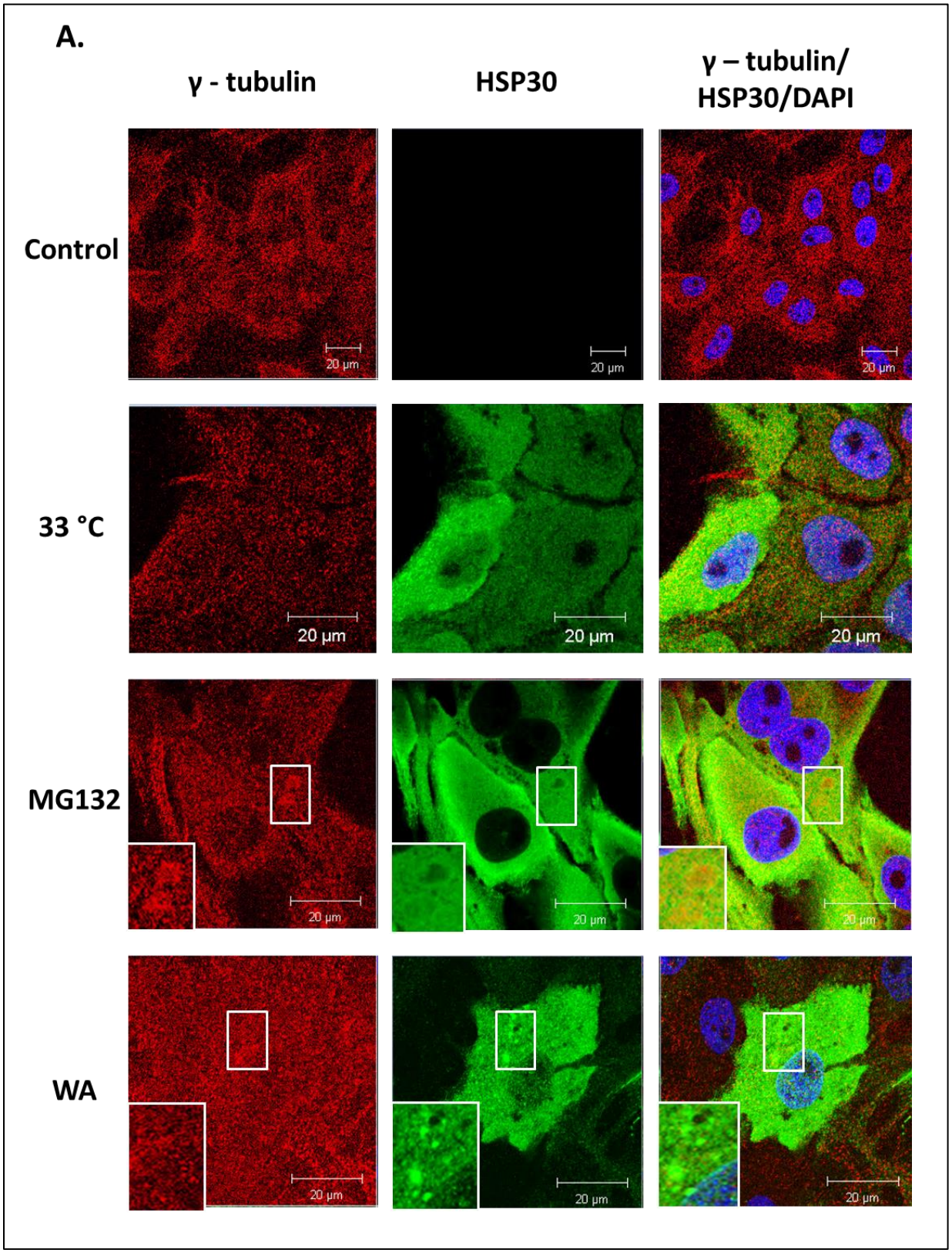
A.
γ - tubulin
HSP30
γ – tubulin/
HSP30/DAPI
Control
33 °C
MG132
WA
20 µm

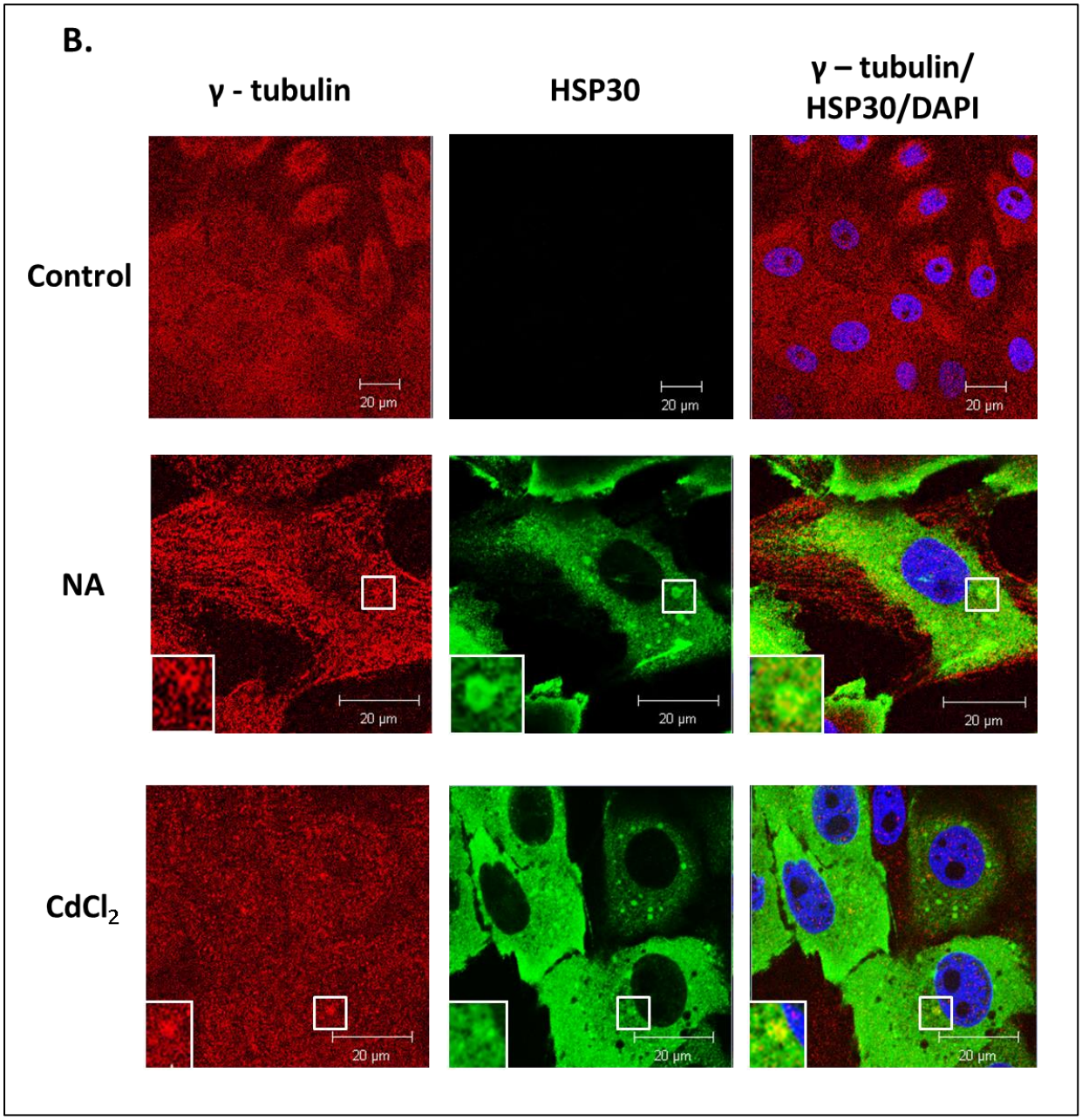
B.
γ - tubulin
HSP30
γ – tubulin/
HSP30/DAPI
Control
NA
CdCl2
20 µm

Figure 35. HSP30 associates with γ-tubulin and β-actin in cells treated with MG132, withaferin A, sodium arsenite or cadmium chloride. Cells were maintained at 22 °C or treated with 30 μM MG132 for 16 h, 5 μM withaferin A (WA) for 16 h, 20 μM sodium arsenite (NA) for 16 h or 100 μM cadmium chloride ($CdCl_2$) for 16 h at 22 °C. Proteins were isolated using non-denaturing conditions and immunoprecipitated (IP) using the anti-*Xenopus* HSP30 antibody. Whole cell lysates (L), flow through (FT) and immunocomplexes (IC) were then analyzed by Western blot analysis using anti- *Xenopus* HSP30, anti-γ-tubulin, anti-actin or anti-BiP antibodies as described in Material and methods. These results are representative of 3 different experiments.

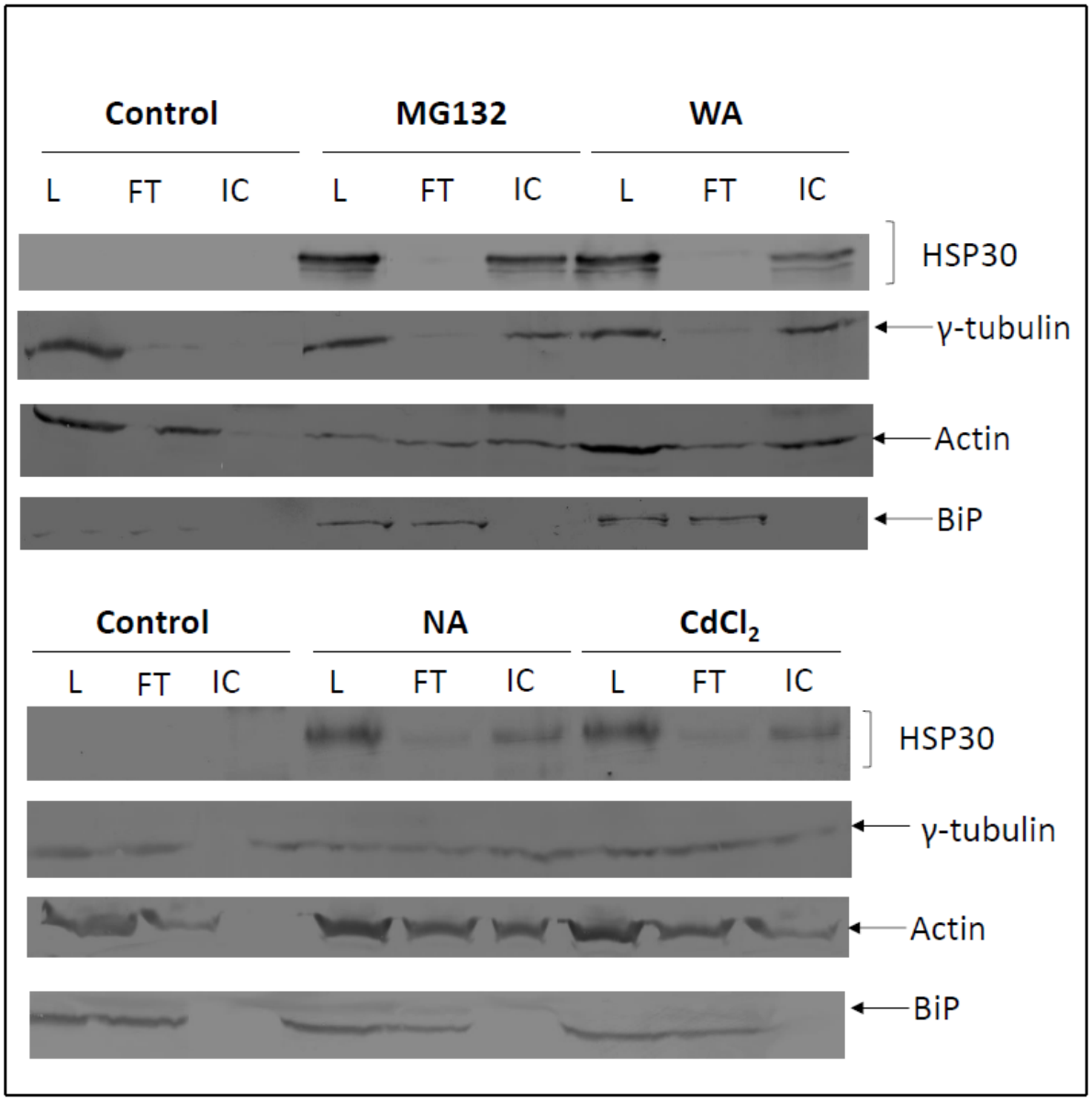
Control
MG132
WA
L
FT
IC
HSP30
γ-tubulin
Actin
BiP
Control
NA
CdCl2

Western blot analysis revealed that anti-γ-tubulin antibody successfully immunoprecipitated γ-tubulin in control cells (Fig. 36). In contrast, no HSP30 was associated with γ-tubulin in control cells. Additionally, γ-tubulin and HSP30 co-immunoprecipitated in cells treated with MG132, withaferin A, sodium arsenite and cadmium chloride (Fig. 36). In comparison, β-actin and BiP did not associate with γ-tubulin and were not co-immunoprecipitated in control or treated cells.

Finally, to investigate a possible association of HSP30 with vimentin, comparable immunocytochemical studies were performed. The vimentin antibody that worked well with immunocytochemistry did not recognize vimentin in immunoblot or co-immunoprecipitation experiments. As shown in Figure 37, treatment with MG132, withaferin A, sodium arsenite and cadmium chloride resulted in enhanced accumulation of HSP30 in the cytoplasm in a granular pattern when compared to control cells. Additionally, cells treated with MG132 or withaferin A showed an increased in vimentin accumulation in the perinuclear region (Fig. 37A). Some areas of intense vimentin staining also co-localized with large HSP30 granules as indicated in white insets (Fig. 37A). Similar results were observed in cells treated with sodium arsenite and cadmium chloride when compared to control cells (Fig. 37B).

Figure 36. Co-immunoprecipitation of HSP30 with γ-tubulin in cells treated with MG132, withaferin A, sodium arsenite and cadmium chloride. Cells were maintained at 22 °C or treated with 30 μM MG132 for 16 h, 5 μM withaferin A (WA) for 16 h, 20 μM sodium arsenite (NA) for 16 h or 100 μM cadmium chloride ($CdCl_2$) for 16 h at 22 °C. Proteins were isolated in non-denaturing conditions and immunoprecipitated (IP) using anti γ-tubulin antibody as described in the Materials and methods. Whole cell lysates (L), flow through (FT) and immunocomplexes (IC) were then analyzed by Western blot analysis using anti-*Xenopus* HSP30, anti-γ-tubulin, anti-actin or anti-BiP antibodies as described in Material and methods. These results are a representation of 3 separate experiments.

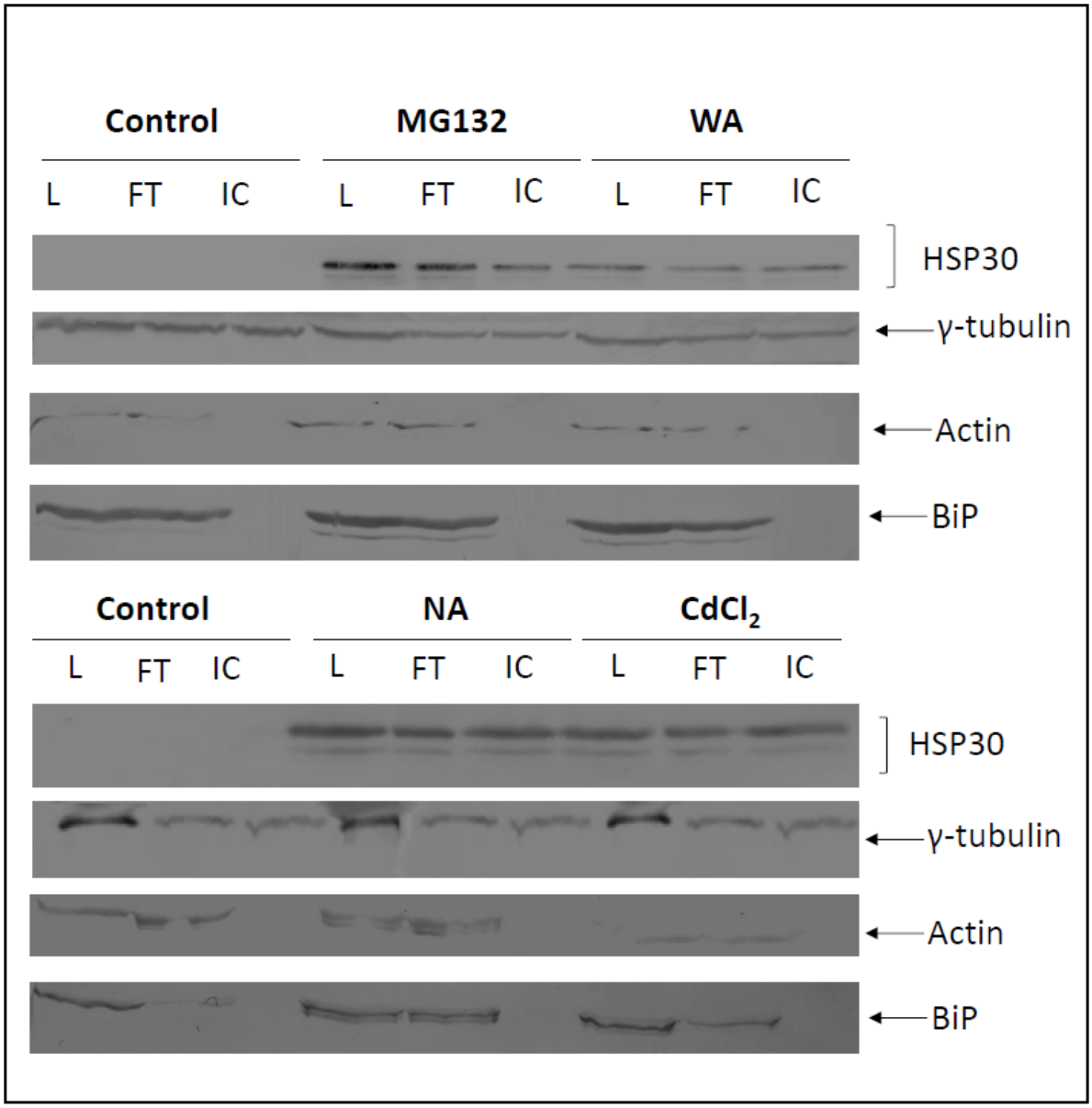
Control
MG132
WA
L
FT
IC
HSP30
γ-tubulin
Actin
BiP
Control
NA
CdCl2
L
FT
IC
HSP30
γ-tubulin
Actin
BiP

Figure 37. Association of large HSP30 structures with vimentin in response to proteasome inhibition. A & B) Cells were grown on glass coverslips and were maintained at 22 °C (Control) or treated with 30 μM MG132 for 16 h or 5 μM withaferin A (WA) for 16 h at 22 °C. B) Cells were also treated with 20 μM sodium arsenite (NA) or 100 μM cadmium chloride ($CdCl_2$) for 16 h at 22 °C. Vimentin was detected indirectly with an anti-vimentin antibody and a secondary antibody conjugated to Alexa-555 (red). HSP30 was detected indirectly using an anti-X*enopus* HSP30 antibody and a secondary antibody conjugated to Alexa-488 (green). Nuclei were stained directly DAPI (blue). From left to right, the columns display fluorescence detection channels for vimentin, HSP30, and merger of HSP30, DAPI and vimentin. Large HSP30 staining structures along with areas of vimentin staining are enlarged, delineated with a white box and shown as a figure inset. These results are representative of 3 separate experiments.

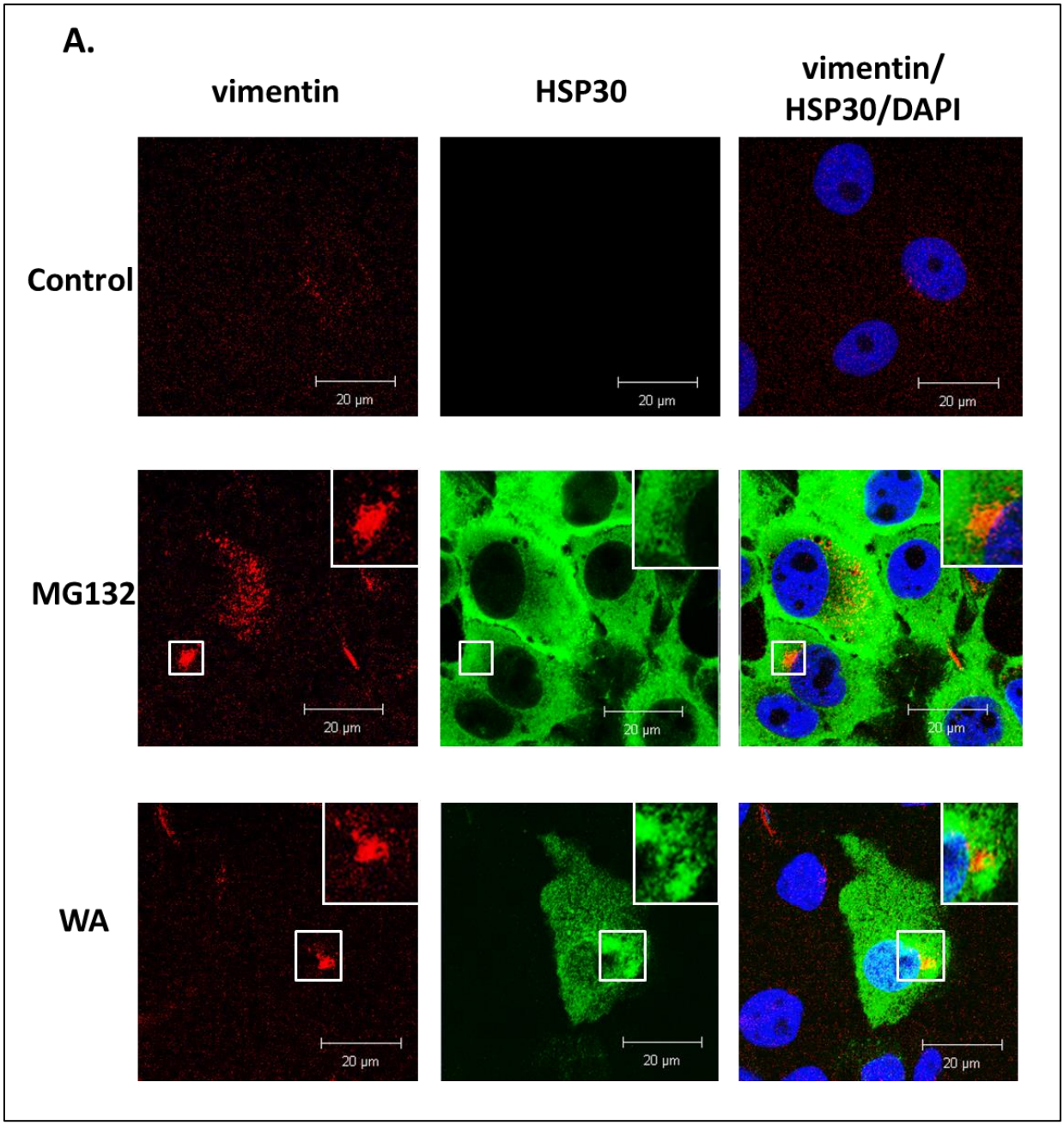
A.
vimentin
HSP30
vimentin/
HSP30/DAPI
Control
MG132
WA
20 μm

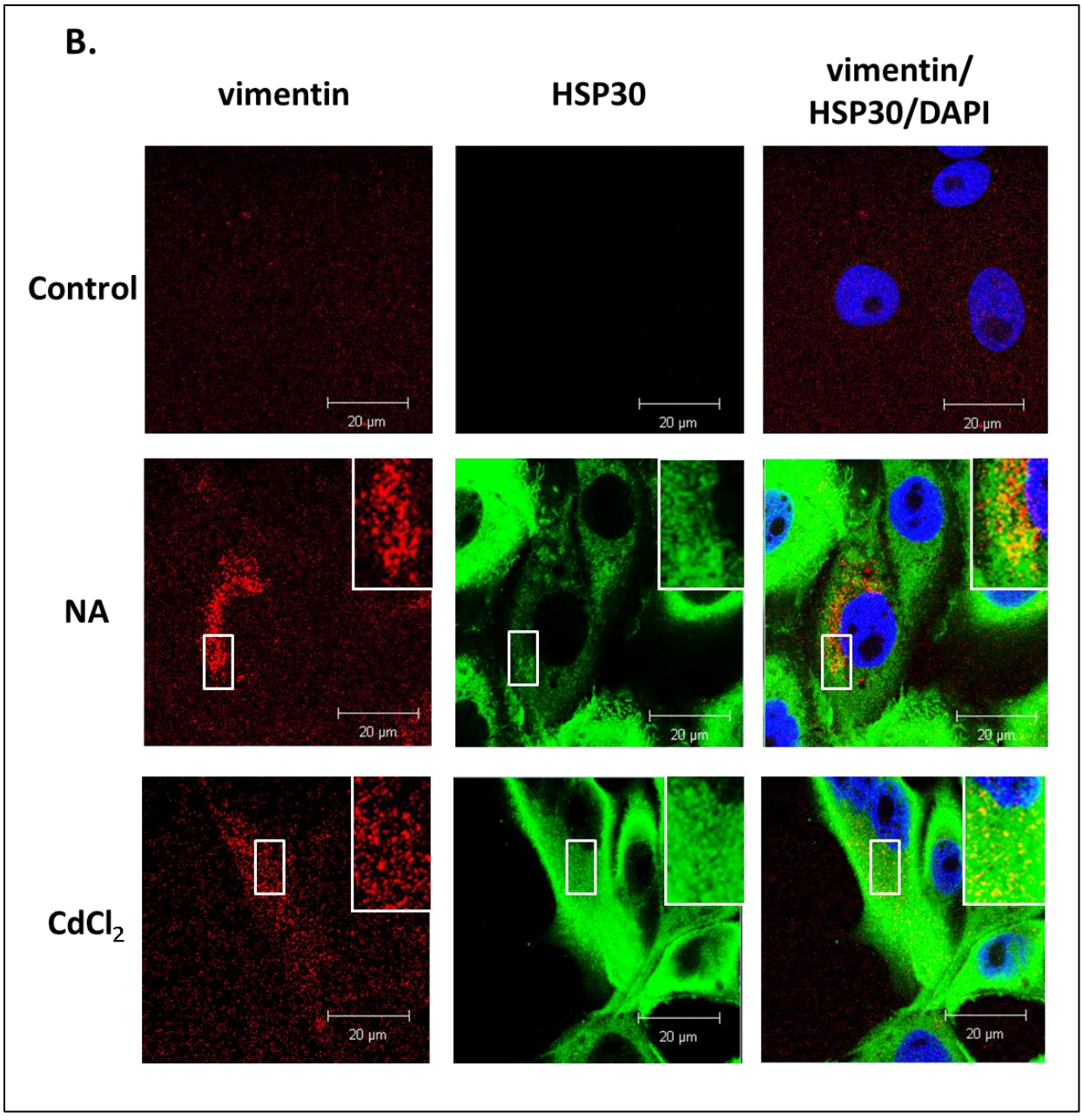
B.
vimentin
HSP30
vimentin/
HSP30/DAPI
Control
NA
CdCl2
20 µm

Chapter 4: Discussion

This thesis has investigated the pattern of HSP30 accumulation in *Xenopus laevis* A6 kidney epithelial cells recovering from heat stress as well as the effect of proteasomal inhibitors, MG132, withaferin A and celastrol on HSP30 accumulation and its possible association with aggresome-like structures.

4.1 HSP30 degradation pattern in cells recovering from heat stress

In initial studies examining the pattern and relative levels of HSP30 during recovery from heat shock, immunoblot analysis revealed that the relative levels of HSP30 declined gradually during recovery with elevated levels still present after 3 days. In comparison, the decay of heat shock-induced HSP70 during recovery occurred much faster. This prolonged accumulation of HSP30 during recovery from heat shock was not correlated with its mRNA levels since both *hsp30* and *hsp70* mRNA levels declined in a similar fashion with undetectable levels at 48 h. Additionally, incubation of A6 cells in the presence of cycloheximide, a translational inhibitor, displayed elevated levels of HSP30 during recovery from heat shock after 36 h in contrast to HSP70 levels, which declined rapidly to non-detectable amounts at 24 h. The longer time period involved in HSP30 decay compared to HSP70 in A6 cells is comparable to that found with HSP27 and HSP70 in Chinese hamster cells (Landry et al., 1991). In this latter study HSP27 had a half-life of 13 h while the value for HSP70 was 4 h. A similar comparison was made with sHSPs and HSP70 in *Drosophila* Schneider S2 cells (Li and Duncan, 1995).

In the present study, treatment of cells recovering from heat shock in the presence of cycloheximide plus MG132 did not have a marked effect on the relative levels of HSP30

compared to cycloheximide alone. Given these results, it raises the possibility that the UPS may not have a major role in the degradation of HSP30 as this treatment should have increased the relative levels of HSP30. In studies with a human neuroblastoma SK-N-SH cell line, it was determined the HSP27 degradation did not occur via the UPS and suggested that it could occur through the autophagy-lysosomal pathway (Chang et al., 2009). Nevertheless, we cannot exclude the possibility that some of the *Xenopus* HSP30 family members may be degraded by the UPS. In contrast to HSP30, MG132 inhibited the cycloheximide-associated decline in HSP70 levels, suggesting that it was degraded via the UPS. These latter results are in agreement with Qian et al. (2006) who found that HSP70 degradation in HEK-293 cells recovering from heat stress occurred via the UPS. Also, Kundrat and Regan (2010) identified 6 lysine residues of human HSP70 that were targeted by ubiquitination for proteasomal degradation via the 26S proteasome.

In *Xenopus*, the differences in the patterns of HSP30 and HSP70 degradation may be associated with their function. While the primary role of HSP70 occurs in protein refolding, HSP30 binds to stress-induced unfolded/damaged protein to prevent their aggregation. It is possible that HSP30 oligomers hold client proteins for an extended amount of time until the cellular machinery can recover sufficiently to either refold or degrade the unfolded protein. Our previous studies determined that HSP30 forms multimeric structures, which bind to unfolded protein, prevent their aggregation and maintain them in a folding-competent state (Fernando and Heikkila, 2000; Abdulle et al., 2002; Fernando et al., 2002). Furthermore, phosphorylation of HSP30 multimers, which is mediated by the p38/MAP kinase pathway, resulted in their breakdown into smaller units (Ohan et al., 1998; Fernando et al., 2003). A similar phenomenon was found with HSP27 and αB crystallin in which phosphorylation was

shown to favor small oligomeric structures (such as dimers), while dephosphorylation was associated with large oligomeric structure formation (Parcellier et al., 2005). In the present study, A6 cells that were pretreated with SB203580 to inhibit HSP30 phosphorylation prior to heat shock and recovery in the presence of cycloheximide resulted in enhanced stability of HSP30 compared to cycloheximide alone.

Additionally, in cells recovering from heat shock, immunocytochemistry revealed the presence of large perinuclear HSP30-immunoreactive structures that were larger and greater in number with prolonged recovery time or treatment with SB203580. Previously, similar HSP30 structures were detected in A6 cells treated with proteasome inhibitors such as MG132 and curcumin and were suggested to be associated with aggresomes (Young and Heikkila, 2010; Khan and Heikkila, 2011). Also, in avian cells MG132-induced HSP25, an HSP30-like sHSP, associated with structures that were proposed to be aggresomes (Katoh et al., 2004). In the present study, during recovery from heat shock, a Proteostat aggresome assay revealed the presence of aggresome-like structures that increased in size and number in the presence of SB253080. Aggresomes are perinuclear microtubule-dependent inclusion bodies that arise from the coalescence of individual protein aggregates (Kopito, 2000; Bauer and Richter-Landsberg, 2006; Bolhuis and Richter-Landsberg, 2010; Shen et al., 2011; Driscoll and Chowdhury, 2012; Nakajima and Suzuki, 2013). This process is thought to occur when the capacity of the proteasome to degrade protein is exceeded or inhibited. The aggregates are transported along microtubules by dynein to a perinuclear microtubule-organizing center to form aggresomes until they undergo proteolysis by autophagy/lysosomes. This process reduces the cytoxic effects of scattered cellular protein aggregates. Previously, formation of these aggresome-like structures were detected in

mammalian cells in response to various stressors and co-localized with HSP27 (Ito et al., 2005; Mi et al., 2009; Bolhuis and Richter-Landsberg, 2010).

Since the present study determined that *Xenopus* HSP30 was more stable during recovery from heat shock than HSP70, it is likely that the presence of HSP30 in multimeric/granular complexes and its association with aggresomes may delay its degradation by an as yet unknown mechanism. It is also possible that heat shock-induced large HSP30 granular complexes may bind to unfolded or misfolded protein and that during recovery from stress these complexes become associated with stress granules or aggresomes to minimize the potential toxic effects of aggregated protein on cell function.

4.2 Proteasome inhibition induces cytosolic/nuclear and ER molecular chaperones in A6 cells

The second part of this study examined the effect of proteasomal inhibitors on the accumulation of cytosolic/nuclear HSPs, HSP30 and HSP70, the endoplasmic reticulum HSP members, BiP and GRP94, and heme oxygenase-1 (HO-1), an enzyme that is induced by stressors such as oxidative stress or heavy metals. Treatment of *Xenopus* cells with 30 μM MG132, 5 μM withaferin A and 2.5 μM celastrol induced an inhibition of proteasome activity and the induction of HSP30, HSP70, BiP and GRP94 in a time-dependent manner. MG132-, withaferin A- or celastrol-induced inhibition of proteasomal activity was indicated by an increase in ubiquitinated protein and a decrease in proteasomal CT-like activity. Previously, our laboratory reported that MG132 and celastrol increased the relative level of ubiquitinated proteins in A6 cells in comparison to control cells and that celastrol decreased CT-like activity of the 26S proteasome by 50 % (Young and Heikkila, 2009; Walcott and

Heikkila, 2010). Additionally, Yang et al. (2006) demonstrated that 2.5 μM celastrol treatment of human prostate cells also resulted in an increase in ubiquitinated protein and inhibition in CT-like activity of the proteasome. Furthermore, these results are similar to findings with human prostate cancer cells in which treatment with 5 to 20 μM withaferin A resulted in an increase in ubiquitinated protein in a dose-dependent manner and a 50% inhibition in CT-like activity after treatment with 20 μM withaferin A for 16 h (Yang et al., 2007). In this latter study, it was suggested that withaferin A-induced proteasomal inhibition resulted from a direct interaction between withaferin A and the β5 subunit of the 20S proteasome, which possesses CT-like activity. Recently, Feng et al. (2013) also demonstrated that celastrol interacted with the β1 subunit of the human recombinant proteasome and decreased the CT-like activity *in vitro*. It is possible that celastrol and withaferin A may have a similar effect on the β1 and β5 subunits in *Xenopus* cells, respectively.

The accumulation of HSP30 and HSP70 as well as their mRNAs in cells in which the proteasome is inhibited is likely the result of an activation of the heat shock response. HSP accumulation as a result of proteasome inhibition is a well-documented phenomenon in eukaryotic systems. For example, in previous studies from our laboratory proteasomal inhibition using MG132, lactacystin and celastrol induced HSP30 and HSP70 in *Xenopus* A6 cells (Young and Heikkila, 2010; Walcott and Heikkila, 2010). Similarly, the induction of HSP accumulation by proteasomal inhibitors was described in yeast and mammalian cells (Lee and Goldberg, 1998; Bush et al., 1997; Pritts et al., 2002; Stangl et al., 2002; Westerheide et al., 2004; Awasthi and Wagner, 2005; Chow and Brown, 2007; Zhang and Sarge, 2007; Trott et al., 2008; Kalmar and Greensmith, 2009). Interestingly, MG132, celastrol and withaferin A have different modes of action within cells, but resulted in similar

levels of HSPs suggesting that multiple pathways might exist for proteasomal inhibitor-induced HSP accumulation in A6 cells.

There are at least two possible mechanisms by which proteasome inhibition can induce the accumulation of unfolded or damaged protein which could ultimately activate the heat shock response. Since the proteasome degrades 80 to 90 percent of total cellular protein, it is possible that inhibition of the proteasome by classical proteasome inhibitors such as MG132 may cause an increase in the concentration of misfolded or damaged proteins, which could ultimately activate HSF1 and result in the subsequent upregulation of *hsp* gene expression (Young and Heikkila, 2010; Walcott and Heikkila, 2010; Khan and Heikkila, 2011). Additionally, in a chicken erythroblast cell line, HD6, the activities of HSF1, HSF2, and HSF3 were upregulated by MG132 (Kawazoe et al. 1998). Moreover, in mouse embryonic fibroblast cells, both MG132 and lactacystin, both of which are known proteasome inhibitors, induced hyperphosphorylation, trimerization, and HSE binding activity of HSF1 (Kim et al. 1999).

Another possible mechanism for celastrol or withaferin A-induced damage of cellular protein leading to the activation of the heat shock response involves the direct effect of these proteasomal inhibitors on protein structure. For example, studies with yeast and mammalian cells demonstrated that celastrol interacts with cysteine residues on proteins through its thiol groups and renders proteins inactive (Trott et al., 2008). Additionally, previous studies also found that withaferin A bound to cysteine residues in the C-terminus of HSP90 and inhibited its chaperone activity by disrupting its ability to bind to client proteins (Yu et al., 2010; Grover et al., 2011; Gu et al., 2014). These findings suggest that both celastrol and withaferin A can modify various proteins via thiol reactivity and could ultimately contribute to an

increase in HSPs. More recently, it was determined that the α, β-unsaturated carbonyl motif of withaferin A reacted with proteins by forming adducts with thiol groups in cysteine residues and that this motif was necessary but not sufficient for heat shock activation of green fluorescent protein controlled by a minimal consensus HSE-containing promoter in a reporter cell line (Ozorowski et al., 2012; Santagata et al., 2012). Since monomeric inactive HSF1 is normally bound to HSP90, binding of withaferin A to HSP90 might disrupt this complex allowing HSF1 to trimerize and activate *hsp* expression.

Activation of the unfolded protein response by MG132, celastrol and withaferin A in A6 cells was suggested by the accumulation of *bip* mRNA and BiP and GRP94 protein. These results are in agreement with previously published results in other vertebrate systems, in which, proteasomal inhibitors induced the unfolded protein response (Choi et al., 2011; Park et al., 2011; Nakajima et al., 2011; Feng et al., 2013). For example, MG132 induced the enhanced accumulation of ER stress markers including *bip*, *chop* and *atf4* mRNA in NRK-53E renal tubule epithelial cells (Nakajima et al., 2011). More recently, Feng et al. (2013) demonstrated that celastrol induced the accumulation of ER stress-related proteins including pancreatic ER kinase (PERK), inositol-requiring enzyme 1 (IRE1), BiP and CHOP in HeLa cells. Additionally, a study by Choi et al. (2011) determined that treatment of mammalian Caki cells with 2-6 μM withaferin A induced ER stress as indicated by the enhanced accumulation of *bip* mRNA and encoded protein. While the mechanism responsible for MG132, celastrol and withaferin A induction of the ER chaperones in *Xenopus* cells is not known, it is possible that these chemicals may cause an increase in unfolded and/or misfolded proteins in the ER lumen resulting from the repression of proteasomal activity. As mentioned previously an increase in unfolded protein results in enhanced accumulation of

BiP and GRP94 in order to inhibit the production of protein aggregates and maintain client protein in a competent state for subsequent folding, oligomerization and translocation (Lee and Goldberg, 1998). Furthermore, it is also possible that MG132, celastrol and withaferin A-induced proteasomal inhibition may slightly increase the relative levels of HSP70 after they are induced since it cannot be degraded due to the inhibition of the proteasome. In these experiments, the relative levels of actin were not altered. It is possible that its relatively long half-life and abundance in the cell may mask an increase in its relative levels by proteasomal inhibition.

Immunocytochemistry was employed to determine the localization of HSP30 and BiP in cells treated with MG132, celastrol or withaferin A. A6 cells exposed to MG132, celastrol or withaferin A accumulated HSP30 mainly in the cytoplasm in a granular pattern with a lesser amount of HSP30 staining in the nucleus. The punctate pattern of HSP30 accumulation may reflect the stress-induced formation of HSP30 multimeric structures that are associated with its cellular function in the prevention of toxic aggregates (Johnston et al., 1998; MacRae, 2000; Van Montfort et al., 2002; Heikkila, 2010). Cells treated with A23187, an inducer of the unfolded protein response, did not show any HSP30 accumulation. In comparison, cells treated with A23187, MG132, celastrol or withaferin A had an enhanced accumulation of BiP in a punctate pattern in the perinuclear region and occasionally at the periphery of the cell membrane. The enhanced accumulation and localization pattern of BiP in A6 cells is indicative of an unfolded protein response. For example treatment of cells with ER stressors such as thapsigargin, a Ca^{2+}-ATPase inhibitor, or tunicamycin were reported to upregulate BiP in a punctate pattern with coalescence of BiP in the perinuclear region of mammalian cells (Kitiphongspattana et al., 2005; Sun et al., 2006). A similar response was

also reported with proteasome inhibitors, MG132 and/or lactacystin in mouse pancreatic β-cell cytoplasm and dog MDCK cells (Bush et al., 1997; Kitiphongspattana et al., 2005; Haas et al., 2007).

In some proteasome inhibited A6 cells, a co-localization of HSP30 with actin was observed which is in accord with the potential role of sHSPs in stabilization of the actin cytoskeleton (MacRae, 2000; Van Montfort et al., 2002; Doshi et al., 2009). Furthermore, cells treated with MG132 or withaferin A did not display a disruption in the F-actin cytoskeleton, which has been employed as a positive indicator of cellular health (Wiegent et al., 1987; Ohtsuka et al., 1993). In contrast, treatment of A6 cells with celastrol induced a rounded cell shape and disrupted actin cytoskeleton as indicated by F-actin localization to the cell periphery. The mechanism for the disruption of the actin cytoskeleton in A6 cells is unknown. It is possible that celastrol might inhibit nuclear factor kappaB (NF-κB), which is linked to decreased levels of cell adhesion molecules that are required for proper attachment of the cytoskeleton to the extracellular matrix (Collins et al., 1995; Tozawa et al., 1995).

In an ancillary study, the effect of proteasomal inhibitors on the relative levels of HO-1 was examined in A6 cells. As mentioned previously, HO-1 is a 32 kDa cytosolic protein, which functions as an enzyme that catalyzes the catabolism of heme into bilirubin via biliverdin (Uppu et al., 2010). It is induced in cells in response to oxidative stress (Keyse and Tyrrell, 1989; Turner et al., 1999). In the present study, treatment of A6 cells with withaferin A and celastrol enhanced the accumulation of HO-1 and HSP30 in a time- and concentration-dependent manner. Immunocytochemical analysis utilizing laser scanning confocal microscopy showed that treatment of A6 cells with proteasome inhibitors resulted in HO-1 accumulation primarily in the cytoplasm in a granular pattern. These results are in agreement

with recent studies showing HO-1 induction in response to proteasome inhibition (Wu et al., 2004; Kastle et al., 2012; Furfaro et al., 2014). For example, Kastle et al. (2012) demonstrated that treatment of human foreskin fibroblast and HT29 colon carcinoma cells with lactacystin induced HSP27, HSP70 and HO-1 accumulation. More specifically, proteasome inhibition by lactacystin induced the deacetylation of HDAC6 resulting in the subsequent phosphorylation of p38-MAPK and activation of the NRF-2, which is a transcriptional activator of HO-1. Previously, Wu et al. (2004) also showed enhanced accumulation of HO-1 in murine macrophages in response to MG132 through the activation of the p38-MAPK pathway.

4.3 Proteasomal inhibition, sodium arsenite and cadmium chloride induce large HSP30 multimeric structure, stress granule and aggresome formation in A6 cells

In the final part of this study, I attempted to identify the structures associated with the relatively large HSP30 staining foci induced by the proteasomal inhibitors, MG132, celastrol and withaferin A. Similar large HSP30 staining structures were reported in A6 cells exposed to sodium arsenite or cadmium chloride, which can also inhibit proteasome function (Woolfson and Heikkila, 2009; Young and Heikkila, 2009; Brunt et al., 2011). Although the identity of these HSP30 staining foci is unclear, it is known from studies with mammalian cells that proteasomal inhibitors can induce the formation of RNA stress granules containing stalled translational complexes or aggresome-like structures, which are proteinaceous inclusion bodies that form as a general cellular response to aggregated protein (Garcia-Mata, 1999; Kopito, 2000; Kedersha et al., 2002; Anderson and Kedersha, 2009).

RNA stress granules are RNA-protein complexes composed of stalled pre-initiated mRNA bound to 40S ribosomal subunit, RNA binding proteins such as TIA1 and various eukaryotic protein synthesis initiation factors such as eIF3, eIF4F, eIF4B, and PABP (Kedersha et al., 2007). In the current study, A6 cells treated with MG132 and withaferin A showed enhanced accumulation and co-localization of TIA1 and PABP, markers of stress granule formation (Kedersha et al., 2000; Anderson and Kedersha, 2002; Gilks et al., 2004; Kedersha and Anderson, 2007). Inhibition of the UPS using MG132, lactacystin or Bortezomib was reported to induce stress granule formation in HeLa cells (Mazroui et al., 2007; Fournier et al., 2010). Furthermore, the MG132-induced formation of stress granules required phosphorylation of eIF2α (Mazroui et al., 2007). Sodium arsenite treatment in A6 cells also resulted in an increase in the formation of stress granules. This was in accordance with previous literature reporting that sodium arsenite induced the formation of stress granules in HeLa cells (Kedersha et al., 2000). Additionally, Satoh et al. (2012) demonstrated that RNA-binding protein Nrd1 localized to PABP-positive stress granules in response to heat, arsenite treatment and oxidative stress. In the present study, no co-localization was observed between HSP30 and PABP1 in A6 cells treated with proteasome inhibitors. Studies examining the association of sHSPs with proteasomal inhibitor-induced formation of stress granules in other experimental systems are quite limited. While Mazroui et al. (2007) established that only HSP72 co-localized with stress granules in HeLa cells, Ma et al. (2009) did observe that HSP27 and HSP72 were co-immunoprecipitated with PABP1 and eIF4G in HeLa cells recovering from heat stress.

The present study revealed that treatment of A6 cells with MG132 or withaferin A also induced the formation of aggresomes-like structures. Anti-vimentin and anti-γ-tubulin

antibodies were used as markers for the presence of aggresomes, along with the ProteoStat aggresome assay described previously. Vimentin and γ-tubulin have been extensively used as markers for detecting aggresomes in many cellular systems (Kopito, 2000; Liewluck et al., 2007; Mi et al., 2009; Taylor et al., 2012; Xiong et al., 2013). More recently, Shen et al., 2011 used the ProteoStat aggresome assay to show the presence of aggresomes in HeLa cells treated with MG132. In the present study, ProteoStat co-localized with both vimentin and -γ-tubulin in cells treated with selected proteasome inhibitors. An increase in the appearance of aggresomes was detected using the ProteoStat assay and anti-vimentin and anti-γ-tubulin antibodies in cells treated with MG132, withaferin A, arsenite and cadmium in comparison to control. These results confirm previous mammalian studies demonstrating the formation of aggresomes in cells treated with proteasome inhibitors. For example, Taylor et al. (2012) showed the presence of aggresome formation in human embryonic kidney and neuroblastoma cells in response to MG132. More recently, prolonged exposure to MG132 treatment resulted in the formation of vimentin-caged aggresome-like inclusion bodies in rat mesencephalic dopaminergic cells (Xiong et al., 2013). Additionally, Song et al. (2008) demonstrated that cadmium treatment of HEK293 cells resulted in aggresome formation as determined by means of γ-tubulin, dynein, HDAC6 and ubiquitin co-localization. Also, arsenite-induced aggresome formation was reported in baby hamster kidney (BHK) cells (Heir et al., 2006). Recently, Jacobson et al. (2012) demonstrated that arsenite interfered with protein folding and induced the formation of protein aggregates.

As mentioned previously, formation of aggresome-like structures that were detected in mammalian cells in response to various stressors co-localized with HSP27 (Ito et al., 2005; Mi et al., 2009; Bolhuis and Richter-Landsberg, 2010). In the present study, multimeric

HSP30 complexes were also shown to co-localize with aggresome-like structures as indicated by ProteoStat assay and the presence of vimentin and γ-tubulin in cells treated with MG132, withaferin A, sodium arsenite and cadmium chloride. Moreover, co-immunoprecipitation experiments revealed that HSP30 associated with γ-tubulin and β-actin. Evidence for sHSP association with cytoskeletal proteins exists in a variety of systems especially as part of the aggresomes (Goldbaum et al., 2009; Richter-Landsberg and Leyk, 2013). For example, Goldbaum et al. (2009) demonstrated that treatment of rat astrocytes with MG132 resulted in aggresome formation containing HSP25 (human HSP27 homolog), ubiquitinated protein and cytoskeletal proteins. Additionally, this latter study determined that HSP25 protected astrocyte morphology during MG132 treatment. More recently, Jacobson et al. (2012) demonstrated that arsenite-induced protein aggregates in yeast cells. Cadmium treatment of HEK293 cells also resulted in the formation of aggresomes containing HSP70, HSP40 and ubiquitinated protein (Song et al., 2008). In the current study, we also detected the presence of aggresome-like structures during recovery from heat shock that increased in size and number in the presence of SB253080 using a Proteostat aggresome assay. This suggests that formation of aggresomes is associated with the multimeric nature of sHSPs and not just limited to proteasome inhibition. To this effect, Zhang and Qian (2010) have shown that HSP70 is required for targeting proteins to aggresomes under stressful conditions; however, HSP70 is not a part of the aggresome complex.

Taken together, these findings suggest a link between proteasome inhibition, HSP induction as well as aggresome and stress granule formation in *Xenopus laevis* A6 kidney cells as outlined in Figure 38. Under normal conditions, the association of HSF1 with HSP90 and HDAC6 maintains it in a monomeric inactive state. Upon treatment of cells with

Figure 38. Model of stress-induced HSP30 induction, stress granule and aggresome formation in *Xenopus* A6 kidney epithelial cells. 1) HSF1 exists in cells in a monomeric inactive form, bound to HSP90 and HDAC6. 2) Proteasome inhibition of cells using MG132, celastrol or withaferin A results in an increase in ubiquitinated proteins. 3) Heat shock or chemical stress also causes an increase in unfolded proteins in cells. 4) An increase in unfolded ubiquitinated protein recruits HDAC6 and HSP90 to prevent its aggregation. HSP90 also binds unfolded proteins in stressed cells. 5) Once HSF1 is not bound to HSP90 or HDAC6, it can trimerize and translocate to the nucleus resulting in an increase in HSPs, including HSP30. 6) Stress-induced HSP30s are then recruited towards unfolded protein complexes and keep them in a folding competent state. HSP30 forms multimeric complexes to bind unfolded protein in cells. 7) HDAC6 complexed with ubiquitinated proteins are transported along microtubule networks to stress granules, which contain RNA-binding proteins such as TIA1 and PABP. 8) Large multimeric HSP30s complexes also interact with cytoskeletal proteins such as vimentin or γ-tubulin as well as HDAC6, HSP90 and ubiquitinated protein complexes to form large aggresome-like structures.

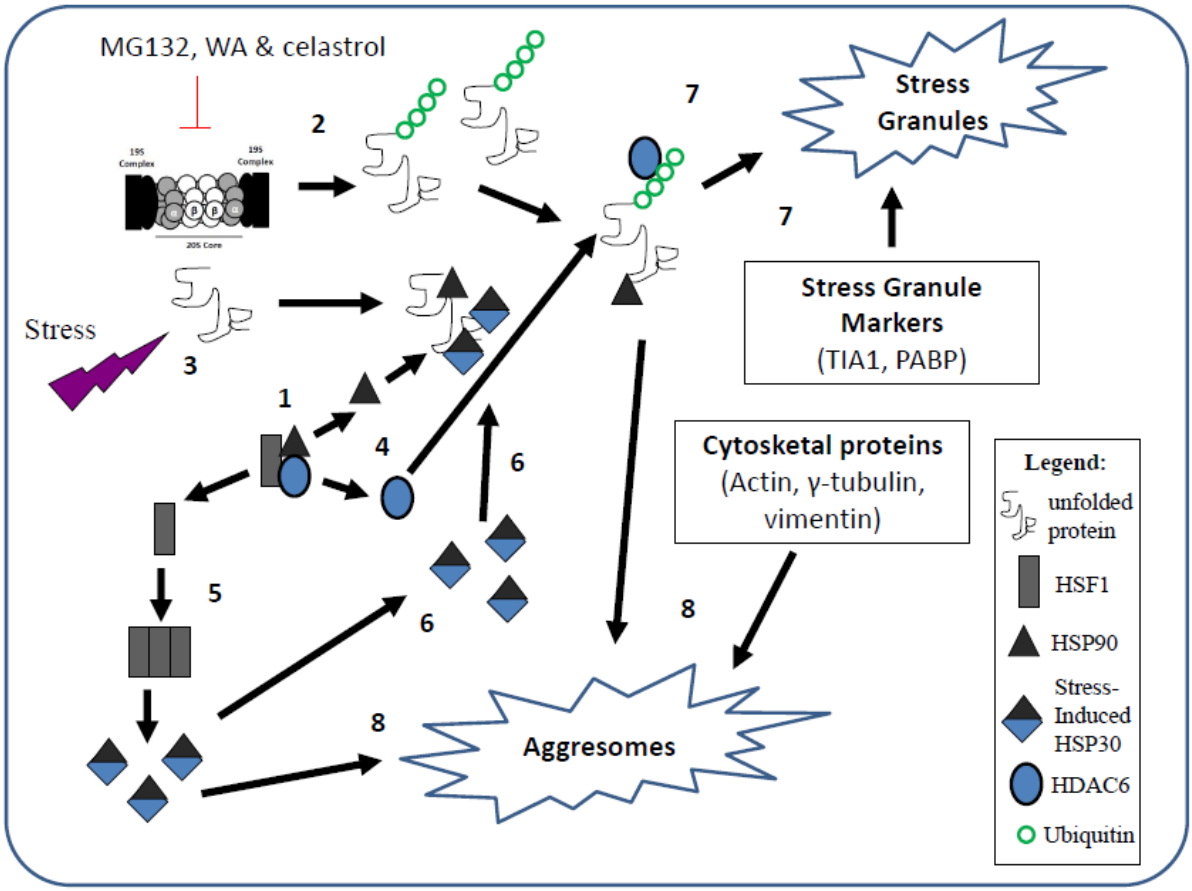
MG132, WA & celastrol
19S Complex
19S Complex
20S Core
Stress
1
2
3
4
5
6
7
8
Stress Granules
Stress Granule Markers (TIA1, PABP)
Cytosketal proteins (Actin, γ-tubulin, vimentin)
Aggresomes
Legend:
unfolded protein
HSF1
HSP90
Stress-Induced HSP30
HDAC6
Ubiquitin

MG132, celastrol or withaferin A, there is an increase in ubiquitinated and misfolded proteins. HDAC6 and HSP90 dissociate from HSF1 as they are recruited to bind ubiquitinated and misfolded proteins, respectively. This causes the trimerization, phosphorylation and binding of HSF1 to HSEs, resulting in stress-induced *hsp* gene expression. HDAC6 bound to ubiquitinated proteins can bind to PABP, TIA1 and G3BP resulting in the formation of stress granules. Additionally, stress-induced sHSPs, particularly, HSP30, forms multimeric complexes and binds misfolded and ubiquitinated proteins to prevent their aggregation. Over an extended period of time, HSP30 also binds cytoskeletal proteins such as tubulin, actin and vimentin, along with misfolded proteins. This results in the formation of aggresome-like structures or inclusion bodies, which are aggregates of cytoskeletal proteins along with misfolded proteins associated with large HSP30 granules.

At present, there is significant evidence available in support of this model. Boyault et al. (2007) have shown that HDAC6 is part of the HSF1 and HSP90 complex. Upon proteasome inhibition, HDAC6 and HSP90 are recruited to bind polyubiquitinated proteins. Additionally, it was demonstrated that HDAC6 binds to polyubiquitinated chains on proteins by means of lysine 63 of ubiquitin (Olzmann and Chin, 2008). This causes monomeric HSF1 to trimerize as it is no longer bound to HSP90 or HDAC6, resulting in stress-induced HSPs (Boyault et al., 2007). HDAC6 also binds tubulin and acts as a bridge between ubiquitinated proteins and the microtubule network by moving aggregated proteins towards the perinuclear region resulting in the formation of aggresomes (Kawaguchi et al., 2003).

More recently, HDAC6 was determined to be a crucial element in the formation of stress granules (Kwon et al., 2007). HDAC6 interacted with G3BP and TIA1 as a result of proteasome inhibition with MG132 and directed the formation of stress granules through the

microtubule network. These findings taken together suggest a prominent role of HDAC6 in the pathway.

4.4 Significance of this thesis

This study has provided significant insight into the detection and understanding of the effect of toxicological agents on protein unfolding and the triggering of both the heat shock and unfolded protein responses in *Xenopus* A6 kidney epithelial cells. For example, my findings that arsenite, cadmium and other proteasomal inhibitors induced HSPs, HO-1, as well as aggresome and stress granule formation suggest that their presence could be used as potential molecular biomarkers of toxicological stress in other aquatic and possibly terrestrial organisms. This study also indicates that sHSPs, such as *Xenopus* HSP30, which has a prolonged decay pattern, may be more useful as molecular biomarkers of recent cell stress events than HSP70. Finally, this thesis research produced basic information on the effects of proteasomal inhibition and sHSP accumulation, which may be of importance in our understanding of human protein misfolding diseases.

4.5 Future directions

In this thesis, I have examined the stress-induced accumulation of multimeric HSP30 complexes and the formation of stress granules and aggresomes in *Xenopus* A6 kidney epithelial cells. Further studies examining the possible involvement of HSP30 and other HSPs, such as HSP70, in the formation of aggresomes should be conducted. In cos7 cells, the involvement of HSP70 with bcl-2-associated athanogene 3 (BAG3) was found to direct chaperone-mediated misfolded proteins to the aggresome (Gamerdinger et al., 2011). One

approach would be to create FLAG-tagged *hsp30* and *hsp70* gene constructs and after their transfection into A6 cells, one could study the role of these HSPs in aggresome formation. An alternative approach would be to overexpress these HSPs in A6 cells by transfecting FLAG-tagged *hsp30* and *hsp70* gene constructs and monitoring the association of these FLAG-tagged HSPs with aggresomes. Furthermore, it is possible to use RNAi or antisense morpholino oligonucleotides (Dirks et al., 2010; Bestman and Kline, 2014; Guo et al., 2014) to inhibit the synthesis of HSP30 or HSP70 in A6 cells and study their effect on the formation of aggresomes. Additionally, nocodazole, which has been shown to inhibit aggresome formation by inhibiting microtubule polymerization (Bauer and Richter-Landsberg, 2006), could be used to study the involvement of HSP30 and HSP70 in the formation of aggresomes in *Xenopus* cells. Finally, it will be interesting to observe the formation of stress granules and aggresomes in response to proteasome inhibition in *Xenopus* embryos in various tissues during development.

An important approach to the study of stress-induced HSPs as well as aggresome and stress-granule formation is to examine the role of HDAC6 in *Xenopus* cells. Unfortunately, due to the lack of an available antibody against *Xenopus* HDAC6, I was not able to investigate the involvement of HDAC6 in the stress-induced formation of aggresomes and stress granules. Since, HDAC6 was found to play a prominent role in mammalian aggresome formation, future research into the role of HDAC6 in the current *Xenopus* model of protein aggregation would be highly beneficial. Finally, the mechanisms by which protein aggregates are cleared from *Xenopus* cells is not well understood and should be assessed. One possible pathway involves autophagy and lysosomes. For example in mammalian cells, it was determined that MG132- and celastrol-induced aggresomes were cleared through autophagy

(Wang et al., 2011; Lee et al., 2012; Williams et al., 2013). Studying the formation and clearance of aggresomes in cells recovering from proteasome inhibition in A6 cells could provide insight into how *Xenopus* cells deal with enhanced levels of aggregated protein.

References

Abane, R., Mezger, V. 2010. Roles of heat shock factors in gametogenesis and development. FEBS J. 277, 4150-4172.

Abdulle, R., Mohindra, A., Fernando, P., Heikkila, J.J. 2002. *Xenopus* small heat shock proteins, Hsp30C and Hsp30D, maintain heat- and chemically denatured luciferase in a folding-competent state. Cell Stress Chaperones 7, 6-16.

Adachi, Y., Yamamoto, K., Okada, T., Yoshida, H., Harada, A., Mori, K. 2008. ATF6 is a transcription factor specializing in the regulation of quality control proteins in the endoplasmic reticulum. Cell Struct Funct. 33, 75-89.

Aghdassi, A., Phillips, P., Dudeja, V., Dhaulakhandi, D., Sharif, R., Dawra, R., Lerch, M.M., Saluja, A. 2007. Heat shock protein 70 increases tumorigenicity and inhibits apoptosis in pancreatic adenocarcinoma. Cancer Res. 67, 616-625.

Alam, J., Wicks, C., Stewart, D., Gong, P., Touchard, C., Otterbein, S., Choi, A.M., Burow, M.E., Tou, J. 2000. Mechanism of heme oxygenase-1 gene activation by cadmium in MCF-7 mammary epithelial cells. Role of p38 kinase and Nrf2 transcription factor. J Biol Chem. 275, 27694-27702.

Ali, A., Salter-Cid, L., Flajnik, M., Heikkila, J.J. 1996a. Isolation and characterization of a cDNA encoding a *Xenopus* 70-kDa heat shock cognate protein, Hsc70.I. Comp Biochem Physiol B Biochem. Mol. Biol. 113, 681-687.

Ali, A., Salter-Cid, L., Flajnik, M., Heikkila, J.J. 1996b. Molecular cloning of a cDNA encoding a *Xenopus laevis* 70-kDa heat shock cognate protein, hsc70.II. Biochim Biophys Acta. 1309, 174-178.

An, L.H., Lei, K., Zheng, B.H. 2014. Use of heat shock protein mRNA expressions as biomarkers in wild crucian carp for monitoring water quality. Environ Toxicol Pharmacol. 37, 248-255.

Anckar, J., Hietakangas, V., Denessiouk, K., Thiele, D.J., Johnson, M.S., Sistonen, L. 2006. Inhibition of DNA binding by differential sumoylation of heat shock factors. Mol Cell Biol. 26, 955-964.

Anderson, P., Kedersha, N. 2006. RNA granules. J Cell Biol. 172, 803-808.

Anttonen, A.K., Mahjneh, I., Hämäläinen, R.H., Lagier-Tourenne, C., Kopra, O., Waris, L., Anttonen, M., Joensuu, T., Kalimo, H., Paetau, A., Tranebjaerg, L., Chaigne, D., Koenig, M., Eeg-Olofsson, O., Udd, B., Somer, M., Somer, H., Lehesjoki, A.E. 2005. The gene disrupted in Marinesco-Sjögren syndrome encodes SIL1, an HSPA5 cochaperone. Nat Genet. 37, 1309-1311.

Arrigo, A.P. 1998. Small stress proteins: chaperones that act as regulators of intracellular redox state and programmed cell death. J Biol Chem. 379, 19-26.

Arrigo, A.P., Gibert, B. 2013. Protein interactomes of three stress inducible small heat shock proteins: HspB1, HspB5 and HspB8. Int J Hyperthermia 29, 409-422.

Arrigo, A.P., Landry, J. 1994. Expression and function of the low-molecular-weight heat shock proteins. In The Biology of Heat Shock Proteins and Molecular Chaperones (ed. R. I. Morimoto, A. Tissières and C. Georgopoulos), pp. 335-373. Cold Spring Harbor Laboratory Press, ColdSpring Harbor, NY.

Arrigo, A.P., Simon, S., Gibert, B., Kretz-Remy, C., Nivon, M., Czekalla, A., Guillet, D., Moulin, M., Diaz-Latoud, C., Vicart, P. 2007. Hsp27 (HspB1) and alphaB-crystallin (HspB5) as therapeutic targets. FEBS Lett. 581, 3665-3674.

Arrigo, A.P., Simon, S. 2010. Expression and functions of heat shock proteins in the normal and pathological mammalian eye. Curr Mol Med.10, 776-793.

Arrigo, A.P., Virot, S., Chaufour, S., Firdaus, W., Kretz-Remy, C., Diaz-Latoud, C. 2005. Hsp27 consolidates intracellular redox homeostasis by upholding glutathione in its reduced form and by decreasing iron intracellular levels. Antioxid Redox Signal. 7, 414-422.

Awasthi, N. and Wagner, B.J. 2005. Upregulation of heat shock protein expression by proteasome inhibition: an antiapoptotic mechanism in the lens. Invest Ophthalmol Vis Sci. 46, 2082-2091.

Balch, W.E., Morimoto, R.I., Dillin A., Kelly J.W. 2008. Adapting proteostasis for disease intervention. Science 319, 916-919.

Bauer, N.G., Richter-Landsberg, C. 2006. The dynamic instability of microtubules is required for aggresome formation in oligodendroglial cells after proteolytic stress. J Mol Neurosci. 29, 153-168.

Beere, H.M., Wolf, B.B., Cain, K., Mosser, D.D., Mahboubi, A., Kuwana, T., Tailor, P., Morimoto, R.I., Cohen, G.M., Green, D.R. 2000. Heat-shock protein 70 inhibits apoptosis by preventing recruitment of procaspase-9 to the apaf-1 apoptosome. Nat Cell Biol. 2, 469-475.

Beere, H.M., Green, D.R. 2001. Stress management - heat shock protein-70 and the regulation of apoptosis. Trends Cell Biol. 11, 6-10.

Bestman, J.E., Cline, H.T. 2014. Morpholino studies in *Xenopus* brain development. Methods Mol Biol. 1082, 155-171.

Bienz, M. 1984. Developmental control of the heat shock response in *Xenopus*. Proc. Natl. Acad. Sci. USA. 81, 3138-3142.

Björk, J.K., Sistonen, L. 2010. Regulation of the members of the mammalian heat shock factor family. FEBS J. 277, 4126-4139.

Blechinger, S.R., Kusch, R.C., Haugo, K., Matz, C., Chivers, D.P., Krone, P.H. 2007. Brief embryonic cadmium exposure induces a stress response and cell death in the developing olfactory system followed by long-term olfactory deficits in juvenile zebrafish. Toxicol Appl Pharmacol. 224, 72-80.

Bode, A.M., Dong, Z. 2002. The paradox of arsenic: molecular mechanisms of cell transformation and chemotherapeutic effects. Crit. Rev. Oncol. Hematol. 42. 5-24.

Bolhuis, S., Richter-Landsberg, C. 2010. Effect of proteasome inhibition by MG-132 on HSP27 oligomerization, phosphorylation, and aggresome formation in the OLN-93 oligodendroglia cell line. J Neurochem 114, 960-971.

Bonham, R.T, Fine, M.R., Pollock, F.M., Shelden, E.A. 2003. Hsp27, Hsp70, and metallothionein in MDCK and LLC-PK1 renal epithelial cells: effects of prolonged exposure to cadmium. Toxicol. Appl. Pharmacol. 191, 63-73.

Boyault, C., Sadoul, K., Pabion, M., Khochbin, S. 2007. HDAC6, at the crossroads between cytoskeleton and cell signaling by acetylation and ubiquitination. Oncogene 26, 5468-5476.

Briant, D., Ohan, N., Heikkila, J.J. 1997. Effect of herbimycin A on *hsp30* and *hsp70* heat shock protein gene expression in *Xenopus* cultured cells. Biochem. Cell Biol. 75, 777-782.

Brunt, J.J., Khan, S., Heikkila, J.J. 2011. Sodium arsenite and cadmium chloride induction of proteasome inhibition and HSP accumulation in *Xenopus laevis* A6 kidney epithelial cells. Comp. Biochem. Physiol. C Toxicol. Pharmacol. 155, 307-317

Bryantsev, A.L., Kurchashova, S.Y., Golyshev, S.A., Polyakov, V.Y., Wunderink, H.F., Kanon, B., Budagova, K.R., Kabakov, A.E., Kampinga, H.H. 2007. Regulation of stress-induced intracellular sorting and chaperone function of Hsp27 (HspB1) in mammalian cells. Biochem J. 407, 407-417.

Buchner, J. 1999. Hsp90 & Co. - a holding for folding. Trends Biochem Sci. 24, 136-141.

Buchner, J., Ehrnsperger, M., Gaestel, M., Walke, S. 1998. Purification and characterization of small heat shock proteins. Methods Enzymol. 290, 339-349.

Buchan, J.R., Parker, R. 2009. Eukaryotic stress granules: the ins and outs of translation. Mol Cell. 36, 932-941.

Bukach, O.V., Glukhova, A.E., Seit-Nebi, A.S., Gusev, N.B. 2009. Heterooligomeric complexes formed by human small heat shock proteins HspB1 (Hsp27) and HspB6 (Hsp20). Biochim Biophys Acta. 1794, 486-495.

Burggren, W.W, Warburton, S. 2007. Amphibians as animal models for laboratory research in physiology. Institute of Laboratory Animal Resources J. 48, 260-269.

Bush, K.T., Goldberg, A.L., Nigam, S.K. 1997. Proteasome inhibition leads to a heat-shock response, induction of endoplasmic reticulum chaperones, and thermotolerance. J. Biol. Chem. 272, 9086-9092.

Chakrabarti, A., Chen, A.W., Varner, J.D. 2011. A review of the mammalian unfolded protein response. Biotechnol. Bioeng. 108, 2777-2793.

Chang, W.H., Tien, C.L., Chen, T.J., Nukina, N., Hsieh, M. 2009. Decreased protein synthesis of Hsp27 associated with cellular toxicity in a cell model of Machado-Joseph disease. Neurosci Lett 454, 152-156.

Chen, X., Shen, J., Prywes, R. 2002. The luminal domain of ATF6 senses endoplasmic reticulum (ER) stress and causes translocation of ATF6 from the ER to the Golgi. J Biol Chem. 277, 13045-13052.

Chen, P., Ji, W., Liu, F.Y., Tang, H.Z., Fu, S., Zhang, X., Liu, M., Gong, L., Deng, M., Hu, W.F., Hu, X.H., Chen, X.W., Li, Z.L., Li, X., Liu, J., Li, D.W. 2012. Alpha-crystallins and tumorigenesis. Curr Mol Med. 12, 1164-1173.

Chow, A.M, Brown, I.R. 2007. Induction of heat shock proteins in differentiated human and rodent neurons by celastrol. Cell Stress Chaperones 12, 237-244.

Ciechanover, A. 1998. The ubiquitin-proteasome pathway: on protein death and cell life. EMBO J. 17, 7151-7160.

Ciocca, D.R., Arrigo, A.P., Calderwood, S.K. 2013. Heat shock proteins and heat shock factor 1 in carcinogenesis and tumor development: an update. Arch Toxicol. 87, 19-48.

Clark, A.R., Lubsen, N.H., Slingsby, C. 2012. sHSP in the eye lens: crystallin mutations, cataract and proteostasis. Int J Biochem Cell Biol. 44, 1687-1697.

Cleren C, Calingasan NY, Chen J, Beal MF. 2005. Celastrol protects against MPTP- and 3-nitropropionic acid-induced neurotoxicity. J Neurochem. 94:995-1004.

Coe, H., Michalak, M. 2009. Calcium binding chaperones of the endoplasmic reticulum. Gen Physiol Biophys. 28, F96-F103.

Collins, T., Read, M.A., Neish, A.S., Whitley, M.Z., Thanos, D., Maniatis, T., 1995. Transcriptional regulation of endothelial cell adhesion molecules: NF-kappa B and cytokine-inducible enhancers. FASEB J. 9, 899–909.

Core, L.J., Lis, J.T. 2008. Transcription regulation through promoter-proximal pausing of RNA polymerase II. Science 319, 1791-1792.

Cui, X., Zhang, J., Du, R., Wang, L., Archacki, S., Zhang, Y., Yuan, M., Ke, T., Li, H., Li, D., Li, C., Li, D.W., Tang, Z., Yin, Z., Liu, M. 2012. HSF4 is involved in DNA damage repair through regulation of Rad51. Biochim Biophys Acta. 1822, 1308-1315.

Darasch, S., Mosser, D.D., Bols, N.C., Heikkila, J.J. 1988. Heat shock gene expression in *Xenopus laevis* A6 cells in response to heat shock and sodium arsenite treatments. Biochem. Cell Biol. 66, 862-868.

Daugaard, M., Rohde, M., Jäättelä, M. 2007. The heat shock protein 70 family: Highly homologous proteins with overlapping and distinct functions. FEBS Lett. 581, 3702-3710.

Davidson, S.M., Loones, M.T., Duverger, O., Morange, M. 2002. The developmental expression of small HSP. Prog Mol Subcell Biol. 28, 103-128.

Davis, R.E., King, M.L., 1989. The developmental expression of the heat-shock response in *Xenopus laevis.* Development 105, 213–222.

de Thonel, A., Le Mouël, A., Mezger, V. Transcriptional regulation of small HSP-HSF1 and beyond. Int J Biochem Cell Biol. 44, 1593-1612.

Del Razo, L.M., Quintanilla-Vega, B., Brambila-Colombres, E., Calderon-Aranda, E.S., Manno M., Albores, A. 2001. Stress proteins induced by arsenic. Toxicol. Appl. Pharmacol. 177, 132-148.

Dirks, R.P., van Geel, R., Hensen, S.M., van Genesen, S.T., Lubsen, N.H. 2010. Manipulating heat shock factor-1 in Xenopus tadpoles: neuronal tissues are refractory to exogenous expression. PLoS One. 5, e10158. doi: 10.1371/journal.pone.0010158.

Doshi, B.M., Hightower, L.E., Lee, J. 2009. The role of Hsp27 and actin in the regulation of movement in human cancer cells responding to heat shock. Cell Stress Chaperones 14, 445-457.

Driscoll, J.J., Chowdhury, R.D., 2012. Molecular crosstalk between the proteasome, aggresomes and autophagy: translational potential and clinical implications. Cancer Lett 325, 147-154.

Drummond, I.A., Lee, A.S., Resendez, E., Steinhardt, R.A. 1987. Depletion of intracellular calcium stores by calcium ionophore A23187 induces the genes for glucose-regulated proteins in hamster fibroblasts. J Biol Chem. 262, 12801-12805.

Dudek, J., Benedix, J., Cappel, S., Greiner, M., Jalal, C., Müller, L., Zimmermann, R. 2009. Functions and pathologies of BiP and its interaction partners. 66, 1555-1569.

El Golli-Bennour, E., Bacha, H. 2011. Hsp70 expression as biomarkers of oxidative stress: mycotoxins' exploration. Toxicology 287, 1-7.

Elbirt, K.K., Whitmarsh, A.J., Davis, R.J., Bonkovsky, H.L. 1998. Mechanism of sodium arsenite-mediated induction of heme oxygenase-1 in hepatoma cells. Role of mitogen-activated protein kinases. J Biol Chem. 273, 8922-8931.

Elicker, K.S., Hutson, L.D. 2007. Genome-wide analysis and expression profiling of the small heat shock proteins in zebrafish. Gene 403, 60-69.

Erlejman, A.G., Lagadari, M., Toneatto, J., Piwien-Pilipuk, G., Galigniana, M.D. 2014. Regulatory role of the 90-kDa-heat-shock protein (Hsp90) and associated factors on gene expression. Biochim Biophys Acta.1839, 71-87.

Etkin, L.D. 1982. Analysis of the mechanisms involved in gene regulation and cell differentiation by microinjection of purified genes and somatic cell nuclei into amphibian oocytes and eggs. Differentiation 21, 149-159.

Evgrafov, O.V., Mersiyanova, I., Irobi, J., Van Den Bosch, L., Dierick, I., Leung, C.L., Schagina, O., Verpoorten, N., Van Impe, K., Fedotov, V., Dadali, E., Auer-Grumbach, M., Windpassinger, C., Wagner, K., Mitrovic, Z., Hilton-Jones, D., Talbot, K., Martin, J.J., Vasserman, N., Tverskaya, S., Polyakov, A., Liem, R.K., Gettemans, J., Robberecht, W., De Jonghe, P., Timmerman, V. 2004. Mutant small heat-shock protein 27 causes axonal Charcot-Marie-Tooth disease and distal hereditary motor neuropathy. Nat Genet. 36, 602-606.

Felts, S.J., Owen, B.A., Nguyen, P., Trepel, J., Donner, D.B., Toft, D.O. 2000. The hsp90-related protein TRAP1 is a mitochondrial protein with distinct functional properties. J Biol Chem. 275, 3305-3312.

Feng, L., Zhang, D., Fan, C., Ma, C., Yang, W., Meng, Y., Wu, W., Guan, S., Jiang, B., Yang, M., Liu, X., Guo, D. 2013. ER stress-mediated apoptosis induced by celastrol in cancer cells and important role of glycogen synthase kinase-3β in the signal network. Cell Death Dis. 4, e715. doi: 10.1038/cddis.2013.222.

Fernando, P., Abdulle, R., Mohindra, A., Guillemette, J.G., Heikkila, J.J. 2002. Mutation or deletion of the C-terminal tail affects the function and structure of *Xenopus laevis* small heat shock protein, hsp30. Comp. Biochem. Physiol. B Biochem. Mol. Biol. 133, 95-103.

Fernando, P., Heikkila, J.J. 2000. Functional characterization of *Xenopus* small heat shock protein, Hsp30C: The carboxyl end is required for stability and chaperone activity. Cell Stress Chaperones 5, 148-159.

Fernando, P., Megeny, L.A., Heikkila, J.J., 2003. Phosphorylation-dependent structural alterations in the small hsp30 chaperone are associated with cellular recovery. Exp. Cell Res. 286, 175–185.

Fournier, M.J., Gareau, C., Mazroui, R. 2010. The chemotherapeutic agent bortezomib induces the formation of stress granules. Cancer Cell Int. 29, 10-12.

Franck, E., Madsen, O., van Rheede, T., Ricard, G., Huynen, M.A., de Jong, W.W. 2004. Evolutionary diversity of vertebrate small heat shock proteins. J Mol Evol. 59, 792-805.

Fujimoto, M., Hayashida, N., Katoh, T., Oshima, K., Shinkawa, T., Prakasam, R., Tan, K., Inouye, S., Takii, R., Nakai, A. 2010. A novel mouse HSF3 has the potential to activate nonclassical heat-shock genes during heat shock. Mol Biol Cell 21, 106-116.

Fujimoto, M., Nakai, A. 2010. The heat shock factor family and adaptation to proteotoxic stress. FEBS J. 277, 4112-4125.

Furfaro, A.L., Piras, S., Passalacqua, M., Domenicotti, C., Parodi, A., Fenoglio, D., Pronzato, M.A., Marinari, U.M., Moretta, L., Traverso, N., Nitti, M. 2014. HO-1 up-regulation: A key point in high-risk neuroblastoma resistance to bortezomib. Biochim Biophys Acta. 1842, 613-622.

Galazyn-Sidorczuk, M., Brzoska, M.M., Jurczuk, M., Moniuszko-Jakoniuk, J. 2009. Oxidative damage to proteins and DNA exposed to cadmium and/or ethanol. Chem. Biol. Interact. 180, 31-38.

Gallastegui, N., Groll, M. 2010. The 26S proteasome: assembly and function of a destructive machine. Trends Biochem Sci. 35, 632-642.

Gal-Yam, E.N., Jeong, S., Tanay, A., Egger, G., Lee, A.S., Jones, P.A. 2006. Constitutive nucleosome depletion and ordered factor assembly at the GRP78 promoter revealed by single molecule footprinting. PLoS Genet. 2, e160.

Gamerdinger, M., Carra, S., Behl, C. 2011. Emerging roles of molecular chaperones and co-chaperones in selective autophagy: focus on BAG proteins. J Mol Med 89, 1175-1182.

Ganea, E. 2001. Chaperone-like activity of α-crystallin and other small heat shock proteins. Curr. Protein Pept. Sci. 2, 205-225.

Garcia-Mata, R., Bebok, Z., Sorscher, E.J., Sztul, E.S. 1999. Characterization and dynamics of aggresome formation by a cytosolic GFP-chimera. J. Cell Biol. 146, 1239-1254.

Garrido, C., Brunet, M., Didelot, C., Zermati, Y., Schmitt, E., Kroemer, G. 2006. Heat shock proteins 27 and 70: anti-apoptotic proteins with tumorigenic properties. Cell Cycle 5, 2592-2601.

Garrido, C., Ottavi, P., Fromentin, A., Hammann, A., Arrigo, A.P., Chauffert, B., Mehlen, P. 1997. HSP27 as a mediator of confluence-dependent resistance to cell death induced by anticancer drugs. Cancer Res. 57, 2661-2667.

Garrido, C., Paul, C., Seigneuric, R., Kampinga, H.H. 2012. The small heat shock proteins family: the long forgotten chaperones. Int J Biochem Cell Biol. 44, 1588-1592.

Gauley, J., Young, J.T.F., Heikkila, J.J. 2008. Intracellular localization of the heat shock protein, HSP110, in *Xenopus laevis* A6 kidney epithelial cells. Comp. Biochem. Physiol. A Mol. Integr. Physiol. 151, 133-138.

Gellalchew, M., Heikkila, J.J. 2005. Intracellular localization of *Xenopus* small heat shock protein, hsp30, in A6 kidney epithelial cells. Cell Biol. Int. 29, 221-227.

Ghayour-Mobarhan, M., Saber, H., Ferns, G.A. 2012. The potential role of heat shock protein 27 in cardiovascular disease. Clin Chim Acta. 413, 15-24.

Goering, P.L., Kish, C.L., Fisher, B.R. 1993. Stress protein synthesis induced by cadmium-cysteine in rat kidney. 85, 25-39.

Goldbaum, O., Riedel, M., Stahnke, T., Richter-Landsberg, C. 2009. The small heat shock protein HSP25 protects astrocytes against stress induced by proteasomal inhibition. Glia. 57, 1566-1577.

Grogan, P.T., Sleder, K.D., Samadi, A.K., Zhang, H., Timmermann, B.N., Cohen, M.S. 2013. Cytotoxicity of withaferin A in glioblastomas involves induction of an oxidative stress-mediated heat shock response while altering Akt/mTOR and MAPK signaling pathways. Invest New Drugs 31, 545-557.

Grover, A., Shandilya, A., Agrawal, V., Pratik, P., Bhasme, D., Bisaria, V.S., Sundar, D. 2011. Hsp90/Cdc37 chaperone/co-chaperone complex, a novel junction anticancer target elucidated by the mode of action of herbal drug Withaferin A. BMC Bioinformatics. 12, S1-S30.

Gu, M., Yu, Y., Gunaherath, G.M., Gunatilaka, A.A., Li, D., Sun, D. 2014. Structure-activity relationship (SAR) of withanolides to inhibit Hsp90 for its activity in pancreatic cancer cells. Invest New Drugs. 32, 68-74.

Guerra, L., Favia, M., Fanelli, T., Calamita, G., Svetlo, M., Bagorda, A., Jacobson, K.A., Reshkin, S.J., Casavola, V. 2004 Stimulation of *Xenopus* P2Y1 receptor activates CFTR in A6 cells. Pflugers Arch. 449, 66-75.

Guo, N., Peng, Z. 2013. MG132, a proteasome inhibitor, induces apoptosis in tumor cells. Asia Pac J Clin Oncol. 9, 6-11.

Guo, K., Gan, L., Zhang, S., Cui, F.J., Cun, W., Li, Y., Kang, N.X., Gao, M.D., Liu, K.Y. 2012. Translocation of HSP27 into liver cancer cell nucleus may be associated with phosphorylation and O-GlcNAc glycosylation. Oncol Rep. 28, 494-500.

Guo, W., Yang, Z., Xia, Q., Liu, J., Yu, Y., Li, J., Zuo, Z., Zhang, D., Li, X., Shi, X., Huang, C. 2011. Arsenite stabilizes HIF-1α protein through p85α-mediated up-regulation of inducible Hsp70 protein expression. Cell Mol Life Sci. 68, 475-488.

Guo, X., Zhang, T., Hu, Z., Zhang, Y., Shi, Z., Wang, Q., Cui, Y., Wang, F., Zhao, H., Chen, Y. 2014. Efficient RNA/Cas9-mediated genome editing in Xenopus tropicalis. Development. 141, 707-714.

Gurgis, F.M., Ziaziaris, W., Munoz, L. 2014. Mitogen-activated protein kinase-activated protein kinase 2 in neuroinflammation, heat shock protein 27 phosphorylation, and cell cycle: role and targeting. Mol Pharmacol. 85, 345-356.

Haas, K.F., Woodruff III, E., Broadie, K. 2007. Proteasome function is required to maintain muscle cellular architecture. Biol Cell 99, 615-626.

Hachfi, L., Simide, R., Richard, S., Couvray, S., Coupe, S., Gaillard, S., Pierre, S., Grillasca, J.P., Prevot-D'Alvise, N. 2012. Effect of water temperature increase on HO-1 expression in European sea bass (Dicentrarchus labrax L.) tissues. Cell Mol Biol (Noisy-le-grand). Suppl. 58, OL1752-OL1756.

Hamilton, A.M., Heikkila, J.J., 2006. Examination of the stress-induced expression of the collagen binding heat shock protein, *hsp47*, in *Xenopus laevis* cultured cells and embryos. Comp. Biochem. Physiol. 143, 133–141.

Heikkila, J.J., Ohan, N., Tam, Y., Ali, A. 1997. Heat shock protein gene expression during Xenopus development. Cell Mol Life Sci. 53, 114-121.

Heikkila, J.J. 2003. Expression and function of small heat shock protein genes during *Xenopus* development. Semin. Cell Dev. Biol. 14, 259-266.

Heikkila, J.J. 2004. Regulation and function of small heat shock protein genes during amphibian development. J. Cell Biochem. 93, 672-680.

Heikkila, J.J. 2010. Heat shock protein gene expression and function in amphibian model systems. Comp. Biochem. Physiol. A Mol. Integr. Physiol. 156, 19-33.

Heir, R., Ablasou, C., Dumontier, E., Elliott, M., Fagotto-Kaufmann, C., Bedford, F.K. 2006. The UBL domain of PLIC-1 regulates aggresome formation. EMBO Rep. 7, 1252-1258.

Helbing, C., Gallimore, C., Atkinson, B.G. 1996. Characterization of a Rana catesbeiana hsp30 gene and its expression in the liver of this amphibian during both spontaneous and thyroid hormone-induced metamorphosis. Dev Genet. 18, 223-233.

Hilario, E., Martin, F.J., Bertolini, M.C., Fan, L. 2011. Crystal structures of *Xanthomonas* small heat shock protein provide a structural basis for an active molecular chaperone oligomer. J Mol Biol. 408, 74-86.

Holmberg, C.I., Tran, S.E., Eriksson, J.E., Sistonen, L. 2002. Multisite phosphorylation provides sophisticated regulation of transcription factors. Trends Biochem. Sci. 27, 619-627.

Ikuzawa, M., Akiduki, S., Asashima, M. 2007. Gene expression profile of *Xenopus* A6 cells cultured under random positioning machine shows downregulation of ion transporter genes and inhibition of dome formation. Adv. Space Res. 40, 1694-1702.

Ito, H., Kamei, K., Iwamoto, I., Inaguma, .Y, García-Mata, R., Sztul, E., Kato, K. 2002. Inhibition of proteasomes induces accumulation, phosphorylation, and recruitment of HSP27 and alphaB-crystallin to aggresomes. J Biochem. 131, 593-603.

Ito, H., Iwamoto, I., Inaguma, Y., Takizawa, T., Nagata, K., Asano, T., Kato, K., 2005. Endoplasmic reticulum stress induces the phosphorylation of small heat shock protein, Hsp27. J Cell Biochem 95, 932-941.

Ivanov, P.A., Chudinova, E.M., Nadezhdina, E.S. 2003. Disruption of microtubules inhibits cytoplasmic ribonucleoprotein stress granule formation. Exp Cell Res. 290, 227-233.

Jacobson, T., Navarrete, C., Sharma, S.K., Sideri, T.C., Ibstedt, S., Priya, S., Grant, C.M., Christen, P., Goloubinoff, P., Tamás, M.J. 2012. Arsenite interferes with protein folding and triggers formation of protein aggregates in yeast. J Cell Sci. 125, 507-5083.

Jankowska, E., Stoj, J., Karpowicz, P., Osmulski, P.A., Gaczynska, M. 2013. The proteasome in health and disease. Curr Pharm Des. 19, 1010-1028.

Johnston, J.A., Ward, C.L., Kopito, R.R. 1998. Aggresomes: a cellular response to misfolded proteins. J Cell Biol. 143, 1883-1898.

Jolly, C., Morimoto, R.I. 2000. Role of the heat shock response and molecular chaperones in oncogenesis and cell death. J. Natl. Cancer Inst. 92, 1564-1572.

Joseph, P., Muchnok, T.K., Klishis, M.L., Roberts, J.R., Antonini, J.M., Whong, W.Z., Ong, T. 2001. Cadmium-induced cell transformation and tumourigenesis are associated with transcriptional activation of c-fos, c-jun, and c-myc proto-oncogenes: role of cellular calcium and reactive oxygen species. Toxicol. Sci. 61, 295-303.

Kaldis, A., Atkinson, B.G., Heikkila, J.J., 2004. Molecular chaperone function of the *Rana catesbeiana* small heat shock protein, Hsp30. Comp. Biochem. Physiol. 139, 175–182.

Kalmar, B., Greensmith, L. 2009. Induction of heat shock proteins for protection against oxidative stress. Adv Drug Deliv Rev. 61, 310-318.

Kästle, M., Woschee, E., Grune, T. 2012. Histone deacetylase 6 (HDAC6) plays a crucial role in p38MAPK-dependent induction of heme oxygenase-1 (HO-1) in response to proteasome inhibition. Free Radic Biol Med. 53, 2092-2101.

Katoh, Y., Fujimoto, M., Nakamura, K., Inouye, S., Sugahara, K., Izu, H., Nakai, A. 2004. Hsp25, a member of the Hsp30 family, promotes inclusion formation in response to stress. FEBS Lett. 565, 28-32.

Katschinski, D. M. 2004. On heat and cells and proteins. News Physiol. Sci. 19, 11-15.

Kawaguchi, Y., Kovacs, J.J., McLaurin, A., Vance, J.M., Ito, A., Yao, T.P. 2003. The deacetylase HDAC6 regulates aggresome formation and cell viability in response to misfolded protein stress. Cell 115, 727-738.

Kawazoe, Y., Tanabe, M., Nakai, A. 1999. Ubiquitous and cell-specific members of the avian small heat shock protein family. FEBS Lett. 455, 271-275.

Kawazoe, Y., Nakai, A., Tanabe, M., Nagata, K. 1998. Proteasome inhibition leads to the activation of all members of the heat shock factor family. Eur. J. Biochem. 255, 356-362.

Kedersha, N.L., Gupta, M., Li, W., Miller, I., Anderson, P. 1999. RNA-binding proteins TIA-1 and TIAR link the phosphorylation of eIF-2 alpha to the assembly of mammalian stress granules. J Cell Biol. 147, 1431-1442.

Kedersha, N., Cho, M.R., Li, W., Yacono, P.W., Chen, S., Gilks, N., Golan, D.E., Anderson, P. 2000. Dynamic shuttling of TIA-1 accompanies the recruitment of mRNA to mammalian stress granules. J Cell Biol. 151, 1257-1268.

Kedersha, N., Chen, S., Gilks, N., Li, W., Miller, I.J., Stahl, J., Anderson, P. 2002. Evidence that ternary complex (eIF2-GTP-tRNA(i)(Met))-deficient preinitiation complexes are core constituents of mammalian stress granules. Mol Biol Cell. 13, 195-210.

Kedersha, N., Stoecklin, G., Ayodele, M., Yacono, P., Lykke-Andersen, J., Fritzler, M.J., Scheuner, D., Kaufman, R.J., Golan, D.E., Anderson, P. 2005. Stress granules and processing bodies are dynamically linked sites of mRNP remodeling. J Cell Biol. 169, 871-884.

Kedersha, N., Tisdale, S., Hickman, T., Anderson, P. 2007. Real-time and quantitative imaging of mammalian stress granules and processing bodies. Methods Enzymol. 448, 521-552.

Kedersha, N., Anderson, P. 2007. Mammalian stress granules and processing bodies. Methods Enzymol. 431, 61-81.

Keyse, S.M., Tyrrell, R.M. 1989. Heme oxygenase is the major 32-kDa stress protein induced in human skin fibroblasts by UVA radiation, hydrogen peroxide, and sodium arsenite. Proc Natl Acad Sci USA. 86, 99-103.

Khalil, S., Luciano, J., Chen, W., Liu, A.Y. 2006. Dynamic regulation and involvement of the heat shock transcriptional response in arsenic carcinogenesis. J Cell Physiol. 207, 562-569.

Khamis, I., Heikkila, J.J. 2013. Enhanced HSP30 and HSP70 accumulation in *Xenopus* cells subjected to concurrent sodium arsenite and cadmium chloride stress. Comp Biochem Physiol C Toxicol Pharmacol. 158, 165-172.

Khan, S., Heikkila, J.J. 2011. Curcumin-induced inhibition of proteasomal activity, enhanced HSP accumulation and the acquisition of thermotolerance in *Xenopus laevis* A6 cells. Comp. Biochem. Physiol. A Mol. Integr. Physiol. 158, 566-576.

Kiaei, M., Kipiani, K., Petri, S., Chen, J., Calingasan, N.Y., Beal, M.F. 2005. Celastrol blocks neuronal cell death and extends life in transgenic mouse model of amyotrophic lateral sclerosis. Neurodegener Dis. 2:246-54.

Kim, Y.E., Hipp, M.S., Bracher, A., Hayer-Hartl, M., Hartl, F.U. 2013. Molecular chaperone functions in protein folding and proteostasis. Annu Rev Biochem. 82, 323-355.

Kim, H.J., Joo, H.J., Kim, Y.H., Ahn, S., Chang, J., Hwang, K.B., Lee, D.H., Lee, K.J. 2011. Systemic analysis of heat shock response induced by heat shock and a proteasome inhibitor MG132. PLoS One 6, e20252. doi: 10.1371/journal.pone.0020252.

Kim, A.J., Shi, Y., Austin, R.C., Werstuck, G.H.. 2005. Valproate protects cells from ER stress-induced lipid accumulation and apoptosis by inhibiting glycogen synthase kinase-3. J Cell Sci. 118, 89-99.

King, L.S., Berg, M., Chevalier, M., Carey, A., Elguindi, E.C., Blond, S.Y. 2001. Isolation, expression, and characterization of fully functional nontoxic BiP/GRP78 mutants. Protein Expr. Purif. 22, 148-158.

Kitiphongspattana, K., Mathews, C.E., Leiter, E.H., Gaskins, H.R. 2005. Proteasome inhibition alters glucose-stimulated (pro) insulin secretion and turnover in pancreatic β-cells. J Biol Chem. 280, 15727-15734.

Koegl, M., Hoppe, T., Schlenker, S., Ulrich, H.D., Mayer, T.U., Jentsch, S. 1999. A novel ubiquitination factor, E4, is involved in multiubiquitin chain assembly. Cell 96, 635-644.

Kondo, H., Harano, R., Nakaya, M., Watabe, S. 2004. Characterization of goldfish heat shock protein-30 induced upon severe heat shock in cultured cells. Cell Stress Chaperones 9, 350-358.

Kopito, R.R. 2000. Aggresomes, inclusion bodies and protein aggregation. Trends Cell Biol. 10, 524-530.

Koteiche HA, Mchaourab HS. 2006. Mechanism of a hereditary cataract phenotype. Mutations in alphaA-crystallin activate substrate binding. J Biol Chem 281, 14273-14279.

Krone, P.H., Heikkila, J.J., 1988. Analysis of hsp30, hsp70, and ubiquitin gene expression in *Xenopus laevis* tadpoles. Development 103, 59–67.

Krone, P.H., Snow, A., Ali, A., Pasternak, J.J., Heikkila, J.J. 1992. Comparison of regulatory and structural regions of the *Xenopus laevis* small heat-shock protein-encoding gene family. Gene 110, 159-166.

Kundrat, L., Regan, L. 2010. Identification of residues on Hsp70 and Hsp90 ubiquitinated by the cochaperone CHIP. J Mol Biol 395, 587-594.

Kwon, S., Zhang, Y., Matthias, P. 2007. The deacetylase HDAC6 is a novel critical component of stress granules involved in the stress response. Genes Dev. 21, 3381-3394.

Lambert, H., Charette, S.J., Bernier, A.F., Guimond, A., Landry, J. 1999. HSP27 multimerization mediated by phosphorylation-sensitive intermolecular interactions at the amino terminus. J. Biol. Chem. 274, 9378-9385.

Landis-Piwowar, K.R., Milacic, V., Chen, D., Yang, H., Zhao, Y., Chan, T.H., Yan, B., Dou, Q.P. 2006. The proteasome as a potential target for novel anticancer drugs and chemosensitizers. Drug Resist. Updat. 9, 263-273.

Landry, J., Chrétien, P., Laszlo, A., Lambert, H., 1991. Phosphorylation of HSP27 during development and decay of thermotolerance in Chinese hamster cells. J Cell Physiol 147, 93-101.

Landry, J., Lambert, H., Zhou, M., Lavoie, J.N., Hickey, E., Weber, L.A., Anderson, C.W. 1992. Human HSP27 is phosphorylated at serines 78 and 82 by heat shock and mitogen-activated kinases that recognize the same amino acid motif as S6 kinase II. J Biol Chem. 267, 794-803.

Lang, L., Miskovic, D., Fernando, P., Heikkila, J.J., 1999. Spatial pattern of constitutive and heat shock-induced expression of the small heat shock protein gene family, Hsp30, in *Xenopus laevis* tailbud embryos. Dev. Genet. 25, 265–374.

Lang, L., Miskovic, D., Lo, M. Heikkila, J.J. 2000. Stress-induced, tissue-specific enrichment of hsp70 mRNA accumulation in *Xenopus laevis* embryos. Cell Stress Chaperones 5, 36-44.

Lavoie, J.N., Gingras-Breton, G., Tanguay, R.M., Landry, J. 1993. Induction of Chinese hamster HSP27 gene expression in mouse cells confers resistance to heat shock. HSP27 stabilization of the microfilament organization. J Biol Chem. 268, 3420-3429.

Lecomte, S., Reverdy, L., Le Quément, C., Le Masson, F., Amon, A., Le Goff, P., Michel, D., Christians, E., Le Dréan, Y. 2013. Unraveling complex interplay between heat shock factor 1 and 2 splicing isoforms. PloS One 8, e56085. doi: 10.1371/journal.pone.0056085

Lee, A.S. 2001. The glucose-regulated proteins: stress induction and clinical applications. Trends Biochem Sci. 26, 504-510.

Lee, P.J., Alam, J., Sylvester, S.L., Inamdar, N., Otterbein, L., Choi, A.M. 1996. Regulation of heme oxygenase-1 expression in vivo and in vitro in hyperoxic lung injury. Am J Respir Cell Mol Biol. 14, 556-568.

Lee, M.J., Lee, J.H., Rubinsztein, D.C. 2013. Tau degradation: the ubiquitin-proteasome system versus the autophagy-lysosome system. Prog Neurobiol. 105, 49-59.

Lehman, N.L. 2009. The ubiquitin proteasome system in neuropathology. Acta Neuropathol. 118, 329-347.

Li, W., Chou, I.N. 1992. Effects of sodium arsenite on the cytoskeleton and cellular glutathione levels in cultured cells. Toxicol. Appl. Pharmacol. 114, 132-139.

Li, D., Duncan, R.F., 1995. Transient acquired thermotolerance in *Drosophila*, correlated with rapid degradation of Hsp70 during recovery. Eur J Biochem 231, 454-465.

Li, L., Li, C.M., Wu, J., Huang, S., Wang, G.L. 2014. Heat shock protein 32/heme oxygenase-1 protects mouse Sertoli cells from hyperthermia-induced apoptosis by CO activation of sGC signalling pathways. Cell Biol Int. 38, 64-71.

Liewluck, T., Hayashi, Y.K., Ohsawa, M., Kurokawa, R., Fujita, M., Noguchi, S., Nonaka, I., Nishino, I. 2007. Unfolded protein response and aggresome formation in hereditary reducing-body myopathy. Muscle Nerve. 35, 322-326.

Lindquist, S. 1986. The heat-shock response. Annu. Rev. Biochem. 55, 1151-1191.

Liu, J., Kadiiska, M.B., Liu, Y., Lu, T., Qu, W., Waalkes, M.P. 2001. Stress-related gene expression in mice treated with inorganic arsenicals. Toxicol. Sci. 61, 314-320.

Lund, S.G., Caissie, D., Cunjak, R.A., Vijayan, M.M., Tufts, B.L. 2002. The effects of environmental heat stress on heat-shock mRNA and protein expression in Miramichi Atlantic salmon (*Salmo salar*) parr. Can J Fish Aquat Sci. 59, 1553-1562.

Ma, S., Bhattacharjee, R.B., Bag, J. 2009. Expression of poly(A)-binding protein is upregulated during recovery from heat shock in HeLa cells. FEBS J. 276, 552-570.

MacRae, T.H. 2000. Structure and function of small heat shock/α-crystallin proteins: Established concepts and emerging ideas. Cell Mol. Life Sci. 57, 899-913.

Mahli, H., Kaufman, R.J. 2011. Endoplasmic reticulum stress in liver disease. J. Hepatol. 54, 795-809.

Malik, F., Kumar, A., Bhushan, S., Khan, S., Bhatia, A., Suri, K.A., Qazi, G.N., Singh, J. 2007. Reactive oxygen species generation and mitochondrial dysfunction in the apoptotic cell death of human myeloid leukemia HL-60 cells by a dietary compound withaferin A with concomitant protection by N-acetyl cysteine. Apoptosis. 12, 2115-2133.

Mandal, C., Dutta, A., Mallick, A., Chandra, S., Misra, L., Sangwan, R. S., Mandal, C. 2008.Withaferin A induces apoptosis by activating p38 mitogen-activated protein kinase signaling cascade in leukemic cells of lymphoid and myeloid origin through mitochondrial death cascade. Apoptosis. 13, 1450-1464.

Mani, A., Gelmann, E.P. 2005. The ubiquitin-proteasome pathway and its role in cancer. J. Clin. Oncol. 23, 4776-4789.

Mao, L., Shelden, E.A. 2006. Developmentally regulated gene expression of the small heat shock protein Hsp27 in zebrafish embryos. Gen Expr Patterns 6, 127-133.

Marzec, M., Eletto, D., Argon, Y. 2012. GRP94: An HSP90-like protein specialized for protein folding and quality control in the endoplasmic reticulum. Biocim Biophys Acta. 1823, 774-787.

Masliah, E., Rockenstein, E., Veinbergs, I., Mallory, M., Hashimoto, M., Takeda, A., Sagara, Y., Sisk, A. and Mucke, L. 2000. Dopaminergic loss and inclusion body formation in alpha-synuclein mice: implications for neurodegenerative disorders. Science 287, 1265-1269.

Mazroui, R., Di Marco, S., Kaufman, R.J., Gallouzi, I.E. 2007. Inhibition of the ubiquitin-proteasome system induces stress granule formation. Mol Biol Cell. 18, 2603-2618.

Mehlen, P., Hickey, E., Weber, L.A., Arrigo, A.P. 1997. Large unphosphorylated aggregates as the active form of hsp27 which controls intracellular reactive oxygen species and glutathione levels and generates a protection against TNFalpha in NIH-3T3-ras cells. Bioxhem Biophys Res Commun. 241, 187-192.

Medina-Díaz, I.M., Estrada-Muñiz, E., Reyes-Hernández, O.D., Ramírez, P., Vega, L., Elizondo, G. 2009. Arsenite and its metabolites, MMA(III) and DMA(III), modify CYP3A4, PXR and RXR alpha expression in the small intestine of CYP3A4 transgenic mice. Toxicol Appl Pharmacol. 239, 162-168.

Mendez-Armenta, M., Rios, C. 2007. Cadmium neurotoxicity. Environ. Toxicol. Pharmacol. 23, 350-358.

Mi, L., Gan, N., Chung, F.L. 2009. Aggresome-like structure induced by isothiocyanates is novel proteasome-dependent degradation machinery. Biochem Biophys Res Commun 388, 456-462.

Michaud, S., Morrow, G., Marchand, J., Tanguay, R.M. 2002. Drosophila small heat shock proteins: cell and organelle-specific chaperones? PRog Mol Subcell Biol. 28, 79-101.

Middleton, R.C., Shelden, E.A. 2013. Small heat shock protein HSPB1 regulates growth of embryonic zebrafish craniofacial muscles. Exp Cell Res. 319, 860-874.

Miskovic, D., Salter-Cid, L., Ohan, N., Flajnik, M., Heikkila, J.J. 1997. Isolation and characterization of a cDNA encoding a *Xenopus* immunoglobulin binding protein, BiP (grp78). Comp. Biochem. Physiol. B Biochem. Mol. Biol. 116, 227-34.

Miskovic, D., Heikkila, J.J. 1999. Constitutive and stress-inducible expression of the endoplasmic reticulum heat shock protein 70 gene family member, Immunoglobulin-Binding Protein (BiP), during *Xenopus laevis* early development. Dev. Genetics 25, 31 – 39.

Mitani, K., Fujita, H., Sassa, S., Kappas, A. 1990. Activation of heme oxygenase and heat shock protein 70 genes by stress in human hepatoma cells. Biochem Biophys Res Commun. 166, 1429-1434.

Mohan, R., Hammers, H.J., Bargagna-Mohan, P., Zhan, X.H., Herbstritt, C.J., Ruiz, A., Zhang, L., Hanson, A.D., Conner, B.P., Rougas, J., Pribluda, V.S. 2004. Withaferin A is a potent inhibitor of angiogenesis. Angiogenesis. 7, 115-122.

Moody, S.A. 2012. Targeted microinjection of synthetic mRNAs to alter retina gene expression in *Xenopus* embryos. Methods Mol Biol. 884, 91-111.

Morimoto, R.I. 1998. Regulation of the heat shock transcriptional response: Cross talk between a family of heat shock factors, molecular chaperones, and negative regulators. Genes Dev. 12, 3788-3796.

Morimoto, R.I, Santoro, M.G. 1998. Stress-inducible responses and heat shock proteins: New pharmacologic targets for cytoprotection. Nat. Biotechnol. 16, 833-838.

Morimoto, R.I. 2008. Proteotoxic stress and inducible chaperone networks in neurodegenerative disease and aging. Genes Dev. 22, 1427-1438.

Morris, A.M., Treweek, T.M., Aquilina, J.A., Carver, J.A., Walker, M.J. 2008. Glutamic acid residues in the C-terminal extension of small heat shock protein 25 are critical for structural and functional integrity. FEBS J. 275, 5885-5898.

Mouchet F, Baudrimont M, Gonzalez P, Cuenot Y, Bourdineaud JP, Boudou A, Gauthier L. 2006. Genotoxic and stress inductive potential of cadmium in *Xenopus laevis* larvae. Aquat Toxicol. 78, 157-166.

Muller, M., Gauley, J., Heikkila, J.J. 2004. Hydrogen peroxide induces heat shock protein and proto-oncogene mRNA accumulation in *Xenopus laevis* A6 kidney epithelial cells. Can. J. Physiol. Pharmacol. 82, 523-529.

Mulligan-Tuttle, A., Heikkila, J.J. 2007. Expression of the small heat shock protein gene, hsp30, in *Rana catesbeiana* fibroblasts. Comp. Biochem. Physiol. 148, 308-316.

Murata, S., Yashiroda, H., Tanaka, K. 2009. Molecular mechanisms of proteasome assembly. Nat Rev Mol Cell Biol. 10, 104-115.

Mymrikov, E.V., Seit-Nebi, A.S., Gusev, N.B. 2012. Heterooligomeric complexes of human small heat shock proteins. Cell Stress Chaperones 17, 157-169.

Nakai, A., Tanabe, M., Kawazoe, Y., Inazawa, J., Morimoto, R.I., Nagata, K. 1997. HSF4, a new member of the human heat shock factor family which lacks properties of a transcriptional activator. Mol Cell Biol. 17, 469-481.

Nakai, A. 1999. New aspects in the vertebrate heat shock factor system: HSF3 and HSF4. Cell Stress Chaperones 4, 86-93.

Nakajima, Y., Suzuki, S., 2013. Environmental stresses induce misfolded protein aggregation in plant cells in a microtubule-dependent manner. Int J Mol Sci 14, 7771-7783.

Nakajima, S., Hiramatsu, N., Hayakawa, K., Saito, Y., Kato, H., Huang, T., Yao, J., Paton, A.W., Paton, J.C., Kitamura, M. 2011. Selective abrogation of BiP/GRP78 blunts activation of NF-κB through the ATF6 branch of the UPR: involvement of C/EBPβ and mTOR-dependent dephosphorylation of Akt. Mol Cell Biol. 31, 1710-1718.

Ni, M., Lee, A.S. 2007. ER chaperones in mammalian development and human disease. FEBS Letters 581, 3641 – 3651.

Norris, C.E., diIorio, P.J., Schultz, R.J., Hightower, L.E. 1995. Variation in heat shock proteins within tropical and desert species of poeciliid fishes. Mol Biol Evol. 12, 1048-1062.

Norris, C.E., Hightower, L.E. 2002. Discovery of two distinct small heat shock protein (HSP) families in the desert fish *Poeciliopsis*. Prog Mol Subcell Biol. 28, 19-35.

Norris, C.E., Brown, M.A., Hickey, E., Weber, L.A., Hightower, L.E., 1997. Low-molecularweight heat shock proteins in a desert fish (*Poeciliopsis lucida*): homologs of human Hsp27 and Xenopus Hsp30. Mol. Biol. Evol. 14, 115–129.

Oguro, T., Hayashi, M., Nakajo, S., Numazawa, S., Yoshida, T. 1998. The expression of heme oxygenase-1 gene responded to oxidative stress produced by phorone, a glutathione depletor, in the rat liver; the relevance to activation of c-jun n-terminal kinase. J Pharmacol Exp Ther. 287, 773-778.

Oh, J.H., Lee, T.J., Kim, S.H., Choi, Y.H., Lee, S.H., Lee, J.M., Kim, Y.H., Park, J.W., Kwon, T.K. 2008. Induction of apoptosis by withaferin A in human leukemia U937 cells through down-regulation of Akt phosphorylation. Apoptosis 13, 1494-1504.

Ohan, N.W., Tam, Y., Fernando, P., Heikkila, J.J. 1998. Characterization of a novel group of basic small heat shock proteins in *Xenopus laevis* A6 kidney epithelial cells. Biochem. Cell Biol. 76, 665-671.

Ohtsuka, K., Liu, Y.C., Kaneda, T. 1993. Cytoskeletal thermotolerance in NRK cells. Int J Hyperthermia 9, 115-124.

Okinaga, S., Takahashi, K., Takeda, K., Yoshizawa, M., Fujita, H., Sasaki, H., Shibahara, S. 1996. Regulation of human heme oxygenase-1 gene expression under thermal stress. Blood. 87, 5074-5084.

Olzmann, J.A., Chin, L.S. 2008. Parkin-mediated K63-linked polyubiquitination: a signal for targeting misfolded proteins to the aggresome-autophagy pathway. Curr Med chem. 15, 47-60.

Otterbein, L.E., Lee, P.J., Chin, B.Y., Petrache, I., Camhi, S.L., Alam, J., Choi, A.M. 1999. Protective effects of heme oxygenase-1 in acute lung injury. Chest. 116, 61S-63S.

Ovsenek, N., Heikkila, J.J., 1990. DNA sequence-specific binding activity of the heat shock transcription factor is heat-inducible before midblastula transition of early *Xenopus* development. Development 110, 427–433.

Ovsenek, N., Williams, G.T., Morimoto, R.I., Heikkila, J.J. 1990. Cis-acting sequences and trans-acting factors required for constitutive expression of a microinjected HSP70 gene after the midblastula transition of Xenopus laevis embryogenesis. Dev. Genet. 11, 97-109.

Ozorowski, G., Ryan, C.M., Whitelegge, J.P., Luecke, H. 2012. Withaferin A binds covalently to the N-terminal domain of annexin A2. Bio Chem. 393, 1151-1163.

Parcellier, A., Schmitt, E., Brunet, M., Hammann, A., Solary, E., Garrido, C. 2005. Small heat shock proteins HSP27 and alphaB-crystallin: cytoprotective and oncogenic functions. Antioxid Redox Signal. 7, 404-413.

Park, H.S., Jun do, Y., Han, C.R., Woo, H.J., Kim, Y.H. 2011. Proteasome inhibitor MG132-induced apoptosis via ER stress-mediated apoptotic pathway and its potentiation by protein tyrosine kinase p56lck in human Jurkat T cells. Biochem Pharmacol. 82, 1110-1125.

Pearl, L.H., Prodromou, C., Workman, P. 2008. The Hsp90 molecular chaperone: an open and shut case for treatment. Biochem J. 410, 439-453.

Phang, D., Joyce, E.M., Heikkila J.J. 1999. Heat shock-induced acquisition of thermotolerance at the levels of cell survival and translation in *Xenopus* A6 kidney epithelial cells. Biochem. Cell Biol. 77, 141-151.

Pirkkala, L., Nykanen, P., Sistonen, L. 2001. Roles of the heat shock transcription factors in regulation of the heat shock response and beyond. Fed. Am. Soc. Exp. Biol. J. 15, 1118-1131.

Pratt, W.B. 1997. The role of the hsp90-based chaperone system in signal transduction by nuclear receptors and receptors signaling via MAP kinase. Annu Rev Pharmacol Toxicol. 37, 297-326.

Pritts, T.A., Hungness, E.S., Hershko, D.D., Robb, B.W., Sun, X., Luo, G.J., Fischer, J.E., Wong, H.R. and Hasselgren, P.O. 2002. Proteasome inhibitors induce heat shock response and increase IL-6 expression in human intestinal epithelial cells. American Journal of Physiology: Regulatory, Integrative and Comparative Physiology 282, 1016-1026.

Qian, S.B., McDonough, H., Boellmann, F., Cyr, D.M., Patterson, C. 2006. CHIP-mediated stress recovery by sequential ubiquitination of substrates and Hsp70. Nature 440, 551-555.

Rafferty, K.A. 1968. Mass culture of amphibian cells: methods and observations concerning stability of cell type. In Biology of Amphibian Tumors (ed. M Mizzel), pp. 52-81. New York, NY, USA: Springer Verlag.

Rallu, M., Loones, M., Lallemand, Y., Morimoto, R.I., Morange, M., Mezger, V. 1997. Function and regulation of heat shock factor 2 during mouse embryogenesis. Proc. Natl. Acad. Sci. U.S.A. 94, 2392-2397.

Raju, V.S., Maines, M.D. 1994. Coordinated expression and mechanism of induction of HSP32 (heme oxygenase-1) mRNA by hyperthermia in rat organs. Biochim Biophys Acta. 1217, 273-280.

Raju, V.S., McCoubrey, W.K., Maines, M.D. 1997. Regulation of heme oxygenase-2 by glucocorticoids in neonatal rat brain: characterization of a functional glucocorticoid response element. Biochem Biophys Acta. 1351, 89-104.

Richter-Landsberg, C., Leyk, J. 2013. Inclusion body formation, macroautophagy, and the role of HDAC6 in neurodegeneration. Acta Neuropathol. 126, 793-807.

Rock, K.L., Gramm, C., Rothstein, L., Clark, K., Stein, R., Dick, L., Hwang, D. and Goldberg, A.L. 1994. Inhibitors of the proteasome block the degradation of most cell proteins and the generation of peptides presented on MHC class I molecules. Cell 78, 761-771.

Rogalla, T., Ehrnsperger, M., Preville, X., Kotlyarov, A., Lutsch, G., Ducasse, C., Paul, C., Wieske, M., Arrigo, A.P., Buchner, J., Gaestel, M. 1999. Regulation of Hsp27 oligomerization, chaperone function, and protective activity against oxidative stress/tumor necrosis factor alpha by phosphorylation. J Biol Chem. 274, 18947-18956.

Ross, C.A., Pickart, C.M. 2004. The ubiquitin–proteasome pathway in Parkinson's disease and other neurodegenerative diseases. Trends Cell Biol. 14, 703-711.

Sahara, K., Kogleck, L., Yashiroda, H., Murata, S. 2014. The mechanism for molecular assembly of the proteasome. Adv Biol Regul. 54C, 51-58.

Sakurai, H., Enoki, Y. 2010. Novel aspects of heat shock factors: DNA recognition, chromatin modulation and gene expression. FEBS J. 277, 4140-4149.

Salminen, A., Lehtonen, M., Paimela, T., Kaarniranta, K. 2010. Celastrol: Molecular targets of Thunder God Vine. Biochem Biophys Res Commun. 394, 439-442.

Sangster, T.A., Lindquist, S., Queitsch, C. 2004. Under cover: causes, effects and implications of Hsp90-mediated genetic capacitance. Bioessays 26, 348-362.

Santagata, S., Xu, Y.M., Wijeratne, E.M., Kontnik, R., Rooney, C., Perley, C.C., Kwon, H., Clardy, J., Kesari, S., Whitesell, L., Lindquist, S., Gunatilaka, A.A. 2012. Using the heat shock response to discover anticancer compounds that target protein homeostasis. ACS Chem Biol. 7, 340-349. Role of the RNA-binding protein Nrd1 in stress granule formation and its implication in the stress response in fission yeast. PLoS One. 7, e29683. doi: 10.1371/journal.pone.0029683.

Satoh, R., Tanaka, A., Kita, A., Morita, T., Matsumura, Y., Umeda, N., Takada, M., Hayashi, S., Tani, T., Shinmyozu, K., Sugiura, R. 2012.

Schlecht, R., Erbse, A.H., Bukau, B., Mayer, M.P. 2011. Mechanics of Hsp70 chaperones enables differential interaction with client proteins. Nat Struct Mol Biol. 18, 345-351.

Schmidt T, Bartelt-Kirbach B, Golenhofen N. Phosphorylation-dependent subcellular localization of the small heat shock proteins HspB1/Hsp25 and HspB5/αB-crystallin in cultured hippocampal neurons. Histochem Cell Biol. 138, 407-418.

Senée, V., Vattem, K.M., Delépine, M., Rainbow, L.A., Haton, C., Lecoq, A., Shaw, N.J., Robert, J.J., Rooman, R., Diatloff-Zito, C., Michaud, J.L., Bin-Abbas, B., Taha, D., Zabel, B., Franceschini, P., Topaloglu, A.K., Lathrop, G.M., Barrett, T.G., Nicolino, M., Wek, R.C., Julier, C. 2004. Wolcott-Rallison Syndrome: clinical, genetic, and functional study of EIF2AK3 mutations and suggestion of genetic heterogeneity. Diabetes 53, 1876-1883.

Shen, D., Coleman, J., Chan, E., Nicholson, T.P., Dai, L., Sheppard, P.W., Patton, W.F., 2011. Novel cell- and tissue-based assays for detecting misfolded and aggregated

protein accumulation within aggresomes and inclusion bodies. Cell Biochem Biophys 60, 173-185.

Sive, H.L., Grainger, R.M., Harland, R.M. 2010. Microinjection of Xenopus oocytes. Cold Spring Harb Protoc. 12, pdb.prot5536. doi: 10.1101/pdb.prot5536.

Smith, J.C., Tata, J.R. 1991. *Xenopus* cell lines. In "Methods in cell biology" 36, pp. 635-654, Academic Press, Inc., London, England.

Song, C., Xiao, Z., Nagashima, K., Li, C.C., Lockett, S.J., Dai, R.M., Cho, E.H., Conrads, T.P., Veenstra, T.D., Colburn, N.H., Wang, Q., Wang, J.M. 2008. The heavy metal cadmium induces valosin-containing protein (VCP)-mediated aggresome formation. Toxicol Appl Pharmacol.

Sreedhar, A.S., Csermely, P. 2004. Heat shock proteins in the regulation of apoptosis: new strategies in tumor therapy: a comprehensive review. Pharmacol. Ther. 101, 227-257.

Stangl, K., Günther, C., Frank, T., Lorenz, M., Meiners, S., Röpke, T., Stelter, L.,Moobed, M., Baumann, G., Kloetzel, P.M. and Stangl, V. 2002. Inhibition of theubiquitin-proteasome pathway induces differential heat-shock protein response incardiomyocytes and renders early cardiac protection. Biochemical andBiophysical Research Communications 291, 542-549.

Stankiewicz, A.R., Livingstone, A.M., Mohseni, N., Mosser, D.D. 2009. Regulation of heat-induced apoptosis by Mcl-1 degradation and its inhibition by Hsp70. Cell Death Differ. 16, 638-647.

Stetler, R.A., Gao, Y., Signore, A.P., Cao, G., Chen, J. 2009. HSP27: mechanisms of cellular protection against neuronal injury. 9, 863-872.

Stromer, T., Ehrnsperger, M., Gaestel, M., Buchner, J. 2003. Analysis of the interaction of small heat shock proteins with unfolding proteins. J Biol Chem. 278, 18015-18021.

Su, R., Li, Z., Li, H., Song, H., Bao, C., Wei, J., Cheng, L. 2010. Grp78 promotes the invasion of hepatocellular carcinoma. BMC Cancer 19, 10-20.

Sun, Y., MacRae, T.H. 2005. Small heat shock proteins: molecular structure and chaperone function. Cell Mol Life Sci. 62, 2460-2476.

Sun, F-C., Wei, S., Li, C-W., Chang, Y-S., Chao, C-C., Lai, Y-K. 2006. Localization of GRP78 to mitochondria under the unfolded protein response. Biochem J. 396, 31-39.

Taipale, M., Jarosz, D.F., Lindquist, S. 2010. HSP90 at the hub of protein homeostasis: emerging mechanistic insights. Nat Rev Mol Cell Biol. 11, 515-528.

Taketani, S., Kohno, H., Yoshinaga, T., Tokunaga, R. 1988. Induction of heme oxygenase in rat hepatoma cells by exposure to heavy metals and hyperthermia. Biochem Int. 17, 665-672.

Tam, Y., Heikkila, J.J., 1995. Identification of members of the hsp30 small heat shock protein family and characterization of their developmental regulation in heat shocked *Xenopus laevis* embryos. Dev. Genet. 17, 331–339.

Tanabe, M., Sasai, N., Nagata, K., Liu, X.D., Liu, P.C., Thiele, D.J., Nakai, A. 1999. The mammalian HSF4 gene generates both an activator and a repressor of heat shock genes by alternative splicing. J. Biol. Chem. 274, 27845-27856.

Tang, S., Buriro, R., Liu, Z., Zhang, M., Ali, I., Adam, A., Hartung, J., Bao, E. 2013. Localization and expression of Hsp27 and αB-crystallin in rat primary myocardial cells during heat stress in vitro. PLoS One 8, e69066. doi: 10.1371/journal.pone.0069066.

Taylor, J.P., Tanaka, F., Robitschek, J., Sandoval, C.M., Taye, A., Markovic-Plese, S., Fischbeck, K.H. 2003. Aggresomes protect cells by enhancing the degradation of toxic polyglutamine-containing protein. Hum Mol Genet. 12, 749-757.

Taylor, J.M., Brody, K.M., Lockhart, P.J. 2012. Parkin co-regulated gene is involved in aggresome formation and autophagy in response to proteasomal impairment. Exp Cell Res. 318, 2059-2070.

Thomas, M.G., Loschi, M., Desbats, M.A., Boccaccio, G.L. 2011. RNA granules: the good, the bad and the ugly. Cell Signal. 23, 324-334.

Tozawa, K., Sakurada, S., Kohri, K., Okamoto, T. 1995. Effects of anti-nuclear factor kappa B reagents in blocking adhesion of human cancer cells to vascular endothelial cells. Cancer Res. 55, 4162–4167.

Trepel, J., Mollapour, M., Giaccone, G., Neckers, L. 2010. Targeting the dynamic HSP90 complex in cancer. Nat. Rev. Cancer 10, 537-549.

Trott, A., West, J.D., Klaic, L., Westerheide, S.D., Silverman, R.B., Morimoto, R.I., Morano, K.A. 2008. Activation of heat shock and antioxidant responses by the natural product celastrol: Transcriptional signatures of a thiol-targeted molecule. Mol Biol Cel.l 19, 1104-1112.

Tsou, T.C., Tsai, F.Y., Hseih, Y.W., Li, L.A., Yeh, S.C., Chang, L.W. 2005. Arsenite induces endothelial cytotoxicity by down-regulation of vascular endothelial nitric oxide synthase. Toxicol. Appl. Pharmacol. 208, 277-284.

Turner, C.P., Panter, S.S., Sharp, F.R. 1999. Anti-oxidants prevent focal rat brain injury as assessed by induction of heat shock proteins (HSP70, HO-1/HSP32, HSP47) following subarachnoid injections of lysed blood. Brain Res Mol Brain Res. 65, 87-102.

Tuttle, A.M., Gauley, J., Chan, N., Heikkila, J.J., 2007. Analysis of the small heat shock protein gene, *hsp27*, in *Xenopus laevis* embryos. Comp. Biochem. Physiol. Part A 147, 112–121.

Van Montfort, R., Slingsby, C., Vierling, E. 2001. Structure and function of the small heat shock protein/alpha-crystallin family of molecular chaperones. Adv. Protein Chem. 59, 105-156.

Vicart, P., Caron, A., Guicheney, P., Li, Z., Prévost, M.C., Faure, A., Chateau, D., Chapon, F., Tomé, F., Dupret, J.M., Paulin, D., Fardeau, M. 1998. A missense mutation in the

alphaB-crystallin chaperone gene causes a desmin-related myopathy. Nat Genet. 20, 92-95.

Vidyasagar, A., Wilson, N.A., Djamali, A. 2012. Heat shock protein 27 (HSP27): biomarker of disease and therapeutic target. Fibrogenesis Tissue Repair 5, 7.

Voellmy, R. 2004. On mechanisms that control heat shock transcription factor activity in metazoan cells. Cell Stress Chaperones 9, 122-133.

Waanders, E., Croes, H.J., Maass, C.N., te Morsche, R.H., van Geffen, H.J., van Krieken, J.H., Fransen, J.A., Drenth, J.P. 2008. Cysts of PRKCSH mutated polycystic liver disease patients lack hepatocystin but express Sec63p. Histochem Cell Biol. 129, 301-310.

Waisberg, M., Pius, J., Hale, B., Beyersmann, D. 2003. Molecular and cellular mechanisms of cadmium carcinogenesis. Toxicology. 192, 95-117.

Walcott, S.E., Heikkila, J.J. 2010. Celastrol can inhibit proteasome activity and upregulate the expression of heat shock protein genes, *hsp30* and *hsp70*, in *Xenopus laevis* A6 cells. Comp Biochem Physiol A Mol Integr Physiol.156, 285-293.

Wang, L., Gallagher, E.P. 2013. Role of Nrf2 antioxidant defense in mitigating cadmium-induced oxidative stress in the olfactory system of zebrafish. Toxicol Appl Pharmacol. 266, 177-186.

Wang, C., Gomer, R.H., Lazarides, E. 1981. Heat shock proteins are methylated in avian and mammalian cells. PNAS 78, 3531-3535.

Wang, J., Wei, Y., Li, X., Cao, H., Xu, M., Dai, J. 2007. The identification of heat shock protein genes in goldfish (Carassius auratus) and their expression in a complex environment in Gaobeidian Lake, Beijing, China. Comp Biochem Physiol C Toxicol Pharmacol. 145, 350-362.

Wang, W.B., Feng, L.X., Yue, Q.X., Wu, W.Y., Guan, S.H., Jiang, B.H., Yang, M., Liu, X., Guo, D.A. 2012. Paraptosis accompanied by autophagy and apoptosis was induced by

celastrol, a natural compound with influence on proteasome, ER stress and Hsp90. J Cell Physiol. 227, 2196-2206.

Wang, S., Liu, K., Wang, X., He, Q., Chen, X. 2011. Toxic effects of celastrol on embryonic development of zebrafish (*Danio rerio*). Drug Chem Toxicol. 34, 61-65.

Wang, J., Zhang, Z., Chou, C., Liang, Y., Gu, Y., Ma, H. 2009. Cyclosporine stimulates the renal epithelial sodium channel by elevating cholesterol. Am. J. Physiol. Renal Physiol. 296, F284-F290.

Weng, S., Zhu, X., Jin, Y., Wang, T., Huang, H. 2011. Protective effect of erythropoietin on myocardial infarction in rats by inhibition of caspase-12 expression. Exp Ther Med. 2, 833-836.

Westerheide S.D., Morimoto, R.I. 2005. Heat shock response modulators as therapeutic tools for diseases of protein conformation. J. Biol. Chem. 280, 33097-33100.

Westerheide, S.D., Bosman, J.D., Mbadugha, B.N., Kawahara, T.L., Matsumoto, G., Kim, S., Gu, W., Devlin, J.P., Silverman, R.B., Morimoto, R.I. 2004. Celastrols as inducers of the heat shock response and cytoprotection. J. Biol. Chem. 279, 56053-56060.

Wettstein, G., Bellaye, P.S., Micheau, O., Bonniaud, P. 2012. Small heat shock proteins and the cytoskeleton: an essential interplay for cell integrity? Int J Biochem Cell Biol. 44, 1680-1686.

Whitesell, L., Lindquist, S.L. 2005. HSP90 and the chaperoning of cancer. Nat Rev Cancer 5, 761-772.

Wiegant, F.A., van Bergen en Henegouwen, P.M., van Dongen, G., Linnemans, W.A. 1987. Stress-induced thermotolerance of the cytoskeleton of mouse neuroblastoma N2A cells and rat Reuber H35 hepatoma cells. Cancer Res. 47, 1674-1680.

Wieske, M., Benndorf, R., Behlke, J., Dölling, R., Grelle, G., Bielka, H., and Lutsch, G. 2001. Defined sequence segments of the small heat shock proteins HSP25 and αB crystallin inhibit actin polymerization. Eur. J. Biochem. 268, 2083-2090.

Williams, J.A., Hou, Y., Ni, H.M., Ding, W.X. 2013. Role of intracellular calcium in proteasome inhibitor-induced endoplasmic reticulum stress, autophagy, and cell death. Pharm Res. 30, 2279-2289.

Winning, R.S., Heikkila, J.J., Bols, N.C., 1989. Induction of glucose-regulated proteins in *Xenopus laevis* A6 cells. J. Cell. Physiol. 140, 239–245.

Winning, R.S., Bols, N.C., Heikkila, J.J., 1991. Tunicamycin-inducible polypeptide synthesis during *Xenopus laevis* embryogenesis. Differentiation 46, 167–172.

Wistow, G. 2012. The human crystallin gene families. Hum Genomics 1, 6-26.

Woolfson, J.P., Heikkila, J.J. 2009. Examination of cadmium-induced expression of the small heat shock protein gene, *hsp30*, in *Xenopus laevis* A6 kidney epithelial cells. Comp. Biochem. Physiol. A Mol. Integr. Physiol. 152, 91-99.

Wu, S., Hong, F., Gewirth, D., Guo, B., Liu, B., Li, Z. 2012. The molecular chaperone gp96/GRP94 interacts with Toll-like receptors and integrins via its C-terminal hydrophobic domain. J Biol Chem. 287, 6735-6742.

Wu, W.T., Chi, K.H., Ho, F.M., Tsao, W.C., Lin, W.W. 2004. Proteasome inhibitors up-regulate haem oxygenase-1 gene expression: requirement of p38 MAPK (mitogen-activated protein kinase) activation but not of NF-kappaB (nuclear factor kappaB) inhibition. Biochem J. 379, 587-593.

Xiong, R., Siegel, D., Ross, D. 2013. The activation sequence of cellular protein handling systems after proteasomal inhibition in dopaminergic cells. Chem Biol Interact. 204, 116-124.

Xu, D., Perez, R.E., Rezaiekhaligh, M.H., Bourdi, M., Truog, W.E. 2009. Knockdown of ERp57 increases BiP/GRP78 induction and protects against hyperoxia and tunicamycin-induced apoptosis. Am J Physiol Lung Cell Mol Physiol. 297, L44-L51.

Yamamoto, N., Izumi, Y., Matsuo, T., Wakita, S., Kume, T., Takada-Takatori, Y., Sawada, H., Akaike, A. 2010. Elevation of heme oxygenase-1 by proteasome inhibition affords dopaminergic neuroprotection. J Neurosci Res. 88, 1934-1942.

Yang, H., Chen, D., Cui, Q.C., Yuan, X., Dou, Q.P. 2006. Celastrol, a triterpene extracted from the Chinese "Thunder of God Vine," is a potent proteasome inhibitor and suppresses human prostate cancer growth in nude mice. Cancer Res. 66, 4758-4765.

Yang, H., Shi, G., Dou, Q.P. 2007. The tumor proteasome is a primary target for the natural anticancer compound withaferin A isolated from "Indian winter cherry". Mol Pharmacol 71, 426-437.

Yang, H., Landis-Piwowar, K.R., Chen, D., Milacic, V., Dou, Q.P. 2008. Natural compounds with proteasome inhibitory activity for cancer prevention and treatment. Curr. Protein Pept. Sci. 9, 227-239.

Yoshida, T., Biro, P., Cohen, T., Müller, R.M., Shibahara, S. 1988. Human heme oxygenase cDNA and induction of its mRNA by hemin. Eur J Biochem. 171, 457-461.

Young, J.T.F., Gauley, J., Heikkila, J.J. 2009. Simultaneous exposure of *Xenopus* A6 kidney epithelial cells to concurrent mild sodium arsenite and heat stress results in enhanced *hsp30* and *hsp70* gene expression and the acquisition of thermotolerance. Comp. Biochem. Physiol. A Mol. Integr. Physiol. 153, 417-424.

Young, J.T., Heikkila, J.J. 2010. Proteasome inhibition induces *hsp30* and *hsp70* gene expression as well as the acquisition of thermotolerance in *Xenopus laevis* A6 cells. Cell Stress Chaperones 15, 323-334.

Yu, X., Hong, S., Faustman, E.M. 2008. Cadmium-induced activation of stress signaling pathways, disruption of ubiquitin-dependent protein degradation and apoptosis in primary rat sertoli cell-gonocyte cocultures. Toxicol. Sci. 104, 385-396.

Yu, Y., Hamza, A., Zhang, T., Gu, M., Zou, P., Newman, B., Li, Y., Gunatilaka, A. A., Zhan, C. G., Sun, D. 2010. Withaferin A targets heat shock protein 90 in pancreatic cancer cells. Biochem. Pharmacol. 79, 542-551.

Zaarur, N., Meriin, A.B., Gabai, V.L., Sherman, M.Y. 2008. Triggering aggresome formation. Dissecting aggresome-targeting and aggregation signals in synphilin 1. J Biol Chem. 283, 27575-27584.

Zhang, X., Qian, S.B. 2011. Chaperone-mediated hierarchical control in targeting misfolded proteins to aggresomes. Mol Biol Cell. 22, 3277-3288.

Zhang YQ, Sarge KD. 2007. Celastrol inhibits polyglutamine aggregation and toxicity though induction of the heat shock response. J Mol Med. 85:1421-8.

Zhang, L.H., Zhang, X. 2010. Roles of GRP78 in physiology and cancer. J Cell Biochem 110, 1299-1305.

Zhao, R., Houry, W.A. 2005. Hsp90: a chaperone for protein folding and gene regulation. Biochem Cell Biol. 83, 703-710.

Zurla, C., Lifland, A.W., Santangelo, P.J. 2011. Characterizing mRNA interactions with RNA granules during translation initiation inhibition. PLoS One 6, e19727. doi: 10.1371/journal.pone.0019727.